



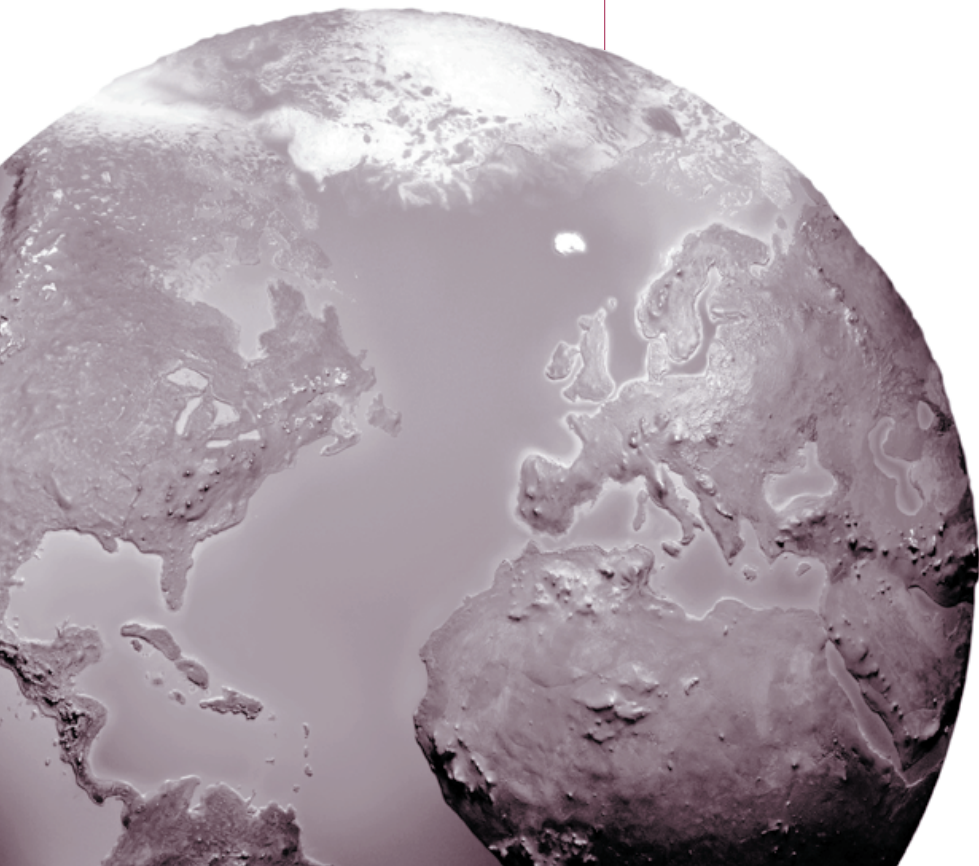
Walter A. Rosenblith New Investigator Award  
**RESEARCH REPORT**

**HEALTH  
EFFECTS  
INSTITUTE**

Number 153  
December 2010

**Improved Source Apportionment  
and Speciation of Low-Volume  
Particulate Matter Samples**

James J. Schauer, Brian J. Majestic,  
Rebecca J. Sheesley, Martin M. Shafer,  
Jeffrey T. DeMinter, and Mark Mieritz





# Improved Source Apportionment and Speciation of Low-Volume Particulate Matter Samples

James J. Schauer, Brian J. Majestic, Rebecca J. Sheesley,  
Martin M. Shafer, Jeffrey T. DeMinter, and Mark Mieritz

with a Critique by the HEI Health Review Committee

---

Research Report 153

Health Effects Institute

Boston, Massachusetts

*Trusted Science • Cleaner Air • Better Health*

Publishing history: The Web version of this document was posted at [www.healtheffects.org](http://www.healtheffects.org) in December 2010.

Citation for document:

Schauer JJ, Majestic BJ, Sheesley RJ, Shafer MM, DeMinter JT, Mieritz M. 2010. Improved Source Apportionment and Speciation of Low-Volume Particulate Matter Samples. Research Report 153. Health Effects Institute, Boston, MA.

---

© 2010 Health Effects Institute, Boston, Mass., U.S.A. Asterisk Typographics, Barre, Vt., Compositor. Printed by Recycled Paper Printing, Boston, Mass. Library of Congress Catalog Number for the HEI Report Series: WA 754 R432.

♻️ Cover paper: made with at least 55% recycled content, of which at least 30% is post-consumer waste; free of acid and elemental chlorine. Text paper: made with 100% post-consumer waste recycled content; acid free; no chlorine used in processing. The book is printed with soy-based inks and is of permanent archival quality.

# CONTENTS

About HEI	v
About This Report	vii
<b>HEI STATEMENT</b>	1
<b>INVESTIGATORS' REPORT</b> by <i>Schauer et al.</i>	3
<b>ABSTRACT</b>	3
<b>INTRODUCTION</b>	4
<b>SPECIFIC AIMS</b>	4
<b>ANALYTIC METHODS</b>	4
Background	4
Improved Characterization of Trace Elements in Personal Exposure Samples	5
Thermal Desorption GC–MS Method	14
Programmable Temperature Vaporization GC–MS Method	20
Wet-Chemical Extractions for Metal Speciation Studies	20
Iron Speciation Techniques	23
Manganese Speciation Techniques	27
Chromium Speciation Techniques	30
Iron L <sub>II</sub> -Edge X-ray Absorption near Edge Structure Spectroscopy	31
<b>SAMPLING AND STUDY DESIGN</b>	33
Intercomparison of Personal Exposure Samplers at University of Southern California	34
Iron Aging Study	35
Manganese Speciation Study	35
St. Louis Truck Terminal Study	36
University of California–Irvine Pilot Health Study	37
<b>RESULTS AND DISCUSSION</b>	37
Intercomparison of Personal Exposure Samplers	37
Iron Aging Study	41
Manganese Speciation Study	49
St. Louis Truck Terminal Results	50
University of California–Irvine Pilot Health Study	62
<b>SUMMARY AND CONCLUSIONS</b>	68
<b>ACKNOWLEDGMENTS</b>	70
<b>REFERENCES</b>	70
<b>APPENDICES AVAILABLE ON THE WEB</b>	73
<b>ABOUT THE AUTHORS</b>	73
<b>OTHER PUBLICATIONS RESULTING FROM THIS RESEARCH</b>	74
<b>ABBREVIATIONS AND OTHER TERMS</b>	74
<b>ABBREVIATIONS OF CHEMICAL ELEMENTS</b>	75

# Research Report 153

---

<b>CRITIQUE</b> <i>by the Health Review Committee</i>	77
<b>INTRODUCTION AND BACKGROUND</b>	77
<b>SPECIFIC AIMS</b>	78
<b>METHODS DEVELOPMENT</b>	78
Acid Digestion for Trace-Element Characterization	78
GC-MS Methods for Quantification of Organic Compounds	80
Wet-Chemical Spectrophotometric Analysis Methods	81
Quantification of Fe(II) and Fe(III) by XANES Spectroscopy	82
<b>REAL-WORLD APPLICATION STUDIES OF LOW-VOLUME PM SAMPLE ANALYSIS METHODS</b>	83
Sampling Campaigns	83
Application Studies	84
<b>HEALTH REVIEW COMMITTEE EVALUATION AND DISCUSSION</b>	87
<b>CONCLUSIONS</b>	88
<b>ACKNOWLEDGMENTS</b>	89
<b>REFERENCES</b>	89
Related HEI Publications	91
HEI Board, Committees, and Staff	93

# ABOUT HEI

The Health Effects Institute is a nonprofit corporation chartered in 1980 as an independent research organization to provide high-quality, impartial, and relevant science on the effects of air pollution on health. To accomplish its mission, the institute

- Identifies the highest-priority areas for health effects research;
- Competitively funds and oversees research projects;
- Provides intensive independent review of HEI-supported studies and related research;
- Integrates HEI's research results with those of other institutions into broader evaluations; and
- Communicates the results of HEI research and analyses to public and private decision makers.

HEI receives half of its core funds from the U.S. Environmental Protection Agency and half from the worldwide motor vehicle industry. Frequently, other public and private organizations in the United States and around the world also support major projects or certain research programs. HEI has funded more than 280 research projects in North America, Europe, Asia, and Latin America, the results of which have informed decisions regarding carbon monoxide, air toxics, nitrogen oxides, diesel exhaust, ozone, particulate matter, and other pollutants. These results have appeared in the peer-reviewed literature and in more than 200 comprehensive reports published by HEI.

HEI's independent Board of Directors consists of leaders in science and policy who are committed to fostering the public-private partnership that is central to the organization. The Health Research Committee solicits input from HEI sponsors and other stakeholders and works with scientific staff to develop a Five-Year Strategic Plan, select research projects for funding, and oversee their conduct. The Health Review Committee, which has no role in selecting or overseeing studies, works with staff to evaluate and interpret the results of funded studies and related research.

All project results and accompanying comments by the Health Review Committee are widely disseminated through HEI's Web site ([www.healtheffects.org](http://www.healtheffects.org)), printed reports, newsletters and other publications, annual conferences, and presentations to legislative bodies and public agencies.



# ABOUT THIS REPORT

Research Report 153, *Improved Source Apportionment and Speciation of Low-Volume Particulate Matter Samples*, presents a research project funded by the Health Effects Institute and conducted by Dr. James J. Schauer of the Department of Civil and Environmental Engineering, University of Wisconsin–Madison, and his colleagues. This research was funded under HEI's Walter A. Rosenblith New Investigator Award Program, which provides support to promising scientists in the early stages of their careers. This report contains three main sections.

**The HEI Statement**, prepared by staff at HEI, is a brief, nontechnical summary of the study and its findings; it also briefly describes the Health Review Committee's comments on the study.

**The Investigators' Report**, prepared by Schauer and colleagues, describes the scientific background, aims, methods, results, and conclusions of the study.

**The Critique** is prepared by members of the Health Review Committee with the assistance of HEI staff; it places the study in a broader scientific context, points out its strengths and limitations, and discusses remaining uncertainties and implications of the study's findings for public health and future research.

This report has gone through HEI's rigorous review process. When an HEI-funded study is completed, the investigators submit a draft final report presenting the background and results of the study. This draft report is first examined by outside technical reviewers and a biostatistician. The report and the reviewers' comments are then evaluated by members of the Health Review Committee, an independent panel of distinguished scientists who have no involvement in selecting or overseeing HEI studies. During the review process, the investigators have an opportunity to exchange comments with the Review Committee and, as necessary, to revise their report. The Critique reflects the information provided in the final version of the report.



# HEI STATEMENT

## Synopsis of Research Report 153

### Improved Source Apportionment and Speciation of Low-Volume Particulate Matter Samples

#### BACKGROUND

As particulate air pollution has increasingly been associated with adverse human health effects, interest has been growing in studying the chemical composition of inhalable particulate matter (PM) and how exposures to its specific constituents are associated with health effects. Much of the general characterization of the composition of PM has been performed on specimens collected by high-volume samplers. Personal sampling, although it improves exposure estimation, makes use of small-scale equipment that traditionally could not collect a sufficient volume of airborne PM for proper speciation analysis. In the current report, Dr. James J. Schauer and his team detail the methods they developed for the detection and quantification of a wide range of trace metals and nonpolar and polar organic species in low-volume PM samples.

#### APPROACH

The investigators' aims were to develop multiple chemical analysis methods for the measurement of concentrations of organic compounds, trace metals, trace-element isotopes, and oxidation states of selected elements in samples of  $PM \leq 2.5 \mu m$  in aerodynamic diameter ( $PM_{2.5}$ ) collected using personal sampling equipment and to analyze existing personal exposure samples from various epidemiologic studies.

Schauer and colleagues developed a number of variations on gas chromatography–mass spectrometry (GC–MS) analysis as well as wet-chemical methods for more economical spectrophotometric analysis of selected metals (iron [Fe], manganese [Mn], and chromium [Cr]) and quantification of the relative proportions of their oxidative states.

The investigators applied rigorous clean-chemistry concepts to their methods development in order to

address the three pillars of quantitative trace-element analysis, namely the control and minimization of background values using blanks; the maximization of sensitivity; and the control, isolation, and removal of interferences.

The following methods were developed or fine-tuned: (1) acid digestion for trace-element characterization, (2) GC–MS techniques for the quantification of organic compounds, (3) wet-chemical spectrophotometric analysis techniques for the analysis of selected metals, and (4) x-ray absorption near edge structure (XANES) spectroscopy for the quantification of the valence states of Fe. The investigators then tested several real-world applications of the methods they had developed in order to demonstrate their utility for low-volume PM samples in a variety of circumstances:

- Using various types of co-located personal samplers, substrate combinations, and ambient samplers, the investigators compared samples from sites in East St. Louis, Illinois, and at the University of Southern California at Los Angeles.
- Samples from sites in East St. Louis; Waukesha, Wisconsin; and the Rancho Los Amigos National Rehabilitation Center, in the Los Angeles Basin, California, were subjected to simulated atmospheric aging for 0 to 10 days to measure changes in Fe oxidation states.
- The investigators undertook a study of Mn speciation in airborne wintertime PM samples from Toronto, Canada (where methylcyclopentadienyl manganese tricarbonyl [MMT] had been used extensively as an octane booster in gasoline prior to 2004).
- Personal samples of PM aerosols were obtained from a large, ongoing cancer study (led by Eric Garshick of Harvard) of dockworkers, mechanics, and drivers at a truck terminal in St. Louis,

This Statement, prepared by the Health Effects Institute, summarizes a research project funded by HEI and conducted by Dr. James J. Schauer of the Department of Civil and Environmental Engineering, University of Wisconsin–Madison, and colleagues. Research Report 153 contains both the full Investigators' Report and a Critique of the study prepared by the Institute's Health Review Committee.

Missouri. The samples were compared with samples obtained in each of four work areas in the terminal and at a nearby urban background monitor, measuring concentrations of elemental carbon, organic carbon, polycyclic aromatic hydrocarbons, steranes, and hopanes.

- The team obtained and compared indoor, outdoor, and personal PM samples from a study of coronary heart disease (led by Ralph Delfino of the University of California–Irvine) in elderly nonsmokers living at a retirement home in the Los Angeles Basin.

### RESULTS AND INTERPRETATION

The team reported good agreement between the size-resolved total PM mass concentrations collected by the co-located PM<sub>2.5</sub> personal samplers in East St. Louis and Los Angeles. Size-resolved trace-metal concentrations for six metals differed by site but showed better agreement within sampler type than between co-located samplers. In the Fe aging study, the greatest changes occurred in the first 6 days, when soluble Fe(II) increased in the coarse fraction over the first day and then decreased steadily. Because the greatest changes occurred in the brief period after sampling, the results were believed to indicate that atmospheric aging could have a substantial effect on exposure to soluble Fe in PM aerosols.

In the wet-chemical analysis of Mn, the greatest concentrations of soluble Mn were found in the coarse fraction of the samples, with decreasing concentrations as particle-size fractions decreased. Compared with speciation results for the East St. Louis samples used in the sampler intercomparison, air concentrations of Mn in Toronto were lower overall. Soluble oxidized Mn was detectable only in the PM<sub>2.5</sub> fraction of the Toronto samples.

Consistency of sampling results for the St. Louis truck terminal was found to vary by job classification and work area. Jobs that included high exposure variation within a job and work area indicated cases where exposures were more highly affected by individual job and personal activities than by area or background air quality.

No relationship was found between air concentrations from the indoor, outdoor, and personal samples for the retirement home residents for all analyzed trace elements except copper. The investigators thought this indicated that the personal exposure samples were not measuring exposure to the same pollutant sources as those represented in the indoor and outdoor samples.

According to the investigators, this study has advanced the PM speciation of personal exposure samples in three key areas: the development of (1) specialized GC–MS methods to measure organic tracers, (2) specialized high-resolution inductively coupled plasma mass spectrometry methods to measure trace elements, and (3) wet-chemical methods to speciate Fe and Mn. The investigators estimated that the cost of the analyses ranged from a high of \$250 per sample for the thermal desorption GC–MS method to a low of \$10 per sample for the wet-chemical method.

The HEI Health Review Committee noted that the description of the methods development and experimental analyses fully addressed the aims proposed at the beginning of the study. Schauer and his team have also demonstrated that their methods are well suited to PM samples collected for health studies.

The Committee noted, however, that the investigators were not able to meet certain goals. They did not test or expand much on their methods for the analysis of polar organic compounds, because the materials caused repeated instrument failures. The investigators also had difficulty measuring Cr(VI), an oxidation state of Cr, because of the extremely small amounts of Cr(VI) present in the PM aerosol found in most environments.

### CONCLUSIONS

Schauer and colleagues have developed methods that have sufficiently high sensitivity and sufficiently low detection limits to measure trace metals, nonpolar organics, and polar organics present in low-volume PM samples, such as those collected by personal sampling equipment. The team has successfully adapted wet-chemical methods for the extraction and quantification of Fe, Mn, and Cr in various oxidation states of interest to researchers.

Results from the St. Louis truck terminal indicated that personal activities, such as smoking and job tasks, had large effects on exposures. Results from the retirement home indicated that trace elements measured in personal PM samples were different from those measured in indoor and outdoor air samples (although the reasons for these discrepancies were not clear). These results indicate the broad suitability of the investigators' methods for use in studies of PM exposure and human health. Further work remains to be done on methods for the analysis of polar organic compounds and for improving detection of Cr(VI) from ambient air samples taken with personal samplers.

## Improved Source Apportionment and Speciation of Low-Volume Particulate Matter Samples

James J. Schauer, Brian J. Majestic, Rebecca J. Sheesley, Martin M. Shafer, Jeffrey T. DeMinter, and Mark Mieritz

*Department of Civil and Environmental Engineering (J.J.S.) and Environmental Chemistry and Technology Program (J.J.S., B.J.M., R.J.S., M.M.S.), University of Wisconsin–Madison; Wisconsin State Laboratory of Hygiene, Madison, Wisconsin (J.J.S., M.M.S., J.T.D., M.M.)*

---

### ABSTRACT

---

New chemical analysis methods for the characterization of atmospheric particulate matter (PM)\* samples were developed and demonstrated in order to expand the number of such methods for use in future health studies involving PM. Three sets of methods were developed, for the analysis (1) of organic tracer compounds in low-volume personal exposure samples (for source apportionment), (2) of trace metals and other trace elements in low-volume personal exposure samples, and (3) of the speciation of the oxidation states of water-soluble iron (Fe), manganese (Mn), and chromium (Cr) in PM samples.

The development of the second set of methods built on previous work by the project team, which had in the past used similar methods in atmospheric source apportionment studies. The principal challenges in adapting these methods to the analysis of personal exposure samples were the improvement of detection limits (DLs) and control of the low-level contamination that can compromise personal exposure samples.

A secondary goal of our development efforts was to reduce the cost and complexity of the three sets of

methods in order to help facilitate their broader use in future health studies.

The goals of the project were achieved, and the ability to integrate the methods into existing health studies was demonstrated by way of conducting two pilot studies. The first study involved analysis of trace elements in size-resolved PM samples that had been collected to represent study subjects' personal exposures along with simultaneous measures of indoor and outdoor PM concentrations. The second study involved analysis of the speciation of organic tracer compounds in personal exposure samples, indoor samples, and outdoor samples in order to understand the diesel PM exposure of study subjects in various job classifications in an occupational setting. Both pilot studies used existing samples from large multi-year health studies and were intended to demonstrate the feasibility and value of using the new chemical analysis methods to better characterize the personal exposure samples. Analysis of the health data and the broader implications of the exposure assessments were not evaluated as part of the present study, but our pilot-study measurements are expected to contribute to investigators' future analyses in the large multi-year health studies.

The methods we developed for the low-cost measurement of the oxidation states of Fe, Mn, and Cr in atmospheric PM samples are extremely sensitive and well suited for use in health studies. To demonstrate the utility of these methods, small-scale studies were conducted to characterize the redox cycling of Fe in PM on the time scale of atmospheric transport from source to personal exposure and to provide preliminary data on the atmospheric concentrations of soluble forms of the target metals in selected urban environments (in order to help focus future research seeking to understand the role of metals in human exposure to PM and its adverse health effects).

---

This Investigators' Report is one part of Health Effects Institute Research Report 153, which also includes a Critique by the Health Review Committee and an HEI Statement about the research project. Correspondence concerning the Investigators' Report may be addressed to Dr. James J. Schauer, 148 Water Science and Engineering Laboratory, 660 North Park Street, Madison, WI 53706-1484; e-mail: jjschauer@wisc.edu.

Although this document was produced with partial funding by the United States Environmental Protection Agency under Assistance Award CR-83234701 to the Health Effects Institute, it has not been subjected to the Agency's peer and administrative review and therefore may not necessarily reflect the views of the Agency, and no official endorsement by it should be inferred. The contents of this document have not been reviewed by private party institutions, including those that support the Health Effects Institute; therefore, it may not reflect the views or policies of these parties, and no endorsement by them should be inferred.

\*Lists of abbreviations and other terms appear at the end of the Investigators' Report.

The present report summarizes the methods that were developed and demonstrated to be suitable for use in health studies and provides pilot-scale data that can be used to develop hypotheses and experimental strategies to further enhance the ability of future health studies to elucidate the role of PM, PM sources, and PM components in the observed associations between atmospheric PM and adverse human health outcomes.

---

### INTRODUCTION

---

A large number of health studies are currently being conducted, or are planned for the future, that are directed toward understanding the effects on human health of exposure to atmospheric PM. Many of these studies address updated research priorities originally identified in the 1998 Nuclear Regulatory Commission report *Research Priorities for Airborne Particulate Matter*, namely (1) to apportion PM exposures to individual sources, (2) to understand the relationship between actual human exposures to PM and the PM present at stationary outdoor monitoring sites, and (3) to identify the biologically important constituents and characteristics of PM in the context of human health effects. Clearly, many of these efforts would be greatly enhanced if cost-effective analytic methods were available that could provide detailed chemical speciation of particle-phase organic compounds and trace metals in personal exposure samples. The measurement of these constituents in PM samples has been shown to be a powerful tool for the apportionment of samples collected at centralized outdoor monitoring sites (Schauer et al. 1996, 2000; Schauer et al. 2002a; Manchester-Neesvig et al. 2003). In the past, analytic methods were not sensitive enough to quantify organic compounds or trace metals in low-volume personal exposure samplers and were too costly to integrate effectively into health studies. This report describes advances in the measurement of organic compounds and trace metals in low-volume personal exposure samples as well as pilot studies that directly integrated these advances into ongoing health studies.

The development and application of the analytic methods described here will provide tools for investigators seeking to better understand (1) human exposures to PM, (2) source contributions to PM exposures, (3) the health effects of exposures to various sources of PM and the constituents present in it, and (4) the use of biomarkers to assess exposure. Ultimately, these new methods will also help provide regulators and engineers with information needed to develop more effective, efficient air pollution control strategies in order to properly protect humans from the adverse effects of exposure to airborne PM.

---

### SPECIFIC AIMS

---

The specific aims of the project were as follows:

1. To develop and validate a gas chromatography–mass spectrometry (GC–MS) technique for the speciation of a broad range of organic compounds present in low-volume personal exposure samples, including all of the molecular markers used in particle-phase organic-compound-based source apportionment models (Schauer et al. 1996, 2000, 2002b; Zheng et al. 2002; Manchester-Neesvig et al. 2003);
2. To develop and validate a low-cost thermal desorption GC–MS (TD-GC–MS) technique for the quantification of a number of selected organic compounds present in PM samples collected with personal exposure samplers that can be integrated effectively into epidemiologic and human exposure studies;
3. To optimize sampling and inductively coupled plasma–mass spectrometry (ICP–MS) analysis techniques for the measurement of trace metals and selected trace-element isotope signatures in PM samples collected with personal exposure samplers;
4. To develop and validate low-cost wet-chemistry methods for the measurement of the oxidation states of selected trace elements (Fe, Mn, and Cr) present in PM samples collected with ambient samplers, personal exposure samplers, and source samplers; and
5. To integrate these analytic techniques into epidemiologic and human exposure studies that are directly or indirectly supported by the Health Effects Institute (HEI). The project’s principal investigator will work with HEI staff and the HEI Research Committee to identify and select appropriate health studies for these unique analytic techniques.

---

### ANALYTIC METHODS

---

#### BACKGROUND

An assessment of breathing-zone exposures to trace metals in atmospheric PM is vital to advancing our understanding of PM’s potential health effects and to better defining its sources and exposure routes. Centralized ambient monitoring sites generally cannot provide the detailed spatial and temporal data required to assess human exposure properly. As a result, personal exposure samplers have been developed to provide better estimates of individuals’ actual exposure to, for example, PM 2.5  $\mu\text{m}$  or smaller in aerodynamic diameter (PM<sub>2.5</sub>). Certain personal exposure samplers provide the additional feature of obtaining detailed size-resolved data (e.g., the Sioutas personal

**Table 1.** Digest Solution Concentrations of Selected Elements Resulting from Solubilization of PM from Personal Exposure Sampler Filters

Concentration (ng/L) <sup>a</sup>	Element
> 5000	Ca, Fe, Na, S
1000–5000	Al, K, Mg, Si
200–1000	Mn, P, Ti, Zn
50–200	Ba, Cu, Pb, Sn, Sr
10–50	As, Cr, Mo, Ni, Rb, Sb
2–10	Ag, Cd, Ce, Co, La, Li, V
0.5–2	Pd, Pt, Tl, W, Y
< 0.5	Be, Cs, Ir, Rh, U, rare earths

<sup>a</sup> Concentrations assume 25 to 150 µg PM on filter and a digest solution volume of 30 mL.

cascade impactor sampler [PCIS]). However, the very low mass loadings (typically 20 to 150 µg) of the PM from these samplers present nontrivial challenges in accurate chemical analysis. Table 1 illustrates this challenge, showing the extremely low concentrations of elements that result from bringing 25 to 150 µg PM into solution. Concentrations for important classes of elements are typically < 50 nanograms (ng)/L and, for many other elements, < 2 ng/L.

Personal exposure samplers are just one example of cases in which the aerosol sample mass available for characterization is small. The growing recognition that atmospheric processes can play out and source vectors can vary on short time scales (on the order of hours) necessitates fine temporal sampling and results, again, in PM samples of restricted mass. Size-resolved sampling in general partitions PM mass into multiple discrete samples of more limited mass, with typically very limited mass in the ultrafine size classes. Because health effects are clearly related to aerosol size and source reconciliation efforts are improved by size fractionation, size-resolved sampling will continue to be a needed tool. For these reasons, the analytic methods developed as part of the present project are expected to have a broad range of applications.

Compounding the challenge posed by limited PM mass is the demand for ever more comprehensive characterization of elemental and organic species. Source reconciliation efforts and tracer development demonstrably benefit from reliable data on larger numbers of trace elements and organic compounds. Unfortunately many of these analytes are present only at very low concentrations in PM, and traditional methods of analysis do not have adequate sensitivity or are plagued with interferences that prevent accurate quantitation.

## IMPROVED CHARACTERIZATION OF TRACE ELEMENTS IN PERSONAL EXPOSURE SAMPLES

With the aim of developing an approach for comprehensive trace-element analysis of micro-samples typical of those obtained from personal exposure samplers, we coupled an enhanced microwave-assisted acid digestion method with state-of-the-art plasma mass spectrometry. Rigorous clean-chemistry concepts were applied throughout the effort. Though not a direct focus of the effort, the analytic mass spectrometry methods we developed will also have direct utility for methods that analyze the soluble, bioavailable fraction of the analyzed elements.

### Approach

A key part of the methods development was aimed at achieving our element-detection and signal-to-noise goals. These efforts were founded on the three pillars of quantitative trace-element analysis, namely (1) blank control or minimization, (2) sensitivity maximization, and (3) interference control, isolation, or removal. Two key accomplishments in the analysis of metals in personal exposure samples were made:

1. The development and validation of an improved micro-volume microwave-assisted acid digestion method. The method was designed to achieve the lowest possible laboratory blanks in order to improve sensitivity.
2. The adaptation of existing quadrupole inductively coupled plasma–mass spectrometry (Q-ICP–MS) aerosol methods to high-resolution magnetic sector ICP–MS (HR-ICP–MS). The use of HR-ICP–MS led to significant improvements in sensitivity and interference management.

These two accomplishments will have a transformative impact on the analysis of trace metals present in PM and are described below:

**Enhanced Microvolume Microwave-Assisted Acid Digestion Method** The goals of establishing a microwave-assisted acid digestion method were as follows:

1. To reduce digestion blank concentrations and variability, which have a direct impact on DLs;
2. To improve the signal-to-noise ratios of the digest for a given digest mass; and
3. To quantitatively recover or solubilize silicon (Si) during the digestion of aerosol samples.

Both a sealed-vial and an open-vessel method were developed to address these goals. The primary reason for this was that all realistic options for attaining goal 3 — quantitative

Si recovery—brought with them some compromises in attaining goals 1 and 2 and reduced overall method robustness. In the sealed-vial method, Si is quantified; in the other, somewhat more robust open-vessel method, Si is not quantified. It should be stressed that both methods exhibited substantially improved performance over previously established analytic methods for trace metals.

Goals 1 and 2 were common to both methods and were addressed as follows:

1. By reducing the quantities of high-purity acids used in digestion from 2.2 to 0.6 mL in the sealed-vial method and from 2.2 to 0.9 mL in the open-vessel method;
2. By adjusting the automated microwave digestion program to compensate for low acid volume, increasing the peak temperature to 200°C in the open-vessel method, and extending dwell times at the peak temperature;
3. By improved blank tracking and validation of the high-purity acids;

4. By employing a new, simplified rotor in the microwave digestion unit; and
5. By reducing the final digestate dilution volume from 30 to 15 mL in both methods.

The reduced acid volumes contributed to substantially lower absolute blank contaminant loading during digestion and, also important, resulted in lower matrix-derived interferences in ICP–MS analysis (see below). Although the latter might not dramatically affect HR-ICP–MS analysis, in which interferences can be mass resolved, it has a significant effect on Q-ICP–MS analysis (the vast majority of ICP–MS users have quadrupole instruments). Total blank contributions from digestion were reduced to < 20 picograms (pg) for many elements.

Method DLs (3-sigma, ng/m<sup>3</sup>) were estimated from blank uncertainties for both the sealed-vial and the open-vessel methods, assuming an air-sampling volume of 14 m<sup>3</sup>. A summary is presented in Figure 1. DLs for all but a few elements (sodium [Na], calcium [Ca], Fe, potassium [K], aluminum [Al], magnesium [Mg], and zinc [Zn]) were

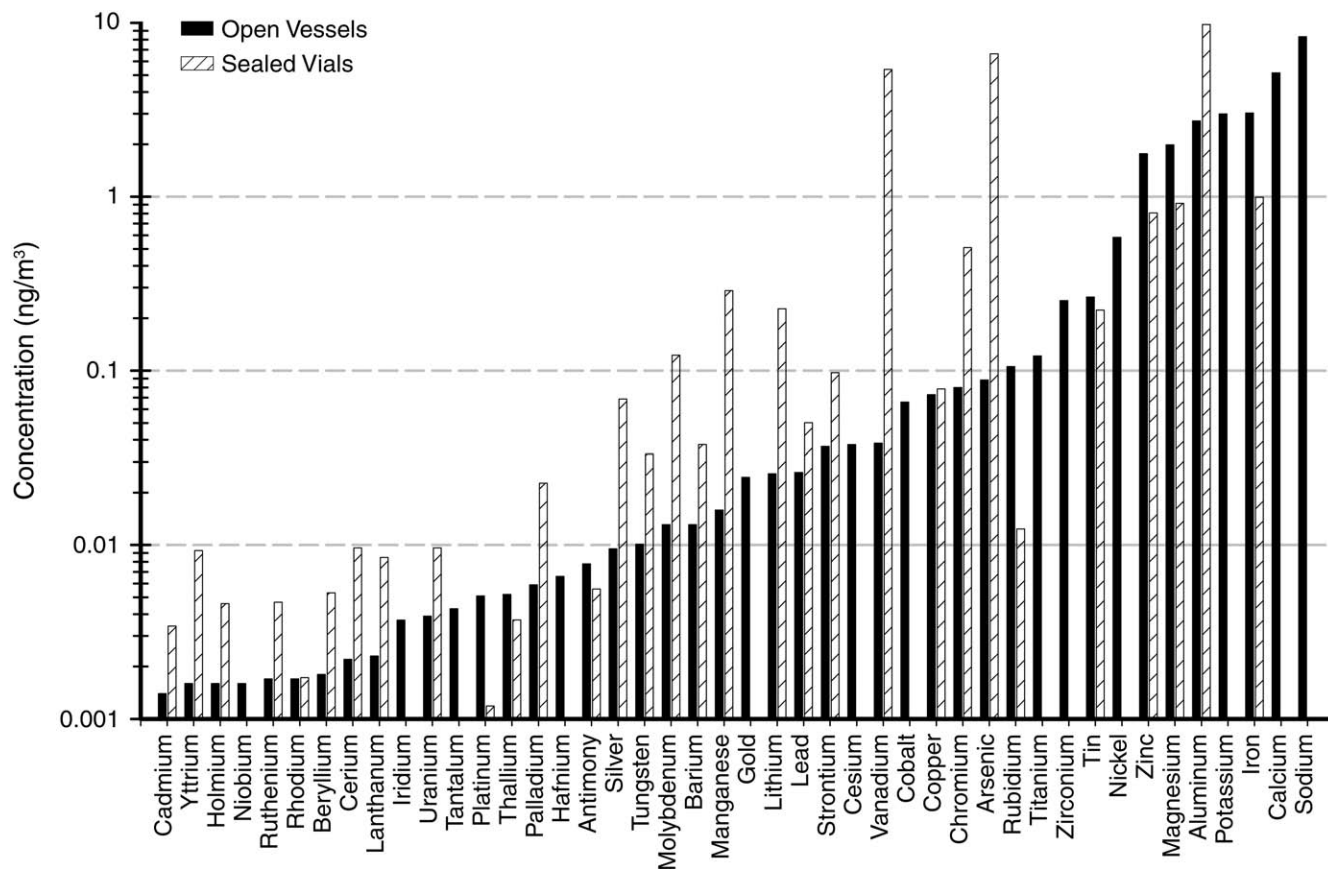


Figure 1. Comparison of method DLs (ng/m<sup>3</sup>) in 44 elements for open-vessel and sealed-vial analytic methods.

$< 1 \text{ ng/m}^3$ . For 33 elements, DLs were  $< 0.1 \text{ ng/m}^3$ , and for 19 elements, DLs were  $< 0.01 \text{ ng/m}^3$ . DLs for many of the rare earth elements, such as cadmium (Cd), rhodium (Rh), and beryllium (Be), approached  $0.001 \text{ ng/m}^3$ . The sealed-vial method exhibited greater blank variability than the open-vessel method for 21 of the 44 elements studied. For most other elements, blank variability was similar in the two methods.

Increasing the microwave peak temperature (and dwell time at that temperature) improved recoveries for a group of refractory elements. By reducing the final digestate dilution volume by a factor of two (thereby doubling analyte concentrations) and lowering blank concentrations by an even larger factor, our effective signal-to-noise ratio was significantly increased.

The microwave vendor (Milestone) introduced a new rotor (model PRO-24) (to hold the digestion “bombs,” or vessels) and digestion-bomb design during the early stages of the project. The digestion bombs incorporated a simplified design and seal system that we felt would reduce stochastic contamination events and therefore contribute to our key goal of improving blank variability. The new rotor also promised to increase productivity, as it held 24 digestion vessels, compared with 12 in the older design. We purchased the new rotor-and-bomb system, and all data for sealed-vessel digestions were generated using the new system. Although blank improvements could not, over the relatively short-term course of the project, be attributed specifically to the bomb design, we expect that over the longer term this will be the case. Throughput, however, was demonstrably improved.

Goal 3 was addressed by validating a new sealed digestion vial (in combination with the new Milestone microwave rotor). In our previously validated microwave-assisted acid digestion method, as well as in the newly optimized method described above, samples (and digest acids) are placed in miniature open-topped TFM-Teflon tubes in the pressure vessel. Si present in the PM samples is brought into solution as silicon tetrafluoride. However, silicon tetrafluoride is volatile and is partially lost from the sample tubes, meaning that Si cannot be quantified using this digestion method. A sealed vial, however, quantitatively retains the solubilized Si. We evaluated several sealable Teflon vials and settled on a 6-mL PFA-Teflon vial manufactured by Savillex (model 201-006-20-023-01). These vials were subjected to a lengthy and exhaustive performance assessment in which, in addition to Si recovery, blanks, standard reference material (SRM) recoveries for the complete set of elements, and robustness were measured.

It was expected that the very low acid volumes employed (sum of all acids = 0.60 mL) and limited surface

area of the sealed vials would result in significant reductions in extract blank concentrations compared with those observed in the open-vessel method. This was indeed what was observed. However, with multiple re-use of the sealed vials, the blank concentrations in the extracts became more variable (even with several cleaning cycles between uses); they were still generally acceptable but did not result in the dramatic gains expected. We attribute this to the more porous nature of the PFA-Teflon in the vials in comparison with the TFM-Teflon in the open tubes. Counterbalancing this issue to some extent is the fact that the Savillex vials are quite inexpensive and can be replaced before blanks become problematic. Also, because three sealed vials can be stacked in a single pressure vessel of the new design, up to 72 samples and controls can be digested as a batch, a substantial improvement in productivity. Potential drawbacks of the Savillex vials include an increased failure rate, which can be minimized by very careful and consistent torquing of the caps, and lower temperature limits ( $190^\circ\text{C}$  compared with  $210^\circ\text{C}$  for the TFM-Teflon tubes).

Although the primary motivation for developing the new solubilization methods was blank reduction, the methods would be of limited utility if aerosol solubilization were incomplete. The recovery efficiency of the new digestion methods was validated using three National Institute of Standards and Technology (NIST) SRMs (Urban Dust #1649a, San Joaquin Soil #2709, and Auto Catalyst #2256) and by demonstrating the comparability of the data from replicate field-collected atmospheric PM samples digested using both the new and the established methods. Recoveries of certified elements in the SRMs were generally acceptable, with traditionally difficult elements such as Cr, palladium, platinum (Pt), Rh, and Si exhibiting quantitative recovery (see Figure 2). A few highly refractory elements (including lanthanum [La], yttrium [Y], and especially hafnium [Hf] and zirconium [Zr]) and gold (Au) exhibited poor recoveries, although these recoveries were no worse than those observed using the established methods, in which, because of inefficient recovery, Au, Hf, and Zr are not reported. The variability of arsenic and cobalt recoveries was greater than is typically observed. Measured elemental recoveries using the sealed-vial and open-vessel methods were comparable, except for silver, antimony (Sb), La, and thallium (Tl), for which the sealed-vial method exhibited superior recoveries.

Goal 3, the quantitative recovery or solubilization of Si, was realized. As illustrated in Figure 3, Si from both liquid spikes and a solid SRM matrix was quantitatively recovered.

**Adapting Methods to High-Resolution Magnetic Sector ICP-MS** HR-ICP-MS instruments possess several attributes that, particularly in the characterization of trace elements

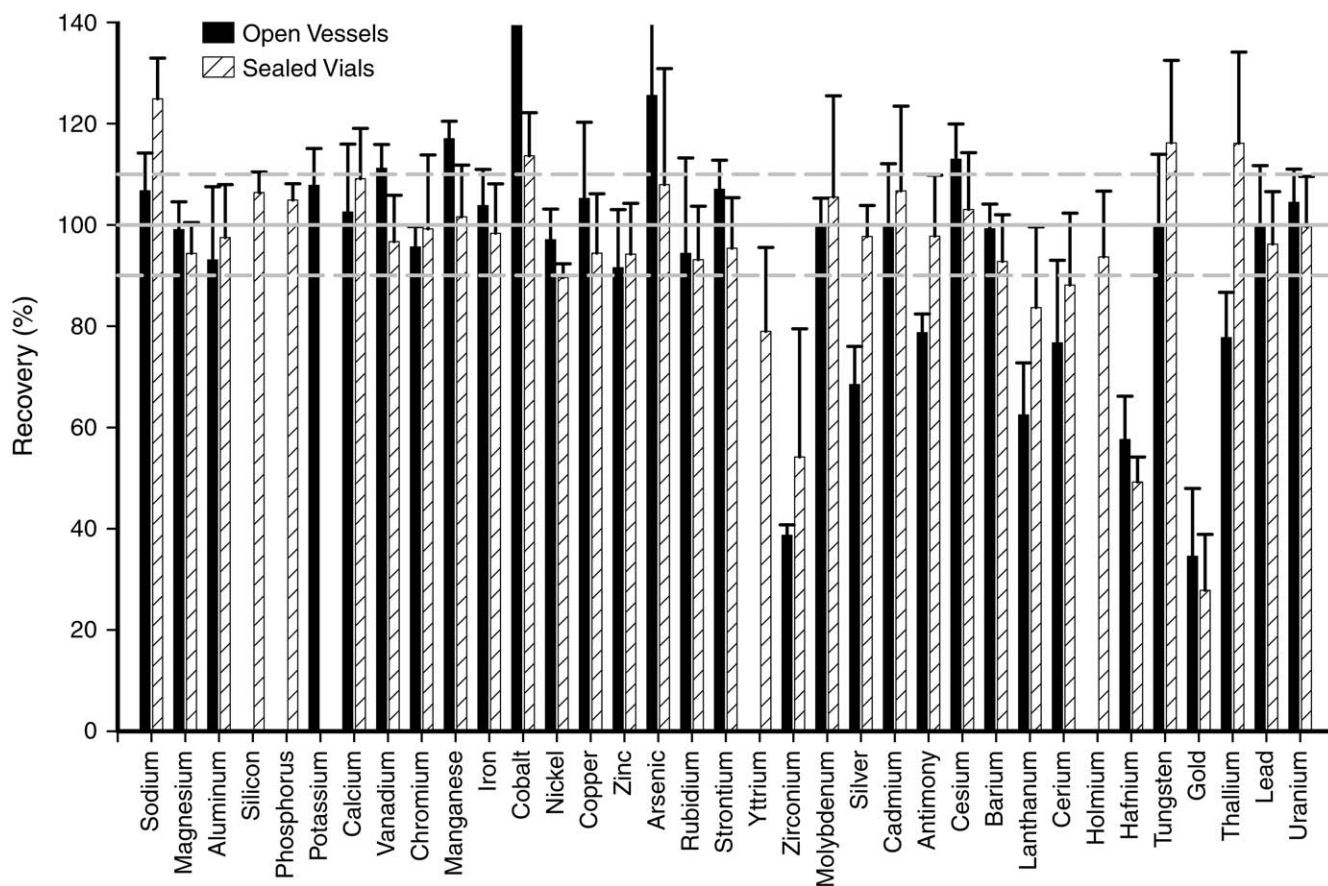


Figure 2. Comparison of element recoveries (% of certified) in NIST SRMs for open-vessel and sealed-vial analytic methods. Results for NIST SRM 2706 (San Joaquin Soil) (first panel) and NIST SRM 1649 (Urban Dust) (second panel). Data in the second panel for rhodium, palladium, and platinum are for NIST SRM 2556 (Auto Catalyst). Numbers near the top of individual bars are percentages that ran off the y-axis scales. Means shown are  $\pm 1$  SD ( $n = 8$ ). The lower dashed, middle solid, and upper dashed horizontal gray lines are reference lines for 90%, 100%, and 110% recoveries, respectively.

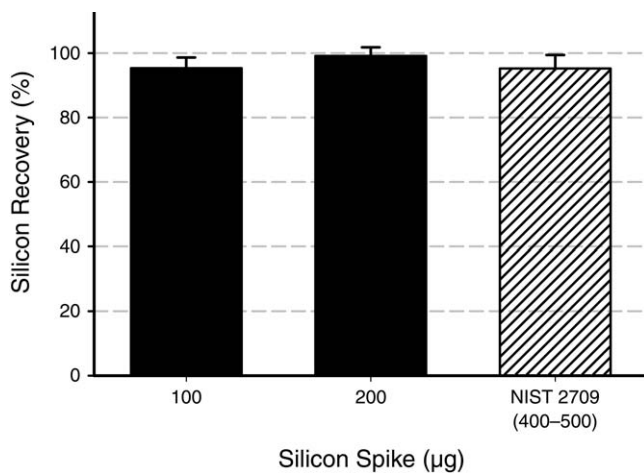


Figure 3. Silicon recovery (% of certified) from liquid spikes and NIST SRM 2709 (San Joaquin Soil) using the sealed-vial analytic method. Means shown are  $\pm 1$  SD ( $n = 8$ ).

in aerosols, make them vastly superior to Q-ICP-MS as an analytic platform. These attributes are outlined below:

1. The sensitivity of HR-ICP-MS is more than an order of magnitude better than that of Q-ICP-MS. Typical counts per second (cps) for a given elemental concentration are 3 billion for HR-ICP-MS compared with 100 million for Q-ICP-MS. This results primarily from the much more efficient ion transmission of the magnetic sector compared with that of the quadrupole mass filter. A comparison of realistic instrument DLs for HR-ICP-MS and Q-ICP-MS is presented in Table 2.
2. Background noise levels of  $< 0.2$  cps are typical for HR-ICP-MS compared with 2 cps or more for Q-ICP-MS.
3. Effective signal-to-noise ratios of  $> 15,000$  for HR-ICP-MS far surpass those of 50–200 that are typical for Q-ICP-MS. As a result, many more elements are quantifiable using HR-ICP-MS (see Table 3), and significant

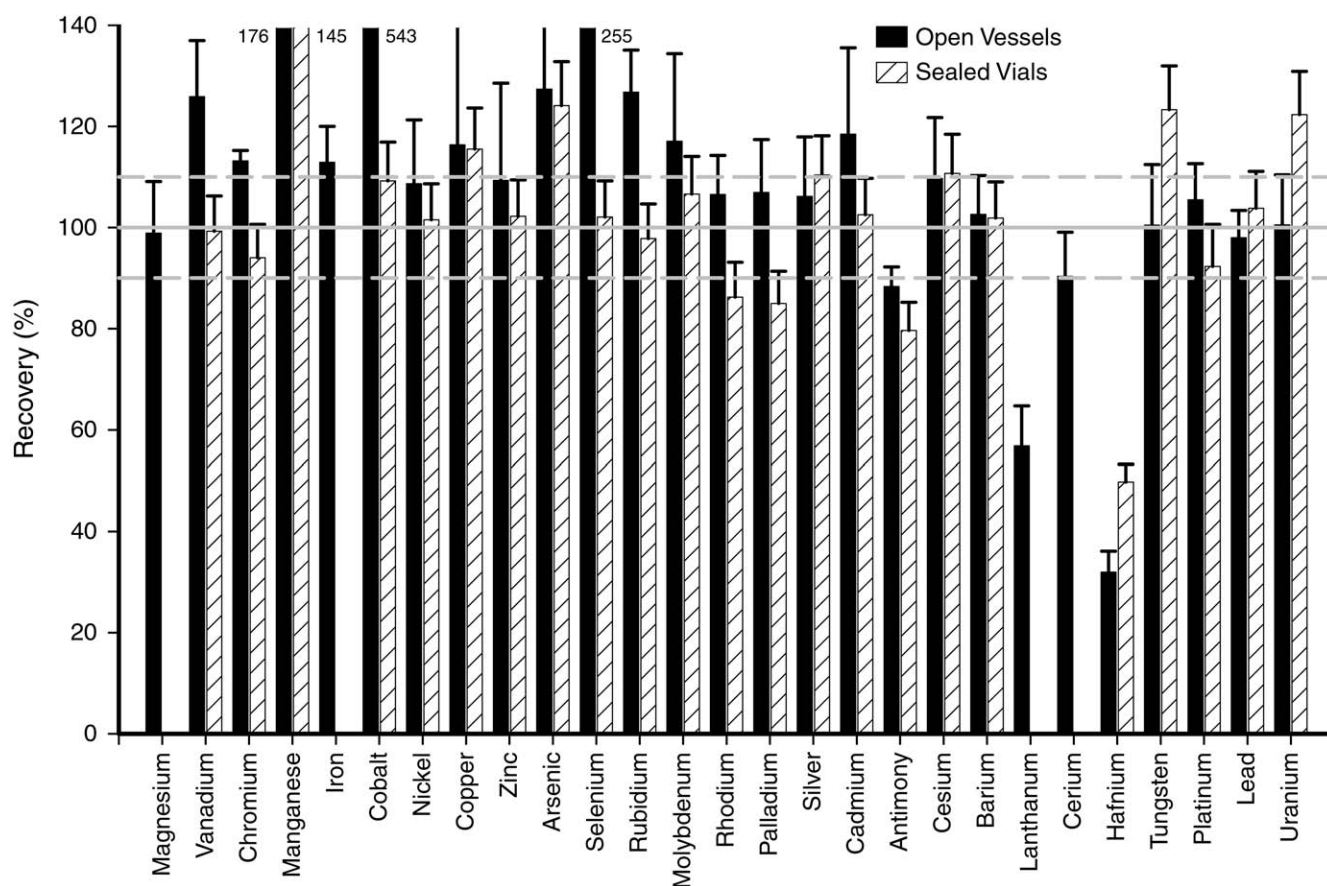


Figure 2 (Continued).

improvements in data quality are apparent for this large set of elements. Signal-to-noise ratio is the best metric of instrument performance.

4. Spectral interferences are isolated (mass-resolved) using HR-ICP-MS, with the result that analyte identification is nearly unequivocal.
5. More elements are quantifiable using HR-ICP-MS. Elements such as phosphorus, Si, and sulfur, nearly impossible to quantify using Q-ICP-MS, are routinely quantifiable using HR-ICP-MS when higher resolution is employed to isolate spectral and matrix interferences. The vastly superior signal-to-noise ratios of HR-ICP-MS mean that a significantly larger number of elements might be quantifiable in low-volume PM samples (see Table 4; more than 50 elements are routinely quantified). To take maximum advantage of these capabilities, obviously, blank concentrations must be minimized.

6. Challenging elements are more readily quantifiable using HR-ICP-MS. Measurement of light elements such as Ca, Fe, K, Mg, and Na is compromised in Q-ICP-MS by severe spectral interferences. Although effective approaches have been developed to address these interferences in Q-ICP-MS, significant compromises are made in terms of sensitivity or sample throughput. Mass-resolving the interfering species using HR-ICP-MS is a more effective and efficient approach.

*Interference Issues* Spectral interferences are a key limiting factor in Q-ICP-MS. Major errors in quantification of a large group of important elements are probable, especially at the low concentrations typically seen in aerosol solutions and digests, if interferences are not properly managed. In many instances, the analyst is unaware that interferences are present, because the conventional quality-control checks might not identify the problem.

## Source Apportionment and Speciation of Low-Volume Particulate Matter Samples

**Table 2.** Comparison of Characteristic DLs for HR-ICP–MS and Q-ICP–MS

Element	Preferred Isotopes	Mass Resolution	Characteristic DL (ng/L)	
			Q-ICP–MS (Hot, Cool)	HR-ICP–MS
Aluminum <sup>a</sup>	27	Medium–high	50, 10	2
Antimony	121	Low	2	0.2
Arsenic <sup>b</sup>	75	High	10	2
Barium	138	Medium	10	0.1
Beryllium	9	Low	5	1
Cadmium	111, 114	Low	2	0.02
Calcium <sup>a</sup>	43, 44	Medium	200, 20	5
Cerium	140	Low	1	0.01
Cesium	133	Low	1	0.02
Chromium <sup>b</sup>	52, 53	Medium	5	1
Cobalt <sup>b</sup>	59	Medium	2	0.5
Copper <sup>b</sup>	63, 65	Medium	10	2
Dysprosium <sup>c</sup>	164, 163	Low–high	0.5	0.01
Europium <sup>c</sup>	153	Low–high	0.5	0.01
Gallium	71, 69	Low	2	1
Hafnium	178	Low–high	1	0.02
Holmium <sup>c</sup>	165	Low–high	0.5	0.01
Iron <sup>a</sup>	54, 56, 57	Medium–high	50, 5	2
Lanthanum	139	Low	0.5	0.01
Lead	208, 207, 206	Low	0.5	0.05
Lithium <sup>a</sup>	7	Low	10, 1	2
Manganese	55	Medium	10	0.5
Magnesium <sup>a</sup>	25	Medium–high	200, 10	2
Molybdenum	95, 98	Medium	5	0.2
Neodymium <sup>c</sup>	146, 143	Low–high	0.5	0.01
Nickel <sup>b</sup>	60	Medium	10	2
Palladium <sup>d</sup>	106, 108	Low	2	0.1
Phosphorus <sup>e</sup>	31	Medium	Problematic	10
Platinum <sup>d</sup>	195	Low	1	0.02
Potassium <sup>a</sup>	39	High	500, 20	10
Rhodium <sup>d</sup>	103	Low	1	0.02
Rubidium	85	Low	5	0.01
Samarium <sup>c</sup>	152	Low–high	0.5	0.01
Scandium <sup>b</sup>	45	Medium	20	2
Selenium <sup>b</sup>	78, 82	Low–high	10	5

*Table continues next page*

<sup>a</sup> Q-ICP–MS: cool plasma elements (Al, Ca, Fe, Li, Mg, K, Na).

<sup>b</sup> Q-ICP–MS: potential interference sources. Acid matrix: As, Co, Cr, V. Sample matrix: Cr, Cu, Ni, Sc, Ti, Zn. Argon: Se.

<sup>c</sup> Lanthanides: typically below DL in standard ambient PM sample by Q-ICP–MS.

<sup>d</sup> Platinum group: typically below DL in standard ambient PM sample by Q-ICP–MS.

<sup>e</sup> Q-ICP–MS: extremely problematic elements (P, S, Si).

**Table 2 (Continued).** Comparison of Characteristic DLs for HR-ICP-MS and Q-ICP-MS

Element	Preferred Isotopes	Mass Resolution	Characteristic DL (ng/L)	
			Q-ICP-MS (Hot, Cool)	HR-ICP-MS
Silicon <sup>e</sup>	29, 28	High	Problematic	50
Silver	109	Low	0.5	0.1
Sodium <sup>a</sup>	23	High	1000, 20	5
Strontium	88	Medium	5	0.1
Sulfur <sup>e</sup>	32	Medium-high	Problematic	10
Thallium	205	Low	2	0.05
Thorium	232	Low	0.5	0.002
Tin	120, 118	Low-medium	10	0.5
Titanium <sup>b</sup>	48, 49	Medium	20	0.5
Tungsten	182, 184	Low-medium	2	0.02
Uranium	238	Low	0.5	0.002
Vanadium <sup>b</sup>	51	Medium	5	0.1
Ytterbium <sup>c</sup>	174	Low-high	0.5	0.01
Yttrium	89	Low	2	0.2
Zinc <sup>b</sup>	66, 68	Medium	10	2
Zirconium	90, 91	Medium	10	0.05

<sup>a</sup> Q-ICP-MS: cool plasma elements (Al, Ca, Fe, Li, Mg, K, Na).

<sup>b</sup> Q-ICP-MS: potential interference sources. Acid matrix: As, Co, Cr, V. Sample matrix: Cr, Cu, Ni, Sc, Ti, Zn. Argon: Se.

<sup>c</sup> Lanthanides: typically below DL in standard ambient PM sample by Q-ICP-MS.

<sup>d</sup> Platinum group: typically below DL in standard ambient PM sample by Q-ICP-MS.

<sup>e</sup> Q-ICP-MS: extremely problematic elements (P, S, Si).

**Table 3.** Air Concentrations of Selected Elements and Resulting Digest Solution Concentrations: Comparison of Analytic Methods

Concentration in Air (ng/m <sup>3</sup> )	PM Mass on Filter (ng)		Digest Concentration (µg/L)		Representative Elements
	20 m <sup>3</sup> Air	2 m <sup>3</sup> Air	20 m <sup>3</sup> Air	2 m <sup>3</sup> Air	
1000	20000	2000	1000 <sup>a</sup>	100 <sup>a</sup>	S, Ca
100	2000	200	100 <sup>a</sup>	10 <sup>a</sup>	N, Al, K, Fe, Si
10	200	20	10 <sup>a</sup>	1 <sup>b</sup>	Mg, Zn, Ba
1	20	2	1 <sup>b</sup>	0.1 <sup>b</sup>	Ti, Cr, Mn, Ni, Cu, Pb, Rb, Sr, Sn
0.1	2	0.2	0.1 <sup>b</sup>	0.01 <sup>b</sup>	V, Co, As, Se, Mo, Cd, Sb, Cs, Ce, W
0.01	0.2	0.02	0.01 <sup>b</sup>	0.001 <sup>c</sup>	Rh, Ag, Pd, Pt, Tl, U, Eu, La, Lu
0.001	0.02	0.002	0.001 <sup>c</sup>	0.0001 <sup>c</sup>	Th, Nd, Sm, Dy, Er, Yb

<sup>a</sup> Inductively coupled plasma optical emission spectroscopy range.

<sup>b</sup> Q-ICP-MS required.

<sup>c</sup> HR-ICP-MS required.

**Source Apportionment and Speciation of Low-Volume Particulate Matter Samples**

**Table 4.** Elements Routinely Quantifiable When Using Optimized Solubilization Methods and HR-ICP-MS

Element Group	Elements
Alkali metals	Li, Na, K, Rb, Cs
Alkaline earths	Be, Mg, Ca, Sr, Ba
Transition groups 3, 4	Sc, Y, Ti, Zr, Hf
Transition groups 5, 6	V, Cr, Mo, W
Transition groups 7, 8, 9, 10	Mn, Fe, Co, Ni
Platinum group	Rh, Pd, Pt
Transition groups 11, 12	Cu, Ag, Zn, Cd
Lanthanides	La, Ce, Nd, Sm, Eu, Tb, Dy, Ho, Er, Yb
Actinides	Th, U
Semimetals	Al, Ga, Sn, Sb, Tl, Pb
Nonmetals	Si, P, S, As, Se

Robust aerosol solubilization and digestion methods necessarily incorporate acids such as hydrochloric acid (HCl) and hydrofluoric acid; however, the use of these acids compounds the interference issue by creating additional polyatomic interferences. Table 5 shows many of the common plasma-gas- and matrix-sourced spectral interferences that affect and limit traditional Q-ICP-MS. As shown in the table, HR-ICP-MS is capable of mass-resolving nearly all of the spectral interferences on the elements of interest. By routinely analyzing these “problematic” elements under conditions where all known interferences are mass-resolved, one can be assured of unequivocal analyte quantification.

With the improvement in the method’s blanks, the capabilities of the HR-ICP-MS approach were better realized. Quantification at concentrations of < 100 pg/L was shown

**Table 5.** Elements Affected by Plasma-Gas (Cool-Plasma Effective), Digest Acid, or Sample Matrix Sourced Interferences

Analyte (Mass)	Abundance (%)	Interferences	Source	Resolution Required	Control Options <sup>a</sup>
<sup>27</sup> Al (26.9815)	100	<sup>12</sup> C <sup>15</sup> N, <sup>12</sup> C <sup>14</sup> NH	Plasma	1500, 920	CP, CCT, HR
<sup>44</sup> Ca (43.9555)	2.13	<sup>12</sup> C <sup>16</sup> O <sup>16</sup> O, <sup>14</sup> N <sup>14</sup> N <sup>16</sup> O	Plasma	1300, 970	CP, CCT, HR
<sup>54</sup> Fe (53.9396)	5.80	<sup>40</sup> Ar <sup>14</sup> N, <sup>54</sup> Cr	Plasma, sample	2100	CP, CCT, IE, HR
<sup>56</sup> Fe (55.9349)	91.7	<sup>40</sup> Ar <sup>16</sup> O, <sup>40</sup> Ca <sup>16</sup> O	Plasma, sample	2500, 2500	CP, CCT, HR
<sup>57</sup> Fe (56.9354)	2.20	<sup>40</sup> Ar <sup>16</sup> OH, <sup>40</sup> Ca <sup>16</sup> OH	Plasma, sample	1950	CP, CCT, HR
<sup>25</sup> Mg (24.9858)	10.1	<sup>12</sup> C <sup>12</sup> CH (25.0078)	Plasma	1200	CP, CCT, HR
<sup>39</sup> K (38.9637)	93.1	<sup>38</sup> ArH (38.9705)	Plasma	5700	CP, CCT, HR
<sup>78</sup> Se (77.9173)	23.6	<sup>38</sup> Ar <sup>40</sup> Ar (77.9251), <sup>78</sup> Kr	Plasma	9990	CCT, HR
<sup>80</sup> Se (79.9165)	49.9	<sup>40</sup> Ar <sup>40</sup> Ar (79.9248), <sup>80</sup> Kr	Plasma	9700	CCT, HR
<sup>82</sup> Se (81.9167)	8.84	<sup>40</sup> Ar <sup>40</sup> ArHH, <sup>82</sup> Kr	Plasma	3500	CCT, HR
<sup>28</sup> Si (27.9769)	92.2	<sup>14</sup> N <sup>14</sup> N, <sup>12</sup> C <sup>16</sup> O	Plasma	960, 1600	CCT, HR
<sup>29</sup> Si (28.9765)	4.71	<sup>14</sup> N <sup>14</sup> NH, <sup>12</sup> C <sup>16</sup> OH	Plasma	780, 1100	CCT, HR
<sup>31</sup> P (30.9738)	100	<sup>16</sup> O <sup>14</sup> NH	Plasma	970	CCT, HR
<sup>32</sup> S (31.9721)	95.0	<sup>16</sup> O <sup>16</sup> O, <sup>14</sup> N <sup>18</sup> O	Plasma	1800, 1060	CCT, HR
<sup>34</sup> S (33.9679)	4.22	<sup>16</sup> O <sup>18</sup> O	Plasma	1300	CCT, HR
<sup>48</sup> Ti (47.9479)	73.5	<sup>36</sup> Ar <sup>12</sup> C, <sup>32</sup> S <sup>16</sup> O, <sup>48</sup> Ca	Plasma, sample	2500, 2500	CCT, HR, IE
<sup>49</sup> Ti (48.9479)	5.51	<sup>35</sup> Cl <sup>14</sup> N, <sup>37</sup> Cl <sup>12</sup> C, <sup>32</sup> S <sup>16</sup> OH	Acid, sample	2100, 2700	CCT, MCN, HR
<sup>51</sup> V (50.9440)	99.8	<sup>35</sup> Cl <sup>16</sup> O, <sup>37</sup> Cl <sup>14</sup> N	Acid	2600, 2100	CCT, MCN, HR
<sup>52</sup> Cr (51.9405)	83.8	<sup>40</sup> Ar <sup>12</sup> C, <sup>36</sup> Ar <sup>16</sup> O, <sup>35</sup> Cl <sup>16</sup> OH	Plasma, acid	2400, 2400	CCT, MCN, HR
<sup>53</sup> Cr (52.9407)	9.55	<sup>36</sup> Ar <sup>16</sup> OH, <sup>37</sup> Cl <sup>16</sup> O,	Plasma, acid	1800, 2600	CCT, MCN, HR
<sup>59</sup> Co (58.9332)	100	<sup>40</sup> Ar <sup>19</sup> F, <sup>24</sup> Mg <sup>35</sup> Cl, <sup>36</sup> Ar <sup>23</sup> Na	Acid, sample	2100, 2900	CCT, MCN, HR
<sup>60</sup> Ni (59.9308)	26.2	<sup>44</sup> Ca <sup>16</sup> O, <sup>23</sup> Na <sup>37</sup> Cl, <sup>25</sup> Mg <sup>35</sup> Cl	Acid, sample	3100, 2500	CCT, MCN, HR
<sup>63</sup> Cu (62.9296)	69.2	<sup>40</sup> Ar <sup>23</sup> Na, <sup>40</sup> Ca <sup>23</sup> Na	Sample	2800, 2800	CCT, MCN, HR
<sup>65</sup> Cu (64.9278)	30.8	<sup>40</sup> Ar <sup>25</sup> Mg	Sample	3200	CCT, MCN, HR
<sup>66</sup> Zn (65.9260)	27.8	<sup>32</sup> S <sup>34</sup> S (65.9400)	Sample	4700	CCT, MCN, HR
<sup>68</sup> Zn (67.9248)	18.6	<sup>40</sup> Ar <sup>14</sup> N <sup>14</sup> N, <sup>36</sup> Ar <sup>32</sup> S	Plasma, sample	1550, 4600	CCT, MCN, HR
<sup>75</sup> As (74.9216)	100	<sup>40</sup> Ar <sup>35</sup> Cl (74.9312)	Acid, sample	7800	CCT, MCN, HR, IE
<sup>111</sup> Cd (110.9042)	12.9	<sup>95</sup> Mo <sup>16</sup> O (110.9007)	Sample	32000	CCT, MCN, IE
<sup>114</sup> Cd (113.9034)	28.8	<sup>98</sup> Mo <sup>16</sup> O (113.9003), <sup>114</sup> Sn	Sample	37000	CCT, MCN, IE

<sup>a</sup> CP indicates cool plasma; CCT indicates collision/reaction cell; HR indicates high resolution; IE indicates interference equation; MCN indicates microconcentric desolvating nebulizer.

to be practical; this equates to ~15 ppb analyte in 100 µg filter-collected aerosol.

### Summary

Order-of-magnitude improvements in method DLs were demonstrated for a large set of elements (see Figure 4). For cesium (Cs), iridium (Ir), Rh, and Tl, improvements of nearly three orders of magnitude over previous ICP-MS methods were observed when using the new microvolume digestion HR-ICP-MS methods. For Pt, rubidium (Rb), Be, copper (Cu), Cd, ruthenium (Ru), Sb, Y, holmium (Ho), La, barium (Ba), and Cs, improvements of one to two orders of magnitude were observed.

By ratioing the elemental masses measured in, say, 100 µg PM with their respective method blank uncertainties, the general detectability of elements in samples of this

type can be estimated. The results of such an exercise are shown in Figure 5. At a signal-to-noise ratio of three or greater, more than 30 elements would be quantifiable.

The sealed-vial method that was developed opens up the additional option of routine measurements of Si in low-volume PM collections.

These new tools will enable advanced characterization of PM from low-volume personal exposure samplers and thereby provide heretofore unobtainable data for improved assessments of human exposures and source contributions to elemental components of atmospheric PM.

Details on the digestion and instrumental analysis of atmospheric PM samples using our microwave-assisted digestions and HR-ICP-MS methods are presented in Appendices C and D (available from HEI on the Web at [www.healtheffects.org](http://www.healtheffects.org) or by request).

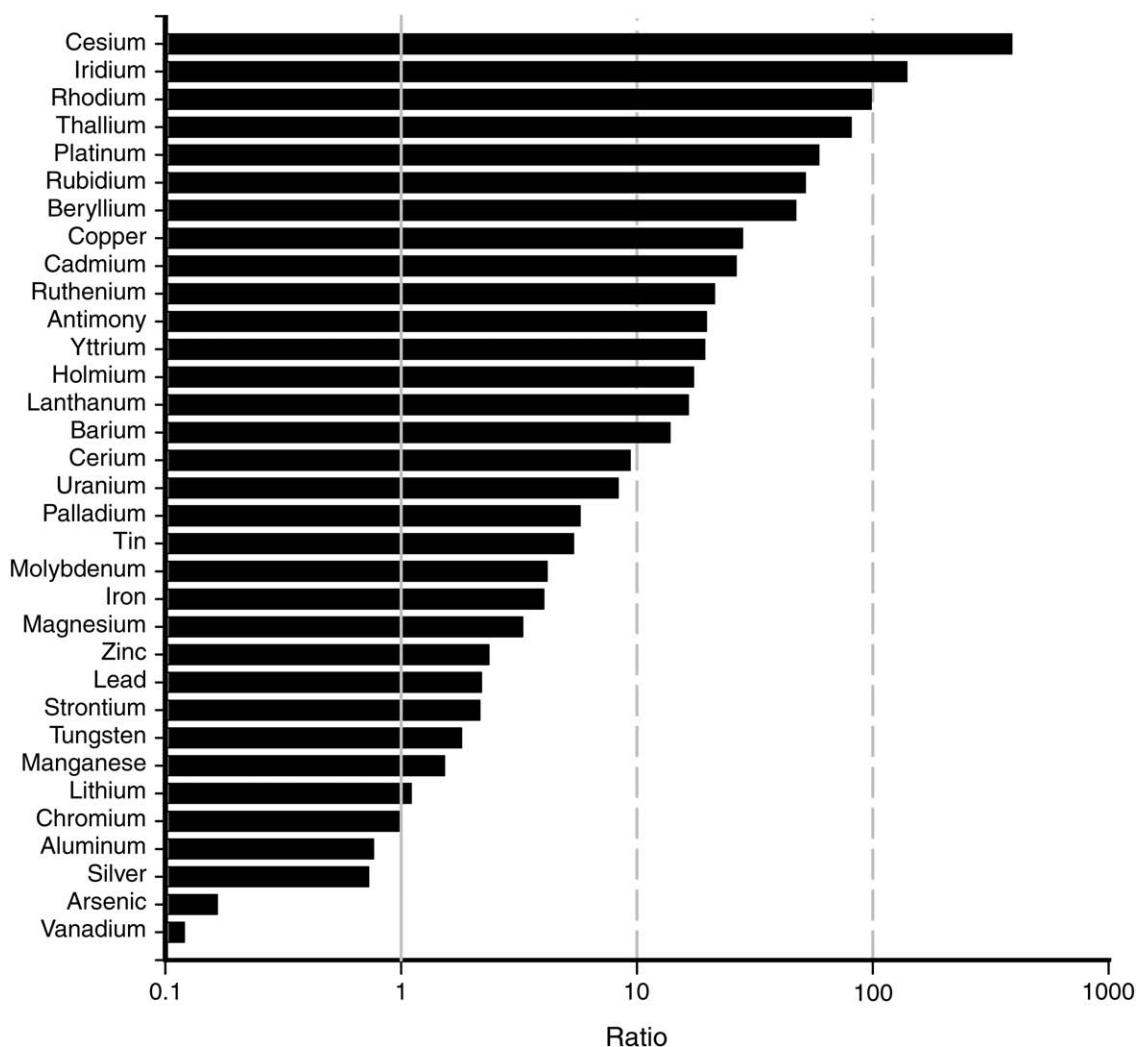


Figure 4. Comparison of method DLs in 33 elements for new open-vessel HR-ICP-MS method and old ICP-MS method. Ratios of new to old DLs are shown.

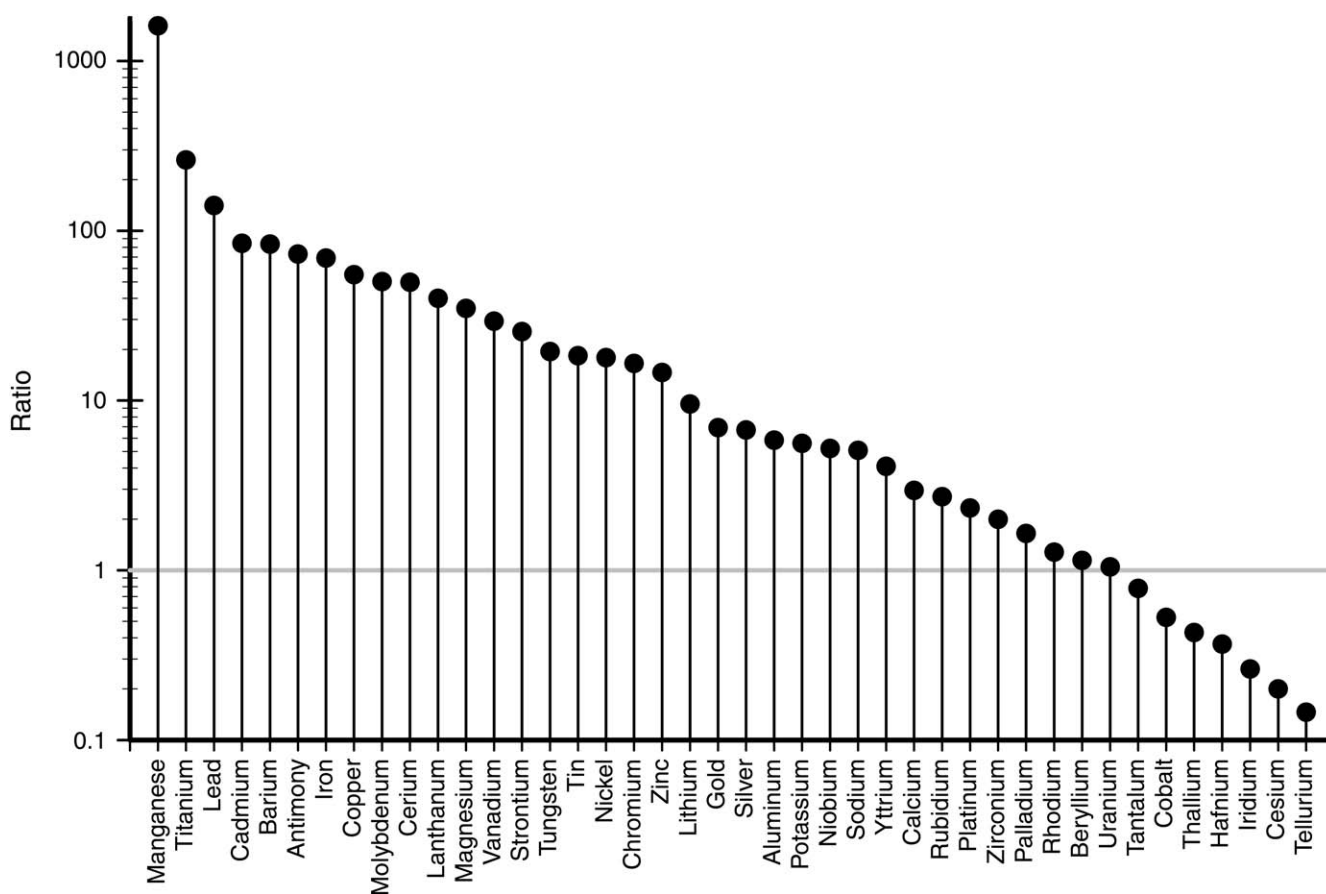


Figure 5. Signal-to-noise ratio — i.e., the ratio of the median elemental mass (ng) from personal exposure sampler filters to the analytic method's blank uncertainties (1-sigma) — for 42 elements.

## THERMAL DESORPTION GC-MS METHOD

### Goals

A TD-GC-MS analytic method was developed in order to address specific concerns related to traditional GC-MS methods for the speciation of organic compounds. The goals of developing this alternative GC-MS method were (1) to significantly reduce the organic carbon (OC) loading necessary for analysis and (2) to minimize sample handling and preparation. Traditional techniques extract the filter with an organic solvent and then analyze a small fraction of it (typically 1% to 5% of the extract). Our TD-GC-MS method bypasses the extraction step by directly analyzing the filter portion, which reduces the required OC loading and eliminates the extra sample handling and time involved in the extraction procedure. The TD-GC-MS method is thus ideal for filters that operate with low flow rates and have low OC loadings (as low as 15  $\mu\text{g}$  OC), such as personal exposure samples. Because the method is only quantitative for nonpolar compounds (polycyclic aromatic hydrocarbons [PAHs], alkanes, and hopanes), it is ideal for projects that focus on motor vehicle exhaust emissions.

### Instrumentation

The TD-GC-MS method developed here builds on existing GC-MS methods for the analysis of organic compounds in atmospheric PM samples. It focuses on the modification of the methods used to introduce the sample to the system and uses the same GC-MS conditions and quantification procedures as commonly used solvent extraction GC-MS. The method uses a Markes International Thermal Desorption Unit (Model M-10140, Foster City, CA) coupled with a 5973 GC-MS (Agilent Technologies, Wilmington, DE) for sample analysis. The system is optimized for loadings ranging from 15 to 40  $\mu\text{g}$  OC. The loading on a filter determines the size of the filter fraction used for the analysis; a single punch from a filter (1–1.45  $\text{cm}^2$ ) or an entire filter (25–37 mm) can be used. The filter sample is first spiked with isotopically labeled internal standard at the same mass present in the quantification standards. The internal standard contains several PAHs, 1 sterane, and several *n*-alkanes that are used as surrogates for compounds of similar structure and molecular weight. The solvent is allowed to evaporate before the filter is inserted into a glass desorption tube and placed in the autosampler. Figure 6 shows a

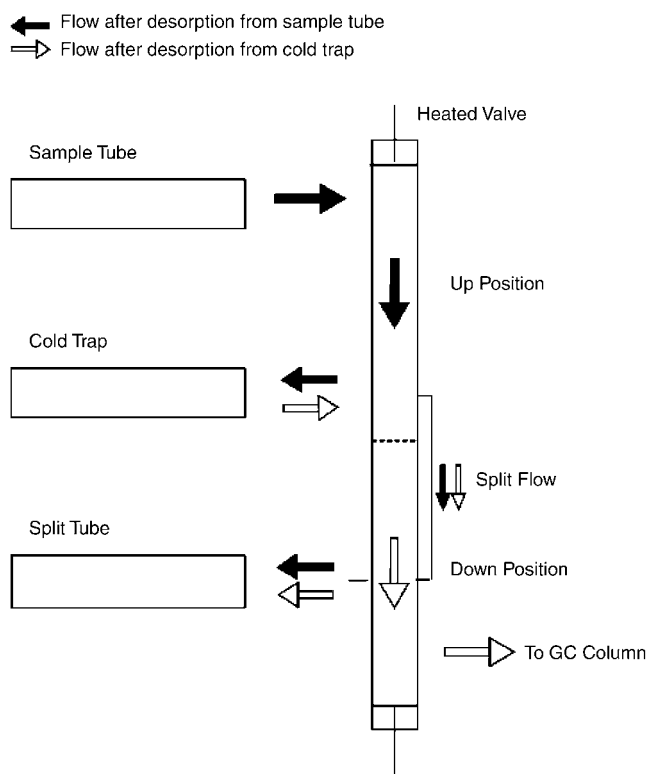


Figure 6. Schematic of the thermal desorption unit used for TD-GC-MS analysis.

schematic of the desorption process. The sample is collected on the cold trap (the flow is shown by the solid black arrows in the figure) during the sample-tube desorption step. It is then transferred into the gas chromatography column (the flow is shown by the white arrows in the figure). In the first step, the sample tube is ramped to 360°C over 20 minutes to desorb the compounds of interest from the filter. In the second step, a glass-bead trap (0°C) is used to focus the sample before the temperature is ramped to 360°C again and desorbed onto the gas chromatography column. This two-step process concentrates the analytes desorbed from the filter into a smaller volume of vapor, which improves detection in GC-MS.

The GC-MS parameters are similar to those previously published for solvent extraction GC-MS (Sheesley et al. 2000). A three-point calibration curve is run at the start of each sample set. The quantification standard includes 17 PAHs, 12 alkanes, and 7 hopanes and steranes that are used to quantify the corresponding compounds in the filter samples as well as compounds of similar structure and molecular weight. The quantification standards are spiked onto a blank filter punch, and the solvent is allowed to evaporate before analysis; this is done to parallel the PM samples more closely. After every five samples, the middle

calibration standard is rerun and quantified to verify the continued accuracy of the calibration curve; this is referred to as the check standard. A duplicate filter sample or matrix spike (a quantification standard spiked directly onto a sample filter) is alternated every 10 samples to assess reproducibility and matrix effects.

### Method Validation Samples

Medium-volume samples were used for method validation. (Data from low-volume personal exposure samples will be discussed in detail in the Results section.) Although the method validation samples were medium-volume ambient samples, only a small fraction of the filter was used for analysis; a 1.45-cm<sup>2</sup> punch of the filter was used, in this instance. In this way, the method validation was based on the analysis of samples similar in volume to personal exposure samples.

Fifteen samples collected at a U.S. Environmental Protection Agency (U.S. EPA)-funded Supersite in East St. Louis, Illinois, in July 2001 were analyzed by both solvent extraction GC-MS and TD-GC-MS. The solvent extraction results were previously published by Bae (2005). The filters were 90-mm quartz fiber filters sampled at 90 L/min for 24 hours, which led to OC loadings averaging 12 µg/cm<sup>2</sup>. The results were blank-subtracted using field blanks collected during the sampling period.

### Method Validation: Check Standards

A variety of quality-control measures were instituted to verify the reproducibility and overall robustness of the TD-GC-MS method for PM analysis. Quantification was derived from the quantification used for solvent extraction GC-MS (Sheesley et al. 2004). Examples of three-point calibration curves for four different compounds representing the various nonpolar-compound classes quantified by this method are shown in Figure 7. The use of surrogate internal standards enables stable calibration for the quantification. Establishing consistent calibration curves is the first step in method development. Maintaining a stable calibration through the course of the analysis of real-world samples is a critical requirement for a robust method, because the matrix of ambient PM samples can affect the calibration curves over time. Check standards were therefore included in the runs to determine when a calibration curve needed to be recalculated. The middle calibration standard was analyzed as a check standard every five samples to assess the stability of the calibration curve. The average recovery of these check standards, with the standard deviation as a measure of uncertainty, is shown in Figure 8. This illustrates that the calibration curve was stable over the course of the sample runs and that the internal standards were tracking the response of the target compounds well.

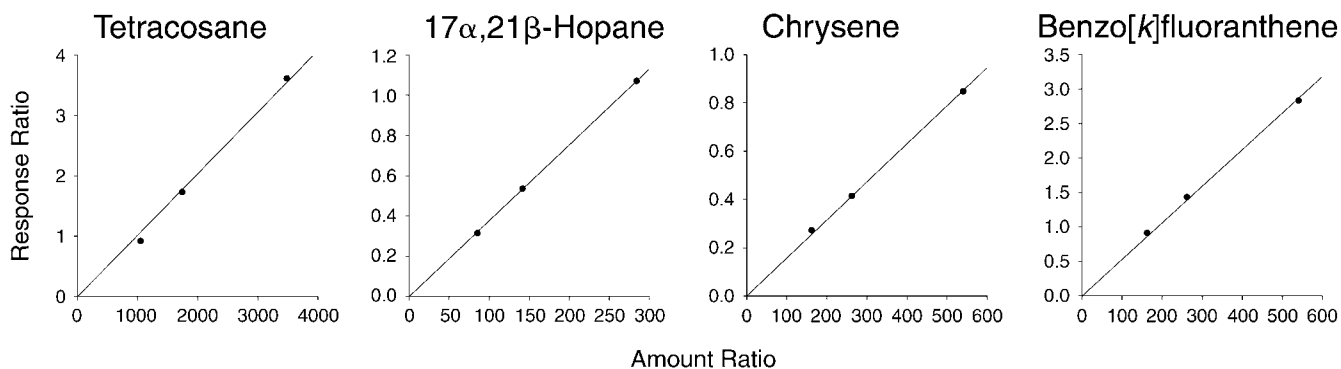


Figure 7. Calibration curves for TD-GC-MS generated by spiking surrogate internal standards onto blank filters. Note that some of the x- and y-axis scales differ from panel to panel.

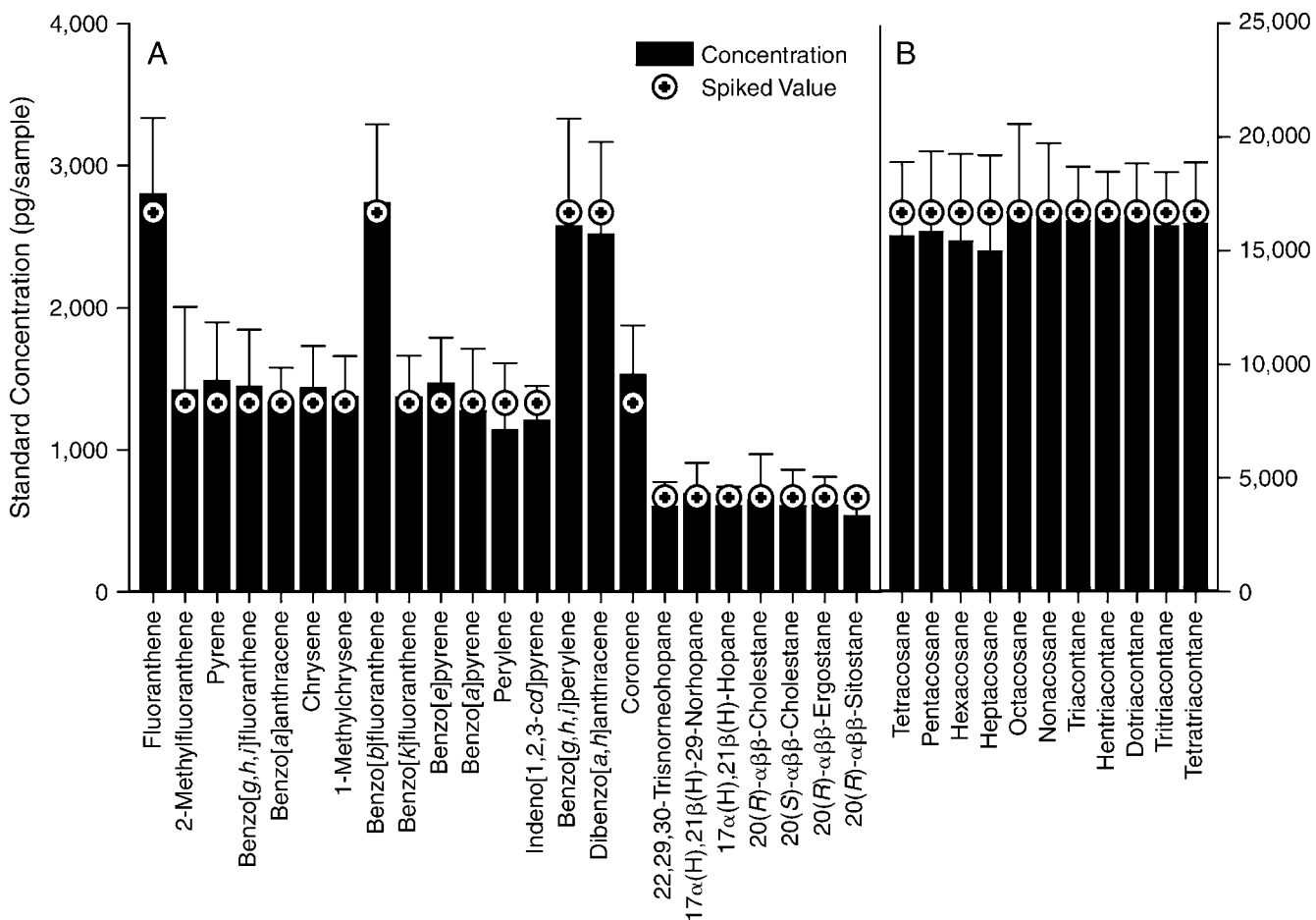


Figure 8. Average spike and associated standard deviation in 34 compounds for the TD-GC-MS method. Note that the scales (but not the units) differ on sides A and B of the y-axis.

### Method Validation: Duplicate Samples

Another advantage of the TD-GC-MS method for ambient PM analysis is that true duplicate analyses can be made more easily because of the method's low loading requirement and the nature of the sample preparation. Duplicate analyses can therefore be a routine aspect of TD-GC-MS, which is not possible with solvent extraction GC-MS. A compilation of six duplicate sample analyses is shown in Figure 9, tracking the reproducibility of the method. The correlation for all three classes of compounds was very good across the range of compound masses. This is particularly important because the nominal DL for these compounds is reduced to 50 pg per sample for PAHs, hopanes, and steranes; to 1 ng for alkanes; and to as low as 15 to 20 ng for other compounds. (For the specific set of personal exposure samples used in the project, duplicate analysis was not possible, because the analysis required use of the entire sample.) The results in Figure 9 represent

duplicate analysis of ambient samples collected at the East St. Louis Supersite using 1.45-cm<sup>2</sup> sample punches.

### Method Validation: Matrix Spikes

To assess the effect of the aerosol matrix on the recovery of target compounds, seven matrix spikes were performed over the course of the analysis of the East St. Louis Supersite ambient samples. Most of the compounds showed an average recovery of  $\pm 20\%$  (see Figure 10); the uncertainty of the recovery is the standard error. Matrix spikes are typically not demonstrated for organic speciation analysis because of the limited amount of sample available for analysis. Thanks to its smaller minimum sample requirements, the TD-GC-MS method can provide validation for organic speciation by GC-MS, which was previously not practical. From a quality-assurance perspective, the ability to perform matrix spikes is a crucial advantage over solvent extraction.

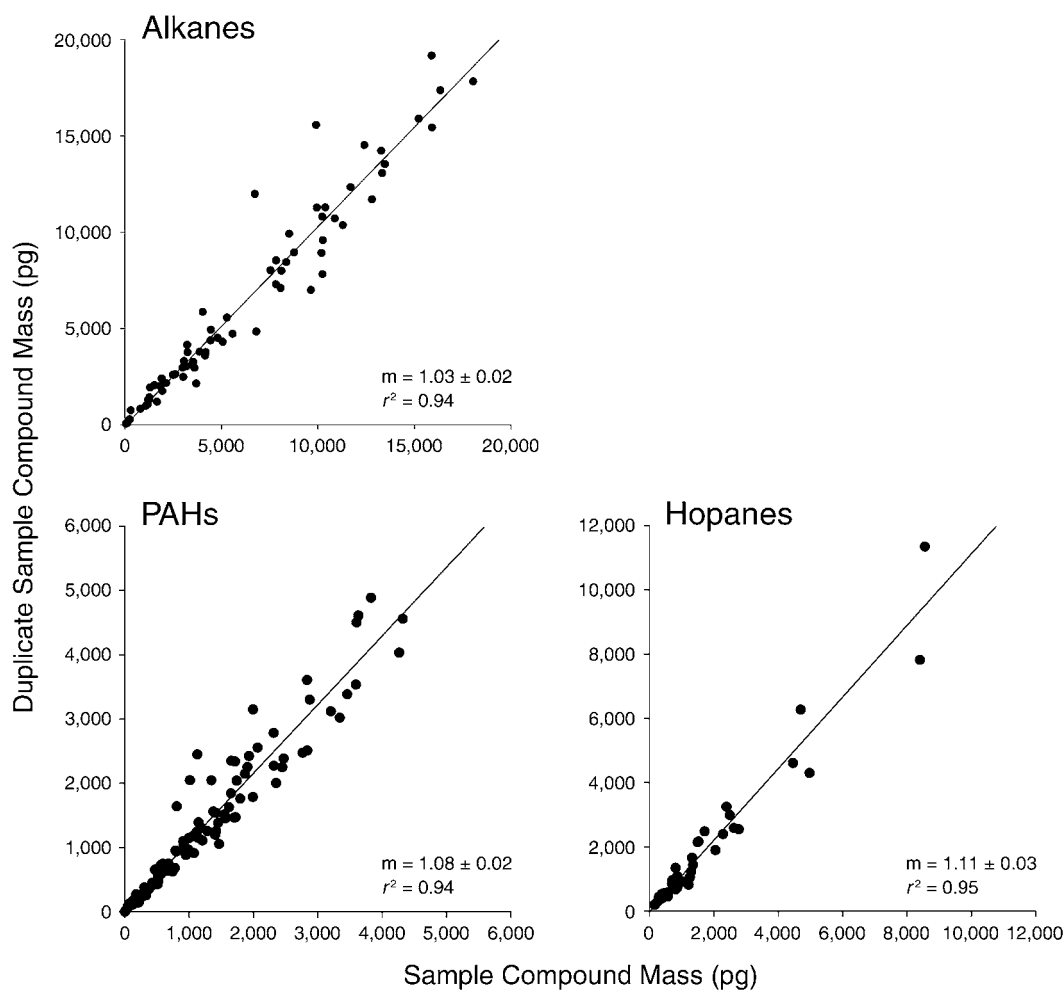


Figure 9. Duplicate analyses by TD-GC-MS of alkanes, PAHs (molecular weights 202 to 300), and hopanes in atmospheric PM samples collected in East St. Louis, demonstrating the reproducibility of the TD-GC-MS method. Note that the x- and y-axis scales differ from panel to panel.

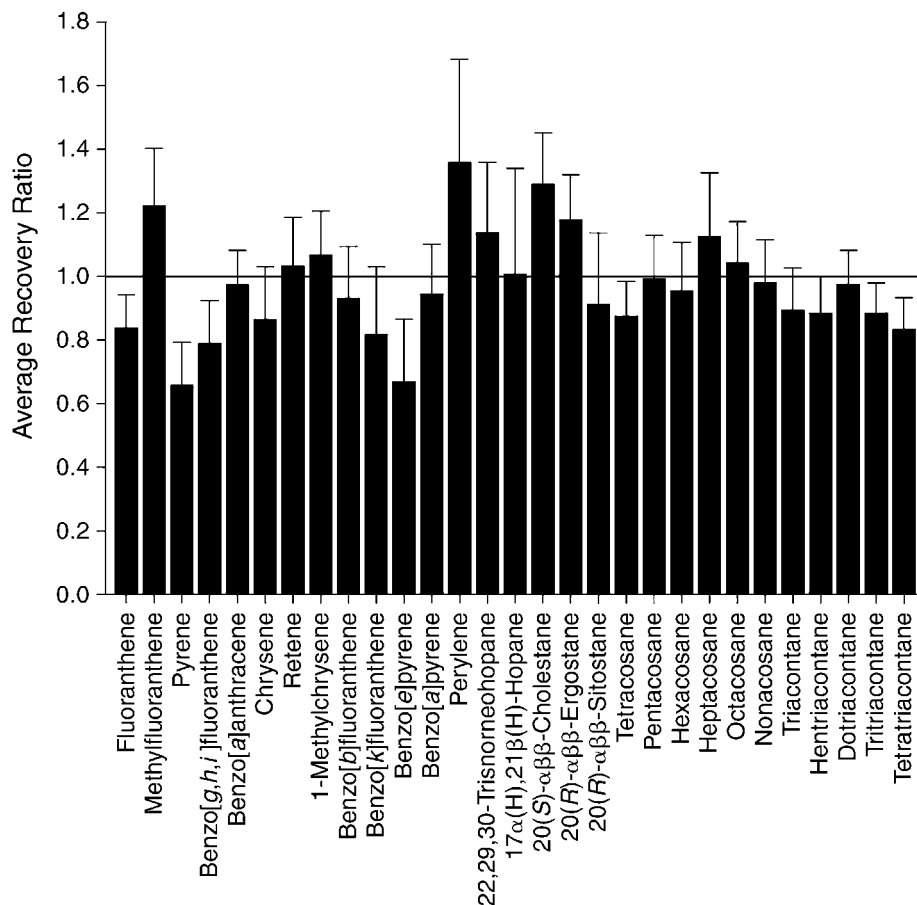


Figure 10. Average recovery and associated standard error for 29 standards spiked onto atmospheric PM samples collected in East St. Louis.

### Method Validation: Intercomparison Study

In order to demonstrate that our TD-GC-MS data were compatible with solvent extraction GC-MS data, an intercomparison study was undertaken. A set of 28 ambient samples collected at the East St. Louis Supersite that had previously been analyzed by solvent extraction GC-MS were run using the TD-GC-MS method (see Figure 11). The samples showed a wide range of compound concentrations (50 pg to 20 ng per sample). Although solvent extraction GC-MS is the standard method for analyzing the organic speciation of PM, it is difficult to assess the accuracy of its results. Our validation efforts for the TD-GC-MS data illustrated the good levels of precision and accuracy of the method, and the intercomparison study showed reasonable compatibility between the two methods, with slopes of 0.93 for PAHs, 1.26 for alkanes, and 0.90 for hopanes and steranes. There was some scatter in the results, which can be expected when two different methods are being compared. The solvent extraction GC-MS alkanes were biased high; the reason for this was unclear.

In the end, the data compatibility between the two methods depends on the level of accuracy that is required. Small, incremental differences will be lost in the scatter if both methods are used. However, the two methods are sufficiently compatible for source apportionment, which is the primary use of the methods' results.

### Thermal Desorption GC-MS Uncertainty Analysis

The increasing use of organic tracers in statistical models demands more accurate estimates of the analytic uncertainty associated with the GC-MS method. The TD-GC-MS protocol includes check standards run every five samples. In large projects such as this one, where there were more than 100 samples, this provides more than 20 check standards with which to calculate the uncertainty. The standard deviation of the recovery of the check standards run in a Harvard study (led by principal investigator Eric Garshick) of samples from a St. Louis truck terminal provided a good approximation of the uncertainty of the analysis by compound (Davis et al. 2009). By calculating

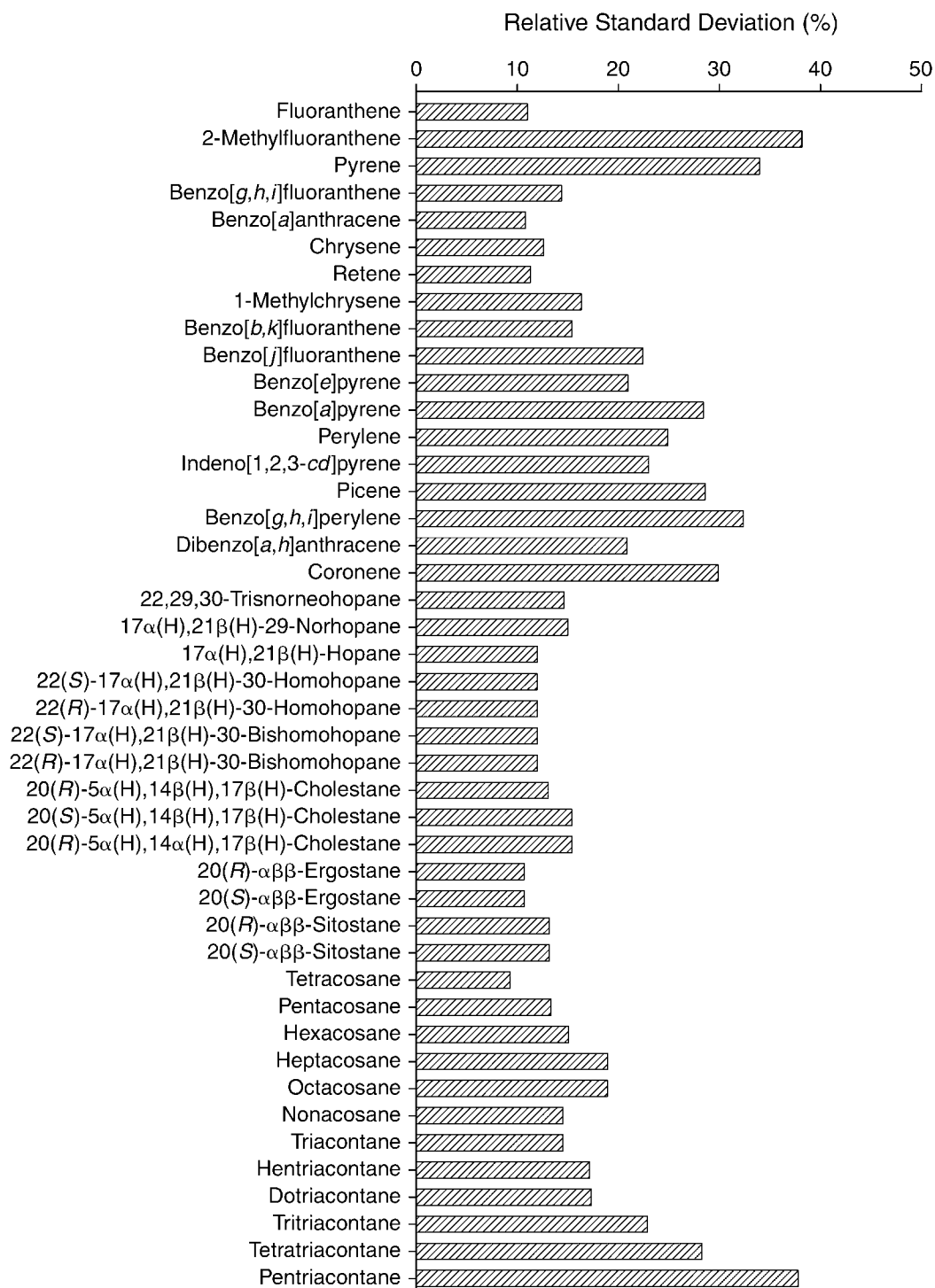


Figure 11. Relative uncertainty of the TD-GC-MS method for replicate analysis of filter spike recoveries for 44 compounds.

uncertainty in this manner, batch conditions specific to the study were taken into account. Figure 11 shows the relative uncertainty by compound. Compounds not included in the standard used the relative standard deviation of a surrogate compound.

### PROGRAMMABLE TEMPERATURE VAPORIZATION GC-MS METHOD

#### Goals

The programmable temperature vaporization GC-MS (PTV-GC-MS) method is designed for the solvent extraction and organic speciation of low-concentration atmospheric samples. In traditional low-volume injection GC-MS, samples have to be composited to achieve high enough concentrations (400  $\mu\text{g}$  OC per 100  $\mu\text{L}$  sample). PTV-GC-MS limits the need for compositing and thus allows higher time resolution. Levoglucosan (a tracer for biomass-burning sources) and nonpolar compounds such as hopanes and PAHs can be done well by PTV-GC-MS, making it a good option for source apportionment projects that collect low-loading atmospheric samples.

#### Method

The PTV-GC-MS method is performed using a commercially available GC-MS with a high-volume injector operated as specified by the manufacturer. Extraction can be done either on a mini-scale with low levels of extraction solvent (5 mL) or in a Soxhlet extractor with high levels of solvent (300 mL). The extracts are evaporated to approximately 100  $\mu\text{L}$ , but it is the injection volume and method that vary the most from those of traditional solvent extraction (Schauer et al. 1996; Sheesley et al. 2000). In PTV-GC-MS (6890 GC with HP PTV inlet and 5973 MSD, Agilent Technologies), the injection volume is at least 10 times higher, at 30  $\mu\text{L}$ , than in traditional low-volume injection GC-MS, which uses injection volumes of 1 to 3  $\mu\text{L}$ . Because of the higher volume, the solvent is vented first, and the analyte transfer to the column is slower than in low-volume splitless injection.

#### Nonpolar Intercomparison

A limited intercomparison study was conducted to compare the PTV-GC-MS method with both the traditional low-volume injection GC-MS and the TD-GC-MS methods. The samples used for the intercomparison were from the same sampling project used for the earlier TD-GC-MS intercomparison. Figure 12 shows the results for 10 samples from the East St. Louis Supersite, collected in July 2001. For this intercomparison a limited number of compounds—PAHs, alkanes, hopanes, and steranes (the same compounds

as in the nonpolar TD-GC-MS method)—were quantified. Figure 13 compares the same PTV-GC-MS data with the TD-GC-MS data. The agreement among all three methods was quite good, with an  $r^2$  of 0.82 for the low-volume comparison and an  $r^2$  of 0.78 for the TD-GC-MS comparison. The slopes indicated that the results for the PTV-GC-MS method were biased approximately 20% high compared with those of the other two methods ( $28 \pm 2\%$  compared with low-volume injection GC-MS and  $12 \pm 2\%$  compared with TD-GC-MS), but PTV-GC-MS should still be considered a good alternative to low-volume injection GC-MS for low-concentration samples.

#### Polar Method

The PTV-GC-MS method was expanded to include derivatization (methylation and silylation) prior to analysis to quantify acids and other polar species. The entire sample was methylated and run by GC-MS. Then an aliquot was silylated and run using low-volume injection GC-MS. Calibration curves looked good for most acids, with correlation coefficients above 0.97. The difficulty with the high-volume injection systems for the methylation-and-acid analysis was twofold: higher blank contamination and poorer recovery of volatile species compared with low-volume injection. Aliphatic diacids do not currently have good recovery by the PTV-GC-MS method for diacids with less than 8 carbons, and ubiquitous species such as palmitic and stearic acid have high blank values.

The silylation technique, which used low-volume injection of the PTV extract, was successful for measurement of levoglucosan and cholesterol in ambient samples. A small intercomparison of the silylation technique using PTV samples and samples extracted for low-volume injection GC-MS showed excellent agreement (see Figure 14).

Our conclusions about PTV-GC-MS are that the method appears to be viable but that additional work is needed to better characterize its reproducibility and accuracy. Future work needs to be directed toward stable, accurate analysis of the large batches of samples typically needed for health studies.

### WET-CHEMICAL EXTRACTIONS FOR METAL SPECIATION STUDIES

#### Background

Studies have clearly shown that, because the chemical reactivity and solubility of an element are often controlled by its oxidation state and immediate bonding environment, the potential health effects of transition metals are likewise dependent on their oxidation state. In the present study, we focused on the development of wet-chemical

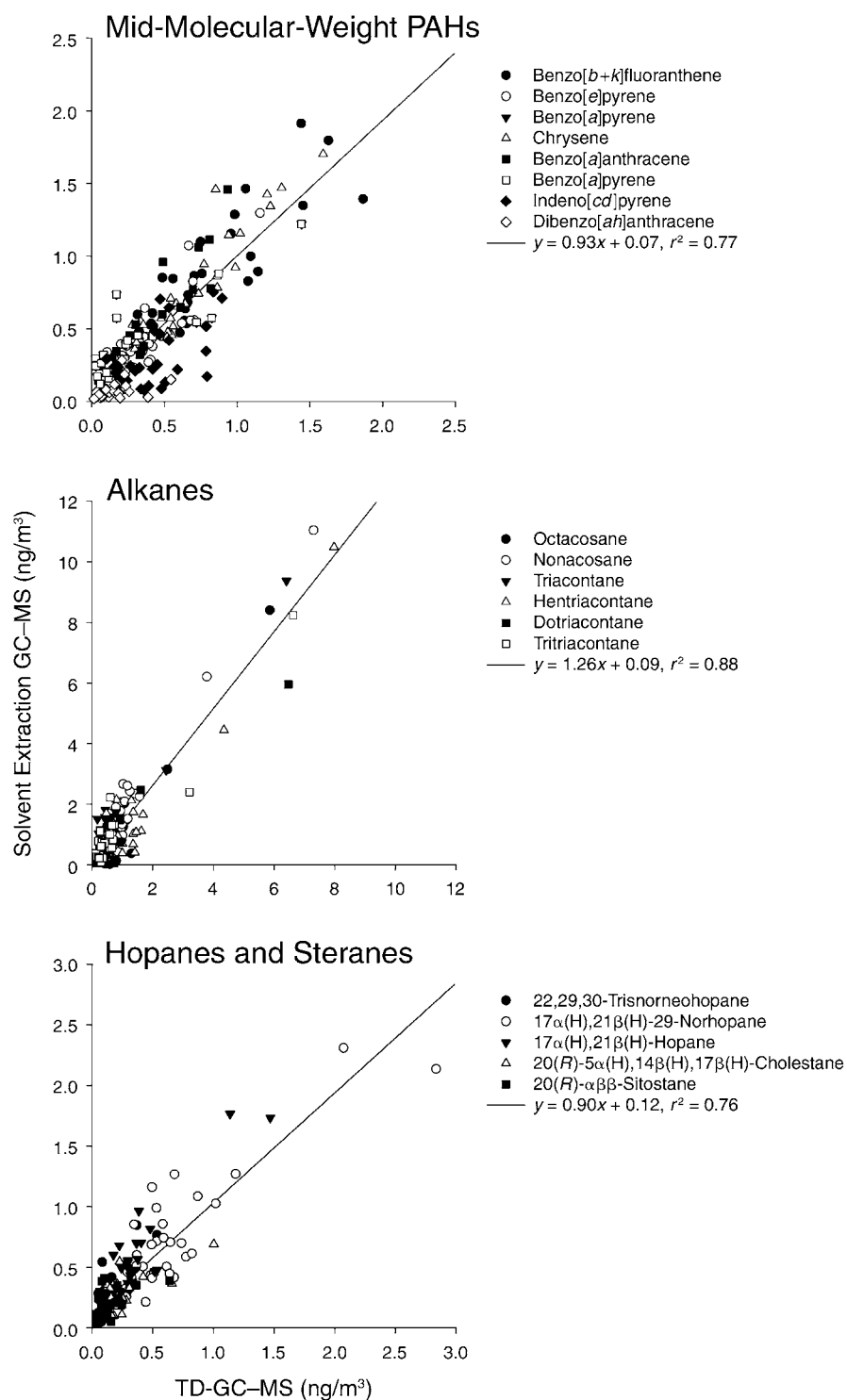


Figure 12. Intercomparison of TD-GC-MS and solvent extraction GC-MS results for three compound classes from atmospheric PM samples collected in East St. Louis.

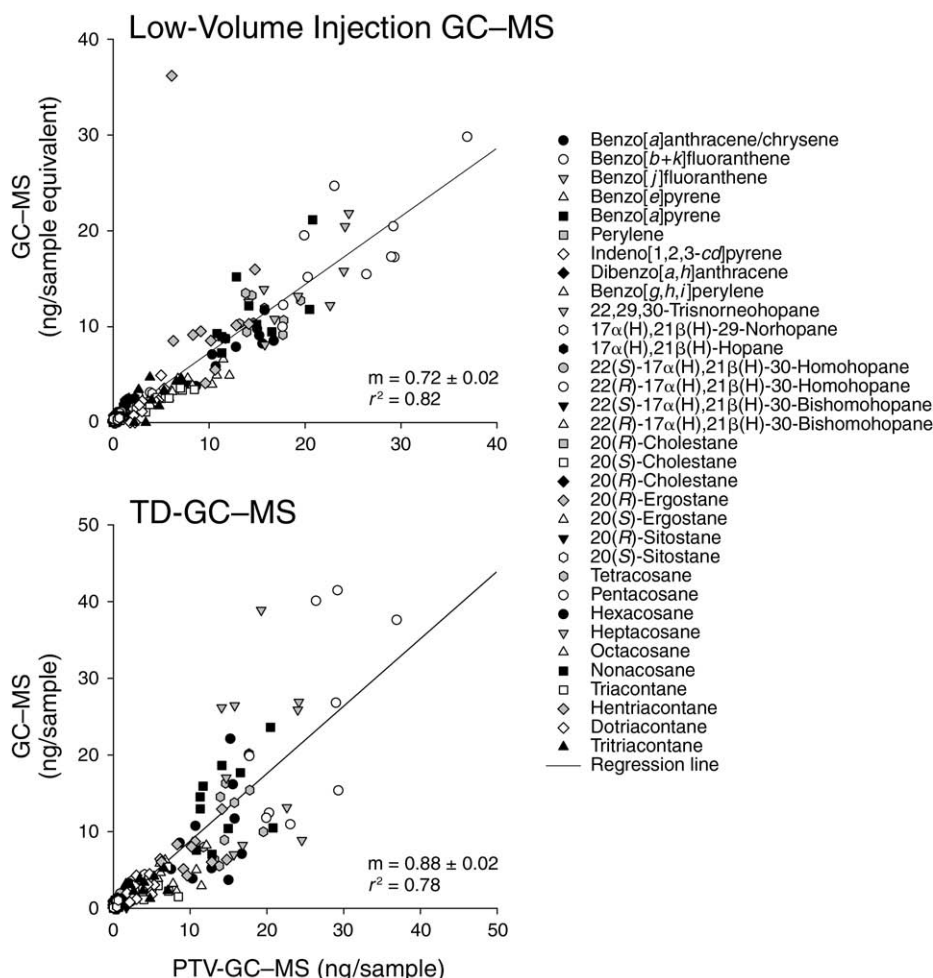


Figure 13. Intercomparison of results for PTV-GC-MS and (top panel) low-volume injection GC-MS and (bottom panel) TD-GC-MS for 33 nonpolar organic compounds from atmospheric PM samples collected in East St. Louis. Note that the x- and y-axis scales differ slightly from panel to panel.

speciation methods for Fe (as Fe[II] and Fe[III]), Cr (as Cr[VI]), and Mn (as total soluble Mn and soluble oxidized Mn). The goal was to develop methods that are sufficiently sensitive and specific and to utilize them to quantify metal species in personal exposure samples using techniques that most adequately equipped laboratories could perform. Because spectrophotometric techniques are generally inexpensive and easy to perform, our methods employed spectrophotometry as adapted to liquid waveguide spectrophotometry. We utilized a sample cell with a 1-m path length that provided almost 100 times more signal (there was some light loss through the cell) than a standard 1-cm path length. The cell was combined with an ultralow-noise photodiode array detector and fiber-optic cables (to minimize light loss), resulting in scan times of < 1 second and DLs that were generally lower than those of ICP atomic emission spectroscopy and approaching those of HR-ICP-MS for a very small fraction of the cost.

## Methods

All extractions were performed in acid-cleaned polypropylene vials by immersing an exposed Teflon substrate into a maximum of 10 mL of one of four extractants:

1. pH = 7.4 sodium bicarbonate ( $\text{NaHCO}_3$ ) solution
2. Sodium chloride ( $\text{NaCl}$ ) solution
3. pH = 4.3 acetate buffer
4. Milli-Q (MQ) water ( $> 18.0 \text{ m}\Omega/\text{cm}^2$ )

The compositions of the leachates are shown in Table 6. The  $\text{NaHCO}_3$  solution was chosen because carbonate systems at this pH are physiologically relevant (Sun et al. 2001). The  $\text{NaCl}$  solution was chosen to match the ionic strength of the  $\text{NaHCO}_3$  buffer but with a minimal buffering capacity. The acetate buffer was chosen because it is a lower-pH buffer with environmental applications (i.e., it is a good approximation of fog and rain water, and similar

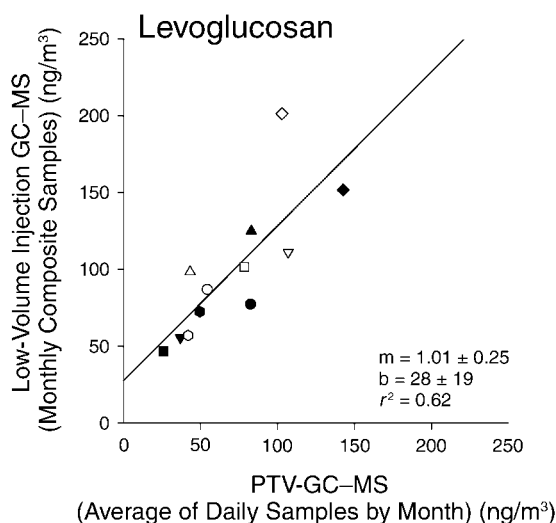


**Figure 14.** Intercomparison of monthly average levoglucosan concentrations measured in daily samples by PTV-GC-MS and in monthly composite samples by low-volume injection GC-MS.

extractants have been used to define labile metal pools in other studies [Siefert et al. 1998a]. Finally, the MQ water was chosen as a clean, simple, standard solution to be compared with the other leaches.

Tests to determine the kinetic release of Fe and Mn into solution from ambient PM samples were conducted. During the leaching period, small aliquots (2 mL) were removed from the leaching solution at intervals of approximately 20 to 30 minutes. The aliquots were then analyzed for soluble Fe and Mn using the wet-chemical speciation methods described below. In these tests, no Fe or Mn was detected in the leach solutions after 100 and 120 minutes, respectively. For all samples reported here, the filters were leached under laboratory conditions (20–22°C and diffuse light) while being slowly rocked back and forth using a

rotisserie shaker for 2 hours, and the leachate was immediately filtered through a 0.2- $\mu\text{m}$ -pore acid-cleaned (1.2 N trace-metal-grade HCl) polypropylene filter (Whatman).

## IRON SPECIATION TECHNIQUES

### Soluble Iron Determination

The purpose of this portion of the project was to develop an inexpensive wet-chemical method capable of quantifying labile Fe(II) and Fe(III) at the concentrations typically present in personal exposure samples. From a human-health perspective, Fe oxidation states can be an important parameter in atmospheric PM in urban settings. It has been shown that Fe, especially as Fe(III), is able to produce reactive oxygen species effectively in human lungs, thus leading to tissue inflammation. In remote settings (e.g., when studying marine aerosols over the open ocean), the ability to measure Fe(II) and Fe(III) in atmospheric PM will provide better insights into the modes of redox transformations as the aerosols are transported through the atmosphere. Further, many aquatic organisms for which Fe is a limiting nutrient depend on Fe deposition from the atmosphere. Because various metal species have different physical and chemical properties, the availability of these nutrients to organisms is dependent on the metals' oxidation state.

Oxidation-state-resolved measurements of Fe can give indications of the redox chemistry occurring in an environment. Resolution of Fe(II) and Fe(III) in atmospheric PM has been successfully achieved using Mössbauer spectroscopy [Hoffmann et al. 1996], although large amounts of PM are required. Other redox-sensitive methods used for these measurements include voltammetric techniques, chemiluminescence, and the ferrozine method [Stookey 1970; King et al. 1991; Viollier et al. 2000; Bowie et al. 2002; Ensafi et al. 2004]. Spectrophotometric techniques (such as the ferrozine method) are powerful and sensitive tools for the characterization of Fe species in atmospheric PM when dissolved in solution [Johansen et al. 2000; Chen and Siefert 2003]. However, few studies have been performed that link the release of soluble Fe(II) and Fe(III) to the nature of the extractant, and no studies have determined whether storage time changes the Fe speciation of atmospheric PM. This section describes a wet-chemical method for determining the Fe speciation of atmospheric PM and presents data on soluble Fe(II) and Fe(III). The project was carried out in order to develop a wet-chemical method that was sensitive to the oxidation state of Fe and to use the method (1) to test the Fe(II) extraction efficiency of various aqueous leaching solutions for Fe, (2) to estimate the time for Fe(II) oxidation to occur in ambient PM samples while in storage, and (3) to apply the method to mobile sources.

**Table 6.** Composition of the Solutions Used as Leachates for Determination of Soluble Metals

Leachate	Composition	Concentration ( $\mu\text{M}$ )	pH
Sodium bicarbonate solution	$\text{NaHCO}_3$	140	7.4
Sodium chloride solution	$\text{NaCl}$	140	6.1
Acetate buffer	Glacial acetic acid, sodium acetate	500	4.3
MQ water	$> 18.0 \text{ M}\Omega/\text{cm}^2$	—	6.3

### Ambient Sampling for Validation of Iron Speciation Method

Atmospheric PM was collected from the East St. Louis Supersite. Working with samplers built specifically for the study, two URG inlets were used to collect atmospheric PM 10  $\mu\text{m}$  or smaller in aerodynamic diameter ( $\text{PM}_{10}$ ) at a total flow of 64 L/min per inlet. Downstream of each inlet, the flow was separated into five airstreams and passed through five URG aluminum filter holders, yielding 10 co-located filters and PM samples each sampling day. The samples were collected at a flow rate of 6.4 L/min for 24 hours on 47-mm acid-cleaned Teflon filters (Teflo, 2.0- $\mu\text{m}$  pore size, Pall Life Sciences). Sampling was carried out every other day for 7 days between March 13 and March 31, 2005. Airflows were calibrated in the laboratory and checked in the field before and after sampling.

### Soluble Iron Detection Method

After filtration, ferrozine solution (Stookey 1970) was added to each filtrate (final ferrozine concentration = 55  $\mu\text{M}$ ), and the resulting solution was analyzed immediately or stored in the dark at 4°C and analyzed within 24 hours. Several samples were selected at random to be analyzed immediately after the ferrozine addition as well as 24 hours after the addition. Delays in analysis of the solution of up to 24 hours after the ferrozine addition were demonstrated not to have an effect on the Fe signal when the solution had been stored in the dark at 4°C. For Fe(II) analysis, about 1.5 mL filtrate (including the ferrozine) was pumped using a peristaltic pump through a liquid waveguide fiberoptic cell with a 1-m path length (volume = 600  $\mu\text{L}$ ), where the absorbance spectrum from 400 to 700 nm was obtained (World Precision Instruments, Sarasota, FL). Prior to analysis, the cell was rinsed with a surfactant (triethanolamine), methanol, and then 2 N HCl. Between each sample, the spectrum of a ferrozine blank in the same matrix as the extractant was obtained. All spectrophotometric experiments were carried out with a Tidas I photodiode array detector using a D<sub>2</sub>H tungsten light source (World Precision Instruments). The absorption of the Fe(II)–ferrozine complex, and therefore of soluble Fe(II) ( $\text{Fe}[\text{II}]_{\text{sol}}$ ), was monitored at 562 nm and compared with a matrix-matched calibration curve. This instrumentation and method allowed for DLs of less than 0.100  $\mu\text{g}/\text{L}$  (or 1.7 nM)  $\text{Fe}[\text{II}]_{\text{sol}}$ . When sampling atmospheric PM for 24 hours at 6 L/min, this corresponds to a DL of less than 0.11 ng soluble Fe(II)/m<sup>3</sup> air, assuming 10 mL of extract.

### Fe(III) Determination

Using the remaining filtrate (approximately 6 mL), Fe(III) was reduced to Fe(II) by adding hydroxylamine hydrochloride (HA) solution (final concentration = 55  $\mu\text{M}$ ). After

about 5 minutes, total soluble iron ( $\text{Fe}[\text{II}]_{\text{sol,tot}}$ ) (as defined by the 0.2- $\mu\text{m}$  filter) was measured in the solution by the ferrozine method outlined above. Soluble Fe(III) ( $\text{Fe}[\text{III}]_{\text{sol}}$ ) could then be determined by subtraction:

$$\text{Fe}[\text{III}]_{\text{sol}} = \text{Fe}[\text{II}]_{\text{sol,tot}} - \text{Fe}[\text{II}]_{\text{sol}} \quad [1]$$

Calibration curves from 0.5 to 20  $\mu\text{g}/\text{L}$  extract of selected leachates are shown in Figure 15. For all curves,  $r^2$  values of > 0.99 were achieved, with slopes ranging from 0.045 absorbance units (AU)/ppb (for  $\text{NaHCO}_3$ ) to 0.052 AU/ppb (for acetate buffer + HA). For the calibration range shown here, the analytic uncertainty of this measurement (as  $\pm 1$  standard deviation from the mean,  $n = 3$ ) was less than 0.4%. Comparison of the acetate and acetate + HA calibration curves indicates that the addition of HA had very little effect on the calibration slope or intercept.

Seven co-located  $\text{PM}_{10}$  samples from the East St. Louis sampling site were extracted in an identical fashion using a pH = 4.3 acetate buffer. Fe(II) in each leachate was measured spectrophotometrically at least twice per sample using the ferrozine method. An average of  $19.6 \pm 1.4$  ng soluble Fe(II)/m<sup>3</sup> air was found, where the uncertainty was one standard deviation of all trials ( $n = 7$ ). This corresponded to a 7.1% relative standard deviation and reflected the overall precision of the technique (including sampling, extraction, and analysis uncertainty).

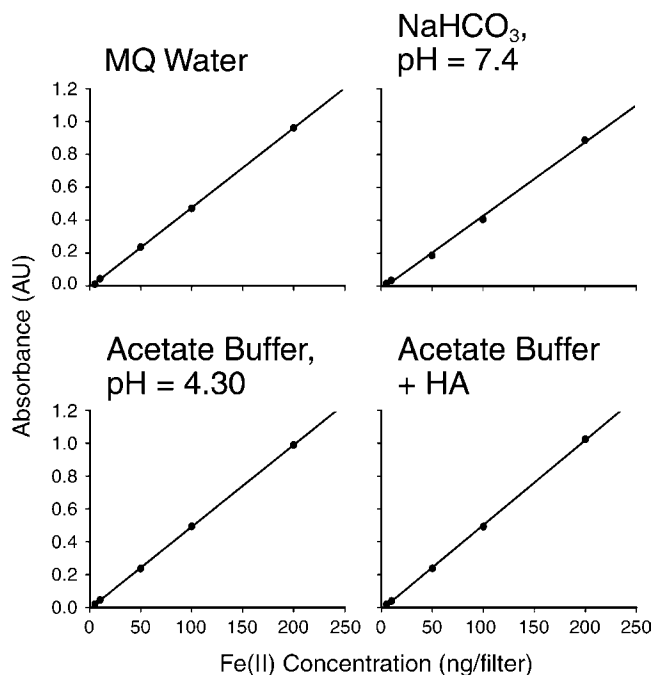
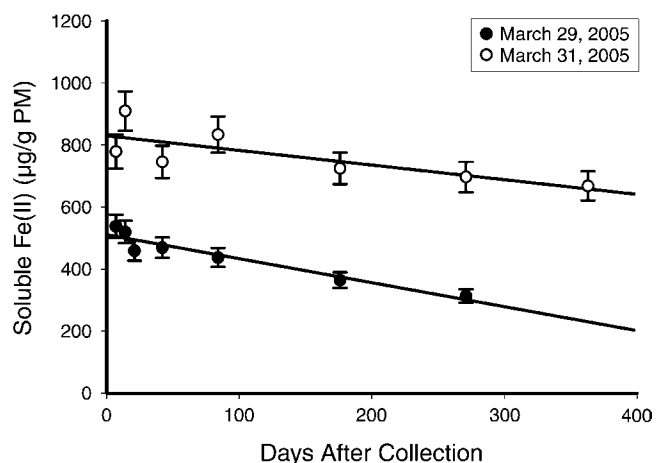


Figure 15. Fe(II) calibration curves in selected leachates. Calibration ranges are from 0.5 to 20  $\mu\text{g}$  Fe(II)/L.

Both the photoreduction of Fe(III) and the oxidation of Fe(II) can alter the redox speciation of Fe in atmospheric aerosols; however, the magnitude and relative importance of these processes are unclear. Real-time or very rapid analysis might be required, but considering that, in most field sampling campaigns it is not always practical or feasible to analyze particles in this manner, experiments were carried out to test how soluble Fe(II) in particles changes while stored in a dark freezer at  $-20^{\circ}\text{C}$ . Co-located samples collected at the East St. Louis Supersite on March 29 and March 31, 2005, were tested for soluble Fe(II) over the course of 12 months. At intervals of 1 week, 2 weeks, 3 weeks, 6 weeks, 3 months, 6 months, 9 months, and 12 months (March 31 sample only) from the sampling date, separate filters were processed for Fe(II) measurement using the pH = 4.3 acetate buffer. The results are shown in Figure 16. For the March 29 sample, an Fe(II) concentration of  $538\ \mu\text{g Fe(II)/g PM}$  was measured 1 week after sample collection. This corresponded to 4.6% of the total Fe in the PM (as measured by ICP-MS). The average decrease in soluble Fe(II) was found to be  $0.77\ \text{ng per day}$  for the March 29 sample and  $0.47\ \text{ng per day}$  for the March 31 sample. These values represent the slope of the regression lines shown in Figure 16. At a 95% confidence level, it was found that there was no statistically significant decrease in Fe(II) over 6 months for the March 31 sample. The March 29 sample did not show a significant decrease over 3 months, although the decrease over 6 months was significant ( $P = 0.007$ ). The March 31 sample at 21 days was set aside because of analytic errors.

Because each leachate listed in Table 6 provides estimates for various environmental and biotic-fluid matrices



**Figure 16.** Stability of soluble Fe(II) in two atmospheric PM samples stored in the dark at  $-20^{\circ}\text{C}$  for 12 months. Samples were leached in pH = 4.3 acetate buffer. The fraction of the total Fe extracted was approximately 5%.

that atmospheric PM might encounter, tests for Fe(II) content in each leachate were carried out. Four co-located PM<sub>10</sub> samples from each of 4 sampling days in East St. Louis, with particulate-mass loadings in agreement to within 10%, were each subjected to one of the four leachates listed in Table 6 and analyzed for soluble Fe(II) and Fe(III) content. The results of these experiments are summarized in Figure 17. In terms of Fe(II) solubility (the white fraction of the bars in Figure 17), the MQ water and NaCl leaches were statistically indistinguishable (two-tailed  $t$  test, 95% confidence level); the pH = 4.3 acetate solution consistently recovered the greatest amount of Fe(II). Aside from March 27 (the only weekend day shown here), the amount of Fe(II) leached from the NaHCO<sub>3</sub> was similar to that of the MQ water and NaCl ( $t$  test, 95% confidence level). This implies that the Fe-release mechanisms for the East St. Louis samples were similar in the three extractants (MQ water, NaCl, and NaHCO<sub>3</sub>) for each day except March 27. Further, only very small deviations in Fe(III)<sub>sol</sub>/Fe(II)<sub>sol</sub> were observed across the various extractants for a given sampling day. The data show that the very labile Fe(II) pool was changing to a greater extent than the less labile Fe(III) pool across the extractants. The relative differences observed among the MQ water, NaCl, and NaHCO<sub>3</sub> extracts indicate that the various emission sources and atmospheric processes associated with day-to-day meteorology can have an effect on how Fe is bound in particles.

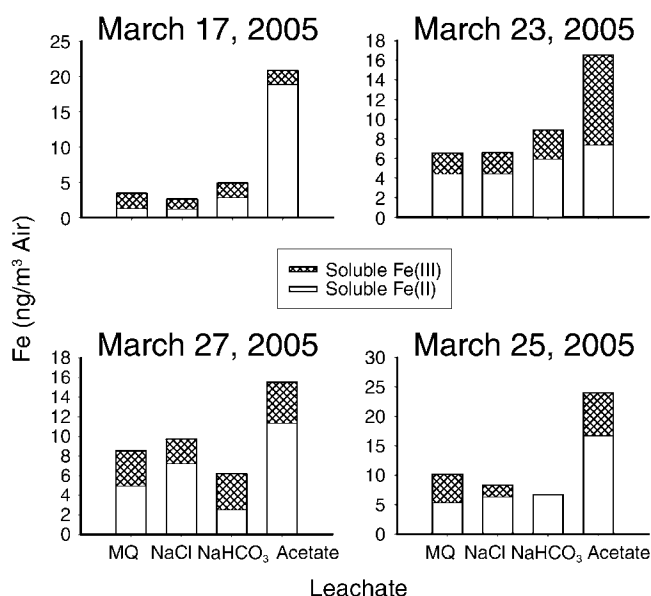


**Figure 17.** Comparison of the ability of leachates to recover soluble Fe(II) from PM<sub>10</sub> samples collected in East St. Louis. For each date, four co-located samples were subjected to a different leachate. The acetate solution consistently recovered the greatest amounts — i.e., 5.7%, 10%, 13%, and 7.4% of the total Fe extracted from samples for March 17, 23, 25, and 27, respectively. Note that the y-axis scales differ from panel to panel.

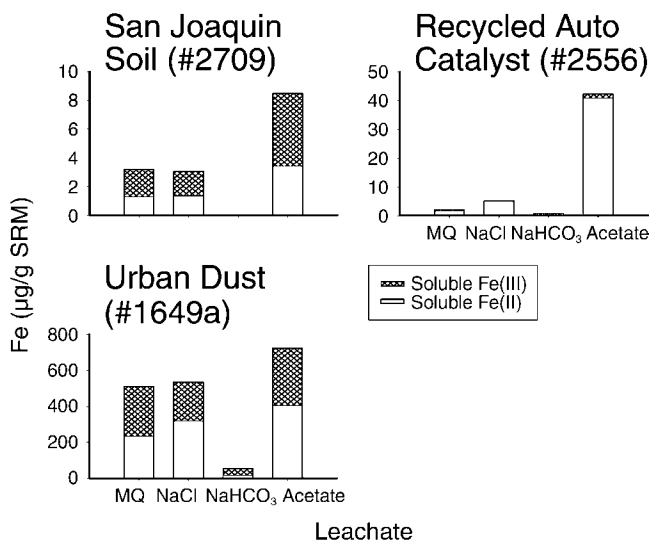


**Figure 18. Comparison of the ability of leachates to recover soluble Fe(II) from NIST SRMs.** The acetate solution consistently recovered the greatest amounts — i.e., 0.01%, 1.4%, and 0.51% of the total Fe extracted from samples of San Joaquin Soil, Urban Dust, and Recycled Auto Catalyst SRMs, respectively. Note that the y-axis scales differ from panel to panel.

Tests to determine the relative Fe pools addressable by the various extractions were also performed on NIST SRMs, including Recycled Auto Catalyst (#2556), Urban Dust (#1649a), and San Joaquin Soil (#2709). The results of these tests are presented in Figure 18. Overall, the SRMs showed a dependence of soluble Fe(II) on extractant composition that was similar to that of the East St. Louis samples. It can be seen from Figure 18 that the labile Fe fraction in the Urban Dust SRM was significantly greater than in the Recycled Auto Catalyst and San Joaquin Soil SRMs. In the acetate solution, the relative soluble Fe was 0.51%, 1.4%, and 0.01% for the Recycled Auto Catalyst, Urban Dust, and San Joaquin Soil, respectively. Further, when combining the results for all leachates for the Urban Dust

and San Joaquin Soil, it was found that, of the total soluble Fe, about half was in the form of Fe(II) (53% and 41%, respectively, for the two SRMs). In contrast, about 98% of all soluble Fe for the Recycled Auto Catalyst was in the form of Fe(II).

#### Caldecott Motor Vehicle Tunnel Study for Soluble Iron Emissions

PM was collected at the Caldecott motor vehicle tunnel in northern California using a Sioutas PCIS (SKC, Eighty Four, PA) (Misra et al. 2002). A series of 6-hour samples was obtained at the inlets and outlets of tunnel bore 1 (whose traffic consisted of approximately 4% diesel vehicles and 96% gasoline-fueled vehicles) and bore 2 (gasoline-fueled vehicles only). Each bore was sampled on 4 separate days during afternoon rush hour. Impactor substrates on the first four stages of the PCIS were acid-cleaned 2.0-µm 25-mm Teflo filters (Pall Life Sciences); precleaned 37-mm 2.0-µm Teflo substrates (Pall Life Sciences) were used in the smallest size-cut (< 0.25 µm, after-filter). For all sampling, substrates were pooled and then placed in a freezer at -20°C until analysis.

Determination of soluble Fe(II) emissions (ng/m<sup>3</sup>) was made by subtracting the Fe(II) concentration at the outlet from that of the inlet of each bore. Table 7 shows the soluble Fe(II) fraction compared with total Fe present in the sample (PM<sub>2.5</sub>). Total Fe analysis by x-ray fluorescence on co-located substrates showed that less than 2% (0.2% to 1.6%) of the total Fe collected was detected as soluble Fe(II). The table suggests that labile Fe(II) might be dependent both on the source (bore 1 or bore 2) and on the extractant. PM<sub>2.5</sub>/PM<sub>10</sub> ratios for soluble Fe(II) and overall PM mass at the outlets of the tunnel are compared in Table 8. These data show that a relatively small addition of coarse PM results in a large proportional increase in soluble Fe(II).

**Table 7. Soluble and Total PM<sub>2.5</sub> Fe in Samples from the Caldecott Motor Vehicle Tunnel<sup>a,b</sup>**

Date	Bore	Leachate	Fe(II) Emission ± SD (ng/m <sup>3</sup> )	Total Fe Emission ± SD (ng/m <sup>3</sup> )	% Soluble Fe ± SD (as Fe(II))
Aug. 25, 2004	2	Acetate buffer	12.2 ± 0.7	760 ± 390	1.6 ± 0.9
Aug. 26, 2004	2	NaHCO <sub>3</sub> solution	1.9 ± 0.4	1200 ± 500	0.2 ± 0.1
Aug. 30, 2004	1	Acetate buffer	10.5 ± 1.8	890 ± 460	1.2 ± 0.8
Aug. 31, 2004	1	Acetate buffer	6.4 ± 2.0	1200 ± 500	0.6 ± 0.4

<sup>a</sup> Substrates were analyzed individually, and labile iron was summed across stages.

<sup>b</sup> SD indicates standard deviation.

**Table 8.** Contributions of the Coarse Fraction to Fe(II) in PM Collected at the Caldecott Tunnel Outlets Compared with Overall PM Concentrations<sup>a</sup>

Date	PM <sub>2.5</sub> Fe(II) (ng/m <sup>3</sup> )	PM <sub>10</sub> Fe(II) (ng/m <sup>3</sup> )	Fe(II) <sub>PM<sub>2.5</sub></sub> / Fe(II) <sub>PM<sub>10</sub></sub>	PM <sub>2.5</sub> (μg/m <sup>3</sup> )	PM <sub>10</sub> (μg/m <sup>3</sup> )	PM <sub>2.5</sub> / PM <sub>10</sub>
Aug. 25, 2004	17.1	30.2	0.57	36.7	43.7	0.84
Aug. 30, 2004	38.9	59.6	0.65	70	85.4	0.82
Aug. 31, 2004	36.5	66.7	0.55	80	94.3	0.85

<sup>a</sup> All filters were extracted in acetate buffer.

## MANGANESE SPECIATION TECHNIQUES

### Background

Mn is known to be a highly toxic metal, linked primarily to neurologic diseases, and is on the U.S. EPA list of hazardous air pollutants. The purpose of this section of the study was to develop a method that could quantify various species of labile Mn bound to atmospheric PM in personal exposure samples. Although Mn can exist in several different oxidation states (Mn[0], Mn[II], Mn[III], Mn[IV], Mn[VI], and Mn[VII]) depending on the surrounding redox environment, we expected most of the Mn in atmospheric PM to be in the forms of Mn(II), Mn(III), and Mn(IV). It is quite difficult using spectrophotometric techniques to measure the Mn(III) and Mn(IV) species independently. However, because Mn(III) and Mn(IV) both have significantly higher redox potentials than Mn(II), they can be measured collectively as oxidized Mn. The goal of this section was therefore to develop methods of measuring overall soluble Mn and soluble oxidized Mn in atmospheric PM samples. The soluble fraction of Mn(II) can be calculated by subtraction. The techniques developed here can be used for the quantification of soluble Mn, oxidized Mn, and various Mn species in ambient samples but are best suited for personal occupational exposures where individuals have been exposed to elevated concentrations of Mn.

In small doses, Mn is an essential element that is found in many enzymes and is necessary for proper development in mammals (Heilbronn and Eriksson 1997; Brown and Taylor 1999). Although it is not clear what effects chronic elevated Mn concentrations have on human health, it is likely that subpopulations such as the elderly are at a higher risk (Weiss and Rehul 1994). When ingested or inhaled in larger doses, Mn is primarily associated with neurotoxic effects such as manganism, a neurologic disorder similar to Parkinson disease (Calne et al. 1994; Witholt et al. 2000). Studies have suggested that, even in smaller doses, transition metals like Mn might play a large part in the toxicity of atmospheric PM because of their ability to transfer

electrons and generate reactive oxygen species. Transformations between the Mn(III) and Mn(IV) states (oxidized Mn) can occur under ambient conditions; transformations to Mn(II) are much more difficult because of the high redox potential of the oxidized Mn. Another difference between Mn(II) and oxidized Mn that might have a direct influence on toxicity is their degrees of solubility. The solubility of the oxidized Mn species depends on their surroundings; Mn(II) is in general much more soluble.

Over the years, several methods have been proposed to estimate soluble Mn in aqueous solution (Nonova and Evtimova 1973; Chiswell and O'Halloran 1991; Kargosha and Noroozifar 2003) as well as the oxidizing equivalents of Mn (Kessick et al. 1972). In many cases, it is difficult to apply these techniques to atmospheric PM because the DLs are not suitable or because of gross interferences that are inherent in the methods. Only the leucocystal violet method has been applied to the quantification of oxidized Mn in atmospheric aerosols, and it has often resulted in measurements that were below the DL or that seemed to show Mn(IV) was present in larger quantities than overall Mn (Siefert et al. 1998b). One technique that shows great promise for the measurement of soluble Mn is a modified version of the formaldoxime (FAD) method of Morgan and Stumm (1965). This method has the advantages that the starting materials are very inexpensive, the Mn–FAD complex has a very high molar absorptivity constant, and the method itself is relatively free from interferences (except from Fe). To complement the FAD method, the oxidation of *o*-tolidine has been found to be suitable for the measurement of oxidized species of Mn at the concentrations found in atmospheric PM.

### Determination of Total Soluble Manganese

Total soluble Mn was quantified using the FAD method (Morgan and Stumm 1965), where a DL of 10 μg soluble Mn/L was reported (Brewer and Spencer 1971). FAD strongly complexes both Mn and Fe in solution and

absorbs light at peak wavelengths of 450 and 525 nm for the two metals, respectively. The FAD-Fe complex also shows a smaller absorption band at 450 nm, giving rise to a potential interference with the Mn measurement. For the present study, this interference was quantified as having added an estimated 25% false signal at a given Fe and Mn concentration, as has been done in other Fe interference studies (Goto et al. 1962). Given that Fe > Mn in most atmospheric PM, it is important to find a way to remove this false signal. The method of Goto and colleagues (1962) was employed, adding ethylenediaminetetraacetic acid (EDTA) and lowering the pH. In our study, HA was also added, and the pH of the extract was lowered to approximately 7.5. In these conditions, the Fe-FAD complex breaks down, while the Mn-FAD complex remains stable

for the analysis time (about 5 minutes). Because the experiments of Goto and colleagues (1962) were performed at Mn concentrations approximately 1000 times higher than those found in atmospheric aerosols, we adapted their method for the lower Fe concentrations encountered in atmospheric PM. Figure 19 presents the absorption spectra of 5 ppb Mn with 0 ppb Fe and with 10 ppb Fe. These spectra show that the addition of EDTA and HA adequately removed Fe interference up to at least 10 ppb Fe, the maximum expected Fe in our PM samples (Majestic et al. 2006), while retaining the Mn signal.

For analysis, stock FAD solution (20 mM) was prepared in the laboratory by combining equimolar amounts of formaldehyde and HA. A stock 100 mg/L Mn(II) solution was prepared from Mn(II)Cl<sub>2</sub> salt in 1% trace-metal-grade HCl (Fisher). Dilutions of this stock solution were prepared for calibration standards. The following reagents were added to 1.950 mL of the standard or the sample in the indicated order:

1. 10 µL 2.5% sodium hydroxide
2. 20 µL 20 mM FAD
3. 10 µL 0.08 N EDTA
4. 8.5 µL 600 mM HA (approximate amount needed to lower solution pH to 7.5)

Five minutes after the addition of the HA, the approximately 1.5-mL sample was pumped into a liquid waveguide cell with a 1-m path length, and the absorbance spectrum was obtained from 400 to 700 nm. The spectra were baseline-subtracted, and the absorbance was recorded at 450 nm. Figure 20 shows the Mn-FAD calibration curve from 0.1 to 5 ppb (1–50 ng/filter, assuming 10 mL extract). The measured slope = 0.0142 AU/ppb, and the *r*<sup>2</sup> value = 1.000.

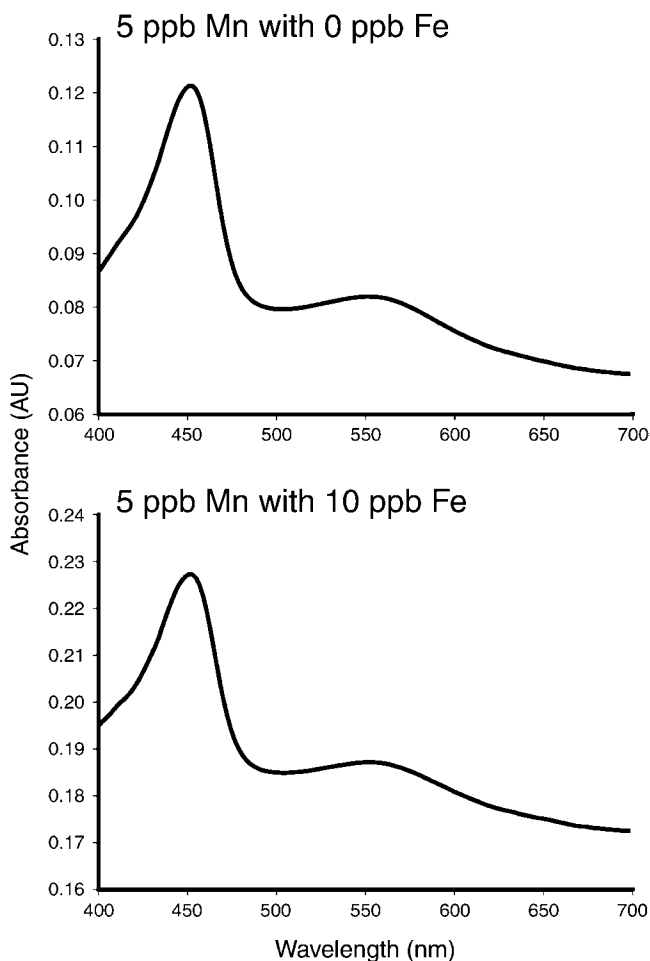


Figure 19. Example spectra for the FAD method of measuring soluble Mn in the presence of soluble Fe. Equivalent spectra were obtained for two solutions of equal Mn concentrations but different Fe concentrations, demonstrating that Fe interference can be adequately reduced at ppb concentrations by complexation with EDTA and HA in slightly basic conditions (pH = 7.5). Note that the y-axis scales differ from panel to panel.

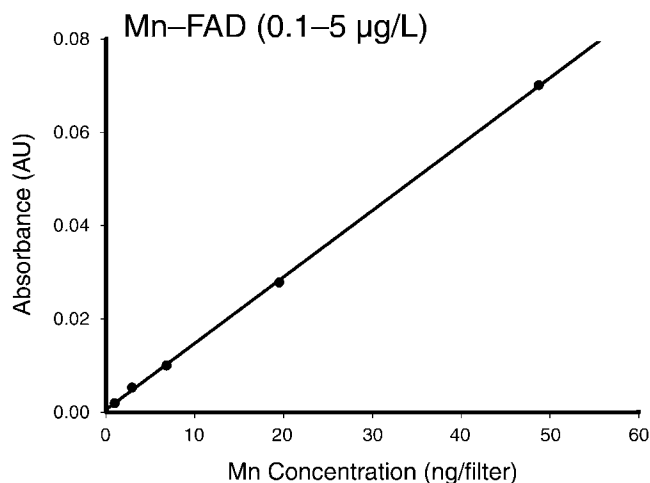


Figure 20. Calibration curve using Mn(II) chloride as the Mn source, showing excellent linearity at concentrations down to 0.1 ppb Mn.

Based on the calibration curves, the DL of this method is approximately 0.09 ppb, or 0.11 ng/m<sup>3</sup> for 24-hour sampling at 6 L/min, assuming a 10-mL extraction volume.

Because the reduction in pH is associated with a subsequent decrease in maximum color loss, Mn-FAD calibration curves were prepared at pH = 6.0, 6.9, 7.2, 7.5, and > 9.0. For these pH values, the observed slopes (in AU/ppb) were  $9.55 \times 10^{-3}$ , 0.013, 0.013, 0.014, and 0.019, respectively. A 26.3% decrease in color was observed when decreasing the pH from > 9.0 to 7.5. However, this percentage remained relatively stable down to a pH of at least 6.9. Further, as shown by the results from duplicate samples from the East St. Louis Supersite, we were still able to achieve reasonable precision (9.1% relative standard deviation [RSD],  $n = 7$ ) and DL (0.10 ppb) after decreasing the pH.

### Determination of Soluble Oxidized Manganese

Soluble oxidized Mn was quantified using the *o*-tolidine method (Morgan and Stumm 1965). In the presence of higher oxidation states of Mn (i.e., Mn[III] and Mn[IV]), *o*-tolidine oxidizes and a maximum absorbance at 440 nm is observed. Mn(III) compounds oxidize one molecule of *o*-tolidine; Mn(IV) (and Mn[VII]) compounds oxidize two. As a result, the method measures *oxidizing equivalents* of Mn rather than absolute Mn concentrations, and our calibration curves were accordingly prepared from two sources of oxidized Mn—Mn(III) and Mn(VII).

A stock solution of 100 ppm Mn(III) pyrophosphate was prepared as described by Klewicki and Morgan (1998) at pH = 7.3 and a 50-times molar excess in pyrophosphate ligand relative to total Mn. Dilutions of the stock solution were initially prepared in MQ water but were found to degrade quickly. Dilutions were then made in pyrophosphate solution, and the stability of the Mn(III) compound was verified spectrophotometrically and found to be stable for at least 30 minutes. In practice, experiments were always completed within 5 minutes of Mn(III) addition. Stock Mn(VII) was purchased from LabChem (Pittsburgh, PA) as a 5% potassium permanganate solution and diluted as needed.

For analysis, 1.750 mL standard (or filtered sample) was drawn into a 2-mL acid-cleaned vial. 10  $\mu$ L 0.1% *o*-tolidine was then added, followed by 142  $\mu$ L concentrated perchloric acid. Preliminary experiments showed that *o*-tolidine oxidizes in this environment in a predictable manner even when no Mn is present, likely because of ambient light. To control for this, the blanks and samples were placed in the dark for 30 minutes and allowed to come to equilibrium before analysis and were then measured in triplicate. This was proven to remove any extra oxidation effects in the blanks and standards. Immediately after the

addition of the perchloric acid, therefore, the samples were placed in the dark for 30 minutes and then analyzed within 2 minutes. Calibration curves for concentrations ranging from 0.10 to 5 ppb (for Mn[III]) and from 0.30 to 1.0 ppb (for Mn[VII]) were prepared using this method and are shown in Figure 21. It should be noted that the slope in the Mn(VII) plot (0.14 AU/ppb) is almost exactly twice that of the Mn(III) plot (0.063 AU/ppb), indicating twice the oxidizing equivalents.

Co-located PM<sub>10</sub> samples were collected at the East St. Louis Supersite to test the variability of the labile Mn measurements. Seven co-located PM<sub>10</sub> samples from March 19, 2005, were extracted in MQ water, and an air concentration of  $0.83 \pm 0.08$  ng soluble Mn/m<sup>3</sup> air was obtained. This corresponds to an RSD of 9.1% and is considered the

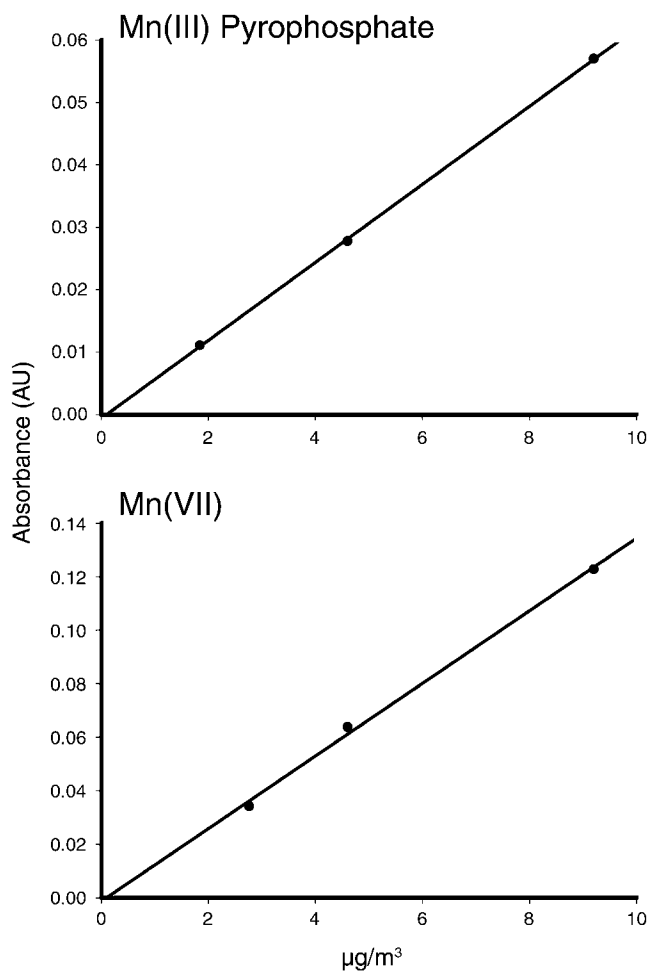


**Figure 21. Calibration curves for soluble oxidized Mn using the *o*-tolidine method.** The two sources of oxidized Mn—Mn(III) and Mn(VII)—have different oxidation states, leading to different levels of *o*-tolidine oxidation that are proportional to the reduction of Mn. Note that the y-axis scales differ from panel to panel.

overall precision for the FAD technique, including sampling, extraction, and analytic uncertainties. No oxidized Mn was observed in any of these extracts.

Because no oxidized Mn was observed in the overall Mn precision test from these samples, eight test solutions of equal concentrations of Mn(VII) were prepared at 0.46 and 0.92 ppb. The variations in these (as % RSD) were found to be 13.8% for the 0.46 ppb Mn(VII) and 8.5% for the 0.92 ppb Mn(VII), with absorbance values ranging from 0.046 to 0.069 AU and from 0.110 to 0.134 AU, respectively. Although great care was taken to prepare samples in a standard fashion and to ensure that the standards were used within minutes of dilution, it is still likely that the scatter was caused by either or both of the following factors:

1. Oxidation of *o*-tolidine caused by ambient light or light from the spectrophotometer during analysis or
2. Breakdown of the very dilute (< 1.0 ppb) Mn(VII) standard to lower oxidation states of Mn that do not oxidize *o*-tolidine, thus causing a lower absorbance signal.

Using PM<sub>10</sub> samples collected on co-located Teflon filters at the East St. Louis Supersite on March 17, March 19, and March 21, 2005, leachate comparisons were conducted for Mn extraction efficiency using the extract solutions listed in Table 6. Both overall soluble Mn and oxidizing Mn equivalents were measured, and the results are shown in Figure 22. The most efficient leachate tested for the release of Mn was the pH = 4.3 acetate buffer. The abilities of the other three leachates to extract Mn were all similar to each other and approximately half that of the acetate buffer. The overall solubility (with total Mn determined by ICP-MS) of Mn is shown in Table 9. The table shows that for the days measured, 6% to 20% of the Mn was soluble, depending on the extract. It should also be noted that no oxidized Mn was detected in these PM<sub>10</sub> samples.

Twenty-four hours after extraction, duplicate measurements of total soluble and soluble oxidized Mn were also obtained in each leachate for the March 17, 2005, samples.

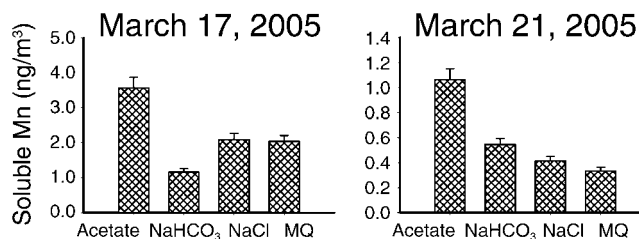


Figure 22. Comparison of the ability of leachates to recover soluble Mn from PM<sub>10</sub> samples collected in East St. Louis. For each date, four co-located samples were subjected to a different leachate. The acetate solution consistently recovered the greatest amounts — i.e., 20% and 13% of the total Mn extracted from samples for March 17 and 21, respectively. Note that the y-axis scales differ from panel to panel.

The resulting measurements of total soluble Mn ranged from 3% higher (in acetate buffer) to 31% higher (in NaHCO<sub>3</sub>) than the original measurements shown in Figure 22, and again no oxidized Mn was detected. These results imply that Mn measurements made in this way are moderately reproducible even after being exposed to laboratory conditions for 24 hours. The ability to recover low concentrations (0.5 ppb) of Mn successfully is essential to measuring soluble Mn accurately in personal exposure samples. Each extract from the March 17, 2005, samples was spiked with 0.5 ppb excess Mn(II). The resulting spike recoveries of total soluble Mn ranged from 94% higher (in MQ water) to 126% higher (in NaHCO<sub>3</sub>) than the original measurements. This suggests that the soluble Mn detection method described here can successfully measure quantities generally associated with personal exposure samples.

### CHROMIUM SPECIATION TECHNIQUES

#### Background

Like many transition elements, Cr can be present in a variety of oxidation states, ranging from -2 to +6. Because of the stability of certain compounds, however, the environmentally relevant Cr species are found as Cr(III) or

Table 9. Comparison of Soluble Mn with Total Mn in PM<sub>10</sub> Samples from East St. Louis

Date	Leachate	Soluble Mn (ng/m <sup>3</sup> )	Total Mn (ng/m <sup>3</sup> )	% Soluble <sup>a</sup>
Mar. 17, 2005	NaCl	2.04	18.31	11.3
Mar. 17, 2005	Acetate buffer	3.57	18.31	20.2
Mar. 17, 2005	NaHCO <sub>3</sub>	1.16	18.31	6.3
Mar. 17, 2005	MQ water	2.09	18.31	11.8
Mar. 19, 2005	MQ water	0.83	7.73	11.0
Mar. 21, 2005	Acetate buffer	1.1	8.3	12.8

<sup>a</sup> From ICP-MS values.

Cr(VI). Cr(III) has been shown to be an essential nutrient; Cr(VI) has been shown to be highly carcinogenic, because it is reduced to Cr(III) in cells and forms reactive oxygen species that are capable of damaging DNA (Cohen et al. 1993). The goal of this section of the study was to develop a spectrophotometric method capable of measuring soluble Cr(VI) at concentrations typical of those found in personal exposure samples. The primary application of the method will be the measurement of occupational exposures to Cr(VI) in high-exposure work, such as chrome plating and steel production.

Cr(VI) determination was achieved using the diphenylcarbazide (DPC) method (Bartlett and James 1979). The DPC solid was obtained from Sigma-Aldrich, and the stock solution (2.35 mM) was prepared in spectrophotometric-grade ethanol. Cr standards were prepared from 1000 mg/L Cr(VI) stock solutions obtained from High Purity Standards (Charleston, SC). The working standards were prepared by dilution of the stock solution in either MQ water or pH = 7.4 NaHCO<sub>3</sub> solution. In 10 mL of each standard, 50  $\mu$ L 85% phosphoric acid and 100  $\mu$ L 2.35 mM DPC were added. The Cr(VI)-DPC complex was then quantified by injecting about 1.5 mL of it into the 1-m liquid waveguide capillary cell, measuring its absorbance at 540 nm, and comparing it against a calibration curve. Figure 23 shows the calibration curves for Cr(VI) concentrations ranging from 0.010 to 10  $\mu$ g Cr(VI)/L in MQ water and in NaHCO<sub>3</sub> solution. The curves show excellent linearity across three orders of magnitude and very minimal dependence on the matrix used (MQ-water slope = 0.067 AU/ppb; NaHCO<sub>3</sub> slope = 0.069 AU/ppb). Judging from the calibration curves, the estimated DL for this method is below 0.010  $\mu$ g Cr(VI)/L (or 0.19 nM), which corresponds to 0.011 ng/m<sup>3</sup> for a 24-hour sampling period at 6 L/min and a 10-mL extract volume.

Four co-located filters from the East St. Louis Supersite were leached and analyzed for Cr(VI) using the DPC method. The results for these samples, however, were below the estimated DL.

### IRON L<sub>II</sub>-EDGE X-RAY ABSORPTION NEAR EDGE STRUCTURE SPECTROSCOPY

#### Background

In the report thus far, all of the speciation methods described have focused on wet-chemical extraction followed by analysis using spectrophotometric techniques. Although these measurements are important from the biologic and environmental perspectives, they generally account for only a small fraction of the total analyte. In order to obtain a more complete picture of the metal speciation and redox

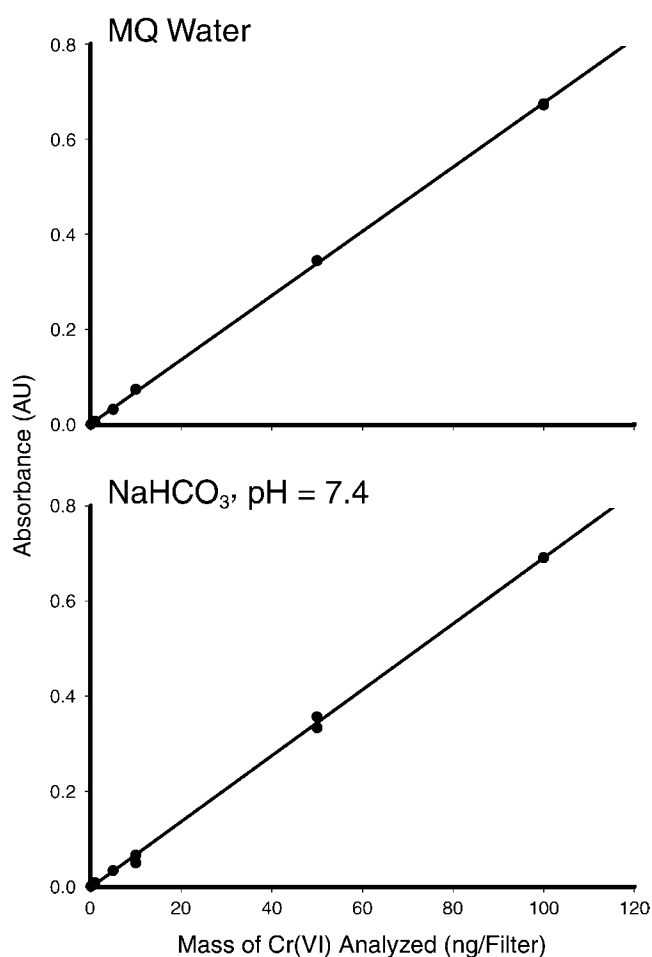


Figure 23. Cr(VI) calibration curves for selected leachates over the calibration range 0.01–5  $\mu$ g Cr(VI)/L.

chemistry occurring in aerosols, we developed a technique suited to measuring total Fe(II) and Fe(III) in personal exposure samples. This technique, known as x-ray absorption near edge structure (XANES) spectroscopy, is synchrotron based and exploits the splitting of the 2p energy level of Fe caused by its oxidation states. Because of this splitting, we were able to determine the relative ratios of Fe(II) and Fe(III) in solid samples. Then, using a method that measures total Fe, such as ICP-MS, we extracted the air concentration of these species. XANES measurements complement wet-chemical measurements, allowing the soluble fraction of Fe(II), for example, to be compared with both the total Fe and total Fe(II) fractions of an aerosol. XANES spectroscopy also allows researchers to observe overall changes in oxidation states, and therefore in redox environments, as particles are transported over long distances.

A study by Zhuang and colleagues (1992) revealed that significant amounts of Fe(II) can be found in remote

marine aerosols. The study also indicated that Fe in atmospheric particles that are transferred over long distances might undergo oxidation and reduction transformations in which Fe(II) and Fe(III) can be interconverted. Because atmospheric aerosols are generally complex mixtures containing a variety of organic and inorganic species, it is extremely difficult to determine how redox-active transition metals behave in PM. Laboratory studies of Fe-containing particles have shown that the oxidation and reduction of Fe(II) and Fe(III) in atmospheric PM can depend on many factors, including the electron donors present and the pH. One study showed that a formate solution was most effective for the photoreduction of Fe(III) compared with other common electron donors such as acetate and oxalate (Pehkonen et al. 1993). Another study showed that the rate of Fe(III) photoreduction depended on the type of Fe(III) as well as the concentration and type of inorganic ions (such as sea salts) present in the PM (Zhu et al. 1993). The current study was undertaken in order to gain insights into the transformations of Fe associated with ambient atmospheric PM collected from three urban sites.

## Methods

We collected XANES data at the Synchrotron Radiation Center (operated in part by the University of Wisconsin–Madison in Stoughton, Wisconsin) using the High Energy Resolution Monochromator (HERMON) beamline. The initial beam current was approximately 280 mA, and the electron energy was constant at 800 MeV. Experiments were performed under ultrahigh-vacuum conditions ( $\sim 10^{-10}$  Torr) using a total electron yield (TEY) detection apparatus. Spectra were obtained at 0.33-eV intervals in replicates of 10 across a scan range that included the zero-valent Fe  $L_{II}$  (719.9 eV) and  $L_{III}$  (706.8 eV) edges and were normalized against a gold mesh current to account for beam decay.

There are currently no well-established methods available for performing ultrahigh-vacuum XANES spectroscopy on atmospheric PM. It was thus necessary to choose a PM sampler and collection substrate that were compatible with ultrahigh-vacuum TEY analysis. The PCIS (Singh et al. 2002) was found to be ideal as a PM sampler because it concentrates PM into a line at which the x-ray beam can be focused. As for a substrate, our preliminary studies had shown that, if direct analysis on the substrate was sought, the PM must be collected on a substrate that conducts, has a smooth surface, has low interference with target species, and is compatible with PM samplers.

The standard filters used as substrates for trace-metal collection are generally made of Teflon. Although Teflon is not a conducting material, commercial products such as

silver pastes can be used to increase conductivity. However, Teflon substrates are extremely troublesome in that the fluorine of which they are composed has a very strong K-edge (1s energy level) absorption at around 697 eV. The extreme intensity of this edge causes a strong interference with the Fe L-edge at around 707 eV, and therefore Teflon filters cannot be used in this application. Quartz is another substrate commonly used in atmospheric samplers. Although quartz is generally a conductive material, the lack of a smooth surface precludes its use in Fe L-edge measurements. High-purity aluminum foil substrates, however, possess all of the qualities required of a substrate to be used in TEY XANES spectroscopy analysis. A PCIS (Singh et al. 2002) with high-purity (99.9995%) aluminum foil as impactor substrates was therefore used for all XANES spectroscopy analyses.

At the  $L_{III}$ -edge, Fe(II) shows a sharp absorption peak at 707.8 eV and a less intense peak at 710.5 eV; Fe(III) shows a less intense peak at around 708.0 eV and a very intense peak at 709.5 eV (van Aken et al. 1998). Many researchers have introduced methods of calculating Fe(II)/Fe(III) ratios from unknown XANES spectra (Garvie and Buseck 1998; van Aken et al. 1998; van Aken and Liebscher 2002). In general, these methods include calculations based on both the  $L_{II}$  and the  $L_{III}$  regions on the spectra. As can be seen in Figure 24, in the sample spectra showing a 70% Fe(II) standard and an actual ambient sample, the  $L_{II}$ -edge in our samples was generally not observed or was very noisy because of the relatively low Fe concentration in them compared with the Fe standards and unknown samples used by other researchers. We therefore devised a method of calculating Fe(II)/Fe(III) in dilute Fe samples using only the  $L_{III}$ -edge as a reference. The  $L_{III}$ -edge (or “white-line”) portion of the mesh-normalized spectrum was first baseline-subtracted, and the relative Fe(II) and Fe(III) peak heights were determined individually. The ratio of the peak heights was then found to depend on the Fe(II)/Fe(III) ratio.

Fe(II) and Fe(III) standards were prepared from Fe(II) and Fe(III) ammonium sulfate salts in mixed proportions. A standard calibration curve, shown in Figure 25, was prepared from these at Fe(II)/Fe(III) ratios of 0, 0.1, 0.3, 0.5, 0.7, 0.9, and 1. The figure shows that the curve is nonlinear and is best described as a second-power polynomial ( $r^2 = 1.000$ ). The nonlinearity of the calibration curve has important implications for the relative uncertainty of the measurement and highlights the fact that extreme care should be given to the selection of the calibration points used for sample quantification.

The precision of the XANES spectroscopy measurement was estimated by measuring the 0.5-to-0.25- $\mu\text{m}$  size fraction at the 40-day time point, collected on February 13,

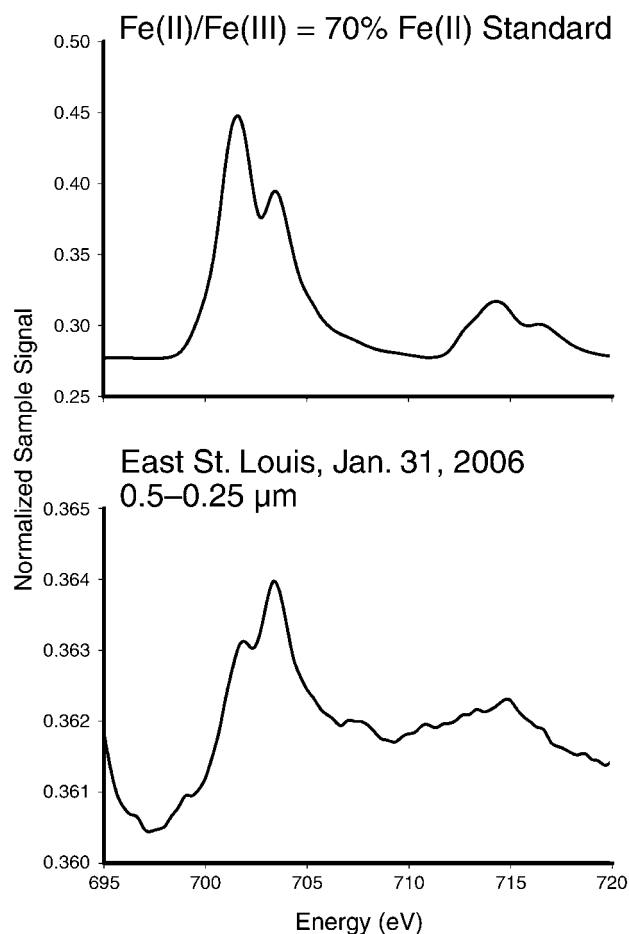


Figure 24. Example XANES spectra for a 70% Fe(II)/30% Fe(III) standard and an ambient sample from East St. Louis. Note that the  $L_{II}$  portion of the ambient sample's spectrum is relatively flat and buried in noise.

2006, from a sampling site at the Rancho Los Amigos National Rehabilitation Center in the Los Angeles Basin, in California. This sample was measured at five different spots on the PCIS sample line. The final Fe(II) concentration was found to be  $5.94 \pm 0.84 \text{ ng/m}^3$ , which corresponds to an RSD of 14.2% and is the overall uncertainty associated with this measurement.

## SAMPLING AND STUDY DESIGN

The new chemical analysis methods developed as part of this study were intended to be suitable for use in health studies. Three key advances from the study are (1) the measurement of organic tracers in personal exposure samples by TD-GC-MS, (2) the measurement of trace elements in personal exposure samples by HR-ICP-MS, and (3) the speciation of Fe and Mn in personal exposure samples by

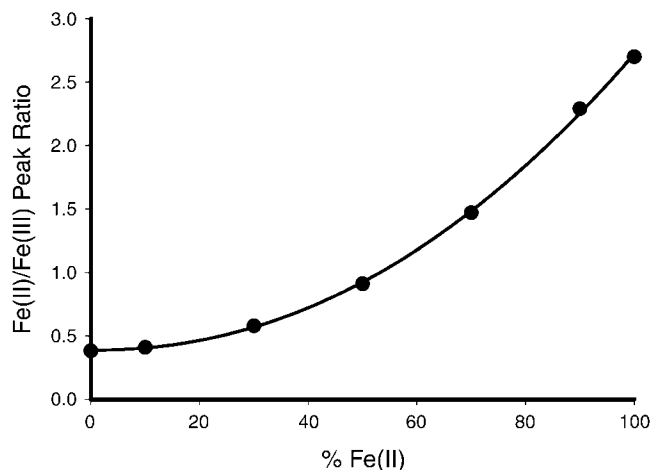


Figure 25. Relative peak heights for Fe(II) and Fe(III) on the  $L_{III}$ -edge for various Fe(II) fractions (prepared and analyzed by XANES spectroscopy) as a function of the Fe(II) fractions. The curve fit shown is a second-power polynomial.

wet-chemical methods. Although the resources and time needed to analyze samples vary considerably across laboratories, estimates can be provided of the current costs of these analyses as conducted in an efficient laboratory with highly trained staff. The nominal costs in 2007 dollars for batches in the range of 100 to 500 samples would be approximately \$250 per sample for TD-GC-MS, \$75 per sample for HR-ICP-MS, and \$10 per sample for the wet-chemical methods.

The TD-GC-MS and wet-chemical methods can readily be used on samples collected for routine analysis of EC (elemental carbon), OC, and water-soluble ions. Standard substrate preparation and sample-handling procedures would be adequate to protect samples from excessive contamination. The HR-ICP-MS method would require additional precautions not typically used for trace-metals analysis by x-ray fluorescence. Filters would need to be precleaned with dilute acid and rinsed with high-purity water to reduce filter blanks to concentrations that would allow the DLs of HR-ICP-MS to be fully exploited. Likewise, the samples would need to be collected and handled with metal-free materials. The TD-GC-MS and wet-chemical methods could, in addition, be integrated retrospectively into health studies; the HR-ICP-MS methods would need to be integrated into studies before sample collection. The methods could be widely used for PM sample analysis and would be equally applicable to atmospheric samples and samples of emission from air pollution sources. Although TD-GC-MS is not expected to completely replace the use of solvent extraction methods for GC-MS analysis of organic tracers, our lab is now using HR-ICP-MS exclusively for the analysis of elements in PM samples.

The following section presents proof-of-concept examples of the application to health studies of the methods developed in our project. Details of the sampling efforts that provided the samples for the data discussed in the Results section of this report are presented below. Extra samples were collected for the Fe aging and Mn speciation studies; samples from existing health studies were obtained from the St. Louis truck terminal and University of California (UC)–Irvine pilot health studies.

### INTERCOMPARISON OF PERSONAL EXPOSURE SAMPLERS AT UNIVERSITY OF SOUTHERN CALIFORNIA

It is becoming increasingly common for researchers to use personal exposure samplers in order to better quantify and characterize a person's actual exposure to PM (Hopke et al. 2003; Keeler et al. 2004). Personal exposure samplers also allow for a more direct measurement of personal exposure to trace metals. Validation of PM samplers is generally a two-step process. First, the individual size fractions are measured by generating spherical aerosols of a known diameter, and the collection efficiency of the relevant sizes is then tested (Misra et al. 2002; Hering et al. 2003). Further validation is accomplished by performing field studies of the sampler against well-characterized samplers. Historically, personal exposure samplers have been validated using measures of mass concentration, major ion concentrations (e.g., nitrate and sulfate), or EC and OC comparisons (Singh et al. 2002; Hering et al. 2003). Validation of personal exposure samplers for the measurement of trace metals has not been reported, yet they have been assumed by some research groups to be adequate for trace-metal sampling (Graney et al. 2004).

In the current study, we collected and compared trace-metals data from five co-located samplers: one standard atmospheric sampler that employed the AIHL cyclone with two PM<sub>2.5</sub>-filter holders (John and Reischl 1980) and four types of personal exposure samplers, including a BGI PM<sub>2.5</sub> KTL (GK 2.05) cyclone, a URG PM<sub>2.5</sub> minicyclone, two PCISs (Misra et al. 2002; Singh et al. 2003), and an Aerosol Dynamics PM<sub>2.5</sub> personal exposure sampler (Hering et al. 2003). The PCISs are capable of collecting particles in five aerodynamic size ranges: 10–2.5 μm, 2.5–1 μm, 1–0.5 μm, 0.5–0.25 μm, and < 0.25 μm. The metals examined were Fe, Mn, Ba, Cu, Pb, and vanadium (V) and were chosen based on one or both of the following criteria: (1) their unique source-apportionment characteristics and (2) their roles in human health and the health of the environment. Fe in particulate phases with an aerodynamic diameter of 2.5 to 10 μm has primary sources in both resuspended crustal material and automobile-brake wear. Ba is also a common element found in automobile-brake wear.

The primary source of Fe found in PM<sub>2.5</sub> aerosols has been reported to be steel mills and coal combustion (Ondov and Suarez 2002). In areas such as the Los Angeles Basin, however, mobile sources are an important source of fine particulate Fe. Vanadium is used as a tracer for fuel-oil combustion (Divita et al. 1996). Mn and Pb were chosen as markers in human toxicity because both elements are well-known neurotoxins. Fe, V, Cu, and Ba are known to cause inflammation in lung tissue (Carter et al. 1997; Camner and Johansson 1992).

The sampling site in Los Angeles was at the main campus of the University of Southern California (USC), near downtown Los Angeles. It was about 150 m downwind of a major freeway and represented an urban mix of industrial, vehicular, and construction sources of PM. An ambient AIHL PM<sub>2.5</sub> cyclone (John and Reischl 1980) was operated at an air flow of 21.5 L/min with the flow split for two collection substrates (47-mm Teflon filters [Teflo, 2.0-μm pore size, Pall Life Sciences]) and was co-located with four types of personal exposure samplers: (1) two PM<sub>10</sub> PCISs (Misra et al. 2002; Singh et al. 2003) with five size-resolved stages operated at 9 L/min with 25-mm impactor substrates (Zefluor, 3.0-μm pore size, or high-purity aluminum foils) for all stages except a 37-mm substrate as an after-filter (Zefluor, 3.0-μm pore size, Pall Life Sciences), (2) a BGI PM<sub>2.5</sub> KTL (GK 2.05) cyclone operated at 3.5 L/min using 37-mm substrates (Teflo, 2.0-μm pore size), (3) a URG PM<sub>2.5</sub> minicyclone operating at 3.0 L/min with 25-mm substrates (Teflo, 2.0-μm pore size) and (4) an Aerosol Dynamics PM<sub>2.5</sub> personal exposure sampler (Hering et al. 2003) operated at 1.97 L/min using 25-mm substrates (Teflo, 2.0-μm pore size). Samples were collected for 24-hour periods over the course of 5 sampling days.

The sampling site in East St. Louis was at a Supersite in an Illinois urban residential–light commercial area about 3 km east of (and across the Mississippi River from) St. Louis, Missouri. As an extension of the Los Angeles study described above, this study not only focused on the comparison of personal exposure samplers with an ambient sampler, but also compared trace-metals data from co-located duplicate personal exposure samplers. An ambient URG PM<sub>2.5</sub> cyclone was operated at 24 L/min with the flow split for three collection substrates (47-mm Teflon filters [Teflo, 2.0-μm pore size, Pall Life Sciences]) and was co-located with three types of personal exposure samplers: (1) two PM<sub>10</sub> PCISs (Misra et al. 2002; Singh et al. 2003) with five size-resolved stages operated at 9 L/min with 25-mm impactor substrates (Zefluor, 3.0-μm pore size, or high-purity aluminum foils) for all stages except a 37-mm substrate as an after-filter (Teflo, 2.0-μm pore size, Pall Life Sciences), (2) two BGI PM<sub>2.5</sub> KTL (GK 2.05) cyclones operated at 3.5 L/min using 37-mm substrates (Teflo, 2.0-μm

pore size), and (3) two URG PM<sub>2.5</sub> minicyclones operating at 3.0 L/min with 25-mm substrates (Teflo, 2.0- $\mu$ m pore size). Samples were collected for 24-hour periods over the course of 5 sampling days.

## IRON AGING STUDY

### Sample Collection at Rancho Los Amigos National Rehabilitation Center

For the Fe aging study, size-fractionated PM<sub>10</sub> samples were collected for 2 days each in the East St. Louis Super-site; in the Los Angeles Basin site; and in Waukesha, Wisconsin. The East St. Louis site was in an urban residential-light commercial area. The Los Angeles Basin site was located at the Rancho Los Amigos National Rehabilitation Center. It is known to have some of the highest PM<sub>10</sub> concentrations in the United States, often exceeding the National Ambient Air Quality Standards primary standard of 150  $\mu$ g/m<sup>3</sup> (Singh et al. 2002). The Waukesha site was approximately 20 km west of Milwaukee, Wisconsin, on a four-lane suburban road. It was fenced in, and the samplers were raised to fence level, approximately 2.5 m above the ground. The area was a mix of residences and heavy industry, and the site itself was adjacent to an automobile-body shop.

Four co-located PCISs (Misra et al. 2002; Singh et al. 2003) were used, each operating at 9 L/min for 24 hours. In three of them, Teflon (Zefluor, 3.0- $\mu$ m pore size) impactor substrates were used; in the fourth, high-purity aluminum foil substrates (Alfa Aesar) were used. In all four, the after-filter was a 37-mm Teflon (Teflo, 2.0- $\mu$ m pore size) substrate.

Trace-metal clean techniques were used throughout the substrate preparation, PM collection, sample handling, and analysis. All pre- and post-sampling handling of the substrates was performed in a dedicated trace-metal cleanroom. Before use, the Teflon substrates were subjected to rigorous acid-washing protocols that have been shown to minimize trace-metal contamination, including a series of three rinses: trace-metal-grade HCl (Fisher) and trace-metal-grade nitric acid (HNO<sub>3</sub>) (Fisher) followed by MQ water. The aluminum substrates were rinsed and sonicated in dichloromethane followed by methanol. All the substrates were conditioned at a constant temperature and relative humidity for at least 24 hours and weighed on a microbalance before and after sampling.

### Aerosol Aging

PM samples collected on the Teflon and aluminum foil substrates were placed in acid-cleaned Petri dishes that were

then sealed with Teflon tape, double bagged under nitrogen, and stored in a cooler for shipment to our laboratories at the University of Wisconsin–Madison. Upon arrival, the substrates were taken to a trace-metal cleanroom and cut into sections using either a ceramic knife or ceramic scissors. For each size fraction on each sampling day, the Teflon filters (25-mm Zefluor and 37-mm Teflo) were cut in half; the aluminum substrates were cut into fourths. This resulted in six identical Teflon and four identical aluminum substrates for each size fraction (no aluminum substrates were used for the after-filters) for each day. One Teflon half and one aluminum quarter were immediately placed in a dark nitrogen atmosphere at  $-20^{\circ}\text{C}$ , representing time  $t = \text{day } 0$ . The others were artificially aged in an environment with tightly controlled temperature ( $20.7 \pm 0.2^{\circ}\text{C}$ ), relative humidity ( $42.8 \pm 1.1\%$ ), and light (250  $\mu$ Einsteins, 16 hours on, 8 hours off) at the university's Biotron controlled-environments facility for various aging times. The East St. Louis and Los Angeles Basin filters were selected to represent long-term aerosol transport and were artificially aged for periods of 0, 10, 20, and 40 days. The Waukesha aerosols were selected to represent short-term aerosol transport and were aged for 0, 1, 3, 6, and 10 days.

For each stage, total Fe determinations were made by ICP-MS using a Teflon filter half and low-volume microwave-assisted acid digestion. For each time point and size fraction, Fe L<sub>II</sub>- and L<sub>III</sub>-edge XANES spectra were acquired using aluminum substrate quarters on the HERMON beamline at the university's Synchrotron Radiation Center. Soluble Fe(II) and Fe(III) were determined from the Teflon sections using the ferrozine method as applied to atmospheric aerosols (Majestic et al. 2006) at each time point.

## MANGANESE SPECIATION STUDY

### Background

As a replacement for the fuel additive tetraethyl lead, now banned in several countries, the Mn-containing additive methylcyclopentadienyl manganese tricarbonyl (MMT) has been used as an octane booster in gasoline. Since its introduction, the use of MMT has been highly debated. Two major concerns about MMT have been (1) that the Mn in it fouls catalytic converters in automobiles, causing them to degrade quickly (Hurley et al. 1991), and (2) that Mn is (like Pb) on the U.S. EPA's list of hazardous air pollutants. It is currently unclear what effects chronic exposure to elevated Mn concentrations has on human health (Zayed 2001).

It has been found that less than half of the Mn added to fuels as MMT makes its way out of the tailpipe (Hammerle et al. 1991). One study determined that, over a 25-year

period of MMT use in Canada, there had not been any significant increase in Mn concentrations in soils along roadways (Bhuie and Roy 2001). The fraction of Mn emitted into the atmosphere has been characterized in a few studies using both low- and high-mileage vehicles. Data obtained from x-ray spectroscopy of engine exhaust have suggested that the Mn was in the form of oxides, sulfates, and phosphates; MMT itself degrades photolytically primarily to solid Mn oxides and carbonates (Terhaar et al. 1975; Ressler et al. 2000).

Despite chemical analyses of MMT and its exhaust products, it is still unclear if excess Mn exhaust leads to adverse human health effects. Although MMT has been approved for use in the United States, France, Russia, and other nations, it has been used extensively only in Canada, and surprisingly few studies have been performed that measure the quantities and speciation of Mn present in urban areas. We therefore applied the Mn speciation method described earlier in this report to PM collected in Toronto, a major urban center in Canada, hypothesizing (1) that, because of the relatively heavy industry present at many sites in the United States, the concentrations of Mn found in PM in Toronto might not be significantly higher than those in the United States and yet (2) that, because MMT combustion in Canada provides a source not seen in the United States (or most other parts of the world), the speciation of the Mn in Toronto might be different from that of the United States.

### Sample Collection

The sampling site was located in a residential neighborhood just west of Toronto, on a third-floor balcony. The site was between two subway stations and was one block north of the main thoroughfare through the neighborhood.

One PCIS (Misra et al. 2002; Singh et al. 2003) was employed, operating at 9 L/min for 24 hours. The sampler was equipped with Teflon (25-mm Zefluor, 3.0- $\mu$ m pore size) impactor substrates and a Teflon (37-mm Teflo, 2.0- $\mu$ m pore size) after-filter. Twenty-four-hour sampling took place intermittently for 12 days between December 30, 2005, and January 22, 2006, and the PM was then analyzed for total labile and soluble oxidized Mn.

### ST. LOUIS TRUCK TERMINAL STUDY

Personal exposure samples were collected at a truck terminal in St. Louis, Missouri, as part of an epidemiologic cancer study funded by the National Cancer Institute (NCI) and led by principal investigator Eric Garshick. A component of this study was to assess the exposure of terminal workers to carbonaceous fine PM. Samples from the study

were provided to our team at the University of Wisconsin–Madison to use in a pilot study measuring organic tracers in personal exposure samples. The mixture of personal exposure samples, ambient worksite samples, and ambient urban background samples (from the East St. Louis Super-site) provided a unique opportunity to track work-related exposure to carbonaceous fine PM in a truck terminal. Detailed analysis of the chemical speciation results provided information on the EC and OC in the personal exposure samples as originating from sources in the urban background, on the worksite, or in personal activity. The exposure model that was tested in the pilot study can be described by the following equation:

$$\text{Personal exposure} = \text{urban background} + \text{worksite background} + \text{personal activity} \quad [2]$$

All samples were collected using the same low-volume model of personal exposure sampling to minimize differences caused by sample collection. Samples of PM 1.0  $\mu$ m or smaller in aerodynamic diameter were collected on 25-mm quartz-fiber filters and were split for OC and EC analysis and organic speciation. A 1.45-cm<sup>2</sup> punch was analyzed for OC and EC, and the remaining filter was used for organic speciation.

To accurately assess the contribution of PM emission sources, particularly motor vehicle exhaust, TD-GC–MS analyses of OC, EC, and markers for nonpolar organic molecules were conducted on all of the PM samples. OC is the least source-specific of the components measured for the study. EC has been used as a tracer for diesel exhaust in urban areas. However, the emission profile for diesel exhaust depends on the operating conditions of the vehicle and can vary considerably within a fleet (Kweon et al. 2003). Additionally, there can be significant contributions of EC from other primary emission sources (Schauer 2003). Hopanes are source-specific organic-molecular markers for the presence of lubricating oil in motor vehicle exhaust (Schauer et al. 2002b). PAHs are indicative of combustion in general. Alkanes (tetracosane through pentriacontane) are emitted from a variety of combustion and biogenic sources (when cigarette smoke is present in high concentrations, however, alkanes are markers mainly for the smoke [Kavouras et al. 1998]). Steranes are markers for motor vehicle exhaust but have higher uncertainty than hopanes. The concentrations of the OC, EC, and organic tracers were averaged to obtain average profiles to assess differences in the personal, worksite, and urban background samples and were correlated individually by sample time to evaluate the exposure model in equation 2. Health data were collected as part of the NCI study but were not provided to our team and were not analyzed as part of this report.

## UNIVERSITY OF CALIFORNIA–IRVINE PILOT HEALTH STUDY

### Background

As part of a study funded by the National Institutes of Health (NIH) and led by principal investigator Ralph Delfino, researchers at the University of California–Irvine are following 72 nonsmoking elderly individuals with coronary heart disease living in a retirement home in an area with high concentrations of air pollution in the Los Angeles Basin of California (Polidori et al. 2007). The following health outcomes have been recorded for all participants during 10-day sampling periods:

1. PDA diary entries every waking hour (diary completion takes less than 5 minutes) for anginal symptoms, medication use, stress levels, and time–activity information during periods of intensive ambulatory monitoring;
2. Continuous ambulatory ECG monitoring 24 hours per day except when bathing;
3. Ambulatory monitoring of systolic and diastolic blood pressure every hour while awake;
4. 12 weekly blood draws over a 7-month period for circulating biomarkers of inflammation and thrombosis; and
5. 12 weekly breath samples for nitric oxide collected by exhalation into a sampling device.

### PM Sampling at Retirement Home

In addition to these health outcomes, exposure to PM and its speciated components are being measured. Individuals in the study were equipped with a PCIS (Misra et al. 2002; Singh et al. 2003) and a small personal exposure sampling pump. The study is focusing on the personal exposure measurement of size-fractionated source tracers using the microvolume microwave-assisted acid digestion method described earlier in this report. For this study, the PCISs were modified by removing two of the intermediate stages in order to collect particles in the coarse ( $> 2.5 \mu\text{m}$ ), accumulation ( $0.25\text{--}2.5 \mu\text{m}$ ), and ultrafine ( $< 0.25 \mu\text{m}$ ) size fractions, and the samplers were operated at 9 L/min. Indoor and outdoor PM was collected simultaneously at an outdoor site in the Los Angeles Basin and inside the retirement home. Samples from the study were provided to our team at the university for analysis by ICP–MS to compare personal exposure, indoor, and outdoor size-resolved metal concentrations. Health and personal subject data were not provided to us and are not included in this report.

For our pilot study, the PCISs were equipped with 25-mm Teflon (Zefluor, 3.0- $\mu\text{m}$  pore size, Pall Life Sciences) impactor substrates for size fractions  $> 0.25 \mu\text{m}$  and a 37-mm (Teflo, 2.0- $\mu\text{m}$  pore size, Pall Life Sciences) substrate to

collect the ultrafine fraction. All filters were subjected to a rigorous acid-cleaning protocol that included rinses in 10% HCl and 10% HNO<sub>3</sub> followed by at least three rinses in MQ water. PM mass was obtained by weighing the filter on a microbalance pre- and post-sampling after equilibration at a constant temperature and relative humidity for at least 24 hours. The filters containing the aerosol samples were then cut in half and analyzed by ICP–MS, as described earlier.

## RESULTS AND DISCUSSION

### INTERCOMPARISON OF PERSONAL EXPOSURE SAMPLERS

Figure 26 presents a comparison of PM<sub>2.5</sub> mass collected from the BGI PM<sub>2.5</sub> KTL (GK 2.05) cyclone (over 2 days in East St. Louis), the URG PM<sub>2.5</sub> minicyclone (over 2 days in East St. Louis), and the two Sioutas PCISs (over 4 days from the existing Los Angeles study and 2 days from the existing East St. Louis study). Loadings for the BGI and URG samplers were typically around 100  $\mu\text{g}$ , ranging from 35 to 160  $\mu\text{g}$  per filter; the mass of each size fraction for the PCISs ranged from 15 to 200  $\mu\text{g}$ . The graph in Figure 26 shows good agreement between the co-located personal exposure samplers (most were within 10% of the 1:1 line). As shown in the graph, the most significant outlier was a filter collected using the BGI sampler on June 2, 2006. Upon visual inspection of the two filters collected from the BGI sampler on this day and comparison of their filter masses with a co-located ambient-PM<sub>2.5</sub> sample, it became apparent that one of the BGI samplers had not been

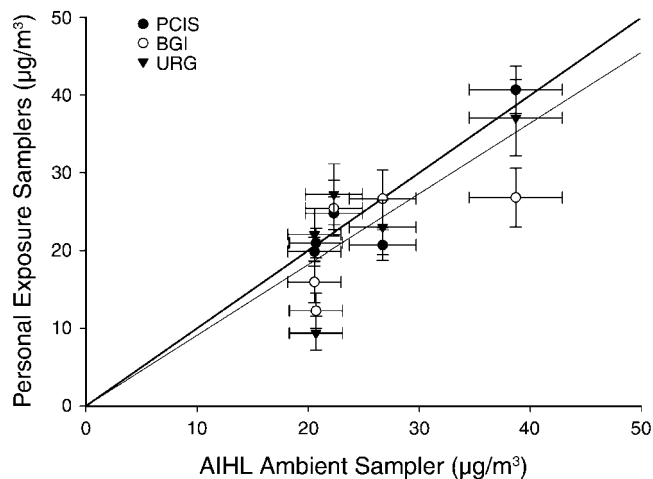


Figure 26. Comparison of PM<sub>2.5</sub> mass measures from samples collected at USC (in Los Angeles) and East St. Louis using co-located PCIS, BGI, and URG personal exposure samplers and a standard AIHL ambient sampler.

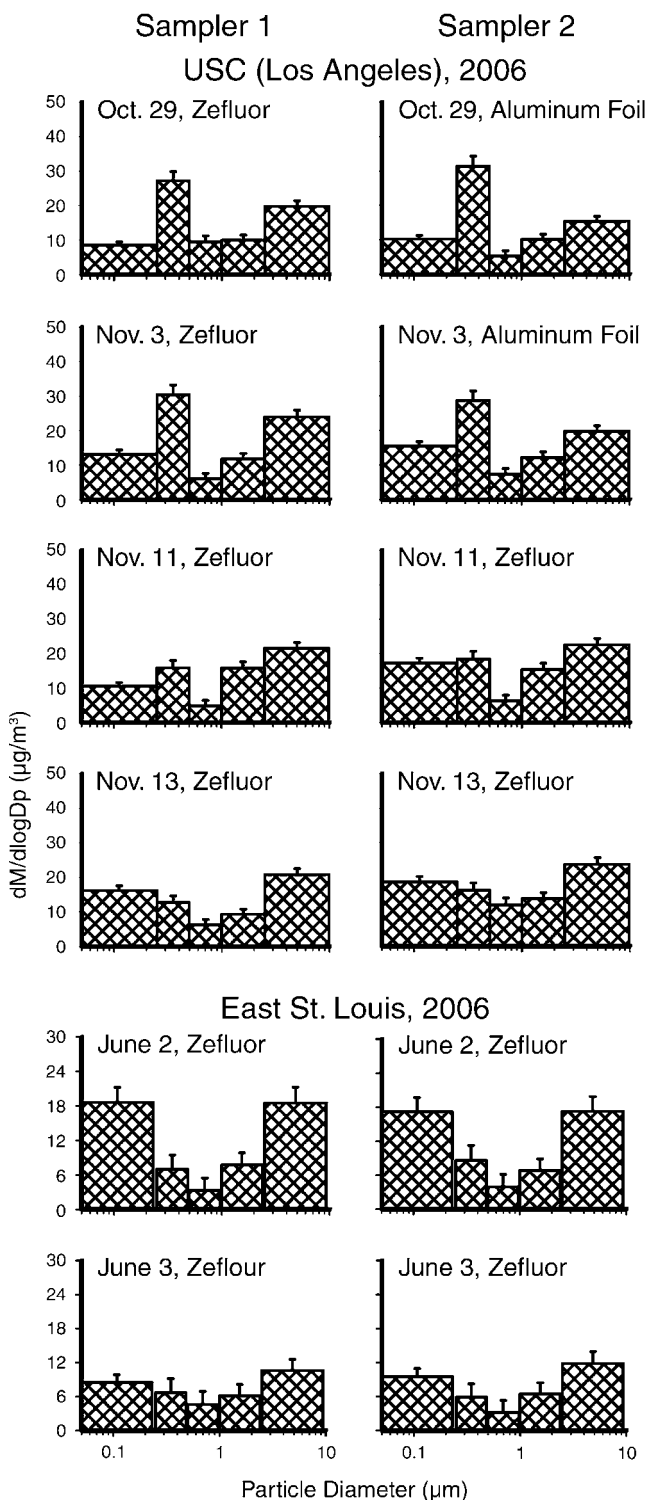


Figure 27. Comparison of size distributions for total PM mass concentrations from samples collected at USC (in Los Angeles) and East St. Louis using PCISs on Zefluor and aluminum foil substrates.

functioning properly, and it was therefore not used for any of the subsequent metal comparisons. Size-resolved total PM concentrations for the co-located PCISs are shown in Figure 27. The plots generally show excellent agreement between the PCISs for each size fraction regardless of the collection substrate. (The PCIS size distribution for November 6, 2003, is not shown here, because no co-located PCIS was used on this day.)

Figure 28 presents PCIS size distributions for six trace metals from samples collected at the site near the main USC campus, near downtown Los Angeles, on October 29, 2003. The plots show a typical distribution for the site during the sampling campaign. With the exception of Pb and V, the coarse fraction (size 2.5 µm or greater) was richer in trace metals compared with PM<sub>2.5</sub>-size fractions. Vanadium, however, exhibited the largest relative contribution in the fine and ultrafine fractions, which implies that the primary source of V was related to the combustion of fossil fuels. The size distribution of Pb revealed a mode at approximately 0.5 µm, which is consistent with findings from past studies (Allen et al. 2001). As expected, Fe concentrations far exceeded those of the other metals presented

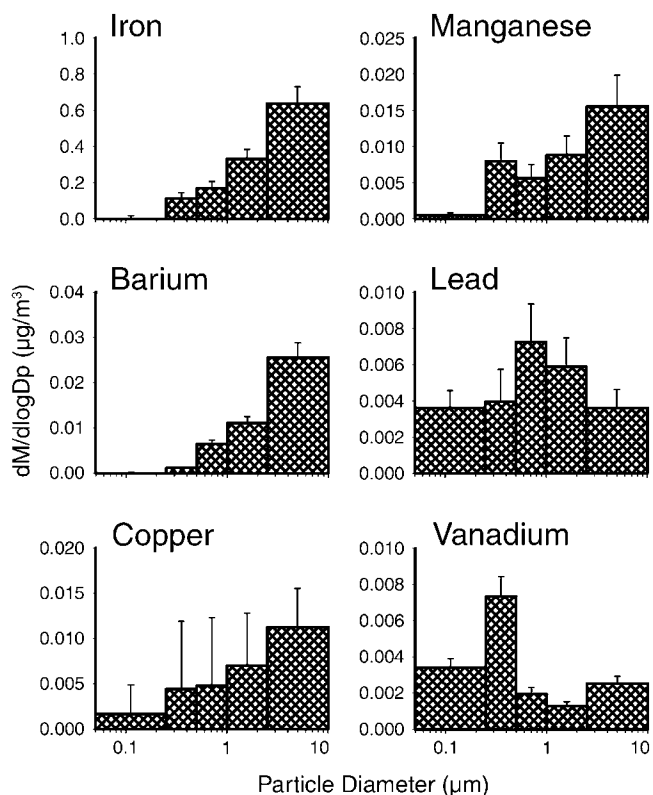


Figure 28. Size distributions for six trace metals from samples collected at USC (in Los Angeles) on October 29, 2003, using PCISs on Zefluor substrates. Note that the y-axis scales differ from panel to panel.

here (ranging from about 50 to 100 times higher than those of the other metals). As can be seen in the figure, it is also clear that total Fe concentrations were dominated by the Fe in the coarse fraction, meaning that the likely sources were resuspended road dust, brake dust, and crustal material. A large fraction of the Ba was also present in the coarse fraction, whose likely source was brake dust and crustal material. As can be seen, Mn had a bimodal distribution, with a small mode at around 1–0.5  $\mu\text{m}$  and a larger mode in the 10- $\mu\text{m}$  range. This, too, is in agreement with findings from past studies (Allen et al. 2001) and probably indicates multiple sources. Past studies indicated that resuspended road dust can be a source of Mn in the coarse fraction and that brake wear can be a significant source in both the sub-micron and coarse fractions (Schauer et al. 2006).

Size-distribution plots paralleling those for the USC site are shown in Figure 29 for the East St. Louis site on June 2, 2006. In general, air concentrations of the six metals were approximately two to four times lower than those from USC. The size distributions were also quite different. In Los Angeles, Fe, Mn, Ba, and Cu showed a consistent decreasing trend as particle size decreased. In East St. Louis, each of these metals had a significant coarse component

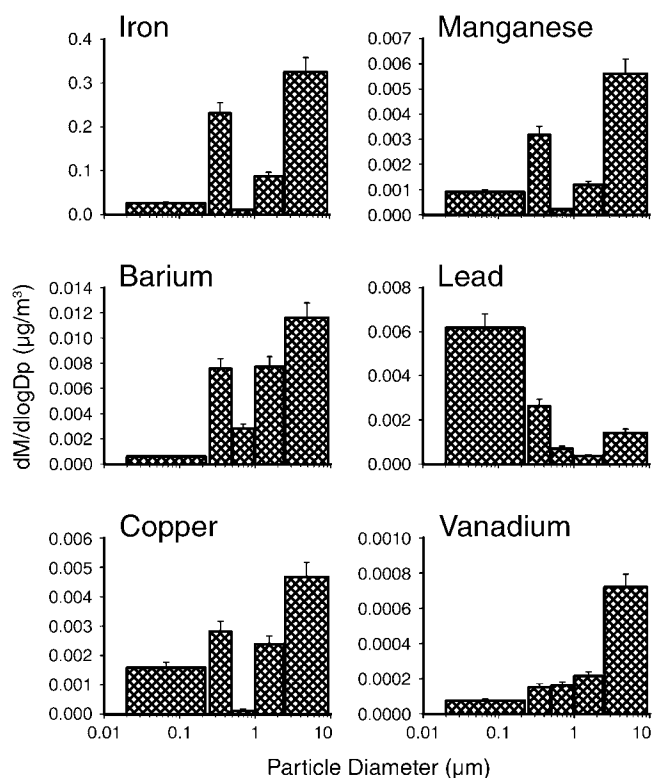


Figure 29. Size distributions for six trace metals from samples collected in East St. Louis on June 2, 2006, using PCISs on Zeffluor substrates. Note that the y-axis scales differ from panel to panel.

but also showed a relatively large mode in the 1-to-0.5- $\mu\text{m}$  fraction that was absent in the USC samples. The Pb size distribution in East St. Louis had a very large ultrafine component with a very small relative coarse component, whereas the Los Angeles site had a relatively even size distribution, including significant coarse and fine fractions. The V size distributions at the two sites were also dramatically different. In East St. Louis, the V was concentrated in the coarse fraction; in Los Angeles it was concentrated in the submicron fraction.

In Figure 30, a direct comparison of metal concentrations from co-located personal exposure samples is presented. These samples were all collected in East St. Louis (the BGI sample mentioned earlier was not included, because of the disagreement in total  $\text{PM}_{2.5}$  mass [see Figure 26]). The error bars in the plots represent the analytic uncertainty of the ICP–MS measurement as well as the error associated with the subtraction of the loading blanks. As can be seen, the URG  $\text{PM}_{2.5}$  minicyclone results were the most reproducible for the tests presented here. This might have been

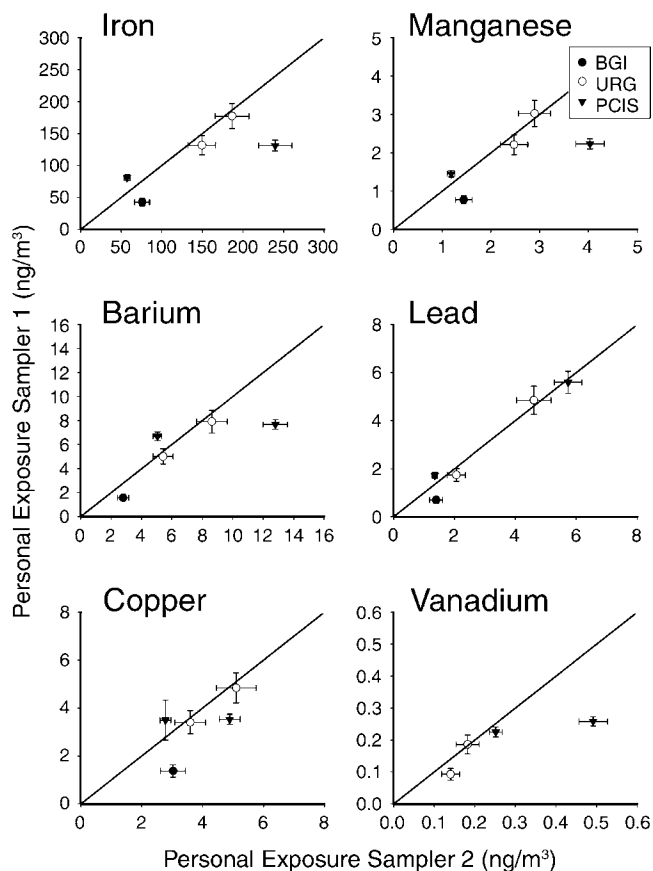


Figure 30. Comparison of air concentrations for six trace metals from replicate  $\text{PM}_{2.5}$  samples collected at USC (in Los Angeles) and East St. Louis using co-located BGI, URG, and PCIS personal exposure samplers. Note that the x- and y-axis scales differ from panel to panel.

caused by sampler design or operation, but it should be noted that the samples were collected under real-world conditions. The PCIS samples collected on June 3, 2006, also generally showed very good agreement. However, significant differences were present for the co-located PCISs on June 2, 2006. This was especially evident for Fe, Mn, Ba, Cu, and V. Upon further inspection of the metal content in the individual size fractions, it was found that in each case a single size fraction (2.5–1 μm) was responsible for the differences. The other four size fractions show very good agreement in terms of metal concentrations (data not shown). The co-located BGI samplers consistently showed different metal contents, with one sampler always showing more than the other. Although the PM<sub>2.5</sub> mass concentrations from the two BGI samplers were statistically similar, it is possible that the slight mass difference (see Figure 26) of the two samplers was associated with the metals discrepancies.

In Figure 31, mass concentrations for trace metals from the personal exposure samples collected in Los Angeles

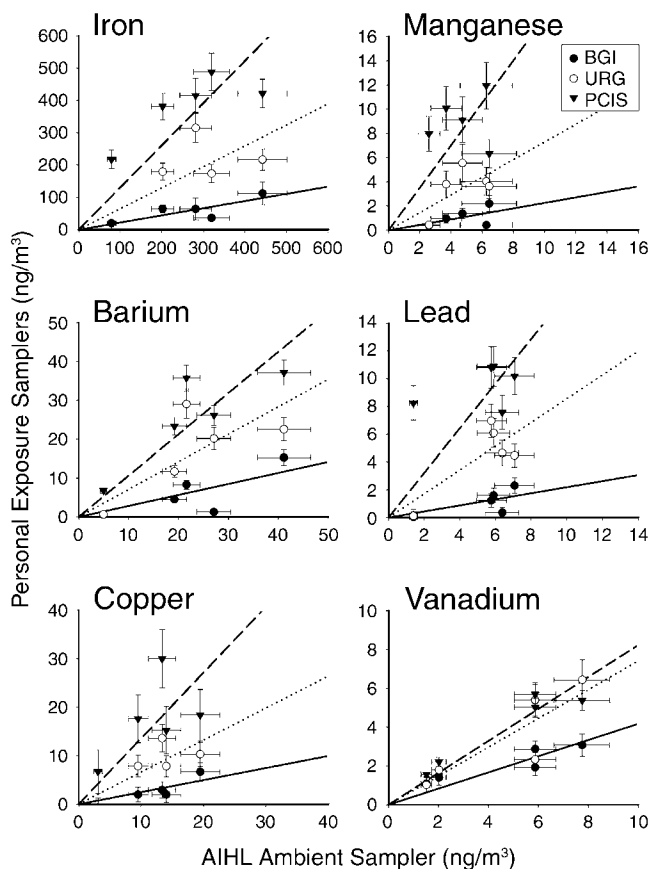


Figure 31. Comparison of mass concentrations for six trace metals from samples collected in Los Angeles using co-located BGI, URG, and PCIS personal exposure samplers and a standard AIHL ambient sampler. Note that the x- and y-axis scales differ from panel to panel.

(PM<sub>2.5</sub> only; summed concentrations of individual stages for the PCISs) are compared with those from the AIHL ambient sampler for each metal. The plots show that the metal concentrations were not consistent across samplers. However, a very clear trend was seen, in that the results for metal PM<sub>2.5</sub> mass concentration ranged from highest to lowest for the co-located PCIS, AIHL, URG, and BGI samplers, respectively, for all metals except V, for which the AIHL results were higher than those for the PCISs. Note also that all the metals except V had a very wide metals distribution across the personal exposure samplers. Figure 32 shows similar plots for the 2 sampling days in East St. Louis, where the personal exposure samplers showed the same trend in metal concentrations — i.e., from highest to lowest for the PCIS, URG, and BGI samplers, respectively — as in Los Angeles. In contrast with the results from Los Angeles, V had the widest distribution across the personal exposure samplers. All of the other metals had narrower distributions across the personal exposure samplers compared with those from the USC site.

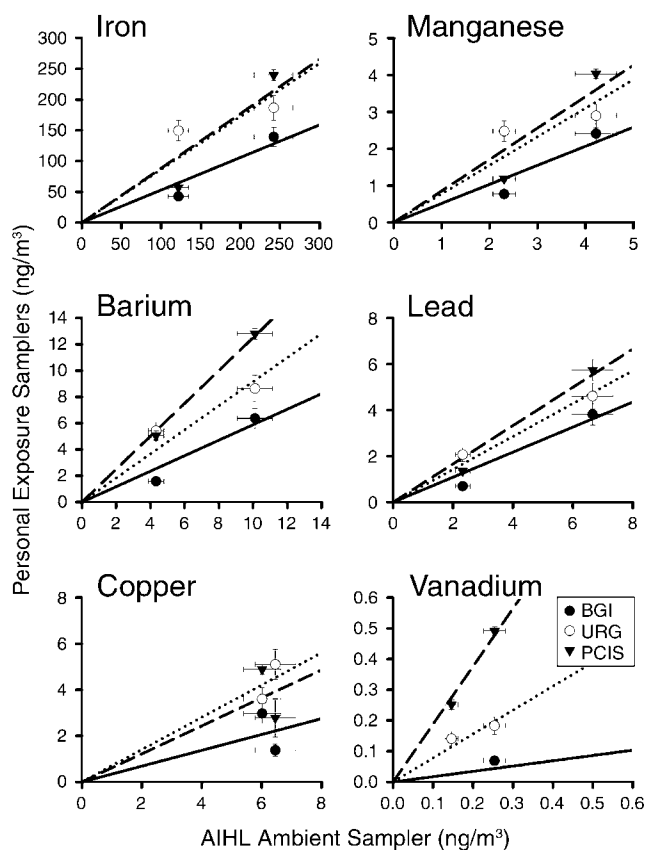


Figure 32. Comparison of mass concentrations for six trace metals from samples collected in East St. Louis using co-located BGI, URG, and PCIS personal exposure samplers and a PM<sub>2.5</sub> ambient sampler. The dashed, dotted, and solid lines represent regression lines for various data points. Note that the x- and y-axis scales differ from panel to panel.

**Table 10.** PM<sub>2.5</sub> Mass and Trace-Metal Comparisons Using Average Ratios and Regression Slopes<sup>a</sup>

	Average Ratio <sup>b</sup>			Regression Slope <sup>c</sup>		
	BGI	URG	PCIS	BGI	URG	PCIS
PM <sub>2.5</sub> mass	0.81 ± 0.23	1.01 ± 0.12	1.12 ± 0.19	0.90	0.98	1.14
Iron	0.30 ± 0.14	0.72 ± 0.42	1.44 ± 0.74	0.27	0.68	1.24
Manganese	0.29 ± 0.16	0.76 ± 0.35	1.72 ± 0.96	0.27	0.73	1.61
Barium	0.31 ± 0.20	0.78 ± 0.42	1.22 ± 0.25	0.29	0.72	1.07
Lead	0.25 ± 0.18	0.75 ± 0.36	1.96 ± 1.81	0.29	0.82	1.42
Copper	0.23 ± 0.15	0.62 ± 0.32	1.36 ± 0.71	0.25	0.66	1.36
Vanadium	0.41 ± 0.25	0.77 ± 0.19	1.19 ± 0.46	0.42	0.74	0.82

<sup>a</sup> The average ratios and the regression slopes take into account the metal concentrations from both Los Angeles and East St. Louis. Note the differences in personal exposure sampler agreement in Figures 31 and 32 when compared with the size distributions of Figures 28 and 29. It is apparent that the agreement is better when a higher fraction of the metal is bound to the submicron size fractions.

<sup>b</sup> Average ( $\pm$  SD) of the ratio of the individual personal exposure sampler and ambient sampler values.

<sup>c</sup> Regression slopes from the plots of the personal exposure sampler versus the ambient sampler (Figures 31 and 32).

The personal exposure samplers showed more variability for some metals than for others, and the degree of variability changed depending on the sampling site. To help determine the cause of these observations, the size distributions shown in Figures 28 and 29 for each metal at each sampling site were examined further. As mentioned before, all of the metals except V showed higher contributions in the coarse fraction in Los Angeles compared with those in East St. Louis. With this in mind, the plots in Figures 31 and 32 were compared, and it was noted that, when a larger fraction of the metal was in the fine and ultrafine fractions, the personal exposure samplers were in closer agreement. This can be seen clearly in the case of V, for example, which at USC was found primarily in the fine fraction (see Figure 28) and for which the personal exposure samplers showed much closer agreement (see Figure 31) than in East St. Louis, where the V was primarily in the coarse fraction (see Figure 29) and the personal exposure samples differed widely (see Figure 32). In fact, better agreement in general was observed across the personal exposure samplers when a higher fraction of the metal was present in the fine and ultrafine fractions compared with the coarse fraction.

The average slopes in Figures 31 and 32 are presented in Table 10, quantifying the average differences between the personal exposure samplers and the ambient sampler. The average slopes for each sampler (i.e., when averaged across all of the metals) were  $0.30 \pm 0.06$ ,  $0.73 \pm 0.06$ , and  $1.25 \pm 0.28$  for the BGI, URG, and PCIS samplers, respectively. The uncertainty represents one standard deviation for all metals. Details for each metal can be seen in Table 10 for the combined Los Angeles and East St. Louis samples. For comparison, the arithmetic mean of the metal concentrations for the personal exposure samplers compared with

those for the ambient sampler for each metal is also shown in the table. This comparison shows that the arithmetic means compared very well with the slopes from the regression.

#### IRON AGING STUDY

Size-resolved Fe concentrations as measured by ICP-MS for the East St. Louis, Los Angeles Basin (Rancho Los Amigos National Rehabilitation Center), and Waukesha sites are shown in Figure 33. The samples from East St. Louis and the Los Angeles Basin showed modes in the coarse fraction of particles, signifying resuspended soil, automobile-brake dust, and road dust as sources, as well as smaller modes in the submicron range, signifying combustion source contributions. The samples from Waukesha for July 12 showed very little in the coarse fraction, signifying very little contribution from crustal elements (Al, Mg, and Ca) in these samples. For July 13 in Waukesha, most of the Fe occurred in the coarse fraction, but there was no mode in the submicron fraction as there had been in East St. Louis and the Los Angeles Basin. The solid-color bars in the plots indicate that speciation (determination of both Fe[II] and Fe[III]) in these size fractions was measured by both XANES spectroscopy and the ferrozine method; the hatch-marked bars (for the smallest size fraction) indicate speciation by the ferrozine method only.

In order to better understand the sources of the aerosols, size-resolved plots of sulfur and common crustal elements (Al, Ca, and Mg) and of other indicators of industrial sources (Mn, Cr, Pb, Ba, and Cu) are shown in Figure 34 and Figure 35, respectively. On July 12, 2006, in Waukesha and February 14, 2006, at the Rancho Los Amigos site, only a small portion of the crustal elements were present

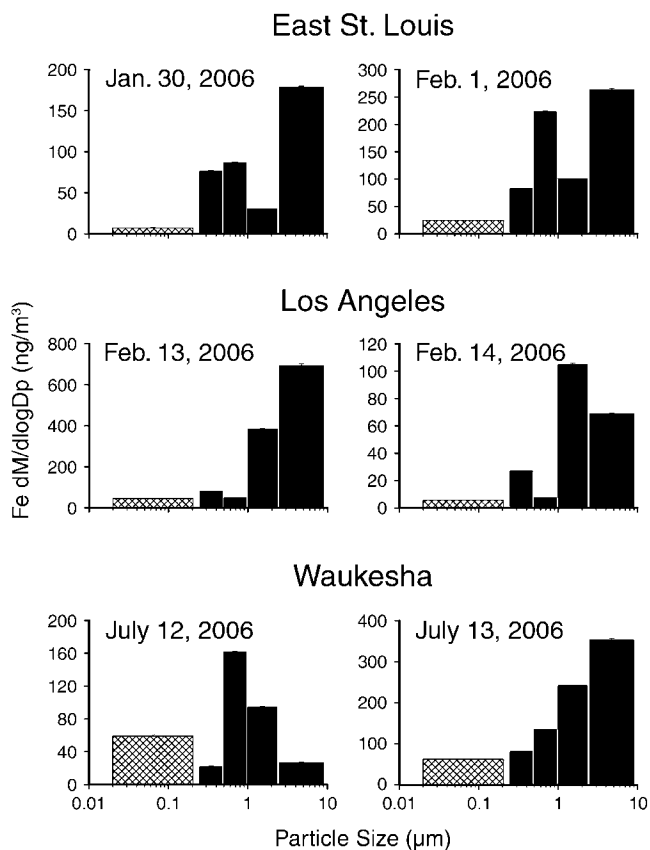


Figure 33. Size distributions for total Fe as measured by ICP-MS from samples collected in East St. Louis, Rancho Los Amigos (in the Los Angeles Basin), and Waukesha. Crosshatched bars indicate collection on a filter that cannot be used for Fe speciation. Solid bars indicate collection from an impactor stage that can be used for Fe(II) and Fe(III) speciation. Note that the y-axis scales differ from panel to panel.

in the coarse fraction, which is consistent with the total Fe data shown in Figure 33. For July 13, an approximately five-fold increase can be observed in crustal contribution in the coarse fraction compared with that of July 12, which is also consistent with the total Fe data shown in Figure 33.

The PM collected at the Rancho Los Amigos site on February 14, 2006, showed a very low air concentration of industrial-source indicator metals (see Figure 35), which indicates that the contributions from anthropogenic sources such as chrome plating and steel manufacturing (i.e., Mn and Cr) were small compared with those of the other sites. The Rancho Los Amigos PM also showed a higher relative contribution from Ba and Cu, which implies a significant contribution from mobile sources (Garg et al. 2000). The East St. Louis PM showed a very high relative contribution from Pb on January 30, 2006, and from both Pb and Ba on February 1, 2006. To a lesser extent, Cu and Mn were also significant in the February 1, 2006, aerosols. Overall, the

Waukesha site showed the greatest amount of industrial-source indicator metals, with a consistent relative metals distribution over the course of the 2 days. These values were about two times those in East St. Louis and about 10 times those in the Los Angeles Basin site. Los Angeles is affected by mobile sources much more than the other two sites are, and the much lower metal concentrations in the Los Angeles Basin demonstrate the impact of industrial sources on the concentrations of metals in PM. Compared with the PM collected at the other two sites, the PM collected in Waukesha showed extremely high concentrations of Cr and Mn, especially in the ultrafine fraction, which were likely caused by the presence of a casting foundry less than a mile east of the sampling site and a facility for stainless-steel fabrication approximately 0.2 miles to the south. A significant amount of Pb was also found in the ultrafine fraction.

The size-resolved plots in Figure 36 show total Fe(II) (solid-color bars) and total Fe(III) (hatchmarked bars) as

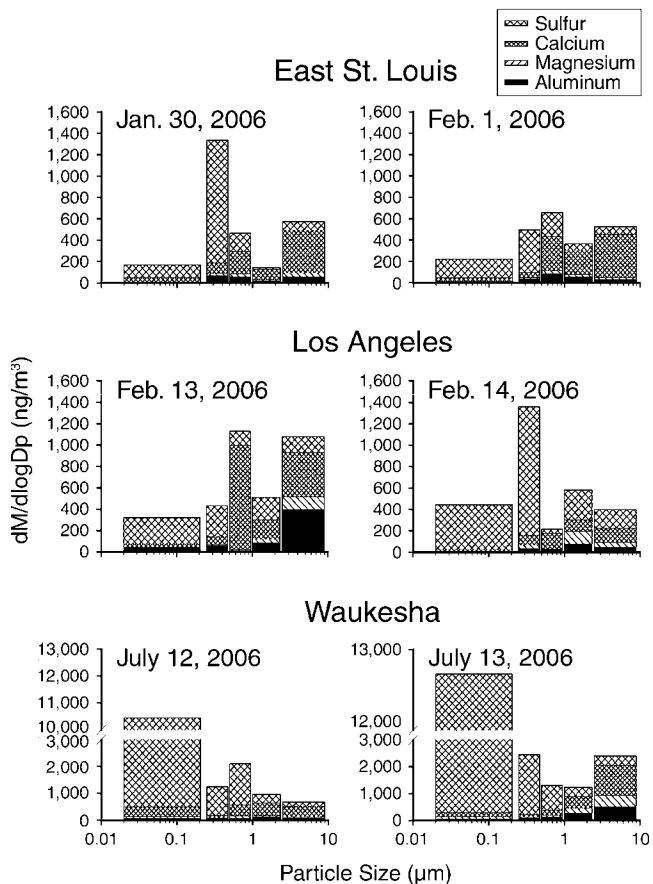


Figure 34. Size distributions for sulfur and three common crustal elements in samples from East St. Louis, Rancho Los Amigos (in the Los Angeles Basin), and Waukesha. Note that some of the y-axis scales differ from panel to panel.

measured by XANES spectroscopy. (Note that there were no data for the  $< 0.25\text{-}\mu\text{m}$  size fraction, because it was not possible to use the necessary Al substrate as the after-filter in the PCISs.) For each sample, all size fractions were dominated by Fe(III), which contributed  $> 50\%$  of the Fe in all cases. We were not able to determine in which chemical form the Fe(III) was bound, but it was likely present as goethite, hematite, or magnetite (Hoffmann et al. 1996). The asterisk (\*) in the Waukesha data for July 13, 2006, indicates that no XANES data were available for this size fraction on that day.

Figure 37 shows size-resolved total Fe(II) and total Fe(III) after aging of the January 30, 2006, sample collected at the East St. Louis Supersite over the course of 40 days in the Biotron. In this sample, a sharp, 100% increase in Fe(II) was observed in the coarse fraction between the zero- and the 10-day aging periods. After 10 days, however, there was very little change in the Fe(II)/Fe(III) ratio for this fraction. In contrast, the smallest size fraction ( $0.5\text{--}0.25\ \mu\text{m}$ )

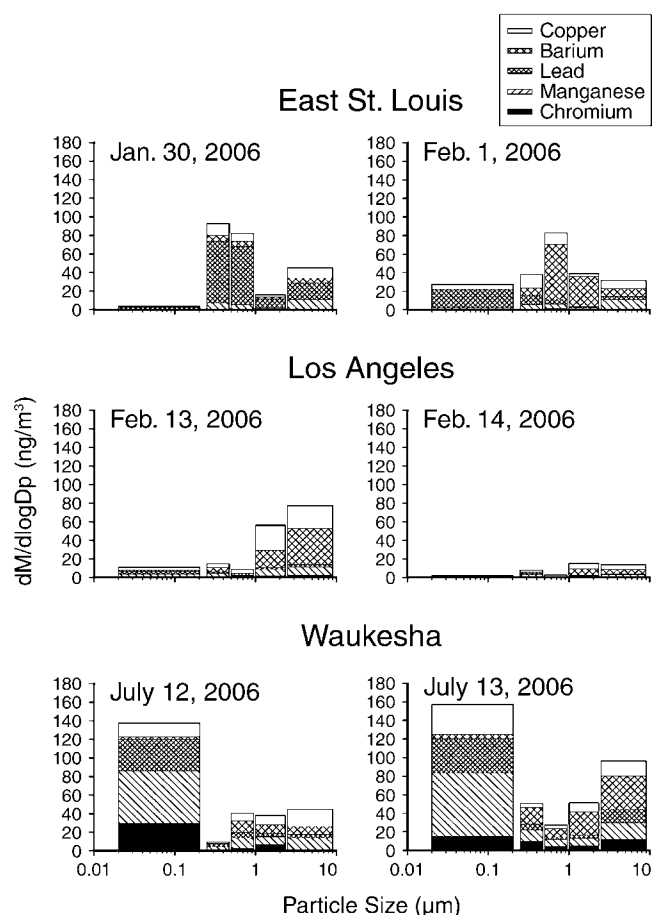


Figure 35. Size distributions for five source-indicator metals from samples collected in East St. Louis, Rancho Los Amigos (in the Los Angeles Basin), and Waukesha.

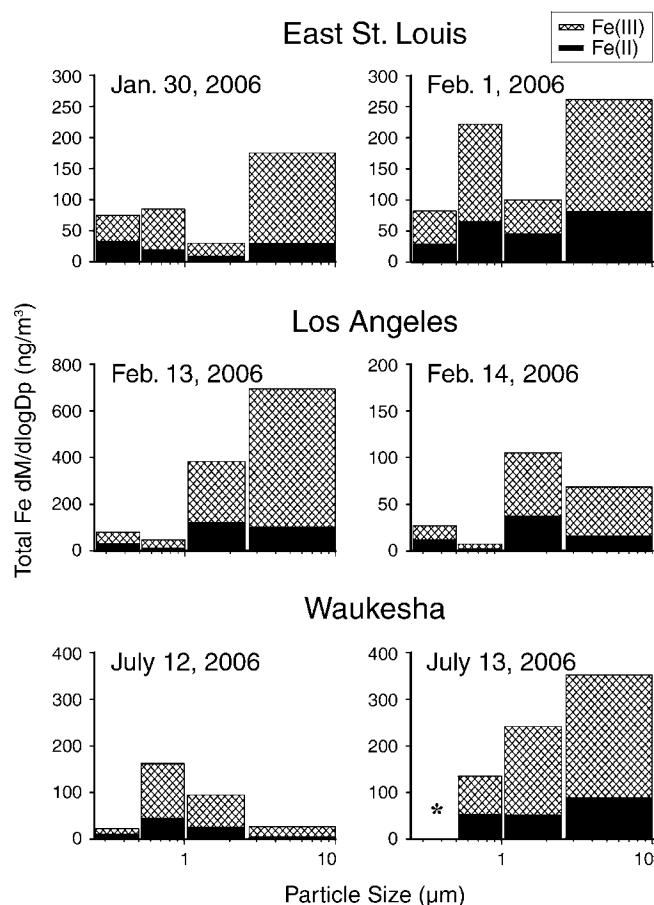


Figure 36. Size distributions for total Fe(II) and Fe(III) as measured by XANES spectroscopy in  $\text{PM}_{10}$  samples collected in East St. Louis, Rancho Los Amigos (in the Los Angeles Basin), and Waukesha. Asterisk indicates unavailable data. Note that some of the y-axis scales differ from panel to panel.

showed a relatively small increase (17%) in the Fe(II) fraction after 10 days of aging but then significant decreases after 20 and 40 days.

The plots in Figure 38 summarize Fe(II) concentrations (in  $\text{ng}/\text{m}^3$ ) for the samples collected in East St. Louis and the Rancho Los Amigos site in the Los Angeles Basin. Each plot shows a different size fraction, and the trends for Fe(II) collected in varying sizes can be seen over the course of aging. In general, the Fe(II) in the coarse fraction ( $> 2.5\ \mu\text{m}$ ) tended to increase over time, while the Fe(II) in the smallest fraction ( $0.5\text{--}0.25\ \mu\text{m}$ ) tended to decrease. The intermediate-size fractions showed very little change.

In addition to the total Fe(II) and Fe(III) measurements made by XANES spectroscopy, soluble Fe(II) and Fe(III) measurements were made on co-located filters using the ferrozine method. Size-fractionated soluble Fe(II) (solid-color bars) and Fe(III) (hatched bars) are shown in

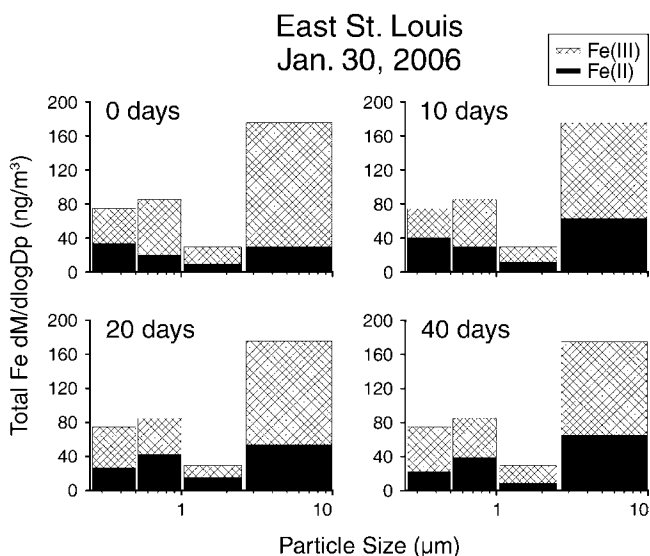


Figure 37. Size distributions for total Fe(II) and Fe(III) as measured by XANES spectroscopy in PM<sub>10</sub> samples collected in East St. Louis, showing changes over 40 days of aging.

Figure 39. The data are for initial soluble Fe(II) and Fe(III) values at a point when they had not yet been artificially aged. It is interesting to note that, regardless of the total Fe concentrations in a given sample, all of the soluble Fe concentrations ranged around 2 to 20 ng/m<sup>3</sup> (on a dM/dlogDp scale). Unlike the relatively low Fe(II)/Fe(III) ratios found in the XANES data, the soluble fractions tended to be primarily Fe(II), although significant amounts of Fe(III) were still present in many samples. It was also observed that each sampling site had a different soluble Fe signature for these 2 sampling days. The PM from Waukesha showed a relatively even Fe size distribution, with a very small mode around 1 µm. Further, for all size fractions on both days in Waukesha, soluble Fe(II) and soluble Fe(III) were approximately equal (i.e., Fe(II)<sub>sol</sub>/Fe(total)<sub>sol</sub> ≈ 0.5). The PM from the Los Angeles Basin site showed a soluble Fe size distribution similar to that of the total Fe distribution prior to aging shown in Figure 33. Of the days sampled, the PM collected in Los Angeles showed the greatest air concentration of soluble Fe. In general, the Fe(II)<sub>sol</sub>/Fe(total)<sub>sol</sub>

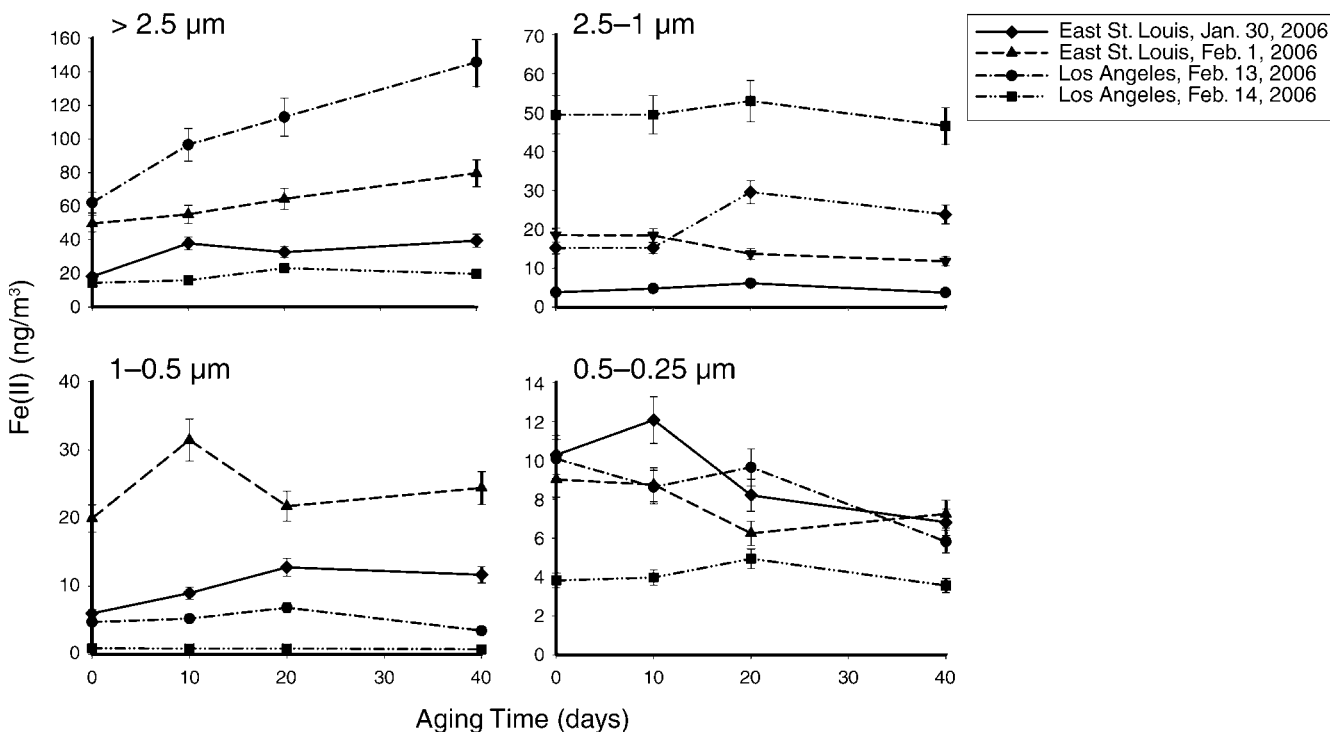
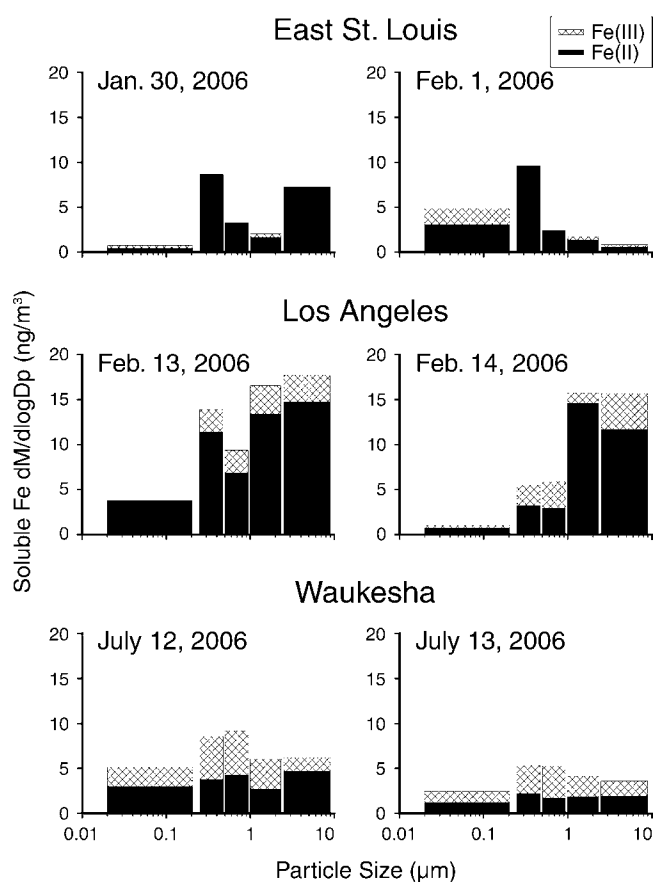


Figure 38. Air concentrations for total Fe(II) in four size fractions as measured by XANES spectroscopy from samples collected in East St. Louis and Rancho Los Amigos (in the Los Angeles Basin), showing changes over 40 days of aging. Note that the y-axis scales differ from panel to panel.



**Figure 39.** Size distributions for soluble Fe(II) and Fe(III) in PM<sub>10</sub> samples collected in East St. Louis, Rancho Los Amigos (in the Los Angeles Basin), and Waukesha. The Fe(II) and Fe(III) were measured using the ferrozine method followed by addition of HA.

fractions in Los Angeles were around 0.75, with the ratio approaching 0.9 for particles  $< 0.25 \mu\text{m}$ , significantly greater than those for Waukesha. Lastly, both East St. Louis samples showed modes at around  $0.5 \mu\text{m}$ , but few other similarities were present. The samples for February 1, 2006, showed by far the greatest discrepancy between coarse and PM<sub>2.5</sub> soluble Fe for all samples, the PM<sub>2.5</sub> fraction being about 32 times larger than the coarse fraction. In contrast with the PM collected in the Los Angeles Basin, the aerosols collected in East St. Louis showed a relatively low Fe(II)<sub>sol</sub>/Fe(total)<sub>sol</sub> ratio of 0.4 for PM  $< 0.25 \mu\text{m}$  and an extremely high ratio (0.98) for all other size fractions, indicating that very little soluble Fe(III) was present in the PM  $> 0.25 \mu\text{m}$  collected in East St. Louis during the sampling period.

To better understand the fraction of labile Fe in the East St. Louis, Rancho Los Amigos, and Waukesha samples, the coarse ( $> \text{PM}_{2.5}$ ) and PM<sub>2.5</sub> fractions of percent soluble Fe compared with total Fe and total Fe(II) are presented in

Table 11. The table shows that the fraction of labile Fe can vary significantly depending on the sample, ranging from  $< 1\%$  to 17% of the total Fe. This likely depends on the “age” of the aerosol at the time of collection as well as on the varying sources. Further, with the exception of the February 14, 2006, sampling date in the Los Angeles Basin and the July 12, 2006, sampling date in Waukesha, the PM<sub>2.5</sub> aerosols had a greater labile fraction than the coarse particles when compared with total Fe. Because of a light rain in the Los Angeles Basin during the February 14, 2006, sampling date, it is likely that aerosols with drastically different compositions were collected during the 2 Los Angeles sampling days. The greater soluble Fe fraction observed in the coarse mode compared with the PM<sub>2.5</sub> fraction for the sample collected in Waukesha on July 12, 2006, was likely caused by the extremely low total Fe concentration in the coarse fraction for this day.

Table 11 also presents a comparison of soluble Fe(II) with total Fe(II). Of the total Fe(II), the soluble fraction of PM<sub>2.5</sub> Fe(II) ranged from 9% up to almost 40%. Although this is a relatively broad range, it is clear that the majority of the Fe(II) in these urban atmospheric aerosols was not in a soluble phase. Size comparisons in Table 11 show that three of the samples had a greater labile fraction in the coarse particles and that two others had a greater labile fraction in the PM<sub>2.5</sub> fraction. This comparison was not possible for the sixth sample, collected on July 13, 2006, in Waukesha, because XANES data were not available. It should be noted, however, that PM  $< 0.25 \mu\text{m}$  was not included in the analysis, because XANES analysis was not possible for this size fraction. Given that a majority of the soluble Fe in the PM  $< 0.25 \mu\text{m}$  was Fe(II), the actual fraction of soluble Fe(II) in the amount of total Fe(II) in the PM<sub>2.5</sub> size range will be greater than is shown in the table. This effect will be marginal, however, because the Fe concentration in this fraction is generally small compared with that of the other size fractions.

Size-fractionated soluble Fe plots over the course of the aging process are shown in Figure 40 for the samples collected on July 12, 2006, in Waukesha. Over the 6-day aging period, the soluble Fe(II) in the coarse fraction is seen to increase slightly by the first day and thereafter to decrease steadily, while the soluble Fe(III) fraction remained relatively steady. This amounts to an overall decrease in soluble Fe in the coarse fraction over time. The most prominent feature of these plots is the overall Fe spike at 3 days in the size ranges of  $0.25$  to  $1 \mu\text{m}$  and the spike at 1 day for PM  $< 0.25 \mu\text{m}$ . The spikes are largely the result of an increase in Fe(II); Fe(III) remained relatively constant. These results indicate that Fe(II) or Fe(III) was undergoing chemical changes that led to a higher solubility for Fe(II). After 6 days, however, both species returned to their approximate initial

**Table 11.** Comparison of Total Soluble Fe with Total Fe and Total Fe(II) with No Aging

Sample	Size Fraction	Total Fe (ng/m <sup>3</sup> )	% Soluble Fe(II) of Total Fe	% Soluble Fe(II) of Total Fe(II) <sup>a</sup>	% Soluble Fe of Total Fe
East St. Louis					
Jan. 30, 2006	> 2.5 μm	107.4	4.1	24.0	4.1
Jan. 30, 2006	PM <sub>2.5</sub>	68.6	7.1	21.3	7.8
Feb. 1, 2006	> 2.5 μm	158.5	0.23	0.7	0.33
Feb. 1, 2006	PM <sub>2.5</sub>	158.9	4.8	8.8	6.1
Los Angeles					
Feb. 13, 2006	> 2.5 μm	417.8	2.1	14.3	2.6
Feb. 13, 2006	PM <sub>2.5</sub>	241.0	6.2	16.9	7.4
Feb. 14, 2006	> 2.5 μm	41.4	17.0	49.1	22.8
Feb. 14, 2006	PM <sub>2.5</sub>	58.2	14.5	38.6	18.6
Waukesha, Wisconsin					
July 12, 2006	> 2.5 μm	16.2	17.5	77.8	23.0
July 12, 2006	PM <sub>2.5</sub>	157.6	4.3	24.5	8.5
July 13, 2006	> 2.5 μm	212.2	0.54	2.1	1.0
July 13, 2006	PM <sub>2.5</sub>	228.6	1.4	N/A	3.3

<sup>a</sup> XANES data were not available for particles < 0.25 μm. For this column only, then, the PM<sub>2.5</sub> rows indicate a particle size range of 0.25 to 2.5 μm.

concentrations, suggesting that insoluble forms of Fe(II) and Fe(III) were being formed.

The PM collected at the other sampling sites were also submitted to an aging study, in which the East St. Louis and Rancho Los Amigos samples were aged for 40 days and the Waukesha samples were aged for 10 days. The

results of the St. Louis and Rancho Los Amigos study are shown in Figure 41, and the results of the Waukesha study are shown in Figure 42. Both figures plot air concentrations (in ng/m<sup>3</sup>) of soluble Fe(II) against aging time.

Four data points (0, 10, 20, and 40 days) were collected over a 40-day period to determine how the Fe(II) content in the aerosol changed (see Figure 41). For 3 of the 4 sampling days in East St. Louis and the Los Angeles Basin, a sharp decrease in soluble Fe(II) was observed within 10 days of sampling. The February 1, 2006, sampling date in East St. Louis was the only one that didn't follow this trend. On this day, both size fractions > 1 μm actually showed an increase in Fe(II) after the initial measurement. The Fe in the submicron particles followed the trend of the other sampling days. The reason for this difference is not yet clear, but it was likely caused in part by the very different initial soluble Fe(II) compared with that of the other days, as shown in Figure 39.

In order to achieve a better understanding of the chemical processes that occur within 10 days of PM collection, the aerosols from Waukesha were aged for shorter times of 0, 1, 3, 6, and 10 days. The air concentrations of the soluble Fe(II) for these time points are shown in Figure 42. The plots show that in the submicron region Fe(II) concentrations spiked at all size fractions at around 1 to 3 days. After this, the values returned to near their initial states. The supermicron particles did not show this behavior. In fact, these particles showed very little if any increase in soluble

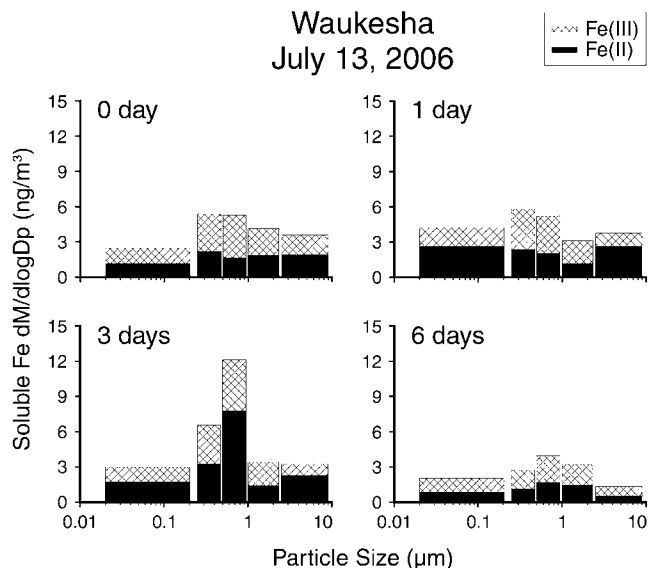


**Figure 40.** Size distributions for soluble Fe(II) and Fe(III) as measured by the ferrozine method from samples collected in Waukesha, showing changes over 6 days of aging.

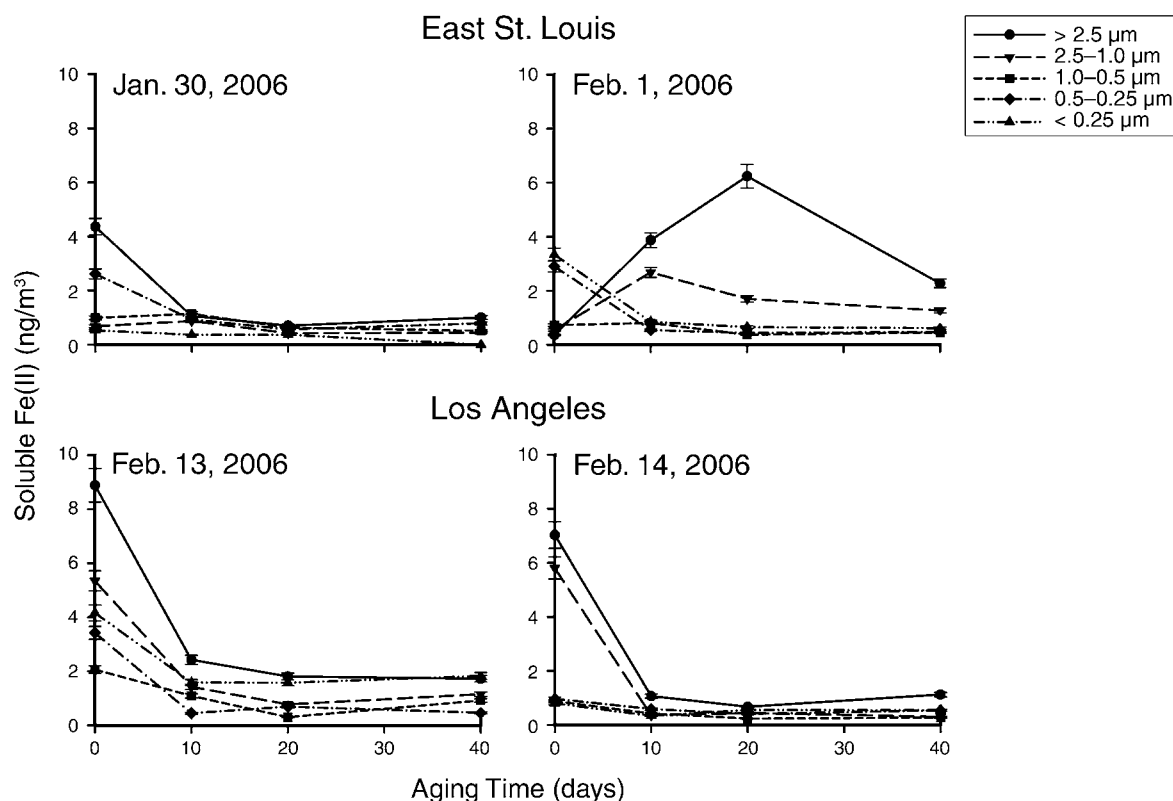


Figure 41. Air concentrations for soluble Fe(II) in five size fractions as measured by the ferrozine method from samples collected in East St. Louis and in Rancho Los Amigos (in the Los Angeles Basin), showing changes over 40 days of aging.

Fe(II) over the course of the study and generally showed a decreasing trend. These results are also summarized in Table 12.

Very little similarity was observed between the total Fe and soluble Fe trends. The XANES data revealed that the overall Fe(II) and Fe(III) trends followed a relatively smooth relationship, with very few (and less pronounced) Fe(II) spikes observed for any size fraction. However, the soluble Fe fraction (especially in the submicron region) showed distinct Fe(II) peaks at around 1 to 3 days. The reason for this apparent contradiction could be twofold. First, the soluble Fe was generally a very small percentage of the total Fe in the sample, ranging from < 1% to about 20% (see Table 11). This would cause small changes in the soluble Fe fraction to remain unnoticed in the less-sensitive total Fe XANES measurements. Second, even though Fe(0) was not observed in the XANES measurements, it is possible that a very small fraction (< 5%) of the total Fe was in fact Fe(0). Ultrafine Fe(0) particles have been observed by other researchers to oxidize to Fe(II) and then Fe(III) (Papaefthymiou et al. 1990; Parkhomenko et al. 1990), which would also explain the behavior of the submicron

soluble Fe fraction in the Waukesha samples during short-term transport.

In this study, we developed a XANES spectroscopy method to determine the total Fe(II) and Fe(III) content of personal exposure samples of atmospheric aerosols. Using a wet-chemical Fe speciation method, the speciation changes in ambient Fe were measured under tightly controlled atmospheric conditions. In all sampling locations, we found that all size fractions > 0.25 μm were primarily in the form of Fe(III) but that most of the soluble fraction was in the form of Fe(II) with strong contributions as Fe(III). It was also found that a majority of the Fe(II) in the PM<sub>2.5</sub> fraction was not labile in our leaching solution (pH = 4.5 acetate buffer).

The XANES results showed that Fe(II) associated with the coarse fraction had a tendency to increase over time and that Fe(II) associated with the smaller 0.5-to-0.25-μm fraction tended to decrease over time. These changes were generally very minor over a long time span (40 days), much longer than the atmospheric residence time of most urban PM. On the timescale of urban aerosols (about 1 week), there was generally very little change in the total Fe(II)

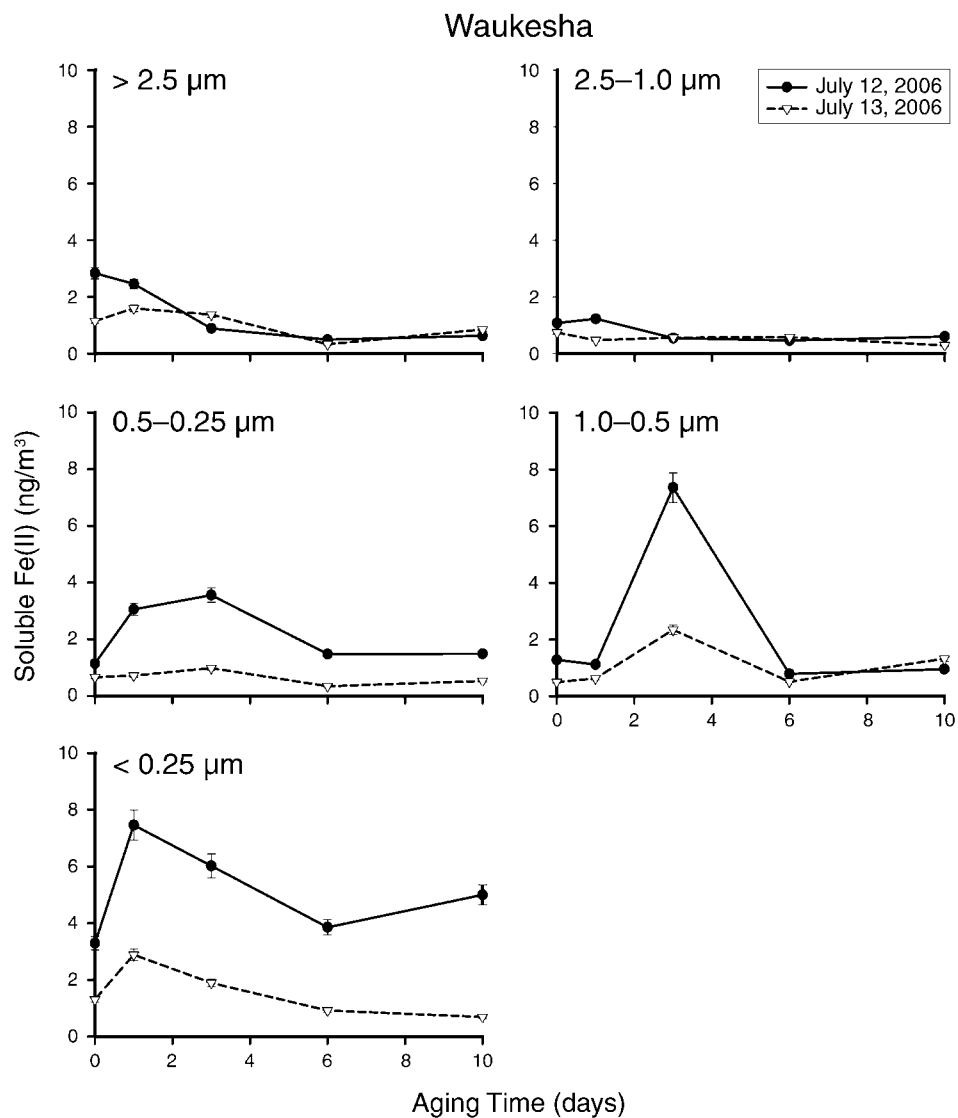


Figure 42. Air concentrations for soluble Fe(II) in five size fractions as measured by the ferrozine method from samples collected in Waukesha, showing changes over 10 days of aging.

**Table 12.** Time Taken for Soluble Fe(II) to Reach Maximum Values in Two Samples Collected in Waukesha

Size Fraction ( $\mu\text{m}$ )	Time Taken	Fe(II) Oxidation Time <sup>a</sup>
> 2.5	No significant peak	Not significant
2.5–1.0	No significant peak	Not significant
1.0–0.5	3 days	6 days
0.5–0.25	3 days	6 days
< 0.25	1 day	6 days

<sup>a</sup> Oxidation time is the time it took for soluble Fe(II) values to come back to equilibrium (from time  $t = 0$ ). Note that Fe(II) peaks were observed only in the submicron fractions.

concentrations. Because of their relevance to long-range transport, however, a brief discussion of the processes that potentially determine species conversion is warranted. Within atmospheric PM, there likely exists a competition between photoreduction to Fe(II) and oxidation to Fe(III). We expect that oxidation is the dominant mechanism for the smaller particles, because of their greater reactive surface area, thus shifting the balance toward Fe(III), and that photoreduction is the dominant mechanism for the larger particles, thus shifting the balance toward Fe(II).

Compared with the total Fe(II) and Fe(III) trends, more drastic changes were noted in the soluble Fe fraction. We observed that (with the exception of the supermicron fraction from February 1) after around 10 days of aging the soluble fraction of Fe(II) was stable for at least 40 days. In the short-term experiments, we observed a spike in submicron soluble Fe(II) after 1 to 3 days, followed by a decline after 6 to 10 days (see Figure 42). The aerosols in the project were aged in an atmosphere that only represented one possible atmospheric condition. It is not clear what changes in Fe speciation might occur under different conditions (i.e., cloudy, very high or low relative humidities, etc.). However, because the changes in soluble Fe occurred rather rapidly (1 to 3 days), our experiments imply that weather conditions can have a large effect on actual exposures to soluble Fe.

### MANGANESE SPECIATION STUDY

A size-resolved plot showing total soluble Mn in samples for 2 days in Toronto using pH = 4.3 acetate buffer is shown in Figure 43. The greatest concentration of soluble Mn was found in the coarse fraction, with concentrations decreasing with size. For PM < 0.5  $\mu\text{m}$ , there was no detectable soluble Mn. This result is similar to that of Allen and colleagues (2001), who found that total Mn concentrations measured by ICP–MS were not detected below

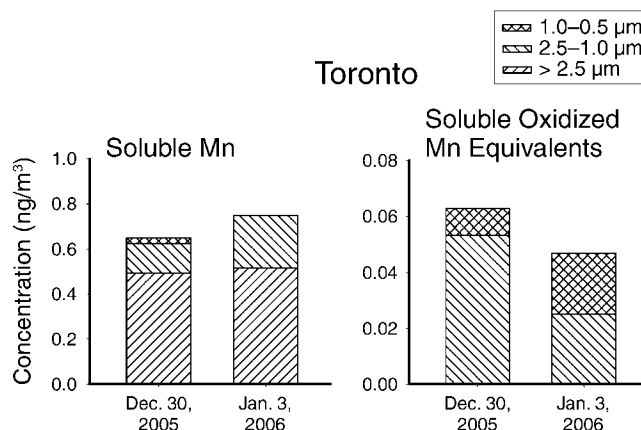


**Figure 43.** Comparison of air concentrations for soluble Mn as measured by the FAD method and soluble oxidized Mn equivalents as measured by the *o*-tolidine method in three size fractions from samples collected in Toronto. Note that the majority of the soluble Mn—and none of the soluble oxidized Mn—was detected in the coarse fraction. Note also that the y-axis scales differ from panel to panel.

0.2  $\mu\text{m}$ . A comparison of these samples with total soluble Mn samples from East St. Louis is shown in Table 13. It was observed that on these sampling days the overall air concentration of Mn was greater at the East St. Louis site and that the PM concentration was roughly similar at both sites. Table 14 shows the relative contribution of the soluble Mn fraction to total Mn for the sampling days in Toronto. The soluble Mn percent of total Mn was found to differ greatly between the sites. Almost 40% of the Mn in the Toronto composite sample was soluble; a maximum of 20% of the Mn in the East St. Louis sample was soluble (see Table 9).

Table 14 also details the relative abundance of oxidized Mn in the total soluble fraction. The table shows that, for

**Table 13.** Comparison of Soluble Mn Air and Particle Concentrations for PM<sub>10</sub> Samples Collected in East St. Louis and Toronto

Sample	PM <sub>10</sub> Mass ( $\mu\text{g}$ )	% Soluble Mn of PM	Soluble Mn ( $\text{ng}/\text{m}^3$ )
East St. Louis			
Mar. 17, 2005	391	0.09	3.57
Mar. 19, 2005	301	0.03	0.83
Mar. 21, 2005	329	0.03	1.06
Toronto <sup>a</sup>			
Dec. 30, 2005	255	0.03	0.64
Jan. 2, 2006	392	0.02	0.75

<sup>a</sup> PM<sub>10</sub> mass values for Toronto were summed for each stage of the PCISs.

**Table 14.** Comparison of Soluble Mn with Soluble Oxidized Mn for PM<sub>2.5</sub> and PM<sub>10</sub> Samples Collected in Toronto<sup>a</sup>

Sample	Total Mn by ICP-MS (ng/filter)	Soluble Mn (ng/filter)	Soluble Oxidized Mn (ng/filter)	% Oxidized Mn of Soluble Mn (as Mn[III])
Dec. 30, 2005				
PM <sub>2.5</sub>	N/A	1.7	0.68	40
PM <sub>10</sub>	N/A	7.0	0.68	9.7
Jan. 2, 2006				
PM <sub>2.5</sub>	N/A	2.3	0.51	21
PM <sub>10</sub>	N/A	7.9	0.51	6.4
Jan. 13 and 19, 2006				
Composite PM <sub>2.5</sub>	45	17	3.1	18
Composite PM <sub>10</sub>	74	28	3.4	12

<sup>a</sup> PM<sub>2.5</sub> and PM<sub>10</sub> mass values were summed for each stage of the PCISs.

the samples measured in this study, a higher fraction of the soluble Mn was always found in the PM<sub>2.5</sub> size fraction compared with the PM<sub>10</sub> size fraction. In PM<sub>2.5</sub>, the oxidized Mn ranged from about 20% to 40% of the total soluble Mn [as Mn(III)]. The data for the limited sampling days presented here, however, should not be taken to represent the sites at all times of the year. Size-fractionated total soluble oxidized Mn equivalents are also shown in Figure 43 for samples from December 30, 2005, and January 3, 2006, at the Toronto site. First, it is interesting to note that oxidized Mn was not detected for either day in the coarse mode (> 2.5 µm), the size fraction with the greatest overall soluble Mn. For both December 30 and January 3, soluble oxidized Mn was found only in the intermediate size fractions (2.5 to 0.5 µm). As was expected, no soluble oxidized Mn was present in the fractions < 0.5 µm. The January 13 and 19 composite sample was very similar to that of December 30 and January 3, except that a small amount of oxidized Mn was detected in the coarse fraction.

The speciation results presented here suggest that the two sites were quite different with respect to their Mn sources. Although similar total Mn concentrations were found in the sites' PM, the aerosols from Toronto showed a significant amount of oxidized Mn, and the oxidized Mn in the PM<sub>10</sub> samples from East St. Louis were below the DL. We also found that no soluble oxidized Mn was detected in the coarse fraction in Toronto, which consisted primarily of resuspended soils and automobile-brake dust. The fact that oxidized Mn was detected only in the PM<sub>2.5</sub> fraction implies that the source of the soluble oxidized Mn was combustion related and might have been a result of the combustion of the Mn-based fuel additive MMT.

## ST. LOUIS TRUCK TERMINAL RESULTS

### Sample Design and Validation

The sample set from the St. Louis truck terminal included personal exposure samples from people with five different job descriptions and area samples from four different worksites and from a nearby urban background location collected over the course of 5 days in August 2003 (see Table 15). In order to match personal exposure samples with the appropriate area samples, an am (time 0:00 to 12:00) percentage and pm (time 12:00 to 23:59) percentage was calculated for each personal exposure sample. The area samples were then classified as am or pm for each date, and a matching area sample was calculated using the am/pm percentage for each personal exposure sample by date. Averages were used when two area samples had been collected simultaneously. The personal exposure samples were used individually for correlation plots.

All personal exposure samples were collected using the same sampler brand and model (to minimize potential differences caused by differences in equipment). Because the urban background sample was collected at the East St. Louis Supersite, it could be validated using co-located OC and EC measurements made by a Sunset Labs semicontinuous OC-EC analyzer (Bae et al. 2004). The analyzer collects samples for 1 hour and then analyzes them for 1 hour, resulting in 12 hours worth of measurements per day. The two sets of measurements were not expected to match exactly but to show the same trends. Figure 44 and Figure 45 offer a comparison of the measurements for OC and EC, respectively. The (undened) personal exposure sampler showed a higher OC concentration for the period than

**Table 15.** Sample Matrix for St. Louis Truck Terminal Study

Personal Exposure Samples Code	Smoker	Start Date	Stop Date	% AM	% PM	Aug.								
						25 AM	25 PM	26 AM	26 PM	27 AM	27 PM	28 AM	28 PM	29 AM
<b>Dockworkers</b>														
D1	No	Aug. 25	Aug. 25	41.2	58.8	x	x							
D2	No	Aug. 25	Aug. 25	0.0	100.0		x							
D3	No	Aug. 25	Aug. 26	60.3	39.7		x	x						
D4	Yes	Aug. 25	Aug. 26	32.4	67.6		x	x						
D5	No	Aug. 26	Aug. 26	70.6	29.4			x	x					
D6	No	Aug. 26	Aug. 27	50.2	49.8				x	x				
D7	No	Aug. 26	Aug. 27	18.6	81.4				x	x				
D8	No	Aug. 26	Aug. 27	40.0	60.0				x	x				
D9	No	Aug. 27	Aug. 27	70.9	29.1					x	x			
D10	No	Aug. 27	Aug. 28	20.1	79.9						x	x		
D11	No	Aug. 27	Aug. 28	38.8	61.2						x	x		
D12		Aug. 27	Aug. 28	50.3	49.7						x	x		
D13	Yes	Aug. 28	Aug. 28	36.1	63.9							x	x	
D14	No	Aug. 28	Aug. 28	65.3	34.7							x	x	
<b>Mechanics</b>														
M1	No	Aug. 25	Aug. 25	0.0	100.0		x							
M2	No	Aug. 25	Aug. 25	0.0	100.0		x							
M3	No	Aug. 25	Aug. 26	75.8	24.2		x	x						
M4	No	Aug. 27	Aug. 27	48.8	51.2					x	x			
M5	No	Aug. 27	Aug. 27	0.0	100.0						x			
M6	No	Aug. 27	Aug. 27	0.0	100.0						x			
M7	No	Aug. 28	Aug. 28	0.0	100.0									x
<b>Hostlers</b>														
H1	No	Aug. 25	Aug. 25	0.0	100.0		x							
H2	No	Aug. 26	Aug. 26	65.9	34.1			x	x					
H3	No	Aug. 27	Aug. 27	100.0	0.0					x				
H4	No	Aug. 27	Aug. 28	66.2	33.8						x	x		
<b>Long-Haul Drivers</b>														
LHD1	No	Aug. 25	Aug. 25	100.0	0.0	x								
LHD2		Aug. 25	Aug. 25	0.0	100.0		x							
LHD3		Aug. 25	Aug. 25	0.0	100.0		x							
LHD4	No	Aug. 25	Aug. 26	34.0	66.0		x	x						
LHD5		Aug. 25	Aug. 26	75.8	24.2		x	x						
LHD6		Aug. 25	Aug. 26	75.8	24.2		x	x						
LHD7	No	Aug. 26	Aug. 26	77.2	22.8			x	x					
LHD8	Yes	Aug. 26	Aug. 27	60.0	40.0				x	x				
LHD9	No	Aug. 26	Aug. 27	77.3	22.7				x	x				
LHD10	Yes	Aug. 26	Aug. 27	60.0	40.0				x	x				
LHD11	Yes	Aug. 26	Aug. 27	81.3	18.7				x	x				
LHD12		Aug. 26	Aug. 27	63.3	36.7				x	x				
LHD13	Yes	Aug. 26	Aug. 27	44.4	55.6				x	x				
LHD14	No	Aug. 27	Aug. 28	74.5	25.5						x	x		
LHD15	Yes	Aug. 27	Aug. 28	32.3	67.7						x	x		
LHD16	Yes	Aug. 27	Aug. 28	77.2	22.8						x	x		
LHD17	No	Aug. 27	Aug. 28	94.5	5.5						x	x		

Table continues next page

**Source Apportionment and Speciation of Low-Volume Particulate Matter Samples**

**Table 15 (Continued).** Sample Matrix for St. Louis Truck Terminal Study

Personal Exposure Samples Code	Smoker	Start Date	Stop Date	% AM	% PM	Aug. 25 AM	Aug. 25 PM	Aug. 26 AM	Aug. 26 PM	Aug. 27 AM	Aug. 27 PM	Aug. 28 AM	Aug. 28 PM	Aug. 29 AM
<b>Long-Haul Drivers (continued)</b>														
LHD18	Yes	Aug. 27	Aug. 28	77.2	22.8						x	x		
LHD19	No	Aug. 27	Aug. 28	38.0	62.0						x	x		
LHD20	No	Aug. 28	Aug. 29	0.0	100.0								x	
LHD21		Aug. 28	Aug. 29	90.8	9.2								x	x
<b>Pickup and Delivery Drivers</b>														
PDD1		Aug. 25	Aug. 25	27.8	72.2	x	x							
PDD2		Aug. 25	Aug. 25	33.7	66.3	x	x							
PDD3		Aug. 25	Aug. 25	28.2	71.8	x	x							
PDD4	No	Aug. 25	Aug. 25	39.7	60.3	x	x							
PDD5		Aug. 26	Aug. 26	19.0	81.0			x	x					
PDD6	No	Aug. 26	Aug. 26	35.7	64.3			x	x					
PDD7		Aug. 26	Aug. 26	21.9	78.1			x	x					
PDD8		Aug. 26	Aug. 26	35.7	64.3			x	x					
PDD9		Aug. 27	Aug. 27	16.1	83.9					x	x			
PDD10		Aug. 27	Aug. 27	24.1	75.9					x	x			
PDD11		Aug. 27	Aug. 27	67.7	32.3					x	x			
PDD12	No	Aug. 27	Aug. 27	29.6	70.4					x	x			
PDD13		Aug. 28	Aug. 28	37.4	62.6							x	x	
PDD14		Aug. 28	Aug. 28	37.5	62.5							x	x	
PDD15		Aug. 28	Aug. 28	21.8	78.2							x	x	
PDD16		Aug. 28	Aug. 28	21.8	78.2							x	x	
PDD17		Aug. 28	Aug. 28	43.6	56.4							x	x	
PDD18		Aug. 28	Aug. 28	39.3	60.7							x	x	
<b>Area Samples</b>														
Area Samples Code	Smoker	Start Date	Stop Date	Time	Aug. 25 AM	Aug. 25 PM	Aug. 26 AM	Aug. 26 PM	Aug. 27 AM	Aug. 27 PM	Aug. 28 AM	Aug. 28 PM	Aug. 29 AM	
<b>Dock</b>														
Aug. 25		Aug. 25	Aug. 25	AM	x									
Aug. 25		Aug. 25	Aug. 25	PM		x								
Aug. 26		Aug. 26	Aug. 26	AM			x							
Aug. 26		Aug. 26	Aug. 26	AM			x							
Aug. 26		Aug. 26	Aug. 26	PM				x						
Aug. 26		Aug. 26	Aug. 26	PM				x						
Aug. 27		Aug. 27	Aug. 27	AM					x					
Aug. 27		Aug. 27	Aug. 27	AM					x					
Aug. 27		Aug. 27	Aug. 27	PM						x				
Aug. 27		Aug. 27	Aug. 27	PM						x				
Aug. 28		Aug. 28	Aug. 28	AM							x			
Aug. 28		Aug. 28	Aug. 28	AM							x			
Aug. 28		Aug. 28	Aug. 28	PM								x		
Aug. 28		Aug. 28	Aug. 28	PM								x		
<b>Shop</b>														
Aug. 25		Aug. 25	Aug. 25	AM	x									
Aug. 25		Aug. 25	Aug. 25	PM		x								

Table continues next page

**Table 15 (Continued).** Sample Matrix for St. Louis Truck Terminal Study

Area Samples Code	Smoker	Start Date	Stop Date	Time	Aug. 25 AM	Aug. 25 PM	Aug. 26 AM	Aug. 26 PM	Aug. 27 AM	Aug. 27 PM	Aug. 28 AM	Aug. 28 PM	Aug. 29 AM
<b>Shop (continued)</b>													
Aug. 26		Aug. 26	Aug. 26	AM			x						
Aug. 26		Aug. 26	Aug. 26	PM				x					
Aug. 27		Aug. 27	Aug. 27	AM					x				
Aug. 27		Aug. 27	Aug. 27	PM						x			
Aug. 28		Aug. 28	Aug. 28	AM							x		
Aug. 28		Aug. 28	Aug. 28	PM								x	
<b>Office</b>													
Aug. 27		Aug. 27	Aug. 27	AM					x				
<b>Yard</b>													
Aug. 25		Aug. 25	Aug. 25	AM	x								
Aug. 25		Aug. 25	Aug. 25	PM		x							
Aug. 26		Aug. 26	Aug. 26	AM			x						
Aug. 26		Aug. 26	Aug. 26	PM				x					
Aug. 27		Aug. 27	Aug. 27	AM					x				
Aug. 28		Aug. 28	Aug. 28	AM							x		
<b>Urban Background</b>													
Aug. 26		Aug. 26	Aug. 26	AM			x						
Aug. 26		Aug. 26	Aug. 26	PM				x					
Aug. 26		Aug. 26	Aug. 26	PM				x					
Aug. 27		Aug. 27	Aug. 27	AM					x				
Aug. 27		Aug. 27	Aug. 27	PM						x			
Aug. 27		Aug. 27	Aug. 27	PM						x			
Aug. 28		Aug. 28	Aug. 28	AM							x		
Aug. 28		Aug. 28	Aug. 28	AM							x		
Aug. 28		Aug. 28	Aug. 29	24 hr								x	x

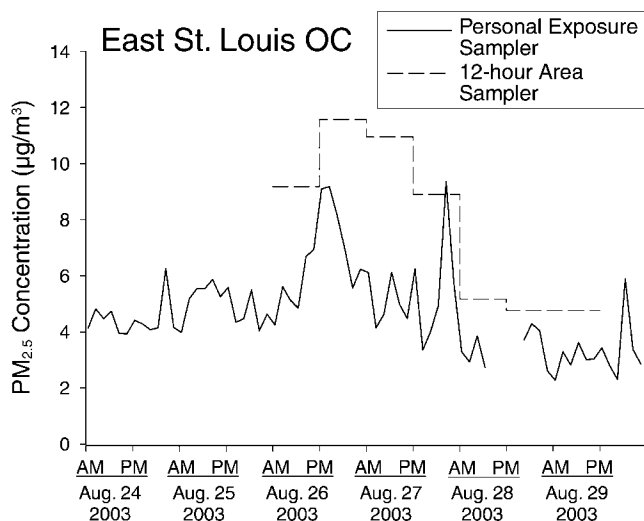


Figure 44. Comparison of urban background OC concentrations as measured by a semicontinuous personal exposure sampler (solid line) and a 12-hour area sampler (dashed line) in PM<sub>2.5</sub> samples collected in East St. Louis.

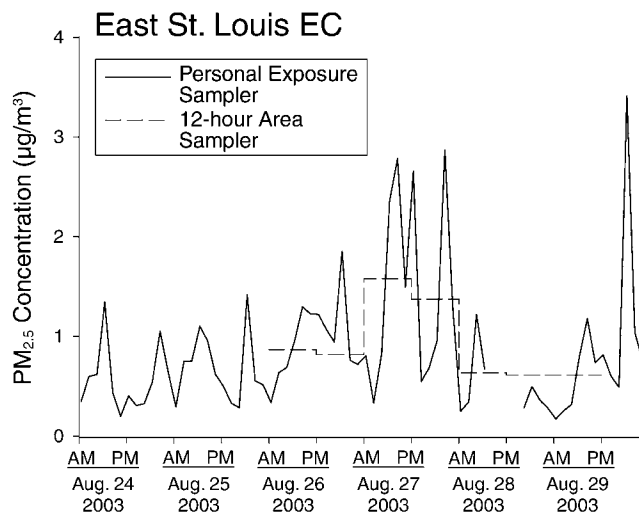


Figure 45. Comparison of urban background EC concentrations as measured by a semicontinuous personal exposure sampler (solid line) and a 12-hour area sampler (dashed line) in PM<sub>2.5</sub> samples collected in East St. Louis.

did the (denuded) OC–EC analyzer. However, it is likely that volatile OC adsorbed onto the personal exposure sampler, causing it to be biased high. Still, the trend in OC, from higher on August 26 and 27 to much lower on August 28 and 29, remained the same.

**Sample Averages**

The samples were first evaluated by calculating averages for each sample type (see Table 16, Table 17, and Figure 46). This helped determine the influence of personal activity on the personal exposure samples and whether each job type and area type had a unique exposure profile. In Tables 16 and 17, the averages for which the standard deviation was equal to or less than one-half of the average (when including the uncertainty) are shown in boldface type. This was used as a rough split to separate groups that had less variability by sample, which would mean less impact caused by date, time, or personal activity. All of the job-type and area-type average OC concentrations had a standard deviation of less than one-half of the average. The samples from the dockworkers and the dock, shop, and yard areas had standard deviations near 20% of the average, which would indicate consistent OC concentrations within each group but not necessarily identical OC source contributions. The average OC concentrations for the personal exposure samples were all higher than those of the worksite and urban background samples. The long-haul drivers' concentrations, at 24 µg/m<sup>3</sup>, were almost twice as high as those of the highest area sample (i.e., the shop, at

13 µg/m<sup>3</sup>). This indicates a significant impact caused by personal activity.

Average EC was generally similar to average OC in terms of consistency among samples within a group (except for the hostlers). Unlike the OC averages, however, the EC personal exposure averages were only marginally elevated, if at all, compared with those of the area samples. The long-haul drivers had by far the highest OC average; the pickup and delivery (P and D) drivers had the highest EC average.

The relative standard deviation was much higher for the molecular markers than for EC and OC. Only norhopane and hopane had standard deviations consistently at or below 50% for all area samples and for the dockworkers, hostlers, and P and D drivers. If a certain mechanic's sample with a hopane concentration more than four times higher than that of the next highest sample is removed, the mechanics' hopane average had a relative standard deviation of 50% or less (with uncertainty). This indicates consistency in the source as being lubricating oil in motor vehicle exhaust, for which hopenes are the markers, in most job and area types. The average personal exposure samples had significantly higher hopenes than did the area samples. This relationship will be explored by looking at correlations among the personal exposure and area samples. The long-haul drivers had high variability for all of the molecular markers, which might indicate that personal activity has a high impact for this job type. The alkanes, C27 through C33 in particular, showed very high variability for all the personal exposure samples.

**Table 16.** Personal Exposure Average Concentrations by Job Title<sup>a</sup>

	Dockworkers (n = 14)			Mechanics (n = 7)			Hostlers (n = 4)			Long-Haul Drivers (n = 21)			P and D Drivers (n = 18)		
	Avg	Unc	SD	Avg	Unc	SD	Avg	Unc	SD	Avg	Unc	SD	Avg	Unc	SD
<b>Carbon (µg/m<sup>3</sup>)</b>															
OC	<b>13.0</b>	<b>1.02</b>	<b>2.92</b>	<b>19.78</b>	<b>1.45</b>	<b>5.81</b>	<b>13.35</b>	<b>1.12</b>	<b>7.48</b>	<b>24.05</b>	<b>1.66</b>	<b>8.75</b>	<b>17.98</b>	<b>1.30</b>	<b>6.80</b>
EC	<b>1.12</b>	<b>0.16</b>	<b>0.41</b>	<b>2.04</b>	<b>0.23</b>	<b>1.02</b>	1.30	0.19	1.00	<b>1.55</b>	<b>0.20</b>	<b>0.42</b>	<b>2.71</b>	<b>0.25</b>	<b>1.37</b>
<b>Compounds (ng/m<sup>3</sup>)</b>															
Benzo[ <i>b+k</i> ]fluoranthene	0.04	0.01	0.03	<b>0.30</b>	<b>0.05</b>	<b>0.19</b>	ND			0.22	0.03	0.21	0.27	0.04	0.39
Benzo[ <i>e</i> ]pyrene	0.19	0.04	0.29	0.11	0.02	0.10	ND			0.11	0.02	0.09	0.30	0.06	0.30
Benzo[ <i>a</i> ]pyrene	0.04	0.01	0.01	0.19	0.05	0.07	ND			0.12	0.03	0.16	0.19	0.05	0.37
Indeno[123- <i>cd</i> ]pyrene	0.08	0.02	0.10	0.05	0.01	0.02	ND			0.07	0.02	0.03	0.11	0.03	0.11
Benzo[ <i>g,h,i</i> ]perylene	1.15	0.37	NA	ND			ND			ND			0.81	0.26	0.38
22,29,30-Trisnorneohopane	<b>0.20</b>	<b>0.03</b>	<b>0.13</b>	0.32	<i>0.05</i>	0.46	0.22	0.03	0.17	0.48	0.07	0.39	<b>0.31</b>	<b>0.04</b>	<b>0.15</b>
17α(H)-21β(H)-29-Norhopane	<b>0.92</b>	<b>0.14</b>	<b>0.51</b>	1.62	<i>0.24</i>	1.93	<b>1.32</b>	<b>0.20</b>	<b>0.60</b>	3.07	0.46	2.40	<b>1.40</b>	<b>0.21</b>	<b>0.67</b>
17α(H)-21β(H)-Hopane	<b>0.50</b>	<b>0.06</b>	<b>0.29</b>	0.87	<i>0.10</i>	0.93	<b>0.72</b>	<b>0.09</b>	<b>0.19</b>	1.40	0.17	1.10	<b>0.68</b>	<b>0.08</b>	<b>0.32</b>
22(S)-17α(H),21β(H)-30-Homohopane	0.25	0.03	0.14	0.45	<i>0.05</i>	0.54	<b>0.40</b>	<b>0.05</b>	<b>0.14</b>	0.78	0.09	0.68	<b>0.29</b>	<b>0.04</b>	<b>0.18</b>
22(R)-17α(H),21β(H)-30-Homohopane	0.18	0.02	0.11	0.34	<i>0.04</i>	0.37	<b>0.31</b>	<b>0.04</b>	<b>0.10</b>	0.57	0.07	0.48	<b>0.21</b>	<b>0.03</b>	<b>0.13</b>
20(R),5α(H),14β(H),17β(H)-Cholestane	0.30	0.04	0.24	0.42	<i>0.06</i>	0.48	<b>0.33</b>	<b>0.04</b>	<b>0.17</b>	0.95	0.12	0.64	<b>0.41</b>	<b>0.05</b>	<b>0.19</b>
20(S),5α(H),14β(H),17β(H)-Cholestane	0.14	0.02	0.11	0.18	<i>0.03</i>	0.16	<b>0.17</b>	<b>0.03</b>	<b>0.08</b>	0.40	0.06	0.27	<b>0.21</b>	<b>0.03</b>	<b>0.09</b>
20(R),αββ-Sitostane	0.18	0.02	0.16	0.31	<i>0.04</i>	0.36	<b>0.25</b>	<b>0.03</b>	<b>0.07</b>	0.55	0.07	0.43	<b>0.22</b>	<b>0.03</b>	<b>0.14</b>
20(S),αββ-Sitostane	0.22	0.03	0.18	0.34	<i>0.05</i>	0.37	<b>0.27</b>	<b>0.04</b>	<b>0.06</b>	0.59	0.08	0.45	<b>0.22</b>	<b>0.03</b>	<b>0.14</b>
Tetracosane	4.90	0.46	3.44	<b>6.42</b>	<b>0.60</b>	<b>2.81</b>	<b>4.17</b>	<b>0.39</b>	<b>1.41</b>	6.84	0.64	4.16	<b>11.27</b>	<b>1.05</b>	<b>6.15</b>
Pentacosane	4.23	0.56	3.21	<b>4.99</b>	<b>0.67</b>	<b>1.90</b>	<b>4.05</b>	<b>0.54</b>	<b>0.44</b>	5.69	0.76	4.55	<b>7.17</b>	<b>0.96</b>	<b>3.14</b>
Hexacosane	2.16	0.33	2.24	<b>2.64</b>	<b>0.40</b>	<b>0.78</b>	<b>2.31</b>	<b>0.35</b>	<b>0.68</b>	3.52	0.53	3.73	2.93	0.44	2.20
Heptacosane	3.11	0.59	1.99	10.47	1.98	14.22	5.20	0.99	4.58	14.60	2.77	22.34	4.37	0.83	6.75
Octacosane	1.24	0.23	0.98	2.67	0.51	2.80	1.93	0.36	1.05	3.27	0.62	4.13	1.47	0.28	1.48
Nonacosane	3.00	0.44	1.70	10.38	1.51	12.4	4.68	0.68	4.40	14.40	2.09	25.73	4.55	0.66	8.29
Triacontane	1.20	0.17	0.67	4.51	0.65	5.42	2.04	0.30	1.33	6.70	0.97	10.14	2.22	0.32	3.55
Hentriacontane	7.04	1.21	6.47	35.93	6.17	43.9	9.58	1.64	16.4	46.90	8.05	84.24	16.19	2.78	37.1
Dotriacontane	1.51	0.26	0.89	6.25	1.08	7.39	2.15	0.37	3.05	9.82	1.70	18.10	3.11	0.54	5.56
Trtriacontane	3.70	0.85	3.77	19.89	4.55	25.2	6.64	1.52	9.95	30.01	6.87	54.86	8.02	1.84	18.7
Tetratriacontane	0.21	0.06	0.21	1.19	0.34	1.21	0.85	0.24	0.26	3.54	1.00	2.92	0.93	0.26	0.78
Pentriacontane	0.03	0.01	0.02	0.17	0.06	0.14	0.09	0.04	0.05	0.24	0.09	0.17	0.07	0.02	0.05

<sup>a</sup> Avg indicates average of all job or area samples; Unc indicates average uncertainty; SD indicates standard deviation of all job or area samples; NA indicates standard deviation not applicable because only 1 value; ND indicates not detected; bold indicates averages with a standard deviation that is less than half the average (when including the uncertainty); italics indicate averages for the mechanics with a standard deviation that is less than half the average only when data for sample individual EC2203 is removed.

Source Apportionment and Speciation of Low-Volume Particulate Matter Samples

Table 17. Area Sample Average Concentrations by Location<sup>a</sup>

	Dock (n = 14)			Shop (n = 8)			Yard (n = 6)			Urban Background (n = 9)		
	Avg	Unc	SD	Avg	Unc	SD	Avg	Unc	SD	Avg	Unc	SD
<b>Carbon (µg/m<sup>3</sup>)</b>												
OC	<b>11.03</b>	<b>0.90</b>	<b>2.21</b>	<b>12.76</b>	<b>0.95</b>	<b>2.49</b>	<b>8.62</b>	<b>0.76</b>	<b>1.77</b>	<b>8.43</b>	<b>0.74</b>	<b>2.83</b>
EC	<b>1.18</b>	<b>0.15</b>	<b>0.38</b>	<b>1.97</b>	<b>0.18</b>	<b>0.82</b>	<b>1.19</b>	<b>0.15</b>	<b>0.38</b>	<b>0.94</b>	<b>0.14</b>	<b>0.34</b>
<b>Compounds (ng/m<sup>3</sup>)</b>												
Benzo[ <i>b+k</i> ]fluoranthene	0.06	0.01	0.19	0.16	0.03	0.21	ND			0.07	0.01	0.05
Benzo[ <i>e</i> ]pyrene	0.04	0.01	0.07	0.10	0.02	0.10	0.04	0.01	0.10	0.05	0.01	0.04
Benzo[ <i>a</i> ]pyrene	0.03	0.01	0.10	0.07	0.02	0.09	ND			0.003	0.001	0.01
Indeno[123- <i>cd</i> ]pyrene	0.08	0.02	0.21	0.10	0.02	0.10	0.00	0.00	0.01	0.03	0.01	0.05
Benzo[ <i>g,h,i</i> ]perylene	0.12	0.04	0.34	0.00	0.00	0.01	0.07	0.02	0.16	0.00	0.00	0.01
22,29,30-Trisnorneohopane	<b>0.18</b>	<b>0.03</b>	<b>0.09</b>	<b>0.24</b>	<b>0.03</b>	<b>0.07</b>	0.05	0.01	0.04	0.03	0.00	0.03
17α(H)-21β(H)-29-Norhopane	<b>0.84</b>	<b>0.13</b>	<b>0.27</b>	<b>0.92</b>	<b>0.14</b>	<b>0.21</b>	<b>0.57</b>	<b>0.09</b>	<b>0.31</b>	<b>0.30</b>	<b>0.04</b>	<b>0.14</b>
17α(H)-21β(H)-Hopane	<b>0.45</b>	<b>0.05</b>	<b>0.18</b>	<b>0.49</b>	<b>0.06</b>	<b>0.19</b>	<b>0.34</b>	<b>0.04</b>	<b>0.18</b>	<b>0.21</b>	<b>0.02</b>	<b>0.09</b>
22( <i>S</i> )-17α(H),21β(H)-30-Homohopane	<b>0.23</b>	<b>0.03</b>	<b>0.11</b>	<b>0.24</b>	<b>0.03</b>	<b>0.13</b>	0.19	0.02	0.12	0.09	0.01	0.06
22( <i>R</i> )-17α(H),21β(H)-30-Homohopane	<b>0.17</b>	<b>0.02</b>	<b>0.09</b>	<b>0.18</b>	<b>0.02</b>	<b>0.10</b>	0.15	0.02	0.10	0.07	0.01	0.05
20( <i>R</i> ),5α(H),14β(H),17β(H)-Cholestane	<b>0.25</b>	<b>0.03</b>	<b>0.13</b>	<b>0.36</b>	<b>0.05</b>	<b>0.11</b>	<b>0.12</b>	<b>0.02</b>	<b>0.07</b>	0.03	0.00	0.05
20( <i>S</i> ),5α(H),14β(H),17β(H)-Cholestane	<b>0.11</b>	<b>0.02</b>	<b>0.05</b>	<b>0.15</b>	<b>0.02</b>	<b>0.05</b>	0.06	0.01	0.04	0.01	0.00	0.02
20( <i>R</i> ), αββ-Sitostane	<b>0.15</b>	<b>0.02</b>	<b>0.06</b>	<b>0.16</b>	<b>0.02</b>	<b>0.06</b>	0.08	0.01	0.07	0.06	0.01	0.04
20( <i>S</i> ), αββ-Sitostane	<b>0.18</b>	<b>0.02</b>	<b>0.11</b>	<b>0.20</b>	<b>0.03</b>	<b>0.09</b>	0.09	0.01	0.07	0.07	0.01	0.05
Tetracosane	5.31	0.49	3.08	<b>7.86</b>	<b>0.73</b>	<b>2.82</b>	1.44	0.13	1.05	1.54	0.14	1.31
Pentacosane	<b>4.59</b>	<b>0.61</b>	<b>1.67</b>	<b>5.46</b>	<b>0.73</b>	<b>2.15</b>	2.26	0.30	1.14	1.62	0.22	0.83
Hexacosane	2.29	0.35	1.67	<b>2.09</b>	<b>0.32</b>	<b>0.85</b>	0.98	0.15	0.63	0.48	0.07	0.50
Heptacosane	2.95	0.56	2.18	<b>1.68</b>	<b>0.32</b>	<b>0.95</b>	0.70	0.13	0.60	0.57	0.11	0.57
Octacosane	1.60	0.30	3.01	<b>0.52</b>	<b>0.10</b>	<b>0.36</b>	0.51	0.10	0.34	0.29	0.06	0.34
Nonacosane	2.80	0.41	2.84	1.36	0.20	0.92	0.54	0.08	0.21	0.47	0.07	0.49
Triacontane	1.28	0.19	1.92	0.65	0.09	0.89	0.08	0.01	0.07	0.22	0.03	0.27
Hentriacontane	6.05	1.04	6.79	3.26	0.56	2.42	0.64	0.11	0.63	0.45	0.08	0.52
Dotriacontane	0.97	0.17	0.90	0.66	0.11	0.82	0.05	0.01	0.07	0.17	0.03	0.22
Tritriacontane	3.31	0.76	3.81	1.72	0.39	1.64	0.53	0.12	0.45	0.21	0.05	0.27
Tetratriacontane	0.35	0.10	0.38	0.18	0.05	0.24	0.04	0.01	0.10	0.11	0.03	0.21
Pentriacontane	0.04	0.01	0.05	0.02	0.01	0.02	0.01	0.00	0.03	0.00	0.00	0.01

<sup>a</sup> Avg indicates average of all job or area samples; Unc indicates average uncertainty; SD indicates standard deviation of all job or area samples; ND indicates not detected; boldface type indicates averages with a standard deviation that is less than half the average (when including the uncertainty).

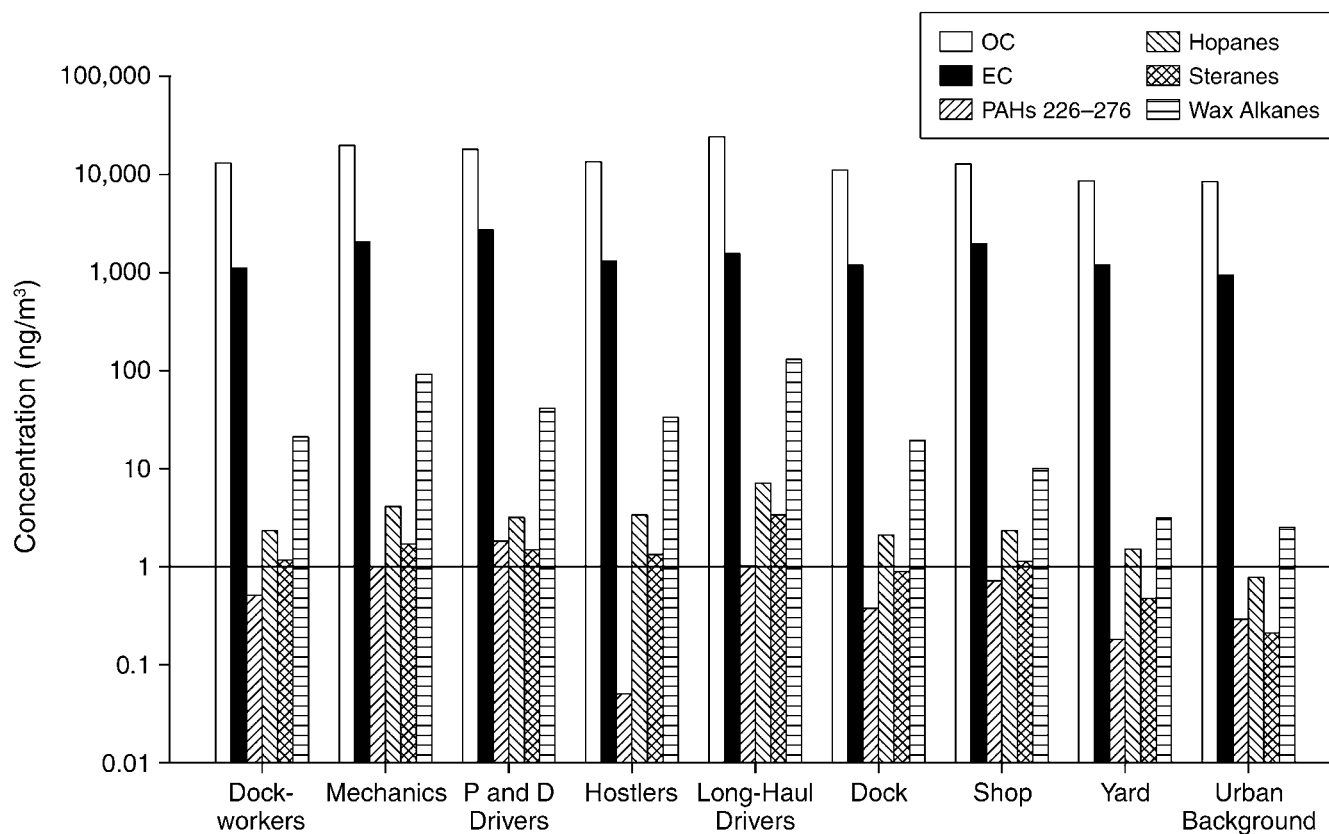


Figure 46. Average concentrations of six compound classes as measured by job type and area type in samples collected at the St. Louis truck terminal.

### Urban Background and Worksite Correlations

The urban background sample (from the Supersite) is plotted against the worksite samples in Figure 47 and Figure 48. The urban background and worksite samples are related in terms of bulk carbon concentrations. The yard and dock measurements came closest to a 1:1 correlation, with the dock consistently biased high compared with the urban background. The shop samples had the highest bias compared with the urban background for OC. The EC plots showed more variability, particularly for the shop samples, one of which was almost three times higher than its respective urban background sample. The worksite EC showed less impact from urban background than did the worksite OC.

The molecular marker plots in Figure 48 can be used to help establish whether differences between worksite and background results are determined by regional worksite emission sources. There was not a correlation among the worksite samples and the urban background samples for PAHs, steranes, or alkanes. For the PAHs, the concentrations were similar, but there was not a correlation. This would seem to indicate that, although there was not a

strong PAH emission source in the truck terminal, the PAHs at the Supersite were not directly transported to the terminal. Sterane and alkane concentrations were considerably higher in the worksite samples, indicating strong emission sources at the truck terminal for both of these compound types. The hopanes had a completely different relationship than any of the other species. There was a strong correlation between the urban background sample and all the worksite samples (0.72), but there was also a high slope (2.5) (see Table 18). The same emission source was thus apparently affecting both the truck terminal and urban background hopanes but to a much greater degree at the truck terminal.

### Personal Exposure and Area Sample Correlations

Personal exposure samples were plotted against their respective worksite samples in Figures 49 through 54. Samples from the hostlers and long-haul drivers were plotted against those from the yard, the urban background, or both. The plots indicate how representative the worksite samples were for personal exposure; because there were also molecular markers (EC, hopanes, alkanes, and PAHs),

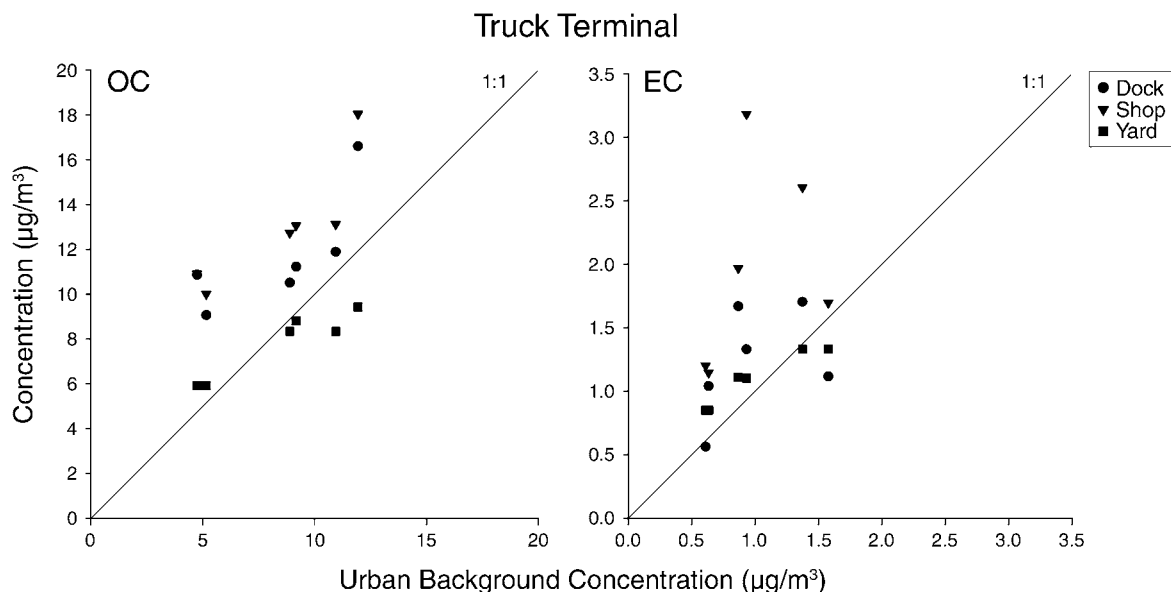


Figure 47. Correlation of shift average OC and EC concentrations from worksite samples collected at the St. Louis truck terminal with urban background samples collected at the East St. Louis Supersite. Note that x- and y-axis scales differ from panel to panel.

the plots also indicate which sources were more affected by personal activity. The regression statistics for Figures 47 through 54 are included in Table 18. Only plots that showed a visual relationship were included in the table.

### Dockworkers

The samples from the dockworkers and the dock did not show clear correlations for OC or EC, although the overall concentrations for each were very similar (see Tables 16 and 17), particularly for EC (see Figure 49). The alkanes were quite variable by sample and in some cases were much higher for the dockworkers than for the dock area. In the samples where the alkanes were systematically high, iso- and anteisoalkanes were also high. These two kinds of branched alkanes were not specifically quantified in the TD-GC-MS method but will be added in the future because they can function as important markers for cigarette smoke (Rogge et al. 1994; Kavouras et al. 1998). It follows, then, that high alkanes in the personal exposure samples in this study can be considered indicative of cigarette smoke. PAHs were very low in both the dockworkers' and dock samples and were similar to those of the urban background measurements, as mentioned previously.

### Mechanics

Although there were not many mechanics' samples, relationships between them and the shop samples were

very clear for EC and hopanes (see Figure 50); both species had correlation coefficients equal to or greater than 0.80. For the hopanes, one mechanic's sample was removed for the regression calculation because, although it had a clear correlation, the slope was closer to 6; his EC concentration was in line with that of the other mechanics (see Figure 50). This individual's personal activity resulted in his being exposed to a much higher concentration of the same sources (i.e., lubricating oil in motor vehicle exhaust) reflected in the other mechanics' and shop samples. Because this study is more interested in characterizing average or typical relationships, the statistics omitting this individual will be used in all further discussions. EC and hopanes potentially represent two different types of motor vehicle exhaust; EC represents diesel exhaust from engines operating at high loads (Kweon et al. 2002), and hopanes represent motor vehicle exhaust affected by lubricating oil (Fraser et al. 2002; Kweon et al. 2002; Schauer et al. 2002b), in this case from diesel smokers (older, dirtier-running diesel engines).

The alkane relationship for the mechanics was similar to that seen for the dockworkers, only more extreme. In this case, one of the mechanics' alkane exposure was 60 times higher than the shop measurement; the sample had high iso- and anteisoalkanes but came from a worker identified as a nonsmoker (see Table 15).

For the mechanics, the shop sample was a good representation of the mechanics' exposure to motor vehicle exhaust

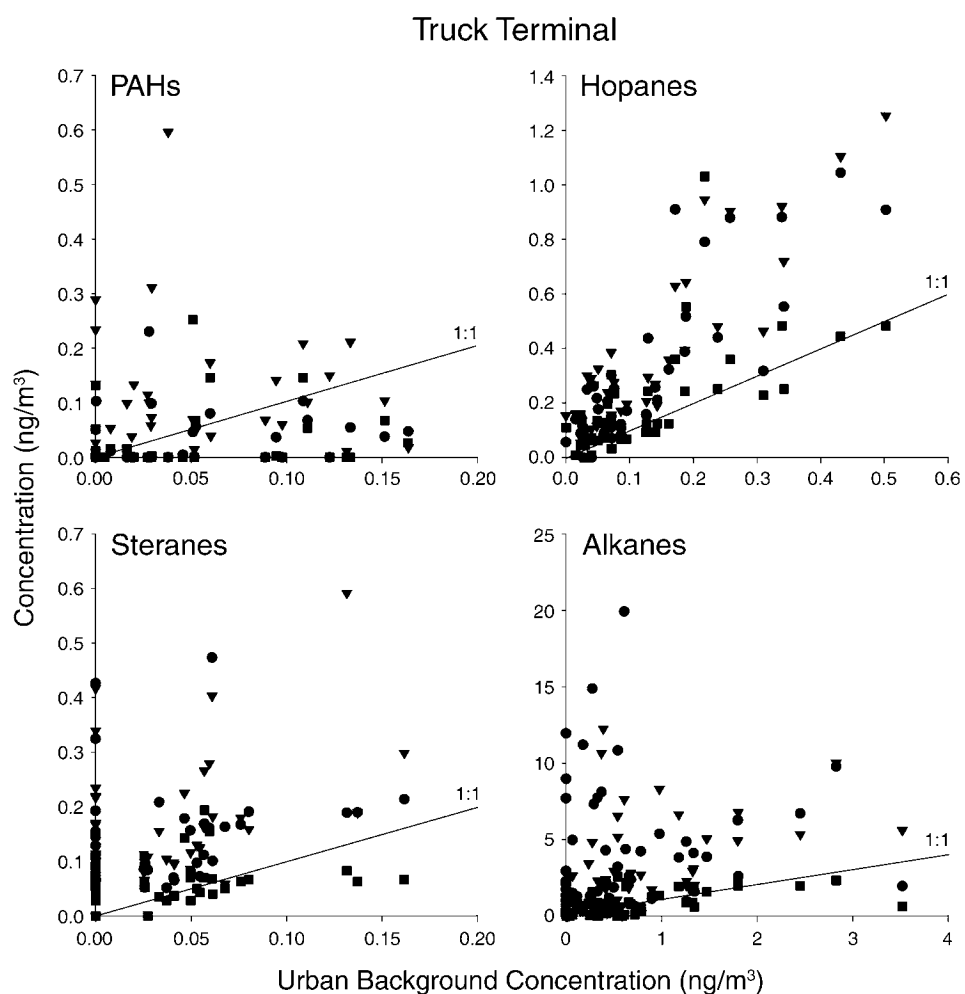


Figure 48. Correlation of shift average concentrations of mid-molecular-weight PAHs, hopanes, steranes, and alkanes from worksite samples collected at the St. Louis truck terminal with urban background samples collected at the East St. Louis Supersite. Note that some of the x- and y-axis scales differ from panel to panel.

Table 18. Regression Statistics for Worksite Versus Job-Type Samples<sup>a</sup>

	EC			Hopanes			Average Area/ Personal EC Ratio	Average Area/ Personal Hopane Ratio
	Intercept	Slope	$r^2$	Intercept	Slope	$r^2$		
Urban background vs. truck terminal	NA	NA	NA	-0.22	2.53	<b>0.72</b>	0.79	0.52
Dock vs. dockworkers	0.51	0.58	0.22	0.02	1.16	<b>0.63</b>	1.06	0.90
Shop vs. mechanics	-0.42	1.38	<b>0.85</b>	0.02	0.86	<b>0.80</b>	0.96	0.56
Yard vs. hostlers	NA	NA	NA	0.18	1.50	0.42	0.91	0.45
Yard vs. P and D drivers	-0.74	3.16	0.20	0.01	2.61	0.55	0.44	0.47
Urban background vs. P and D drivers	0.27	2.73	0.29	0.04	3.94	0.57	0.35	0.25
Urban background vs. long-haul drivers	NA	NA	NA	0.20	8.27	0.26	0.61	0.11

<sup>a</sup> Boldface type indicates  $r^2 > 0.60$ . NA indicates no regression calculated and no relationship apparent.

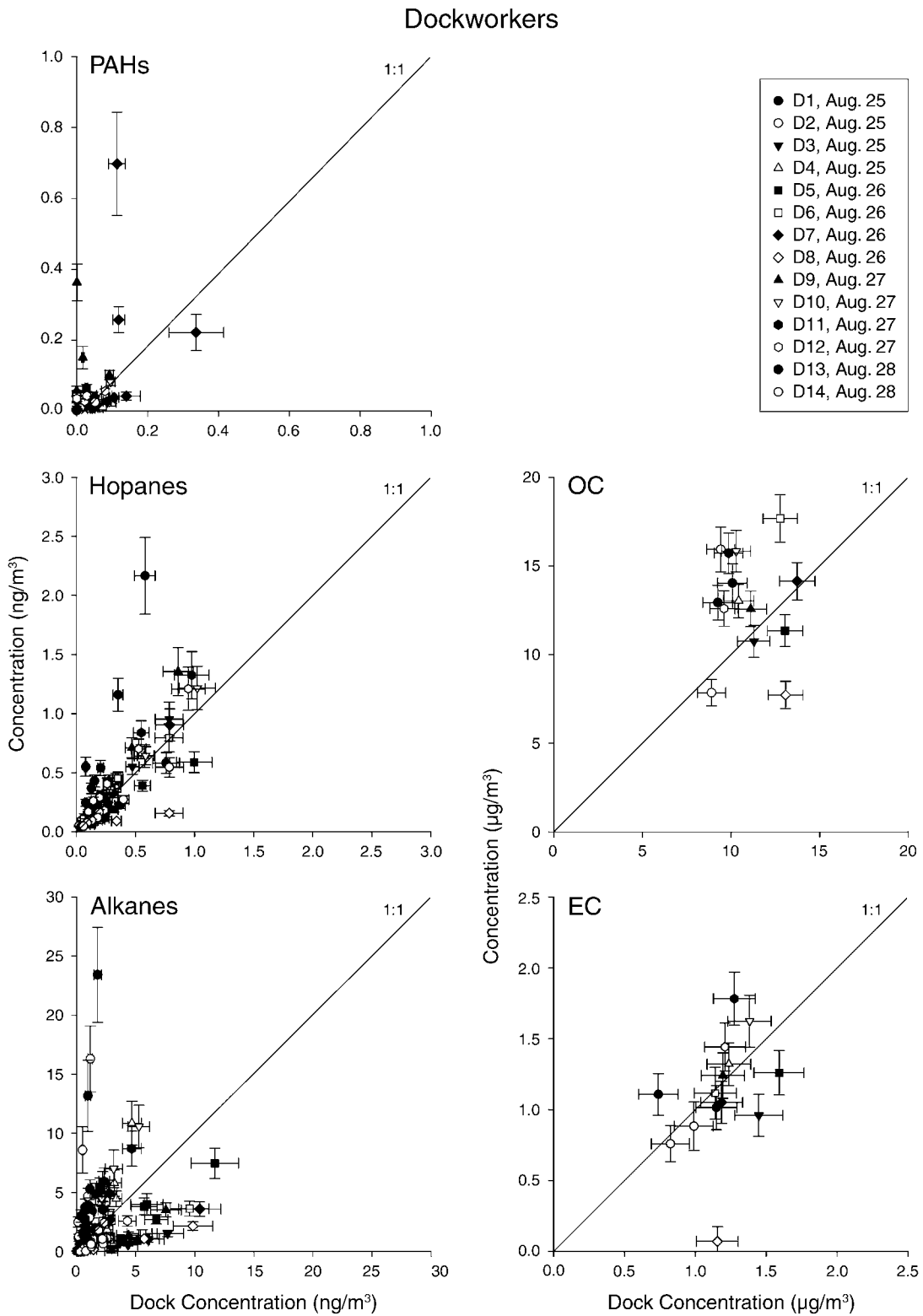


Figure 49. Correlation of shift average concentrations of mid-molecular-weight PAHs, hopanes, OC, alkanes, and EC from dockworkers' personal exposure samples with dock worksite samples collected at the St. Louis truck terminal. Note that some of the x- and y-axis scales differ from panel to panel.

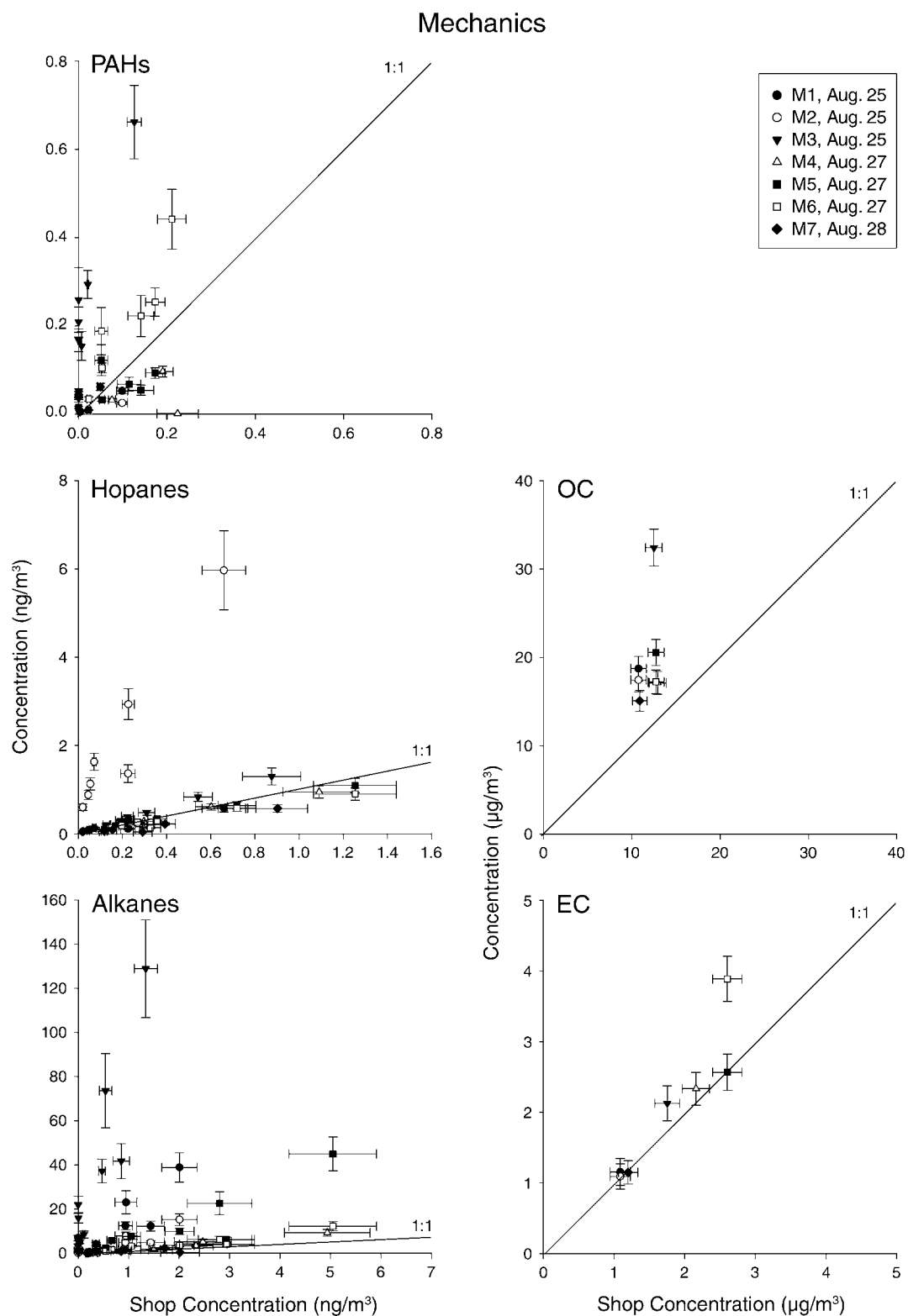


Figure 50. Correlation of shift average concentrations of mid-molecular-weight PAHs, hopanes, OC, alkanes, and EC from mechanics' personal exposure samples with shop worksite samples collected at the St. Louis truck terminal. Note that the x- and y-axis scales differ from panel to panel.

as represented by EC and hopanes (for all but the one individual mentioned above). OC, PAHs, and alkanes showed a lack of correlations between the personal exposure and area samples, much as they showed for the dockworkers.

### Drivers

The three sets of drivers had distinctly different job descriptions. The hostlers drove in the yard, the P and D drivers worked at the local scale, and the long-haul drivers worked at more of a regional scale. With only four hostler samples, good statistical information could not be expected. However, the organic tracers did show patterns similar to those of the dockworkers for both the yard and urban background relationships (see Figure 51). The correlation coefficient for the hopanes was near 0.4 for the yard (see Table 18).

For the P and D drivers, the loadings for the personal exposure samples were consistently much higher compared with those of either the yard or urban background for all measured species (see Figure 52 and Figure 53 and Table 15). There was a slight correlation between the P and D drivers' samples and the yard samples for EC; the correlation was strongest for the hopanes. The correlation coefficients were almost the same for the two area samples, but the slopes were quite different, with a higher slope for the urban background relationship. This was not altogether unexpected, considering the results for the truck terminal and urban background hopanes shown earlier, in Figure 48. The P and D drivers' alkanes were affected by personal activity, as were all the personal exposure samples. PAHs were consistently higher for the P and D drivers compared with either the yard or urban background, which indicates a source specific to the drivers.

Of all the job-type samples, those for the long-haul drivers showed the least correlation with any area samples (see Figure 54). There was only a small correlation for hopanes, and the slopes were quite high ( $m = 8.3$  for the urban background). As with the P and D drivers, the concentrations for all species were significantly higher than those for the urban background. The long-haul drivers clearly were not experiencing the same sources as the St. Louis urban background or truck terminal. The hopanes in the yard and urban background samples were only a fraction of those measured for the drivers (but personal activity increases this source). Because these drivers were exposed to motor vehicle traffic outside of the truck terminal, it cannot be determined from the available data whether the source of the lubricating oil in motor vehicle exhaust for these drivers was diesel smokers; gasoline exhaust, including gasoline smokers (older, dirtier-running gasoline engines); or a mixture.

### Discussion

This data set provided an excellent basis for the discussion of important questions: How well do area samples (local urban or indoor) represent personal exposure? Does the quality of these representations vary by source? Do EC and hopanes track the same motor vehicle source in a diesel-affected environment?

As to the first question, the data set provided a valuable continuum. At one end, the mechanics were in the most contained environment, where the two markers for motor vehicle exhaust showed clear correlations and a near 1:1 relationship between the personal exposure and area samples. At the opposite end, the long-haul drivers worked at a regional scale and showed only a small correlation for hopanes, the most specific motor vehicle marker. In the paradigm of equation 2, contributions from personal activity dominate when a physical area is large, and contributions from the worksite dominate when a physical area is contained. However, this pattern cannot be extrapolated to all sources. As evidenced in the personal exposure samples, contributions of cigarette smoke (as represented quantitatively by alkanes and qualitatively by iso- and anteisoalkanes) are dominated by personal activity regardless of the nature of the work environment. Dockworkers had the least difference between the personal exposure and dock measurements for alkanes, but there was still no correlation. As mentioned previously, the measurement of organic tracers is integral to defining the relationships between personal and worksite exposures, because exposures to sources are not all affected by personal activity in the same way.

An overall assessment of the personal exposure, worksite, and urban background samples indicates that hopanes and EC do not necessarily depict the same source. Only in the case of the mechanics was there a similar relationship for the two types of species, although even in that case the difference in slopes was still 0.5, or roughly 50%. EC measurement would thus not be sufficient to depict the lubricating oil in the exhaust of the diesel source in truck terminals or other high-impact areas.

### UNIVERSITY OF CALIFORNIA–IRVINE PILOT HEALTH STUDY

Table 19 presents raw data from the UC–Irvine pilot health study for 13 elements (chosen on the criterion that at least 60% of the measurements related to them were greater than two times the combined field blank and analytic uncertainties) in samples of PM in three different size fractions (coarse, accumulation, and ultrafine).

The Average columns in the table show the average air concentrations (in  $\text{ng}/\text{m}^3$ ) indoors, outdoors, and from all

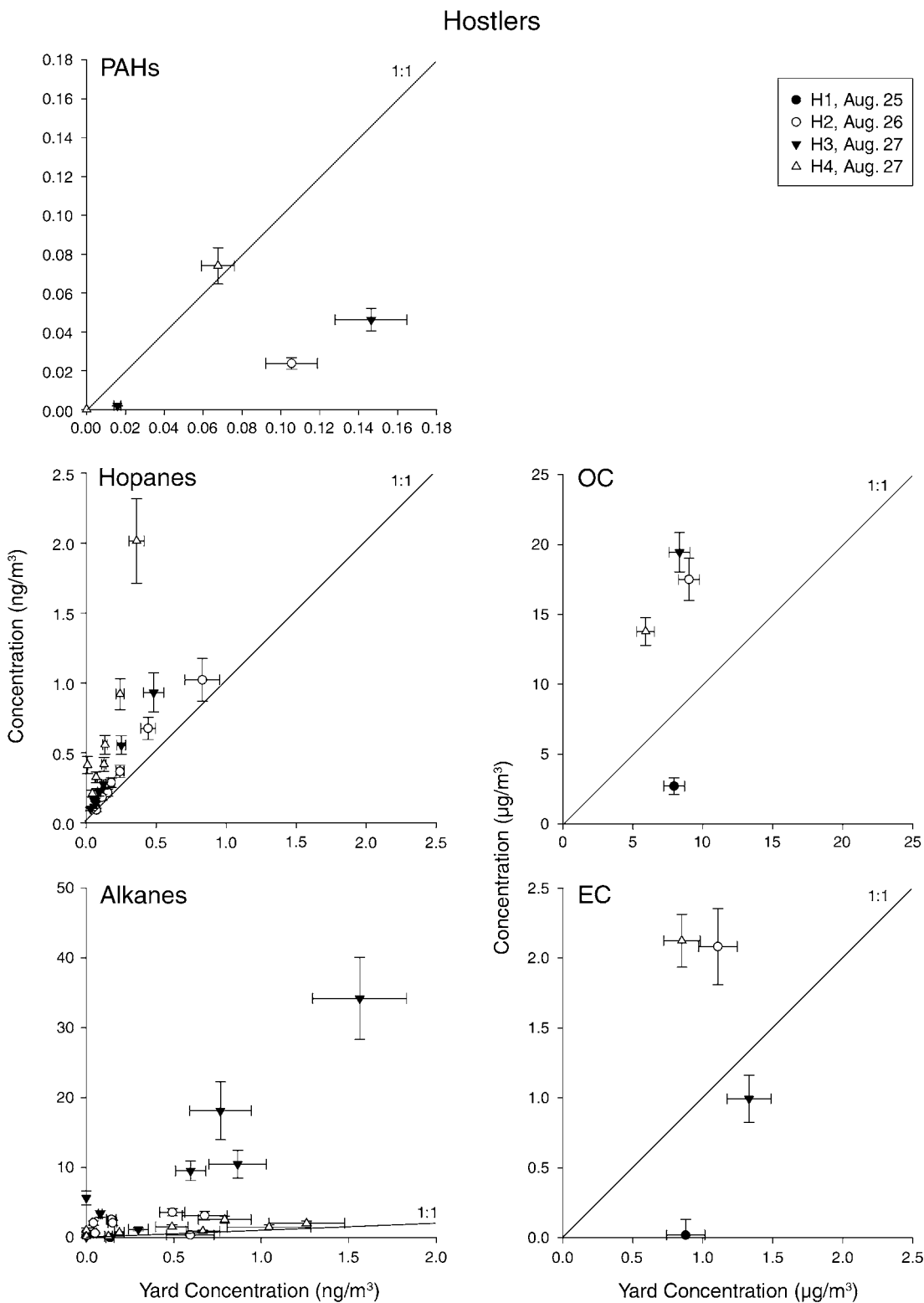


Figure 51. Correlation of shift average concentrations of mid-molecular-weight PAHs, hopanes, OC, alkanes, and EC from hostlers' personal exposure samples with yard worksite samples collected at the St. Louis truck terminal. Note that some of the x- and y-axis scales differ from panel to panel.

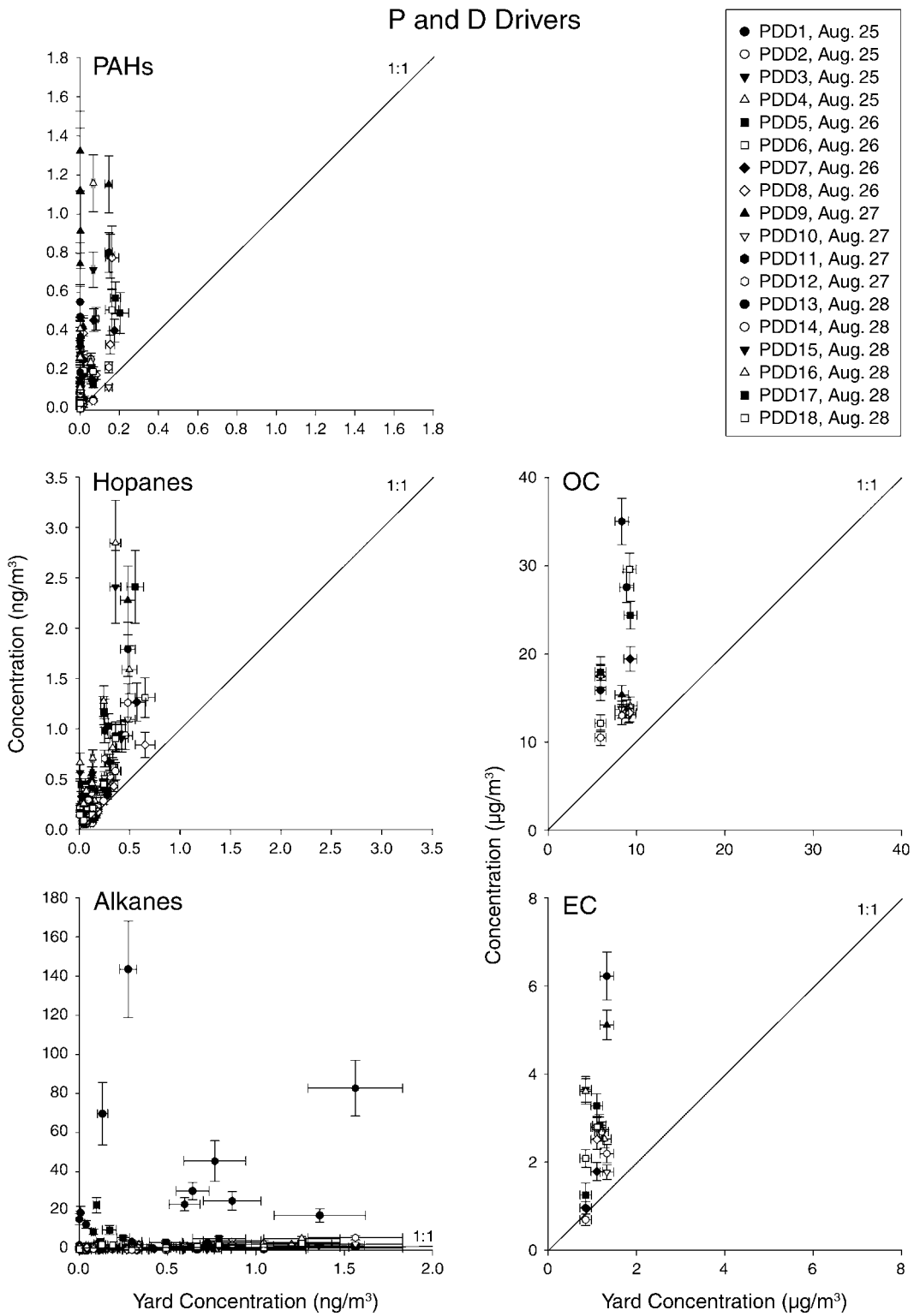


Figure 52. Correlation of shift average concentrations of mid-molecular-weight PAHs, hopanes, OC, alkanes, and EC from P and D drivers' personal exposure samples with yard worksite samples collected at the St. Louis truck terminal. Note that the x- and y-axis scales differ from panel to panel.

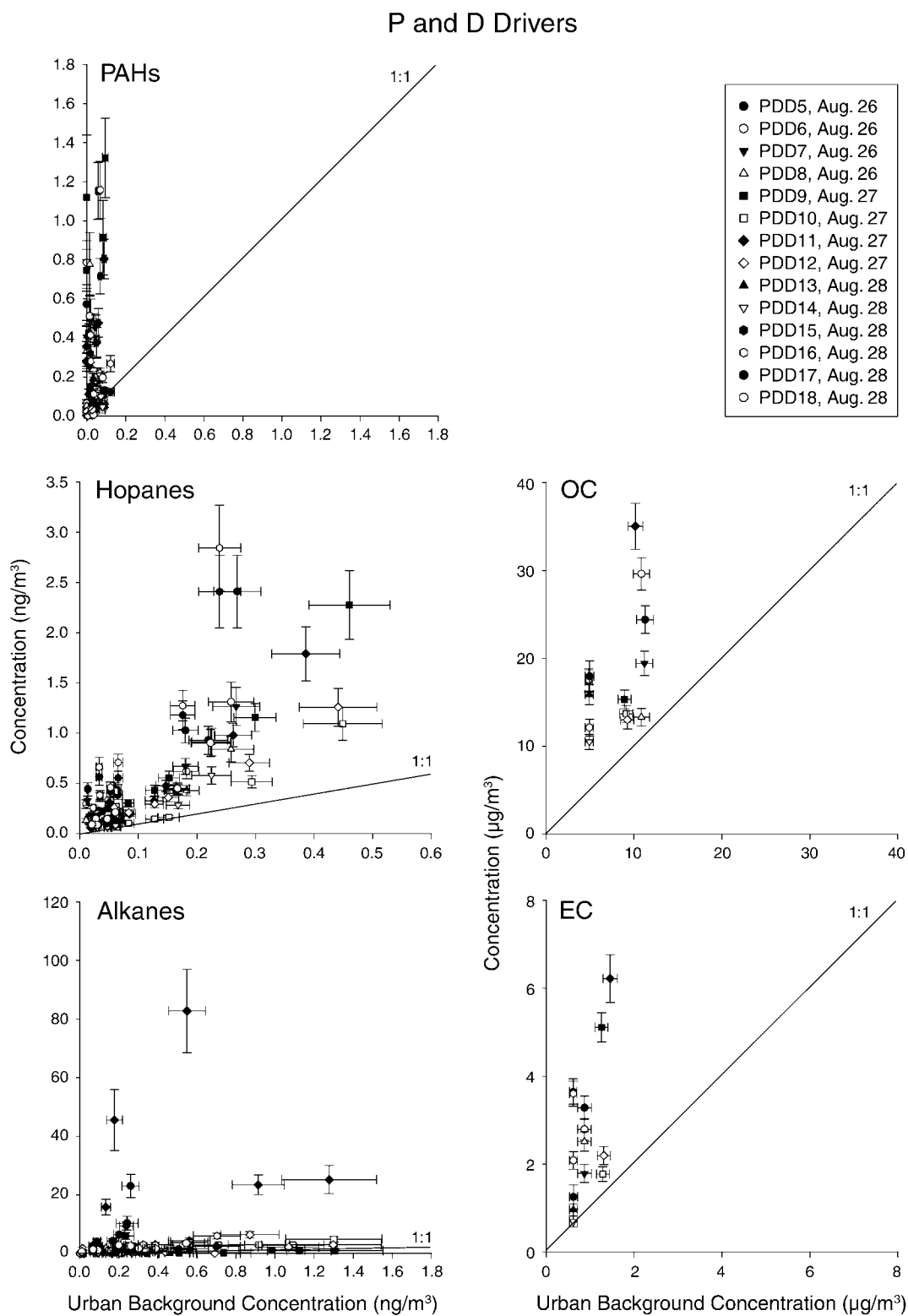


Figure 53. Correlation of shift average concentrations of mid-molecular-weight PAHs, hopanes, OC, alkanes, and EC from P and D drivers' personal exposure samples collected at the St. Louis truck terminal with urban background samples collected at the East St. Louis Supersite. Note that some of the x- and y-axis scales differ from panel to panel.

Long-Haul Drivers

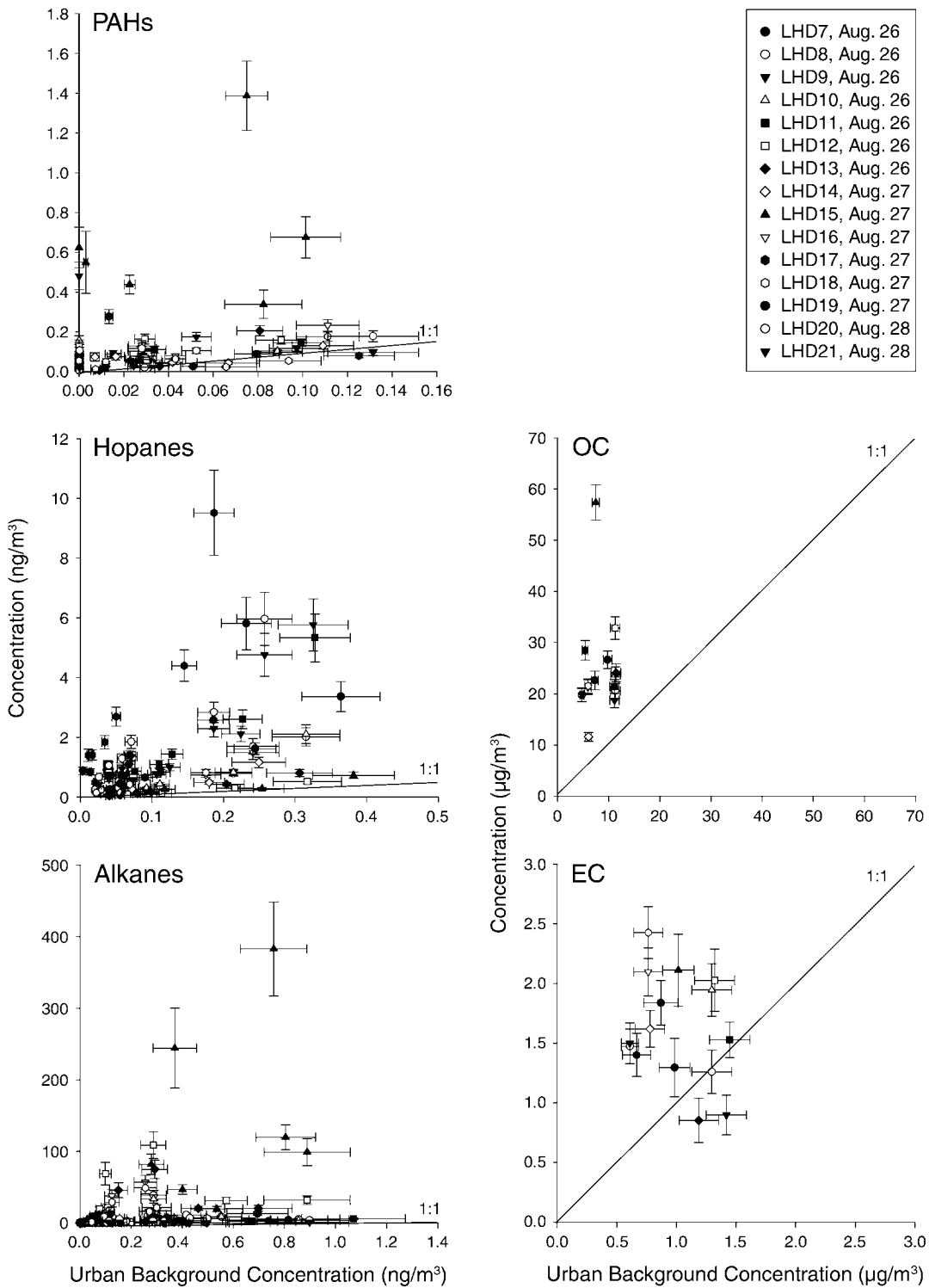


Figure 54. Correlation of shift average concentrations of mid-molecular-weight PAHs, hopanes, OC, alkanes, and EC from long-haul drivers' personal exposure samples collected at the St. Louis truck terminal with urban background samples collected at the East St. Louis Supersite. Note that the x- and y-axis scales differ from panel to panel.

**Table 19.** Comparison of 13 Elements in PM in Three Size Fractions from Indoor, Outdoor, and Personal Exposure Samplers<sup>a</sup>

Element	Average			Average Ratio			Regression Slope		
	Indoor Metals $\pm$ SD (ng/m <sup>3</sup> )	Outdoor Metals $\pm$ SD (ng/m <sup>3</sup> )	Personal Exposure Metals $\pm$ SD (ng/m <sup>3</sup> )	Indoor/ Outdoor	Personal/ Outdoor	Personal/ Indoor	Indoor vs. Outdoor	Personal vs. Outdoor	Personal vs. Indoor
	<b>Coarse Fraction</b>								
Sulfur	101 $\pm$ 79	247 $\pm$ 161	94 $\pm$ 71	0.41	0.38	0.94	0.23	0.27	0.62
Iron	156 $\pm$ 153	556 $\pm$ 503	133 $\pm$ 141	0.28	0.25	0.83	0.12	0.13	0.39
Copper	4.7 $\pm$ 4.4	23 $\pm$ 24	4.9 $\pm$ 13.1	0.21	0.21	0.99	0.15	0.10	0.70
Cadmium	0.02 $\pm$ 0.02	0.11 $\pm$ 0.20	0.05 $\pm$ 0.13	0.19	0.45	2.53	0.02	0.07	1.88
Antimony	0.3 $\pm$ 0.4	2.0 $\pm$ 1.7	0.5 $\pm$ 1.2	0.16	0.27	1.74	0.09	0.23	0.62
Lead	1.7 $\pm$ 2.5	22 $\pm$ 52	1.4 $\pm$ 1.9	0.08	0.06	0.78	0.05	0.01	0.29
Aluminum	155 $\pm$ 218	490 $\pm$ 418	218 $\pm$ 184	0.32	0.28	0.79	0.10	0.14	0.27
Vanadium	0.5 $\pm$ 0.3	5.0 $\pm$ 10.4	9.0 $\pm$ 23.4	0.09	1.68	19.6	0.01	0.19	25.8
Chromium	1.2 $\pm$ 1.7	6.3 $\pm$ 12.2	1.4 $\pm$ 3.5	0.19	0.21	1.11	0.13	0.15	0.88
Manganese	3.3 $\pm$ 3.0	11.0 $\pm$ 10.6	2.6 $\pm$ 2.6	0.30	0.25	0.77	0.13	0.12	0.44
Cobalt	0.12 $\pm$ 0.12	0.28 $\pm$ 0.24	0.09 $\pm$ 0.10	0.43	0.34	0.82	0.28	0.19	0.43
Molybdenum	0.26 $\pm$ 0.26	0.9 $\pm$ 0.6	0.3 $\pm$ 0.4	0.31	0.32	1.04	0.21	0.16	0.56
Barium	4.7 $\pm$ 5.2	26.4 $\pm$ 24.6	4.4 $\pm$ 4.8	0.18	0.17	0.95	0.09	0.08	0.35
<b>Accumulation Mode</b>									
Sulfur	823 $\pm$ 644	553 $\pm$ 544	337 $\pm$ 413	1.49	0.57	0.41	0.82	0.34	0.40
Iron	173 $\pm$ 75	135 $\pm$ 110	67 $\pm$ 70	1.28	0.45	0.40	0.62	0.27	0.34
Copper	15.4 $\pm$ 18.8	12.3 $\pm$ 15.7	4.0 $\pm$ 4.6	1.25	0.30	0.25	1.01	0.12	0.01
Cadmium	0.17 $\pm$ 0.09	0.15 $\pm$ 0.19	0.08 $\pm$ 0.13	1.08	0.45	0.47	0.56	0.33	0.49
Antimony	1.3 $\pm$ 0.7	1.0 $\pm$ 0.8	0.5 $\pm$ 0.6	1.32	0.51	0.45	0.73	0.35	0.36
Lead	11.8 $\pm$ 17.1	15.4 $\pm$ 25.7	2.6 $\pm$ 4.0	0.77	0.15	0.21	0.67	0.05	0.08
Aluminum	153 $\pm$ 156	130 $\pm$ 103	46 $\pm$ 79	1.17	0.33	0.29	0.99	0.22	0.14
Vanadium	2.3 $\pm$ 1.9	2.0 $\pm$ 1.0	6 $\pm$ 22	1.19	2.99	2.56	1.02	1.74	1.52
Chromium	2.7 $\pm$ 4.9	4.1 $\pm$ 7.3	0.7 $\pm$ 1.2	0.67	0.15	0.23	0.63	0.08	0.11
Manganese	6.2 $\pm$ 6.3	3.0 $\pm$ 2.4	1.7 $\pm$ 1.7	2.05	0.52	0.28	0.89	0.31	0.14
Cobalt	0.13 $\pm$ 0.08	0.08 $\pm$ 0.05	0.06 $\pm$ 0.06	1.62	0.64	0.43	0.94	0.45	0.30
Molybdenum	0.6 $\pm$ 0.5	0.5 $\pm$ 0.4	0.22 $\pm$ 0.21	1.18	0.44	0.40	0.60	0.31	0.23
Barium	8.9 $\pm$ 5.9	7.5 $\pm$ 7.0	3.7 $\pm$ 4.5	1.18	0.46	0.47	0.55	0.21	0.38
<b>Ultrafine Fraction</b>									
Sulfur	361 $\pm$ 219	577 $\pm$ 340	301 $\pm$ 187	0.63	0.53	0.83	0.41	0.41	0.66
Iron	189 $\pm$ 261	211 $\pm$ 205	56 $\pm$ 72	0.90	0.26	0.28	0.38	0.20	0.08
Copper	53 $\pm$ 93	68 $\pm$ 96	4.3 $\pm$ 6.3	0.77	0.06	0.07	0.88	0.03	0.03
Cadmium	0.07 $\pm$ 0.08	0.14 $\pm$ 0.16	0.05 $\pm$ 0.05	0.51	0.32	0.62	0.11	0.15	0.25
Antimony	0.6 $\pm$ 0.5	1.5 $\pm$ 1.7	0.4 $\pm$ 0.3	0.39	0.28	0.71	0.23	0.14	0.50
Lead	11.1 $\pm$ 22.1	24 $\pm$ 31	2.4 $\pm$ 1.8	0.46	0.09	0.20	0.57	0.03	0.03
Aluminum	467 $\pm$ 743	989 $\pm$ 956	74 $\pm$ 84	0.47	0.07	0.15	0.56	0.04	0.04
Vanadium	14 $\pm$ 28	5.0 $\pm$ 2.0	7.3 $\pm$ 10.2	2.80	1.50	0.52	1.24	1.30	0.05
Chromium	12 $\pm$ 22	9.3 $\pm$ 11.0	4.6 $\pm$ 6.2	1.34	0.47	0.33	1.22	0.16	0.09
Manganese	4.7 $\pm$ 7.5	4.3 $\pm$ 4.0	2.0 $\pm$ 3.7	1.10	0.45	0.38	0.34	0.42	0.08
Cobalt	0.20 $\pm$ 0.24	0.20 $\pm$ 0.15	0.07 $\pm$ 0.07	1.07	0.37	0.34	0.66	0.25	0.14
Molybdenum	1.02 $\pm$ 1.20	0.9 $\pm$ 0.6	0.4 $\pm$ 0.3	1.17	0.46	0.37	0.56	0.32	0.17
Barium	3.6 $\pm$ 3.9	8.4 $\pm$ 8.3	1.4 $\pm$ 1.7	0.43	0.17	0.38	0.14	0.10	0.16

<sup>a</sup> Averages and regression slopes represent all individuals across all days. The uncertainty in the average is 1 SD of all values.

personal exposure samplers averaged across all sampling days, with the standard deviation of all values marked as a measure of uncertainty. It is interesting to note that the standard deviations generally approached, and sometimes exceeded, the absolute air concentrations. This indicates that there was a wide range of exposures across the sampling days (average relative standard deviation = 104%) and especially across individuals (average relative standard deviation = 143%).

The Average Ratios columns show the average ratios between the various sampling sites averaged over all sampling days. A general trend can be observed in these data when comparing indoor and outdoor concentrations, namely that the coarse and ultrafine fractions generally showed greater outdoor concentrations and the accumulation mode generally showed greater indoor concentrations.

The data from this 2-week pilot study indicated that, for all elements except for Cu, there were no correlations between indoor, outdoor, and personal air concentrations. The outdoor samples were shown to be richer in most of the trace elements than both the indoor and personal exposure samples. Additionally, the personal exposure samples were not as rich in trace elements as were the indoor and outdoor samples. Only V concentrations were consistently higher in the personal exposure samples than in the indoor and outdoor samples in all size fractions. This implies that the metals that were present both indoors and outdoors were associated with local sources and were encountered less by the individuals with the personal exposure samplers. The primary implication of this study was that, for the population studied here, neither indoor nor outdoor ambient measurements can be used as surrogates for measurements of actual exposure to trace metals.

---

### SUMMARY AND CONCLUSIONS

---

It has become more evident in recent years that trace elements, especially transition metals, in atmospheric PM might have a large impact on human health effects. This impact is primarily caused by the fact that transition metals transport electrons efficiently and can therefore help to create reactive oxygen species. It has also been recognized that PM obtained from fixed-site ambient samplers might not be a good surrogate for PM from actual exposures. The motivation of the present study, therefore, was to develop methods to measure trace elements, organic species, and oxidation states of trace elements at the very low concentrations found in personal exposure samples.

HR-ICP-MS digestion methods were developed in order to improve the analytic DLs for a set of trace elements.

Another aim was to recover Si quantitatively. This study focused on reducing acid digestion volumes, increasing microwave digestion temperatures, and using new digestion rotors and vials. Order-of-magnitude improvements in method DLs were demonstrated for a large set of elements (see Figure 4). For Cs, Ir, Rh, and Tl, improvements of nearly three orders of magnitude over previous ICP-MS techniques were observed when microvolume digestion HR-ICP-MS was employed. For a large group of additional elements, the improvement factor associated with the new methods was between 10- and 100-fold (Pt, Rb, Be, Cu, Cd, Ru, Sb, Y, Ho, La, Ba, and Cs). Using a sealed-vial approach, the complete recovery of Si was realized in NIST SRMs.

A TD-GC-MS method was developed in order to address concerns related to traditional GC-MS analysis. The specific goals of developing this alternative GC-MS organic speciation technique were twofold: to significantly reduce the OC loading necessary for analysis and to minimize sample handling and preparation. In this study, 17 PAHs, 12 alkanes, and 7 hopanes and steranes were used as calibration standards. One advantage of the thermal desorption method over solvent extraction GC-MS for ambient PM analysis is that true duplicate analyses can be more easily obtained because of the low loading requirement and the nature of the sample preparation. It was found that duplicate measurements on the same sample showed similar results and that nominal DLs for these compounds were 50 pg per sample for PAHs, hopanes, and steranes; 1 ng per sample for alkanes; and as low as 15 to 20 ng per sample for all other compounds studied. An intercomparison between TD-GC-MS and solvent extraction GC-MS was performed, and good agreement was found between the two methods for all sample classes (with slopes of 0.93 for PAHs, 1.26 for alkanes, and 0.90 for hopanes and steranes).

A PTV-GC-MS method was designed for the solvent extraction and organic speciation of low-concentration atmospheric samples. Upon analysis of nonpolar compounds using PTV-GC-MS, we found the technique to be biased slightly high compared with the solvent extraction GC-MS and TD-GC-MS methods but still a viable option for analysis of these atmospheric aerosols. The PTV-GC-MS method was found to be very good for nonpolar species and good for levoglucosan measurements with silylation and analysis using low-volume injection GC-MS. The methylation method shows promise but will likely not be able to quantify the full range of acids handled by solvent extraction GC-MS. The PTV-GC-MS method developed here, then, can measure nonpolar species, levoglucosan, and a limited selection of acids for low-concentration ambient or personal exposure samples.

To measure the various forms of metals present in atmospheric PM, wet-chemical methods were developed in this study for the measurement of specific oxidation states of Fe, Mn, and Cr. In order for a method to be considered for use, it had to be (1) species specific, (2) sensitive enough to measure the analyte in personal exposure samples, and (3) relatively inexpensive, such that most adequately equipped laboratories could perform the analyses. Because earlier researchers had shown that some spectrophotometric measurements can have extremely low DLs, the wet-chemical methods described here all involved leaching the metal off atmospheric PM into an aqueous extract solution followed by complexation or oxidation with an excess ligand and monitoring of the reaction product using liquid wave-guide spectrophotometry. For both Fe and Mn, we found that the DLs were sufficient to measure the concentrations found in ambient personal exposure samples and that the extractable fraction was heavily dependent on the leachate (with acetate buffer being the most efficient leachate tested in this study). It was also found that, over a period of a few months, the Fe associated with PM oxidizes while in storage (in the dark at  $-20^{\circ}\text{C}$ ), meaning that this fact must be taken into account on field campaigns where the PM cannot be immediately analyzed using the ferrozine ligand. If the PM cannot be analyzed immediately, we recommend that it be stored in the dark in an inert gas atmosphere below  $-15^{\circ}\text{C}$ . An aging study was also carried out to determine how soluble Fe changes as it is processed in the atmosphere. In our short-term experiments (up to 10 days), soluble Fe(II) in the supermicron fraction showed very little change over the course of the experiments. The soluble Fe(II) in the submicron fraction, however, peaked at around 1 to 3 days of exposure and then decreased back to near the initial values after 6 to 10 days.

Despite using the study's most sensitive method (estimated DL was  $< 0.1$  ng per filter), no Cr(VI) was detected in the extracts of any ambient  $\text{PM}_{10}$  samples from East St. Louis. It is therefore recommended that wet-chemical methods for Cr(VI) analysis be used instead in various occupational settings, such as chrome plating, where higher concentrations of Cr(VI) are to be found.

In this study, we also developed a method to measure the oxidation state of Fe in atmospheric samples using XANES spectroscopy. The method, which does not include an extraction step, provides the ability to measure Fe(II) and Fe(III) relative oxidation states in an ambient sample. Combined with a method such as ICP-MS to measure total Fe content, an estimate of the total Fe(II) and Fe(III) in an atmospheric PM sample can be obtained. The method both complements and enhances the speciation data obtained by

the wet-chemical extraction procedures. Both the XANES and wet-chemical methods were used in an atmospheric aerosol aging study using PM collected from three urban sampling sites. The purpose of the study was to examine how iron speciation changes as it is cycled through the atmosphere during short- and long-range transport. XANES spectroscopy results showed that there was very little overall change in Fe(II)/Fe(III) ratios over the course of the experiment. However, there was a tendency for the Fe associated with larger particles ( $> 2.5 \mu\text{m}$ ) to slowly oxidize to Fe(III) over periods of up to 40 days and a tendency for a higher percentage of the Fe in the small size fractions ( $< 0.5 \mu\text{m}$ ) to be present as Fe(II). The midrange fractions did not show any significant change in Fe(II)/Fe(III) ratios over the course of the 40 days of aging.

As part of an NCI-funded cancer study led by principal investigator Eric Garshick, this section of the epidemiologic project aimed to assess the carbonaceous fine PM exposure of workers at a diesel truck terminal. The sample set consisted of personal exposure samples from people with five different job descriptions (dockworkers, mechanics, hostlers, pickup and delivery drivers, and long-haul drivers) and area samples from four different worksites and a nearby urban background location over the course of 5 days. Bulk OC and EC as well as organic markers such as PAHs, hopanes and steranes, and alkanes were quantified. The degree of correlation between personal exposure and background concentration was found to depend on the various job types. The mechanics were in the most contained environment, where the two markers for motor vehicle exhaust showed clear correlations and a near 1:1 relationship between the personal exposure and area samples. The long-haul drivers, who work at a regional scale, had only a small correlation for hopanes, the most specific motor vehicle marker. Contributions from personal activity dominate when a physical area is large; contributions from the work-site dominate when a physical area is contained. However, this pattern cannot be extrapolated to all sources. As evidenced in the personal exposure samples, contributions of cigarette smoke (as represented quantitatively by alkanes and qualitatively by iso- and anteisoalkanes) were dominated by personal activity regardless of the nature of the work environment. Dockworkers had the least differences between personal exposure and dock measurements for alkanes, but there was still no correlation. As mentioned previously, the measurement of organic tracers is integral to defining the relationships between personal and work-site exposures, because exposures to sources are not all affected by personal activity in the same way.

As part of an NIH-funded study led by principal investigator Ralph Delfino, researchers at UC-Irvine are following

72 nonsmoking elderly individuals with coronary heart disease living in an area with high concentrations of air pollution in the Los Angeles Air Basin of California. Indoor, outdoor, and personal exposure samples were compared for 13 elements quantified using the low-volume microwave-assisted acid digestion method coupled with HR-ICP-MS. The data from this 2-week pilot study have indicated that, for all elements except Cu, there were no correlations between the indoor, outdoor, and personal exposure concentrations. The outdoor samples were shown to be richer in most of the trace elements than both the indoor and personal exposure samples. Additionally, the personal exposure samples were not as rich in trace elements as the indoor and outdoor samples. Only concentrations of V were consistently higher in the personal exposure samples than the outdoor and indoor samples in all size fractions. This implies that the metals that were present both indoors and outdoors were associated with local sources and were encountered less by the individuals with the personal exposure samplers. The primary implication of this study is that, for the population studied here, neither indoor nor outdoor ambient measurements can be used as surrogates for measurements of actual exposure to trace elements.

---

### ACKNOWLEDGMENTS

We wish to thank Jay Turner, Jay Hill, and Eric Ryzkiewicz at the Midwest Supersite in East St. Louis, Illinois, for giving us access and assistance in obtaining samples. We also wish to thank Costantinos Sioutas, Philip Fine, and Mike Geller at the University of Southern California for access to sampling sites and collection of samples in Los Angeles.

Many thanks to undergraduate researchers Melissa Wilking, Jackson Helmer, Alex Wong, and Steve Schwanbeck for their great assistance in much of the wet-chemical laboratory work and method development.

Our XANES analyses were conducted at the Synchrotron Radiation Center at the University of Wisconsin-Madison, which is supported by the National Science Foundation under Award Numbers DMR-0084402 and DMR-0537588. We thank Mary Severson, Mark Bissen, and Bob Pedley at the Synchrotron Radiation Center for their assistance in these analyses.

We also thank Chris Worley, Dustan Helmer, Joel Overdier, and Noel Stanton at the Wisconsin State Laboratory of Hygiene for their roles in the ICP-MS analysis.

We thank Ralph Delfino at the University of California-Irvine, Costantinos Sioutas at the University of Southern

California, and their research teams for providing pilot-study samples for trace-metals analysis. We thank Eric Garshick and Francine Laden at the Harvard Medical School, Tom Smith at the Harvard School of Public Health, and their research teams for providing pilot-study samples for organic-tracer analysis.

---

### REFERENCES

- Allen AG, Nemitz E, Shi JP, Harrison JP, Greenwood JC. 2001. Size distributions of trace metals in atmospheric aerosols in the United Kingdom. *Atmos Environ* 35:4581-4591.
- Bae MS. 2005. A Comprehensive Characterization of Carbonaceous Aerosols in St. Louis, Missouri [dissertation]. University of Wisconsin, Madison, WI.
- Bae MS, Schauer JJ, DeMinter JT, Turner JR, Smith D, Cary RA. 2004. Validation of a semi-continuous instrument for elemental carbon and organic carbon using a thermal-optical method. *Atmos Environ* 38:2885-2893.
- Bartlett R, James B. 1979. Behavior of chromium in soils: III. Oxidation. *J Environ Qual* 8:31-35.
- Bhuie AK, Roy DN. 2001. Deposition of Mn from automotive combustion of methylcyclopentadienyl manganese tricarbonyl beside the major highways in the greater Toronto area, Canada. *J Air Waste Manag Assoc* 51:1288-1301.
- Bowie AR, Achterberg EP, Sedwick PN, Ussher S, Worsfold PJ. 2002. Real-time monitoring of picomolar concentrations of iron(II) in marine waters using automated flow injection-chemiluminescence instrumentation. *Environ Sci Technol* 36:4600-4607.
- Brewer PG, Spencer W. 1971. Colorimetric determination of manganese in anoxic waters. *Limnol Oceanogr* 16:107-110.
- Brown S, Taylor NL. 1999. Could mitochondrial dysfunction play a role in manganese toxicity? *Environ Toxicol Pharmacol* 7:49-57.
- Calne DB, Chu NS, Huang CC, Lu CS, Olanow W. 1994. Manganism and idiopathic parkinsonism: Similarities and differences. *Neurology* 44:1583-1586.
- Camner P, Johansson A. 1992. Reaction of alveolar macrophages to inhaled metal aerosols. *Environ Health Perspect* 97:185-188.
- Carter JD, Ghio AJ, Samet JM, Devlin RB. 1997. Cytokine production by human airway epithelial cells after exposure to an air pollution particle is metal-dependent. *Toxicol Appl Pharmacol* 146:180-188.

- Chen Y, Siefert RL. 2003. Determination of various types of labile atmospheric iron over remote oceans. *J Geophys Res* 108(D24).
- Chiswell B, O'Halloran KR. 1991. Comparison of 3 colorimetric methods for the determination of manganese in fresh-waters. *Talanta* 38:641–647.
- Cohen MD, Kargacin B, Klein CB, Costa M. 1993. Mechanisms of chromium carcinogenicity and toxicity. *Crit Rev Toxicol* 23:255–281.
- Davis ME, Laden F, Hart JE, Garshick E, Blicharz A, Smith TJ. 2009. Predicting changes in PM exposure over time at U.S. trucking terminal using structural equation modeling techniques. *J Occup Environ Hyg* 6:396–403.
- Divita F, Ondov JM, Suarez AE. 1996. Size spectra and atmospheric growth of V-containing aerosol in Washington, DC. *Aerosol Sci Technol* 25:256–273.
- Ensafi AA, Chamjangali MA, Mansour HR. 2004. Sequential determination of iron(II) and iron(III) in pharmaceutical by flow-injection analysis with spectrophotometric detection. *Anal Sci* 20:645–650.
- Fraser MP, Lakshmanan K, Fritz SG, Ubanwa B. 2002. Variation in composition of fine particulate emissions from heavy-duty diesel vehicles. *J Geophys Res-Atmos* 107(D21).
- Garg BD, Cadle SH, Mulawa PA, Groblicki PJ, Laroo C, Parr GA. 2000. Brake wear particulate matter emissions. *Environ Sci Technol* 34:4463–4469.
- Garvie LAJ, Buseck PR. 1998. Ratios of ferrous to ferric iron from nanometre-sized areas in minerals. *Nature* 396:667–670.
- Goto K, Tsuyoshi K, Furukawa T. 1962. Rapid colorimetric determination of manganese in waters containing iron: A modification of the formaldoxime method. *Anal Chim Acta* 27:331–334.
- Graney JR, Landis MS, Norris GA. 2004. Concentrations and solubility of metals from indoor and personal exposure PM<sub>2.5</sub> samples. *Atmos Environ* 38:237–247.
- Hammerle RH, Korniski TJ, Weir JE, Chladek E, Gierczak CA, Hurley RG. 1991. Particulate emissions from current model vehicles using gasoline with methylcyclopentadienyl manganese tricarbonyl. Presented at: International fuels and lubricants meeting and exposition; October; Toronto, ON, Canada. Warrendale, PA: SAE technical paper 912436.
- Heilbronn E, Eriksson H. 1997. Implications of manganese in disease, especially central nervous system disorders. In: *Mineral and Metal Neurotoxicology* (Yasui M, Strong MJ, Ota K, Verity MA, eds). CRC Press. Salem, MA.
- Hering S, Kreisberg N, John W. 2003. A Personal Particle Speciation Sampler. Research Report 114. Health Effects Institute, Boston, MA.
- Hoffmann P, Dedik AN, Ensling J, Weinbruch S, Weber S, Sinner T, Gutlich P, Ortner HM. 1996. Speciation of iron in atmospheric aerosol samples. *J Aerosol Sci* 27:325–337.
- Hopke PK, Ramadan Z, Paatero P, Norris GA, Landis MS, Williams RW, Lewis CW. 2003. Receptor modeling of ambient and personal exposure samples: 1998 Baltimore Particulate Matter Epidemiology-Exposure Study. *Atmos Environ* 37:3289–3302.
- Hurley RG, Hansen LA, Guttridge DL, Gandhi HS, Hammerle RH, Matzo AD. 1991. The effect of emission component durability by the fuel additive methylcyclopentadienyl manganese tricarbonyl (MMT). Presented at: International fuels and lubricants meeting and exposition; October; Toronto, ON, Canada. Warrendale, PA: SAE technical paper 912437.
- Janssen NA, Hoek G, Brunekreef B, Harssema H, Mensink I, Zuidhof A. 1998. Personal sampling of particles in adults: Relation among personal, indoor, and outdoor air concentrations. *Am J Epidemiol* 147: 537–547.
- Johansen AM, Siefert RL, Hoffmann MR. 2000. Chemical composition of aerosols collected over the tropical North Atlantic Ocean. *J Geophys Res* 105:15277–15312.
- John W, Reischl G. 1980. A cyclone for size-selective sampling of ambient air. *J Air Pollut Control Assoc* 30:872–876.
- Kargosha K, Noroozifar M. 2003. Flow injection speciation analysis of manganese in real samples by diphenylcarbazide-spectrophotometric determination. *Turkish J Chem* 27: 227–233.
- Kavouras IG, Stratigakis N, Stephanou EG. 1998. Iso- and anteiso-alkanes: Specific tracers of environmental tobacco smoke in indoor and outdoor particle-size distributed urban aerosols. *Environ Sci Technol* 32:1369–1377.
- Keeler KJ, Yip FY, Dvonch JT, Robins GT, Parker EA, Israel BA, Brakefield-Caldwell W. 2004. Personal exposures to particulate matter among children with asthma in Detroit, Michigan. *Atmos Environ* 38:6511–6524.
- Kessick MA, Vuceta J, Morgan JJ. 1972. Spectrophotometric determination of oxidized manganese with leuco crystal violet. *Environ Sci Technol* 6:642–644.

- King DW, Lin J, Kester DR. 1991. Spectrophotometric determination of iron(ii) in seawater at nanomolar concentrations. *Anal Chim Acta* 247:125–132.
- Klewicki JK, Morgan JJ. 1998. Kinetic behavior of Mn(III) complexes of pyrophosphate, EDTA, and Citrate. *Environ Sci Technol* 32:2916–2922.
- Kweon C, Okada S, Foster DE, Bae M, Schauer JJ. 2003. Effect of engine operating conditions on particle-phase organic compounds in engine exhaust of a heavy-duty direct-injection (D.I.) diesel engine. Presented at: SAE 2003 world congress and exhibition; March; Detroit, MI. Warrendale, PA: SAE technical paper 2003-01-0342.
- Kweon C, Okada S, Schauer JJ, Foster DE. 2002. Detailed chemical composition and particle size assessment of diesel engine exhaust. Presented at: SAE powertrain and fluid systems conference; October; San Diego, CA. Warrendale, PA: SAE technical paper 2002-01-2670.
- Lioy PJ, Waldman JM, Buckley T, Butler J, Pietarinen C. 1990. The personal, indoor and outdoor concentrations of PM-10 measured in an industrial community during the winter. *Atmos Environ Part B Urban Atmosphere* 24: 57–66.
- Majestic BJ, Schauer JJ, Shafer MM, Turner JR, Fine PM, Singh M, Sioutas C. 2006. Development of a wet-chemical method for the speciation of iron in atmospheric aerosols. *Environ Sci Technol* 40:2346–2351.
- Manchester-Neesvig JB, Schauer JJ, Cass GR. 2003. The distribution of particle-phase organic compounds in the atmosphere and their use for source apportionment during the southern California children's health study. *J Air Waste Manag Assoc* 53:1065–1079.
- Misra C, Singh M, Shen S, Sioutas C, Hall PA. 2002. Development and evaluation of a personal cascade impactor sampler (PCIS). *J Aerosol Sci* 33:1027–1047.
- Morgan JJ, Stumm W. 1965. Analytical chemistry of aqueous manganese. *J Am Water Works Assoc* 57:107–119.
- Nonova D, Evtimova B. 1973. Spectrophotometric study and analytical application of reaction between manganese(ii) and 4-(2-pyridylazo)resorcinol. *Talanta* 20:1347–1351.
- Ondov JM, Suarez AE. 2002. Ambient aerosol concentrations of elements resolved by size and by source: Contributions of some cytokine-active metals from coal- and oil-fired power plants. *Energy Fuels* 16:562–568.
- Papaefthymiou V, Kostikas A, Simopoulos A, Niarchos D, Gangopadhyay S, Hadjipanayis GC, Sorensen CM, Klabunde KJ. 1990. Magnetic hysteresis and mossbauer studies in ultrafine iron particles. *J Appl Phys* 67:4487–4489.
- Parkhomenko VD, Kolodyazhnyi AT, Galivets YD, Pokholok KV. 1990. Mössbauer spectroscopy applied to surfaces of ultrafine iron powders. *Sov Powder Metall Met Ceram* 29:165–167.
- Pehkonen SO, Siefert R, Erel Y, Webb S, Hoffmann MR. 1993. Photoreduction of iron oxyhydroxides in the presence of important atmospheric organic-compounds. *Environ Sci Technol* 27:2056–2062.
- Polidori A, Arhami M, Sioutas C, Delfino RJ, Allen R. 2007. Indoor/outdoor relationships, trends, and carbonaceous content of fine particulate matter in retirement homes of the Los Angeles Basin. *J Air Waste Manag Assoc* 57:366–379.
- Ressler T, Wong J, Roos J, Smith IL. 2000. Quantitative speciation of Mn-bearing particulates emitted from autos burning (methylcyclopentadienyl)manganese tricarbonyl-added gasolines using XANES spectroscopy. *Environ Sci Technol* 34:950–958.
- Rogge WF, Hildemann LM, Mazurek MA, Cass GR. 1994. Sources of fine organic aerosol.6. Cigarette-smoke in the urban atmosphere. *Environ Sci Technol* 28:1375–1388.
- Schauer JJ. 2003. Evaluation of elemental carbon as a marker for diesel particulate matter. *J Expo Anal Environ Epidemiol* 13:443–453.
- Schauer JJ, Cass GR. 2000. Source apportionment of wintertime gas-phase and particle-phase air pollutants using organic compounds as tracers. *Environ Sci Technol* 34: 1821–1832.
- Schauer JJ, Fraser MP, Cass GR, Simoneit BRT. 2002a. Source reconciliation of atmospheric gas-phase and particle-phase pollutants during a severe photochemical smog episode. *Environ Sci Technol* 36:3806–3814.
- Schauer JJ, Kleeman MJ, Cass GR, Simoneit BRT. 2002b. Measurement of emissions from air pollution sources. 5. C-1-C- 32 organic compounds from gasoline-powered motor vehicles. *Environ Sci Technol* 36:1169–1180.
- Schauer JJ, Lough GC, Shafer MM, Christensen WF, Arndt MF, DeMinter JT, Park J-S. 2006. Characterization of Metals Emitted from Motor Vehicles. Research Report 133. Health Effects Institute, Boston, MA.
- Schauer JJ, Rogge WF, Hildemann LM, Mazurek MA, Cass GR, Simoneit BRT. 1996. Source apportionment of airborne particulate matter using organic compounds as tracers. *Atmos Environ* 30:3837–3855.

- Sheesley RJ, Schauer JJ, Kenski D. 2004. Trends in secondary organic aerosol at a remote site in Michigan's Upper Peninsula. *Environ Sci Technol* 38:6491–6500.
- Sheesley RJ, Schauer JJ, Smith ND, Hays MD. 2000. Development of a Standardized Method for the Analysis of Organic Compounds Present In  $PM_{2.5}$ . In: Proceedings of the AWMA Annual Meeting 2000, Salt Lake City, UT.
- Siefert RL, Johansen AM, Hoffmann MR, Pehkonen SO. 1998a. Measurements of trace metal (Fe, Cu, Mn, Cr) oxidation states in fog and stratus clouds. *J Air Waste Manag Assoc* 48:128–143.
- Siefert RL, Johansen AM, Hoffmann MR, Pehkonen SO. 1998b. Measurements of trace metal (Fe, Cu, Mn, Cr) oxidation states in fog and stratus clouds. *J Air Waste Manag Assoc* 48:128–143.
- Singh M, Jaques PA, Sioutas C. 2002. Size distribution and diurnal characteristics of particle-bound metals in source and receptor sites of the Los Angeles Basin. *Atmos Environ* 36:1675–1689.
- Singh M, Misra C, Sioutas C. 2003. Field evaluation of a personal cascade impactor sampler (PCIS). *Atmos Environ* 37:4781–4793.
- Stookey LL. 1970. Ferrozine: A new spectrophotometric reagent for iron. *Anal Chem* 42:779–781.
- Sun GB, Crissman K, Norwood J, Richards J, Slade R, Hatch GE. 2001. Oxidative interactions of synthetic lung epithelial lining fluid with metal-containing particulate matter. *Am J Physiol Lung Cell Mol Physiol* 281:L807–L815.
- Terhaar GL, Griffing ME, Brandt M, Oberding DG, Kapron M. 1975. Methylcyclopentadienyl manganese tricarbonyl as an antiknock: Composition and fate of manganese exhaust products. *J Air Pollut Control Assoc* 25:858–860.
- van Aken PA, Liebscher B. 2002. Quantification of ferrous/ferric ratios in minerals: new evaluation schemes of Fe L<sub>2,3</sub> electron energy-loss near-edge spectra. *Physics and Chemistry of Minerals* 29: 188–200.
- van Aken PA, Liebscher B, Styrsa VJ. 1998. Quantitative determination of iron oxidation states in minerals using Fe L<sub>2,3</sub>-edge electron energy-loss near-edge structure spectroscopy. *Physics and Chemistry of Minerals* 25:323–327.
- Viollier E, Inglett PW, Hunter K, Roychoudhury AN, Van Cappellen P. 2000. The ferrozine method revisited: Fe(II)/Fe(III) determination in natural waters. *Appl Geochem* 15: 785–790.
- Weiss B, Reuhl K. 1994. Delayed Neurotoxicity: A Silent Toxicity. In: Principles of Neurotoxicity (Chang LW, ed). Marcel Dekker, New York.
- Witholt R, Gwiazda RH, Smith DR. 2000. The neuro-behavioral effects of subchronic manganese exposure in the presence and absence of pre-parkinsonism. *Neurotoxicol Teratol* 22:851–861.
- Zayed J. 2001. Use of MMT in Canadian gasoline: Health and environment issues. *Am J Ind Med* 39:426–433.
- Zheng M, Cass GR, Schauer JJ, Edgerton ES. 2002. Source apportionment of  $PM_{2.5}$  in the southeastern United States using solvent-extractable organic compounds as tracers. *Environ Sci Technol* 36:2361–2371.
- Zhu X, Prospero JM, Savoie DL, Millero FJ, Zika RG, Saltzman ES. 1993. Photoreduction of iron(III) in marine mineral aerosol solutions. *J Geophys Res* 98:9039–9046.
- Zhuang GS, Yi Z, Duce RA, Brown PR. 1992. Link between iron and sulfur cycles suggested by detection of Fe(ii) in remote marine aerosols. *Nature* 355:537–539.

---

#### APPENDICES AVAILABLE ON THE WEB

---

Appendices A, B, C, and D contain supplemental material not included in the printed report. They are available on the HEI Web site at <http://pubs.healtheffects.org>. They may also be requested by contacting the Health Effects Institute at 101 Federal Street, Suite 500, Boston, MA 02110, +1-617-488-2300, fax +1-488-2335, or e-mail [pubs@healtheffects.org](mailto:pubs@healtheffects.org). Please give (1) the first author, full title, and number of the Research Report and (2) the title of the appendix requested.

Appendix A. St. Louis Trucking Terminal Study Organic Speciation Data

Appendix B. UC–Irvine Pilot Study Metals Data

Appendix C. Microwave Digestion of Aerosol Particulate Matter

Appendix D. Determination of Elemental Composition by HR-ICP–MS

---

#### ABOUT THE AUTHORS

---

**James J. Schauer** is professor of civil and environmental engineering at the University of Wisconsin–Madison and also carries appointments in the Environmental Chemistry and Technology Program and as director of air chemistry at the Wisconsin State Laboratory of Hygiene. He is well

known for his work in source apportionment of atmospheric PM.

**Brian J. Majestic** is a doctoral student with Professor Schauer.

**Rebecca J. Sheesley** is a postdoctoral research associate with Professor Schauer.

**Martin M. Shafer** is an associate scientist in the Environmental Chemistry and Technology Program at the University of Wisconsin–Madison. He is an expert in trace-metal analytic chemistry, speciation, biogeochemistry, and field sampling.

**Jeffrey T. DeMinter** is a senior chemist in environmental sciences at the Wisconsin State Laboratory of Hygiene, specializing in the chemical analysis of atmospheric PM.

**Mark Meiritz** is a senior chemist in environmental sciences at the Wisconsin State Laboratory of Hygiene, specializing in chemical analysis using mass spectrometry.

---

OTHER PUBLICATIONS RESULTING FROM THIS RESEARCH

---

Majestic BJ, Schauer JJ, Shafer MM, Turner JR, Fine PM, Singh M, Sioutas C. 2006. Development of a wet-chemical method for the speciation of iron in atmospheric aerosols. *Environ Sci Technol* 40:2346–2351.

---

ABBREVIATIONS AND OTHER TERMS

---

AU	absorbance units
cps	counts per second
DL	detection limit
DPC	diphenylcarbazine
EC	elemental carbon
EDTA	ethylenediaminetetraacetic acid
FAD	formaldehyde
GC–MS	gas chromatography–mass spectrometry
HA	hydroxylamine hydrochloride
HCl	hydrochloric acid

HERMON	High Energy Resolution Monochromator
HNO <sub>3</sub>	nitric acid
HR-ICP–MS	high-resolution inductively coupled plasma–mass spectrometry
ICP–MS	inductively coupled plasma–mass spectrometry
MMT	methylcyclopentadienyl manganese tricarbonyl
MQ water	Milli-Q water (also > 18.0 mΩ/cm <sup>2</sup> water)
NIH	National Institutes of Health
NCI	National Cancer Institute
ng	nanogram
NIST	National Institute of Standards and Technology
OC	organic carbon
PAH	polycyclic aromatic hydrocarbon
P and D	pickup and delivery
PCIS	personal cascade impactor sampler
pg	picogram
PM	particulate matter
PM <sub>2.5</sub>	particulate matter 2.5 μm or smaller in aerodynamic diameter
PM <sub>10</sub>	particulate matter 10 μm or smaller in aerodynamic diameter
PTV-GC–MS	programmable temperature vaporization gas chromatography–mass spectrometry
Q-ICP–MS	quadrupole inductively coupled plasma–mass spectrometry
RFPA	Request for Preliminary Applications
RSD	relative standard deviation
SRM	standard reference material
TD-GC–MS	thermal-desorption gas chromatography–mass spectrometry
TEY	total electron yield
U.S. EPA	U.S. Environmental Protection Agency
UC	University of California
USC	University of Southern California
XANES	x-ray absorption near edge structure

---

 ABBREVIATIONS OF CHEMICAL ELEMENTS
 

---

Ag silver	Cu copper	Mn manganese	Sc scandium
Al aluminum	Dy dysprosium	Mo molybdenum	Se selenium
Ar argon	Er erbium	N nitrogen	Si silicon
As arsenic	Eu europium	Na sodium	Sm samarium
Au gold	Fe iron	Nd niodymium	Sn tin
Ba barium	Ga gallium	Ni nickel	Sr strontium
Be beryllium	Hf hafnium	O oxygen	Ti titanium
C carbon	Ho holmium	P phosphorus	Th thorium
Ca calcium	Ir iridium	Pb lead	Tl thallium
Cd cadmium	K potassium	Pd palladium	U uranium
Ce cerium	Kr krypton	Pt platinum	V vanadium
Cl chlorine	La lanthanum	Rb rubidium	W tungsten
Co cobalt	Li lithium	Rh rhodium	Y yttrium
Cr chromium	Lu lutetium	Ru ruthenium	Yb ytterbium
Cs cesium	Mg magnesium	S sulfur	Zn zinc
		Sb antimony	Zr zirconium



Research Report 153, *Improved Source Apportionment and Speciation of Low-Volume Particulate Matter Samples*, J.J. Schauer et al.

---

## INTRODUCTION AND BACKGROUND

---

Over the past two decades, research on the human health effects of exposure to particulate matter (PM\*) has focused on the role of particle size in assessing PM toxicity. As particulate air pollution has been increasingly associated with adverse health effects, interest has been growing in understanding the chemical composition of inhalable PM and studying how exposures to specific PM constituents are associated with observed health outcomes.

In 1998, HEI initiated a research program aimed at transition metals, some of which can be toxic even at low doses. HEI issued a Request for Preliminary Applications (RFP) 98-4, "Research on Metals Emitted by Motor Vehicles," that solicited studies of metals found in auto emissions and in tailpipe exhaust in particular. Under RFP 98-4, HEI approved three studies for funding, including one by Dr. James Schauer of the University of Wisconsin–Madison. In that earlier study, Schauer had measured metals in emissions of fine PM with an aerodynamic diameter  $\leq 2.5 \mu\text{m}$  (PM<sub>2.5</sub>) and of coarse PM with an aerodynamic diameter  $\leq 10 \mu\text{m}$  (PM<sub>10</sub>) under several conditions: in tunnel studies, during vehicle cold starts in winter and summer, from tire and brake wear, and in ambient samples from various cities in the American Midwest (Schauer et al. 2006).

Much of the general characterization of the composition of PM has been performed on specimens collected by high-volume samplers co-located with ambient air sampling monitors. Data collected by ambient monitors are helpful in understanding the role of various PM<sub>2.5</sub> constituents when assessing human health risks and regional variations in PM<sub>2.5</sub> composition throughout the country. However,

they lack the spatial and temporal resolution needed to serve as a surrogate for dose when assessing human exposures. And personal sampling, although it improves exposure estimation, makes use of small-scale equipment that traditionally does not collect sufficient airborne PM for proper speciation analysis. Likewise, air sampling campaigns aimed at detecting variations in PM<sub>2.5</sub> composition by repeatedly sampling for short periods of time do not produce sufficient material for analysis using existing methods.

Schauer applied to HEI for funding under Request for Applications 02-2, "Walter A. Rosenblith New Investigator Award," which was established to provide support for an outstanding investigator at the Assistant Professor level who is at the beginning of his or her independent research career. The purpose of the award is to encourage talented investigators to conduct research in air pollution and public health.

Schauer submitted his full application, "Source Apportionment and Speciation of Particulate Matter to Support Exposure and Health Studies," on May 1, 2002. At its July 2002 meeting, the HEI Health Research Committee discussed the proposal, the letters of support, the generally positive external and Committee reviews, and Schauer's satisfactory performance on the earlier study for HEI and recommended the study for funding. The Committee was impressed with Schauer's track record in the field as well as his interest in collaborating with researchers in exposure assessment and epidemiology, and thought that his proposed research was important work that needed to be done.

In the current report, Schauer and colleagues detail the methodologic research they conducted on the quantitative measurement of various chemical species and compounds in low-volume PM<sub>2.5</sub> samples collected using personal sampling equipment. The investigators describe the methods they developed for the detection and quantification of a wide range of trace metals and nonpolar and polar organic species in low-volume PM samples using a variety of protocols based on gas chromatography–mass spectrometry (GC–MS); wet-chemical methods for trace metals and their application to the determination of the oxidation states of iron (Fe), chromium (Cr), and manganese (Mn); and the results of the application of these methods to exposure assessments in urban areas and personal sampling studies.

---

Dr. James J. Schauer's 3-year study, "Source Apportionment and Speciation of Particulate Matter to Support Exposure and Health Studies," began in April 2003. Total expenditures were \$273,376. The draft Investigators' Report from Schauer and colleagues was received for review in December 2006. A revised report, received in January 2008, was accepted for publication in February 2008. During the review process, the HEI Health Review Committee and the investigators had the opportunity to exchange comments and to clarify issues in both the Investigators' Report and the Review Committee's Critique.

This document has not been reviewed by public or private party institutions, including those that support the Health Effects Institute; therefore, it may not reflect the views of these parties, and no endorsements by them should be inferred.

\* A list of abbreviations and other terms appears at the end of the Investigators' Report.

---

**SPECIFIC AIMS**

---

The investigators proposed five specific aims for the study, covering multiple chemical analysis methods suitable for measuring concentrations of organic compounds, trace metals, trace-element isotopes, and oxidation states of selected elements in PM<sub>2.5</sub> specimens collected using personal sampling equipment. The five aims were as follows:

1. To develop and validate a GC–MS technique to quantify a broad range of organic compounds present in low-volume personal exposure samples, including all of the molecular markers used in particle-phase organic-compound-based source apportionment models (Schauer et al. 1996, 2002; Schauer and Cass 2000; Zheng et al. 2002; Manchester-Neesvig et al. 2003);
2. To develop and validate a low-cost thermal desorption GC–MS (TD-GC–MS) technique to quantify a list of selected organic compounds present in PM samples collected with personal exposure samplers that can be effectively integrated into human exposure and epidemiologic studies;
3. To optimize sampling and inductively coupled plasma mass spectrometry (ICP–MS) analysis techniques for the measurement of trace metals and selected trace-element isotope signatures in PM samples collected with personal exposure samples;
4. To develop and validate low-cost techniques to measure the oxidation states of trace levels of Fe, Mn, and Cr present in PM samples collected with ambient samplers, personal samplers, and source samplers; and
5. To integrate these analytic techniques with human exposure and epidemiologic studies.

---

**METHODS DEVELOPMENT**

---

In order to address the aims of their research, the investigators developed a set of analytic methods for low-volume PM samples. These methods employed a number of variations on GC–MS analysis adapted to identify and quantify a broad range of trace-metal species, organic carbon (OC) compounds, and polar organic compounds found in PM samples. For more economical analysis of specific metals (Fe, Mn, and Cr) and quantification of the relative proportions of their oxidative states, the investigators also developed and tested a set of wet-chemical methods for spectrophotometric analysis. The methods are briefly described below, and their attributes are summarized in Critique Table 1.

In describing their work, the investigators first outlined a number of overarching quality standards that they

applied to all their attempts to develop methods for the identification and quantification of chemical species in low-volume PM samples. They stated that all methods development employed a rigorous application of clean-chemistry concepts and was intended to address the three pillars of quantitative trace-element analysis, namely the control and minimization of background values using blanks; the maximization of sensitivity; and the control, isolation, and removal of interferences. Detailed descriptions of the methods described here are given in Appendices C and D of the Investigators' Report (available on the HEI Web site at <http://pubs.healtheffects.org> or by request).

**ACID DIGESTION FOR TRACE-ELEMENT CHARACTERIZATION**

Schauer and his team analyzed PM samples from National Institute of Standards and Technology (NIST) standard reference materials and field-derived PM samples for multiple trace elements using the low-volume methods they developed for this project. (A complete list of these elements appears in Table 2 of the Investigators' Report.) They compared retrieval levels (recovery efficiency) in samples processed using established methods and their new methods for a large number of trace elements using quadrupole ICP–MS (Q-ICP–MS) and then adapted their procedures for high-resolution magnetic sector ICP–MS (HR-ICP–MS).

Before spectrometric analysis, each trace-element sample was processed using the investigators' improved micro-volume microwave-assisted acid digestion methods. The goals of improving these methods were to reduce digestion blank concentrations and variability, lower detection limits (DLs) by reducing the amounts of acids used, improve signal-to-noise ratios for a given digested mass, and enable recovery of silicon (Si) during the digestion of aerosol samples. The methods permitted reduction of the amount of high-purity acid used for each sample from 2.2 mL for a conventionally processed sample to 0.9 mL for the open-vessel method and 0.6 mL for the sealed-vial method (as described below). Reducing the acid volume yielded more concentrated samples and lowered blank concentrations (by reducing the amount of background contamination from the acid), both of which improved signal-to-noise ratios and lowered the DL for the samples.

The apparatus consisted of a digestion “bomb” (i.e., a sealed pressure vessel) to hold the samples and a rotor to hold the Teflon vials of acid and PM and move them around during microwave heating. The investigators tested two variations of the system: one in which the vials were open during processing and one in which they were capped. Capping the vials allowed the investigators to successfully

**Critique Table 1.** Overview of Methods for Low-Volume PM Sample Analysis

Method of Analysis	Elements or Compounds Detected	Advantages	Disadvantages
High-resolution inductively coupled plasma–mass spectrometry (HR-ICP–MS)	Extensive list of inorganic trace elements	Low DL for most elements Detects an extensive range of elements	Moderately expensive
Thermal–desorption gas chromatography–mass spectrometry (TD-GC–MS)	A broad range of nonpolar organic compounds	Low DL Detects a range of compounds generated by combustion	Relatively expensive
Programmable temperature vaporization gas chromatography–mass spectrometry (PTV-GC–MS)	Polar organic compounds	Low DL Range of compounds	Relatively expensive Chemicals used in process caused frequent equipment failures
Spectrophotometric measurement of Fe	Quantity and relative amounts of two oxidation states of soluble Fe	Low cost Readily available equipment	
XANES measurement of Fe oxidation states	Insoluble and soluble Fe(II) and Fe(III)	Readily available equipment Compliments spectrophotometric methods	Need access to a laboratory that has experience in and facilities for conducting XANES analyses
Spectrophotometric measurement of Mn	Soluble and oxidized manganese	Low cost Readily available equipment	
Spectrophotometric measurement of Cr(VI)	Hexavalent chromium	Low cost Readily available equipment	DL is too high for most ambient samples

recover Si from the samples (the open-vessel method allowed acid-digested Si to escape as gas-phase silicon tetrafluoride). The investigators reported that they subjected the sealable vials to an extensive performance assessment prior to use. They found that failure rates could be minimized by careful and consistent torquing of the caps and by observing lower temperature limits (190°C) than those used in the open-vessel method (210°C).

When the investigators analyzed processed samples using Q-ICP–MS, they reported that recovery of elements in the NIST standard particulates was acceptable and that certain difficult-to-extract elements (Cr, palladium, platinum, rhodium [Rh], and Si) had been recovered in measurable quantities (see Figure 2 of the Investigators' Report). Lanthanum (La), yttrium, gold (Au), hafnium (Hf), and zirconium (Zr) showed poor recovery using the new methods, but Au, Hf, and Zr usually show poor recovery using established methods as well. The variability in arsenic and cobalt recovery was higher with the microvolume methods than is typical with the established methods. Recovery of most elements was comparable for the open-vessel and sealed-vial methods, with the exception of

improved recovery of silver, antimony, La, and thallium (Tl) when the investigators processed samples in sealed vials. In standard silica samples and samples spiked with known amounts of silica, Si was solubilized and recovered in measurable quantities from solutions processed in the sealed vials.

Schauer and colleagues also developed methods for analysis of trace elements using HR-ICP–MS. HR-ICP–MS has certain advantages over Q-ICP–MS for trace-element analysis, including superior sensitivity, reduced background noise, a much higher effective signal-to-noise ratio, and the removal of spectral interference through isolation (mass resolution). These advantages mean that investigators can detect and quantify more elements using HR-ICP–MS methods and quantify problematic elements, such as Fe, Mg, calcium, potassium, and sodium, that have spectra that are typically masked by spectral interference in Q-ICP–MS. Coupled with the improvements in blank concentrations resulting from microvolume methods, quantification of trace elements at concentrations < 100 pg/L — approximately 15 ppb of analyte per 100 µg of filter-collected aerosol — is practical with HR-ICP–MS analysis.

In Figure 4 of the Investigators' Report, Schauer and colleagues report order-of-magnitude improvements in method DLs for a large group of elements. For Rh, Tl, cesium, and iridium, the team observed an improvement of nearly three orders of magnitude with HR-ICP-MS and microvolume digestion methods over Q-ICP-MS analysis and established digestion methods. They estimated that they would be able to detect around 30 different elements in a 100- $\mu\text{g}$  sample of filter-collected aerosol, assuming observed blank concentrations and a signal-to-noise ratio of three or greater. The sealed-vial method also permitted the quantitative measurement of Si in very low-volume PM samples, of the sort that are commonly collected in low-volume personal samplers.

### GC-MS METHODS FOR QUANTIFICATION OF ORGANIC COMPOUNDS

Because particulate aerosol samples are composed of a broad mixture of elements and compounds, including organic compounds, it is desirable to detect and measure the organic compounds that might be associated with health effects. Organic compounds such as polycyclic aromatic hydrocarbons (PAHs) and levoglucosan are generated by combustion processes, are present in aerosols, and are of interest to health researchers. The investigators developed methods for the extraction of these organic compounds in low-volume PM samples for analysis using TD-GC-MS and programmable temperature vaporization GC-MS (PTV-GC-MS).

The new TD-GC-MS method improves on traditional GC-MS methods by directly analyzing the sample filter. This reduces the amount of carbon necessary for analysis and minimizes sample handling and preparation by eliminating organic-solvent extraction and dilution. These features are important for the analysis of very low-volume samples, because less material is required for analysis and because reduced handling reduces blank concentrations and the potential for sample contamination during processing. The TD-GC-MS methods described here quantify only nonpolar organic compounds, which are common in aerosols from vehicle exhaust emissions. The investigators built on existing GC-MS methods for the analysis of organic compounds in atmospheric PM samples, using the same conditions and quantification procedures used in the TD-GC-MS method.

Filter samples were either used in their entirety or a punch measuring 1 to 1.45  $\text{cm}^2$  was removed for analysis, depending on how much PM was present on the filter. The optimal filter or punch for the TD-GC-MS setup holds 15 to 40  $\mu\text{g}$  of OC, present in organic compounds in the PM. Each filter sample was spiked with an isotopically labeled

internal standard containing several PAHs, a sterane, and several *n*-alkanes to ensure stable calibration for the quantification of the compounds.

Figure 6 of the Investigators' Report schematically shows the desorption process for the samples. Samples were placed in a sample tube that was then heated to 360°C for 20 minutes to desorb the compounds of interest off the filter. In order to concentrate the sample for analysis, the resulting vapor was condensed on a glass-bead focusing trap at 0°C. After condensation, the trap was then heated to 360°C to desorb the analytes, and the sample was introduced onto the GC-MS column for analysis.

Calibration is similar to that published for standard solvent extraction methods for GC-MS. A three-point calibration curve was run at the start of each sample set with a standard for the quantification of compounds on the filter samples. After every five samples, the calibration standard was rerun as a check standard to verify continuing calibration accuracy. A duplicate sample or spike was tested after every 10 samples to assess reproducibility. TD-GC-MS also permits the use of "matrix spikes"—that is, samples that assess the effect of the aerosol matrix on the recovery of target compounds.

To validate the TD-GC-MS methods, the investigators used medium-volume samples collected at a U.S. Environmental Protection Agency (U.S. EPA) Supersite in East St. Louis, Illinois, in July 2001. Because these samples were considerably larger than the samples on filters used in personal samplers, the investigators used a small fraction of the filters to test their methods—a 1.45- $\text{cm}^2$  punch—consistent with samples collected with personal samplers. They analyzed 15 of these samples. Average recovery values for check standards are plotted in Figure 8 of the Investigators' Report; a compilation of six duplicate-sample analyses is shown in Figure 9. An analysis of analytic uncertainty using check standards for every fifth run for compounds of interest is shown in Figure 11 of the Investigators' Report.

The investigators performed a further study comparing results from their TD-GC-MS methods with results from conventional solvent extraction and GC-MS methods using 28 ambient samples collected at the East St. Louis Supersite. These samples had been previously analyzed using conventional methods. The team reported good levels of precision and accuracy when their TD-GC-MS results for PAHs, alkanes, hopanes, and steranes were compared with results from the conventional methods.

The investigators also used programmable temperature vaporization GC-MS (PTV-GC-MS) for sample analysis. PTV-GC-MS improves the potential for GC-MS to identify and quantify certain nonpolar compounds associated with

combustion, such as PAHs and levoglucosan, in low-volume PM samples.

Samples were extracted into either low (5 mL) or high (300 mL) quantities of solvent and evaporated to 0.1 mL before analysis. The PTV-GC-MS method uses about 10 times as much sample volume (30  $\mu$ L) as traditional GC-MS, requiring a commercially available high-volume injection system to vent solvent prior to slow transfer of the analyte to the column.

The investigators performed a small study to compare the results for samples from the Supersite analyzed using the PTV-GC-MS, TD-GC-MS, and traditional low-volume GC-MS systems. Results for the quantification of PAHs, alkanes, hopanes, and steranes were in reasonable agreement among all three methods; however, PTV-GC-MS results generally read approximately 20% higher than TD-GC-MS and traditional GC-MS results. Further detailed analysis, made available by the investigators to the HEI Research Committee (but not included in the report), suggested that the bias was quite variable for individual compounds, particularly for some of the *n*-alkanes. Correlations ranged from as low as  $r^2 = 0.34$  to as high as  $r^2 = 0.95$ , although the majority of correlations were above 0.7.

Schauer and colleagues further adapted the PTV-GC-MS methods to analyze certain polar organic compounds, such as acids, through methylation and silylation prior to analysis. They achieved good calibration curves for most acids, but higher amounts of contaminants in the blanks and poor recovery of volatile species with the high-volume injection resulted in poor recovery of some acids, such as aliphatic diacids and palmitic and stearic acids.

#### WET-CHEMICAL SPECTROPHOTOMETRIC ANALYSIS METHODS

The investigators also developed additional methods for the analysis of aerosol PM samples, including wet-chemical spectrophotometric analysis methods for the detection and quantification of very specific species found in aerosol PM and their oxidation states that are of interest in health researchers. The team developed most of these methods for inexpensive extraction and analysis of samples in laboratories using commonly available laboratory equipment.

Because spectrophotometric techniques are relatively inexpensive and simple, the investigators specified liquid waveguide spectrophotometry using a sample cell with a 1-m path length, an ultralow-noise photodiode array detector, and fiber-optic cables for the purposes of metal speciation. This equipment has DLs for the trace-metal species of interest approaching those of HR-ICP-MS at a fraction of the cost.

Wet-chemical speciation methods for the analysis of oxidation states of Fe (Fe(II) and Fe(III)), Cr (Cr(VI)), and Mn (total and oxidized soluble) involved extraction in acid-cleaned polypropylene vials using up to 10 mL of one of four leachates (see Table 6 of the Investigators' Report). The investigators immersed Teflon filters in each leachate and withdrew aliquots of approximately 2 mL at intervals of 20 to 30 minutes and analyzed them for soluble Fe and Mn; no Fe or Mn was found in solution from the filter blanks after 120 minutes. When leaching PM samples, the investigators used a rotisserie shaker for 2 hours, then immediately filtered the leachate through an acid-cleaned polypropylene filter before spectrophotometric analysis.

Atmospheric PM was collected at the Supersite every other day from March 13 to March 31, 2005, using samplers built specifically for the study. Two larger-volume pumps were used for this sampling campaign, each split five ways, collecting PM onto Teflon filters in personal-sample-scale aluminum filter holders, resulting in 10 co-located samples per day.

Schauer and his team developed measurement methods that resolved the Fe(II) and Fe(III) oxidation states of Fe in PM (there is physiologic and toxicologic evidence that these oxidation states of Fe might behave differently and be associated with different health effects in the human body). They also developed a ferrozine assay that had the potential to detect Fe of various oxidation states in the small volumes of PM collected in personal samplers.

After the samples were leached and the leachate was filtered, the investigators added ferrozine solution to aliquots of the leachate. They analyzed some ferrozine-spiked samples immediately and analyzed others after 24 hours of storage in the dark at 4°C. They measured Fe(II) by pumping about 1.5 mL of the solution through a 1-m path-length liquid waveguide fiber-optic cell, obtaining an absorbance spectrum from 400 to 700 nm. They monitored absorption of the Fe(II)-ferrozine complex at 562 nm. This instrumentation and method allowed the investigators to detect Fe(II) at concentrations of less than 0.100  $\mu$ g/L of solution, corresponding to a DL of under 0.11 ng/m<sup>3</sup> for the tested air samples. Comparison tests of the four leaching solutions demonstrated that the pH 4.3 acetate leach recovered the greatest amounts of Fe(II).

In order to measure Fe(III) in solution, the investigators added hydroxylamine hydrochloride solution to the leachate to convert Fe(III) to Fe(II). After five minutes, they added ferrozine to the mixture, measured Fe(II) concentrations, and determined the Fe(III) content by subtraction of the previously measured Fe(II) concentrations.

Given concerns that photoreduction of Fe(III) and oxidation of Fe(II) in sampled PM might affect results over

time, the investigators designed an experiment to measure changes in results over the course of a year of filter storage. As shown in Figure 16 of the Investigators' Report, they found that storage leads to modest declines in yields (about 150–200 µg soluble Fe(II)/g of PM over the course of a year).

Manganese is a metal that is an essential element of the human diet but is associated with neurologic disease at high doses and is therefore classified as a hazardous air pollutant by the U.S. EPA. Schauer and his team developed a method to measure total soluble Mn and Mn in oxidized states extracted from PM collected using personal air samplers. The method used formaldoxime (FAD) with *o*-toluidine, both inexpensive reagents, to measure oxidized species of Mn at concentrations found in atmospheric PM.

FAD complexes with Mn and Fe in solution and absorbs light at peak wavelengths of 450 nm for Mn and 525 nm for Fe, with a minor interfering peak for Fe at 450 nm. The Fe interference was reduced by adding ethylenediaminetetraacetic acid (EDTA) and hydroxylamine hydrochloride (HA) and lowering the pH of the leachate solution. As shown in Figure 19 of the Investigators' Report, these additions successfully removed the Fe interference for concentrations up to the peak anticipated Fe content of the PM samples. Because pH reductions resulted in some color loss in the solution and color loss is important in spectrophotometric analysis, the investigators tested the effect of the pH reduction on the analysis. They found that, despite a 26.3% decrease in color with a pH decrease from 9.0 to 7.5, reasonable precision and DLs were retained at the reduced pH needed to remove the Fe interference.

Calibration samples for analysis were prepared with dilutions of a stock Mn(II) solution from Mn(II)Cl<sub>2</sub> salt in 1% trace-metal HCl. To each 1.95 mL of a standard or a sample solution, the investigators added specified amounts of sodium hydroxide (NaOH), FAD, EDTA, and HA (to lower the pH of the solution to 7.5). Five minutes after the HA addition, the solution was pumped into the spectrophotometric analysis system to obtain the absorbance spectrum from 400 to 700 nm.

The team also measured soluble oxidized Mn using *o*-toluidine, which oxidizes in the presence of the higher oxidation states of Mn and creates an absorbance peak at 440 nm. Because Mn(III) compounds oxidize one molecule of *o*-toluidine and Mn(IV) and Mn(VII) oxidize two molecules, the method measures the oxidizing potential of Mn in the solution, rather than the absolute quantity of oxidized Mn in solution. The investigators prepared calibration standards for two oxidation states from Mn(III) pyrophosphate and potassium permanganate (Mn(VII)).

The investigators analyzed samples by taking filtered samples or standards and adding first *o*-toluidine, then perchloric acid. They controlled for the effects of light by keeping blanks and samples in the dark for 30 minutes and then measuring them in triplicate, which prevented and removed the effects of photo-oxidation. PM samples were derived from seven co-located PM<sub>10</sub> samplers at the East St. Louis Supersite on March 19, 2005. Although measurable results were obtained for soluble Mn by way of the FAD technique, no oxidized Mn was detected in the sample extracts. Investigation of identical standards prepared from the Mn(VII) solutions demonstrated a wide range of scatter in measured values, possibly caused by breakdown of the standard Mn(VII) to lower oxidation states or photo-oxidation from ambient light or spectrophotometer light. Each of the four leachate solutions was also tested on PM obtained from Supersite sampling on March 17 and March 21, 2005; the highest soluble fraction was shown for the acetate solution (see Figure 22 of the Investigators' Report).

Of all the oxidation states of Cr, only hexavalent Cr (Cr(VI)) is known to form reactive oxygen species capable of damaging DNA and is considered carcinogenic. Chrome plating and steel production generate occupational exposure to Cr(VI). For these reasons, the team adapted the diphenylcarbazide (DPC) wet-chemical method for analyzing Cr(VI) concentrations present in PM from personal samplers run in occupational settings.

The investigators created standards by diluting Cr(VI) stock standards in either high-purity water or sodium bicarbonate solution at pH 7.4. Standards were treated with phosphoric acid and DPC, and the Cr(VI)–DPC complex was quantified using spectrophotometry, with peak absorbance at 540 nm. Based on their calibrations, the investigators estimated the DL to be less than 0.011 ng/m<sup>3</sup> for a 24-hour sampling period at 6 L per minute, which is suitable for measuring likely personal exposures in occupational settings. Although four co-located filters were analyzed from the Supersite, the investigators were not able to detect any Cr(VI), because the sampling sites did not have sufficient exposure concentrations to reach the DL.

#### QUANTIFICATION OF FE(II) AND FE(III) BY XANES SPECTROSCOPY

Schauer and his team wanted to develop even finer methods than the wet-chemical methods described above for analyzing the redox chemistry of aerosol PM collected for the study. To this end, a technique was developed for aerosol PM samples using x-ray absorption near edge structure (XANES) spectroscopy, which allows investigators to observe overall changes in oxidation states. XANES measurements complement ICP–MS measurements of total Fe

and the wet-chemical methods, allowing the soluble fraction of Fe(II) and Fe(III) to be compared with the total Fe and the total Fe(II) and Fe(III) fractions of the aerosol.

Using XANES spectroscopy, the investigators prepared a standard calibration curve from standards created with varying proportions of Fe(II) and Fe(III) from solutions of Fe(II) and Fe(III) ammonium sulfate salts. Because of low amounts of Fe and high spectral noise levels in aerosol PM samples from the Supersite as compared with those of the standards, the  $L_{III}$  rather than the customary  $L_{II}$  edge of the XANES spectra were used in practice to calculate the relative fractions of Fe(II) and Fe(III) (see Figure 25 of the Investigators' Report).

---

#### REAL-WORLD APPLICATION STUDIES OF LOW-VOLUME PM SAMPLE ANALYSIS METHODS

---

Once the basic methods research was completed, Schauer and his team sought real-world applications for the methods they had developed in order to demonstrate the methods'

utility for a range of studies using low-volume PM samples. The investigators used the methods they had developed to analyze low-volume PM samples collected in various locations and situations for a variety of experimental reasons. Because the samples used in the various analyses were sometimes collected by different equipment operating in the same locations, the sampling campaigns are briefly described below and summarized in Critique Table 2.

#### SAMPLING CAMPAIGNS

##### U.S. EPA Supersite in East St. Louis

In addition to collecting samples for use in the validation and testing of methods developed for this study, the investigators also used the U.S. EPA Supersite in East St. Louis, Illinois, to conduct two separate sampling campaigns for two separate methods-application studies. Samples from the first campaign were used for the sampler intercomparison analysis described in the following section. The investigators collected one large-scale ambient sample using a cyclone sampler and six co-located personal-scale samplers

---

**Critique Table 2.** Sampling Sites and Campaigns

---

Location	Sample Analysis	Sampling Details
U.S. EPA Supersite East St. Louis, IL	Sampler intercomparison analysis	Large-scale ambient cyclone Six co-located personal samplers (various designs and filters)
	Fe aging study	Four co-located personal cascade impactors
	Mn speciation analysis	Samples from above campaigns (compared with Toronto levels)
University of Southern California—Main Campus Los Angeles, CA	Sampler intercomparison analysis	Large-scale ambient monitor (split into two samples) Four co-located personal samplers (three designs)
Rancho Los Amigos National Rehabilitation Center Los Angeles, CA	Fe aging study	Four co-located personal cascade impactors
Light industrial neighborhood Waukesha, WI	Fe aging study	Four co-located personal cascade impactors, 2.5 m off the ground
Toronto, Ontario, Canada	Mn speciation analysis	Single personal sampler on residential balcony
St. Louis truck terminal St. Louis, MO	Cohort study of truckers and truck terminal workers	Personal, work area, and outdoor ambient air samplers Personal samples from workers in six job classifications; area samples from four work areas
Retirement home Los Angeles, CA	Epidemiologic study of elderly retirement-home residents	Personal, indoor area, and outdoor ambient air samplers

---

representing three design and substrate combinations. In the second campaign, samples were collected using four co-located personal cascade impactors and analyzed as part of the Fe aging study, described below.

#### **University of Southern California and Rancho Los Amigos**

Schauer and his team used two locations in the Los Angeles Basin for PM sampling for two separate methods-application studies. The first site was at the main campus of the University of Southern California near downtown Los Angeles, where the investigators placed an ambient monitor that collected two split samples and four co-located personal samplers of three designs. The resulting samples were used for the sampler intercomparison analysis, described below. The second site was at the Rancho Los Amigos National Rehabilitation Center (where some of the highest PM<sub>10</sub> concentrations in the United States have been measured [Singh et al. 2002]) in the Los Angeles Basin. The investigators placed four co-located personal cascade impactor samplers (PCISs) to collect size-fractionated PM<sub>10</sub> samples that were used for the Fe aging study.

#### **Waukesha**

Four co-located PCISs were placed in a suburban residential–light industrial site in Waukesha, Wisconsin, to collect PM samples for use in the investigators' Fe aging study. Because the site was fenced, the samplers were placed at the height of the fence, about 2.5 m off the ground.

#### **Toronto**

In addition, a single personal sampler was placed on a third-floor balcony of a residence in a residential area west of Toronto, Canada. The sampler collected 24-hour samples on alternate days for 12 days over a 23-day period in late 2005 and early 2006 for use in the Mn speciation analysis detailed in the following section.

### **APPLICATION STUDIES**

The investigators applied the analytic methods for low-volume PM samples that they had developed to groups of these samples for various reasons. In the sampler intercomparison analysis, the results were compared from simultaneous samples taken using different types of personal and ambient samplers run side by side at the same locations. A study was conducted of the effects of sample aging on the oxidation states of Fe, in an attempt both to assess the effects of storing the samples and to simulate the aging of Fe in PM during atmospheric transport. The Mn content

of low-volume urban PM samples was also assessed. The investigators further applied their new methods to samples taken as part of existing epidemiologic studies, analyzing PM for polar organic compounds in samples from an occupational setting and a group of trace metals in samples from a residential setting. These studies are described briefly below and summarized in Critique Table 3.

#### **Intercomparison of Personal Samplers**

Personal exposure samplers are intended to quantify and characterize a person's actual exposure to PM. The investigators conducted an intercomparison study of personal exposure samplers, applying their methods to generate trace-metals comparison data for the co-located samplers of the various types.

Personal and ambient PM samples from the East St. Louis and Los Angeles (University of Southern California) sites were used for this study. The results were compared for PM samples taken using the various types of personal samplers and substrate combinations and the larger ambient samplers, both between co-located samplers and between sites.

When comparing analytic results in larger-scale PM samples from personal samplers of different designs and the same locations, the investigators noted some important differences and variations. Agreement was good between the size-resolved total PM mass concentrations collected by the co-located PM<sub>2.5</sub> personal samplers in East St. Louis and Los Angeles (see Figure 27 of the Investigators' Report; one personal sampler in East St. Louis was apparently not working properly, and its data were omitted). Size-resolved trace-metal concentrations for the six metals differed by site but showed better agreement within sampler type than between co-located samples and showed consistent trends by sampler type. In Los Angeles, the Fe, Mn, Ba, and Cu content of PM decreased as particle size ranges decreased; samples from East St. Louis had a secondary mode in the 0.5-to-1.0- $\mu\text{m}$  fraction. Lead in Los Angeles had a relatively even size distribution; in East St. Louis it had a small coarse component and a large ultrafine component. Vanadium was concentrated in the submicron fraction in Los Angeles and the coarse fraction in East St. Louis. Better agreement was found across personal samplers when a higher fraction of the metal was present in the fine and ultrafine fractions than in the coarse fraction.

Table 10 of the Investigators' Report shows the average differences between personal samplers and the ambient sampler for both the Los Angeles and the East St. Louis locations. The arithmetic means of the metal concentrations for each metal and sampler type compared favorably when regressed against ambient concentrations measured

**Critique Table 3.** Summary of Application Studies for New Low-Volume PM Analysis Methods

Application Study	Purpose	Methods Used and Species Analyzed
Sampler intercomparison analysis	Compare PM speciation and analysis results between sampler designs and filter types	Trace-metals analysis methods (HR-ICP-MS)
Fe aging study	Assess the effect of atmospheric aging on oxidation states of Fe in PM	Wet-chemical spectrophotometric methods for soluble Fe(II) and Fe(III); XANES spectroscopy
Mn speciation study	Determine the amount and oxidation states of Mn in various size fractions of PM collected at a residential location in an area with high MMT use in gasoline and in an area without MMT use as a reference	Wet-chemical spectrophotometric methods for soluble Mn
Cohort study of truckers and truck terminal workers	Assess and compare concentrations of PAH-, carbon, and organic compounds in PM collected from personal, area, and ambient samplers across work areas and job categories	Nonpolar organic compound analysis methods (TD-GC-MS and PTV-GC-MS)
Epidemiologic study of elderly retirement home residents	Assess and compare concentrations of speciated metals in PM collected from personal samplers, indoor air samplers, and ambient monitoring	Trace-metals analysis methods (HR-ICP-MS)

by the URG and PCIS sampler types but compared favorably with the BGI sampler type only for PM<sub>2.5</sub> mass (and not for the speciated metals).

#### Iron Aging Study Using Wet-Chemical and XANES Analysis

Schauer and his team subjected samples to simulated atmospheric-aging processes, performing a trace-metal analysis of Fe oxidation using their newly developed wet-chemical and XANES methods to ascertain changes in Fe(II) and Fe(III) concentrations over time. The goal of the analysis was to age the aerosols artificially using tightly controlled light, humidity, and temperature conditions for 0 to 10 days in order to assess how trace concentrations of Fe(II) and Fe(III) change during atmospheric transport. The samples used were from sets of PCISs placed at the East St. Louis, Waukesha, and Los Angeles Basin (Rancho Los Amigos) sites.

The investigators found that the largest changes occurred in the first 6 days of aging, when soluble Fe(II) increased in the coarse fraction over the first day (while Fe(III) remained steady), then steadily decreased thereafter. Spikes in soluble Fe(II) were found on the first day in the < 0.25- $\mu$ m fraction and on the third day in the 0.25-to-1.0- $\mu$ m fraction (while Fe(III) remained steady). After 6 days, overall, concentrations of both Fe states returned to near their initial

levels and stabilized. The investigators hypothesized that oxidation of Fe(II) to Fe(III) predominates in smaller particles because of their high surface area and that photo-reduction of Fe(III) to Fe(II) predominates in larger particles. Because the greatest changes occurred in the brief period after sampling, the results were believed to indicate that prevailing weather conditions could have a substantial effect on exposure to soluble Fe in PM aerosols.

#### Wet-Chemical Analysis of Manganese in PM Samples

When tetraethyl lead was banned as an octane booster in gasoline, it was replaced with methylcyclopentadienyl manganese tricarbonyl (MMT), which contained Mn and thus raised concerns about hazardous air pollution. Although MMT has been approved for use in several countries, including the United States, it had been used most extensively in Canada prior to 2004 (Health Canada 2010). (It has not been used much in the United States pending further emissions characterization and health testing.) The investigators thus undertook a study of Mn speciation using their newly developed wet-chemical methods for Mn to analyze wintertime PM samples from Toronto, Canada, although that sampling, in late 2005 and early 2006, took place nearly two years after the cessation of use of MMT in Toronto gasoline.

The investigators' experiments with Mn speciation in the Toronto samples yielded some interesting insights into the sources of Mn in aerosol PM. The greatest concentrations of soluble Mn were found in the coarse fraction, with decreasing concentrations as particle size fractions decreased. When compared with speciation results from East St. Louis samples used in the sampler intercomparison study, the air concentrations of Mn in Toronto were lower overall, with roughly similar particle concentrations. Soluble Mn as a percent of total Mn was twice as high in Toronto (40% versus 20%), and concentrations of oxidized Mn were higher than in East St. Louis. Soluble oxidized Mn was only detectable in the PM<sub>2.5</sub> fraction of the Toronto samples. The investigators suggest this finding may point to combustion of MMT as the source, given the use of MMT in the country. Because that use had ended prior to the sampling, the presence of Mn in the coarse fraction might in part be explained by the previous fuel use (i.e., accumulations in road dust); it seems unlikely that fuel use directly contributed to the presence of Mn in the PM<sub>2.5</sub> fraction, although it remains possible that residual Mn depositions inside the engine continued to contribute to emissions even after the removal of MMT from the fuel.

#### **Epidemiologic Studies with Collaborating Researchers**

The investigators worked with Dr. Eric Garshick of the Channing Laboratory at Harvard Medical School and Dr. Ralph Delfino of the University of California–Irvine, who at the time were both directing health studies involving PM exposure. The investigators obtained personal, area, and ambient samples from Garshick (Davis et al. 2009) and Delfino (Polidori et al. 2007) and analyzed them as a demonstration of the utility of their new low-volume analytic methods for human health research.

**St. Louis Truck Terminal Study** Samples of PM aerosols were obtained from a large, ongoing National Cancer Institute–funded cancer study, run by Garshick, of workers in a truck terminal in St. Louis, Missouri. Schauer and his team obtained personal samples of PM for dockworkers, mechanics, and drivers during their regular shifts and compared them with PM samples from two on-site monitors in each of three work areas in the dock, shop, and yard as well as with samples from an off-site urban background monitor located nearby (but outside the terminal). The investigators applied their newly developed low-volume PM analysis methods for nonpolar organics, comparing measured concentrations of elemental carbon, OC, PAHs, steranes, and hopanes from the personal samplers, area samplers, and background monitors.

Consistency of sampling results varied by job classification and work area, as shown in Tables 16 and 17 of the Investigators' Report. Jobs where there was high variation within a job and within a work area indicated cases where worker exposures were more highly subject to individual job and personal activities than to area or background air quality—i.e., cases where personal monitoring is a more valuable measure of personal exposure than area or background monitoring.

When measures from work-area monitors were compared with those from background monitors, interesting patterns emerged. Figures 47 and 48 of the Investigators' Report show the contrasts between work-area and background concentrations of total carbon. Although the results of work-area monitoring in the yard were close to those of the background monitoring, dock and shop PM was consistently higher in total carbon, with the shop area recording the highest concentrations. For PAHs, there was no correlation between work-area and background concentrations, indicating that these exposures had been dominated by work-area activities. When personal exposures were compared with background concentrations, the investigators noted chemical markers (alkanes) indicative of substantial cigarette-smoke exposure among the dockworkers. Good agreement was found between personal and area samples for elemental carbon and hopanes among the mechanics, suggesting that work-area monitors might be an adequate indicator of diesel exposure. However, there was little correlation for OC, PAHs, or alkanes in the mechanics' personal samples, raising doubts about the appropriateness of area sampling in estimating their personal exposures. Personal samples for pickup and delivery drivers were more heavily loaded with PM than the work-area and background samples—indicating higher overall PM exposures—and showed little correlation with either work-area or background exposure levels. Exposures for long-haul drivers, as measured by personal samplers, had the least correlation to work-area or background measures for any group. As with the pickup and delivery drivers, the personal samples of PM for the long-haul drivers had higher concentrations for all species compared with the background concentrations, likely because of in-cab exposures.

**Los Angeles Heart Disease Study** Schauer and his team obtained indoor, outdoor, and personal PM samples from a coronary heart disease study, run by Delfino, of elderly nonsmokers living in a retirement home in the Los Angeles Basin. Delfino outfitted his subjects with personal PM samplers that separated particulates from aerosols into coarse (> PM<sub>2.5</sub>), fine (PM<sub>0.25–2.5</sub>), and ultrafine (< PM<sub>0.25</sub>) fractions. He also collected PM from air samplers placed

inside and outside the retirement home (on site). Schauer and his team analyzed and compared the concentrations of a group of trace metals found in the PM from the various samples.

The investigators' most important observation from the analysis was that trace-metal concentrations in both the indoor or outdoor PM samples were not correlated with trace-metal concentrations in the PM taken from the personal samples. For all elements except copper, no relationship was found for these retirement-home residents between air concentrations from the indoor, outdoor, and personal samples (see Table 19 of the Investigators' Report). This implies that the personal exposure samples were not measuring exposure to the same pollutant sources represented in the indoor and outdoor samples.

---

#### HEALTH REVIEW COMMITTEE EVALUATION AND DISCUSSION

---

The investigators report that this study has advanced the field of PM speciation in three key areas: The investigators developed (1) methods to measure organic tracers in personal exposure samples using TD-GC-MS, (2) methods to measure trace elements using HR-ICP-MS, and (3) wet-chemical methods to speciate Fe and Mn in personal exposure samples. The investigators estimated that using these methods on a batch of 100 to 500 personal PM samples would cost about \$250 per sample (in 2007 U.S. dollars) for the TD-GC-MS analysis, \$75 per sample for the HR-ICP-MS analysis, and about \$10 per sample for the wet-chemical analysis.

Overall, the Health Review Committee viewed the study as strong and thought that the research was original and thorough in developing methods for the analysis of samples from personal and other low-volume samplers. Both the newly developed methods and the refined methods will be appropriate for the analysis of trace elements and nonpolar organic tracers of interest in personal exposure samples. The Committee also noted that the experimental data that Schauer and his team gathered during the study will be useful in the validation of exposure models and as tools for future health studies. The full range of trace elements and chemicals included in the methods development and analysis should also be of use in performing source apportionment based on PM collected from personal and other low-volume samplers.

The Committee further noted that the methods developed for the study, the experimental analyses, and the report itself fully addressed all five objectives (i.e., the specific aims) proposed at the beginning of the study. The investigators successfully developed and validated a GC-MS

technique to analyze a broad range of organic compounds and a low-cost TD-GC-MS technique to quantify a selected list of organic compounds present in PM samples collected with personal samplers. The investigators optimized and adapted ICP-MS analysis techniques for the measurement of selected trace metals and trace-element isotope signatures and developed and validated low-cost wet-chemistry techniques to measure the oxidation states of selected trace elements (Fe, Mn, and Cr) in PM samples collected with personal samplers, source samplers, and ambient samplers. They also collaborated with two existing epidemiologic studies to provide trace-metal and organic speciation analyses of PM from personal, area, and ambient samplers that were useful for understanding the relationships between personal and ambient exposure measurements.

The Committee noted, however, that the investigators were not able to meet some of their goals in certain areas. Apart from basic method development, the investigators did not test or expand much upon their methods for the analysis of polar organic compounds. In correspondence with the Committee, Schauer explained that, although he and his team were able to demonstrate the methods as a proof of concept, the necessary analysis materials were harsh on the investigators' GC-MS system and caused repeated instrument failures; the investigators were therefore unable to analyze large numbers of samples using the methods as described and are still working to reduce instrument failures and expand the method's capabilities.

The investigators also encountered difficulties in detecting Cr(VI) from ambient air samples taken with personal samplers. The DL for Cr(VI) was simply too low for the amount of Cr(VI) present in the PM aerosol found in most environments. Schauer has stated, however, that the DL for the method is sufficient for occupational-exposure environments, such as chrome-plating shops and steel foundries, where personal Cr(VI) exposure is both high and of interest to health researchers. The investigators were unable to detect Cr(VI) in any study samples and were thus unable to perform the necessary measurements, quality control, and validation (of the sort they performed for their Fe and Mn methods).

The Committee members thought that the cost estimates provided for the various analytic methods developed and discussed as part of the study were helpful, but they added that would have liked to see more information about the amount of worker and laboratory throughput time required for the methods. Schauer did not provide time estimates, because he maintained that the labor and time needed to process a sample are highly dependent on individual laboratory factors, such as equipment availability, staff training, staffing levels, and the number of samples routinely processed using a given method.

The Committee thought that the report lacked sufficiently detailed descriptions of standardized laboratory procedures—in their absence, a reader would need to piece together certain methods from multiple sources—and that any details tailored specifically for the methods developed as a part of the study might not be well integrated into standard method descriptions. Schauer's reasoning was that such procedures are common and well described elsewhere and that most analytic laboratories are well versed in such procedures. The Committee believed that Schauer's subsequent inclusion of a full standard-operating-procedure manual (see Appendix C, available on the HEI Web site at <http://pubs.healtheffects.org> or by request) for the methods and equipment used in the study's microwave digestion of aerosol PM was a valuable addition to the report; it provides more detail about methods that are less commonly referenced in the air pollution literature.

Achieving the large majority of the goals of the study, Schauer and colleagues have extended and enhanced speciation methods for use with low-volume PM samples. With the exception of the trace-element analysis method for Cr(VI), the methods the investigators developed appear to have sufficiently low DLs for use with the quantities of PM collected by most personal samplers operating under typical conditions. The precision and accuracy of these methods appear favorable compared with standard high-volume-sample methods or analyses of standards (with the exception of polar organics, for which the investigators could not assess sufficient samples to validate their methods fully).

With the application of the investigators' methods to actual personal sampling data from a workplace study and a retirement-home study, the team has also demonstrated the potential of the methods for other health studies assessing exposure to a wide variety of compounds. In each case, the methods used were well suited to the types of PM samples originally collected by the study teams and provided interesting insights into the nature of individual exposures and their relationships to potential sources and into speciation results from indoor, outdoor, area, and background PM samples. The new wet-chemical methods, geared toward commonly available equipment and low-cost reagents, will be particularly appropriate to the assessment of commonly encountered toxic-metal exposures at a low estimated cost per sample. The investigators' more sophisticated GC-MS-based methods improved DLs to such an extent that they were suitable for the low PM volume collected with personal samplers, although the cost of the analysis of samples for a typical panel study still appears to be prohibitively high at this time, and it is not clear how much these methods could be scaled up with a concomitant per-sample cost reduction.

---

## CONCLUSIONS

---

Although the composition of PM has been characterized in samples collected by high-volume samplers, there is still a need to assess human exposures on a finer scale by characterizing the smaller samples typically collected by personal exposure samplers. In the current study, the investigators addressed these issues by developing methods that have sufficiently high sensitivity and sufficiently low DLs for the speciation of low-volume PM samples.

For the detection and quantification of a large group of trace-metal constituents of PM<sub>2.5</sub>, the investigators used a novel microvolume microwave digestion process that reduced blank volumes and concentrated the samples sufficiently for analysis by HR-ICP-MS. They further adapted methods for the analysis of nonpolar organic materials by TD-GC-MS. They were less successful in quantifying polar compounds by TD-GC-MS, because the required chemicals caused numerous equipment failures.

In the interest of creating economical ways to meet the challenges of small-sample analysis, the investigators adapted wet-chemical methods for the extraction and quantification of Fe, Mn, and Cr in various oxidation states of interest to health effects researchers. They analyzed samples using specialized spectrophotometric methods and, in the case of the oxidation states of Fe, XANES spectroscopy. These methods are important not only for their cost-saving application in common laboratory settings, but also for their use in health studies for the analysis of the oxidative states of metals.

Most of the methods developed by the investigators were validated by the investigators as being sufficiently sensitive to analyze small PM samples of the sort collected by personal sampling equipment. (Exceptions, again, were the detection of Cr(VI) by way of wet-chemical methods in ambient PM samples and the quantification of polar organic compounds.)

In conclusion, Dr. Schauer and his team have developed methods that have sufficiently high sensitivity and sufficiently low DLs to measure trace metals, nonpolar organics, and polar organics present in low-volume PM samples. The investigators have successfully adapted wet-chemical methods for the extraction and quantification of Fe, Mn, and Cr in various oxidation states of interest to researchers. Most of the methods were validated by the investigators as being sufficiently sensitive to analyze low-volume PM samples of the sort collected by personal sampling equipment.

Results from the St. Louis truck terminal indicated that personal activities, such as smoking and job tasks, had large effects on exposures. Results from the retirement home indicated that trace elements measured in personal

PM samples were different from those measured in indoor and outdoor air samples (although the reasons for these discrepancies were not clear). These results indicate the broader suitability of the investigators' methods for use in studies of PM exposure and human health. Further work remains to be done on methods to analyze polar organic compounds and improving detection of Cr(VI) from ambient air samples taken with personal samplers.

---

#### ACKNOWLEDGMENTS

---

The Health Review Committee thanks the ad hoc reviewers for their help in evaluating the scientific merit of the Investigators' Report. The Committee is also grateful to Annemoon van Erp for her oversight of the study; to Debra Kaden for her assistance in the review of the study; to Kate Adams for her assistance in preparing the study's Critique; to George Simonson for his science editing of the Report and this Critique; and to Suzanne Gabriel, Barbara Gale, Fred Howe, Bernard Jacobson, and Flannery Carey McDermott for their roles in preparing the Report for publication.

---

#### REFERENCES

---

- Davis ME, Laden F, Hart JE, Garshick E, Blicharz A, Smith TJ. 2009. Predicting changes in PM exposure over time at U.S. trucking terminal using structural equation modeling techniques. *J Occup Environ Hyg* 6:396–403.
- Health Canada. 2010. Human Health Risk Assessment for Inhaled Manganese. Minister of Health, Ottawa, ON, Canada. Available from <http://www.hc-sc.gc.ca/ewh-semt/pubs/air/manganese-eng.php>.
- Manchester-Neesvig JB, Schauer JJ, Cass GR. 2003. The distribution of particle-phase organic compounds in the atmosphere and their use for source apportionment during the Southern California Children's Health Study. *J Air Waste Manag Assoc* 53:1065–1079.
- Polidori A, Arhami M, Sioutas C, Delfino RJ, Allen R. 2007. Indoor/outdoor relationships, trends, and carbonaceous content of fine particulate matter in retirement homes of the Los Angeles Basin. *J Air Waste Manag Assoc* 57:366–379.
- Schauer JJ, Cass GR. 2000. Source apportionment of wintertime gas-phase and particle-phase air pollutants using organic compounds as tracers. *Environ Sci Technol* 34:1821–1832.
- Schauer JJ, Fraser MP, Cass GR, Simoneit BR. 2002. Source reconciliation of atmospheric gas-phase and particle-phase pollutants during a severe photochemical smog episode. *Environ Sci Technol* 36:3806–3814.
- Schauer JJ, Lough GC, Shafer MM, Christensen WF, Arndt MF, DeMinter JT, Park J-S. 2006. Characterization of Metals Emitted from Motor Vehicles. Research Report 133. Health Effects Institute, Boston, MA.
- Schauer JJ, Rogge WF, Hildemann LM, Mazurek MA, Cass GR, Simoneit BRT. 1996. Source apportionment of airborne particulate matter using organic compounds as tracers. *Atmos Environ* 30:3837–3855.
- Singh M, Jaques PA, Sioutas C. 2002. Size distribution and diurnal characteristics of particle-bound metals in source and receptor sites of the Los Angeles Basin. *Atmos Environ* 36:1675–1689.
- Zheng M, Cass GR, Schauer JJ, Edgerton ES. 2002. Source apportionment of PM<sub>2.5</sub> in the Southeastern United States using solvent-extractable organic compounds as tracers. *Environ Sci Technol* 36:2361–2371.



## RELATED HEI PUBLICATIONS: PARTICULATE MATTER

Number	Title	Principal Investigator	Date*
<b>Research Reports</b>			
149	Development and Application of a Sensitive Method to Determine Concentrations of Acrolein and Other Carbonyls in Ambient Air	T.M. Cahill	2010
147	Atmospheric Transformation of Diesel Emissions	B. Zielinska	2010
143	Measurement and Modeling of Exposure to Selected Air Toxics for Health Effects Studies and Verification of Biomarkers	R.M. Harrison	2009
133	Characterization of Metals Emitted from Motor Vehicles	J.J. Schauer	2006
131	Characterization of Particulate and Gas Exposures of Sensitive Subpopulations Living in Baltimore and Boston	P. Koutrakis	2005
130	Relationships of Indoor, Outdoor, and Personal Air (RIOPA) <i>Part I. Collection Methods and Descriptive Analyses</i>	C.P. Weisel	2005
	<i>Part II. Analyses of Concentrations of Particulate Matter Species</i>	B.J. Turpin	2007
127	Personal, Indoor, and Outdoor Exposures to PM <sub>2.5</sub> and Its Components for Groups of Cardiovascular Patients in Amsterdam and Helsinki	B. Brunekreef	2005
122	Evaluation of a Personal and Microenvironmental Aerosol Speciation Sampler (PMASS)	A.S. Geyh	2004
121	Field Evaluation of Nanofilm Detectors for Measuring Acidic Particles in Indoor and Outdoor Air	B.S. Cohen	2004
114	A Personal Particle Speciation Sampler	S. Hering	2003
107	Emissions from Diesel and Gasoline Engines Measured in Highway Tunnels Real-World Particulate Matter and Gaseous Emissions from Motor Vehicles in a Highway Tunnel Airborne Carbonyls from Motor Vehicle Emissions in Two Highway Tunnels	A.W. Gertler	2002
95	Association of Particulate Matter Components with Daily Mortality and Morbidity in Urban Populations	M. Lippmann	2000
61	Methods Development Toward the Measurement of Polyaromatic Hydrocarbon–DNA Adducts by Mass Spectrometry	R.W. Giese	1993
56	Characterization of Particle- and Vapor-Phase Organic Fraction Emissions of a Heavy-Duty Diesel Engine Equipped with a Particle Trap and Regeneration Controls	S.T. Bagley	1993

*Continued*

\* Reports published since 1993.

Copies of these reports can be obtained from the Health Effects Institute and many are available at [www.healtheffects.org](http://www.healtheffects.org).

## RELATED HEI PUBLICATIONS: PARTICULATE MATTER

---

Number	Title	Date*
<b>Special Reports</b>		
17	Traffic-Related Air Pollution: A Critical Review of the Literature on Emissions, Exposure, and Health Effects	2010
16	Mobile-Source Air Toxics: A Critical Review of the Literature on Exposure and Health Effects	2007
	Research Directions to Improve Estimates of Human Exposure and Risk from Diesel Exhaust	2002
	Diesel Exhaust: A Critical Analysis of the Institute's Diesel Working Group	1995
<b>HEI Communications</b>		
8	The Health Effects of Fine Particles: Key Questions and the 2003 Review (Report of the Joint Meeting of the EC and HEI)	1999
5	Formation and Characterization of Particles	1997
<b>HEI Research Program Summaries</b>		
	Research on Diesel Exhaust and Other Particles	2003
	Research on Particulate Matter	1999
<b>HEI Perspectives</b>		
	Understanding the Health Effects of Components of the Particulate Matter Mix: Progress and Next Steps	2002

---

\* Reports published since 1993.

Copies of these reports can be obtained from the Health Effects Institute and many are available at [www.healtheffects.org](http://www.healtheffects.org).

# HEI BOARD, COMMITTEES, and STAFF

## Board of Directors

**Richard F. Celeste, Chair** *President, Colorado College*

**Sherwood Boehlert** *Of Counsel, Accord Group; Former Chair, U.S. House of Representatives Science Committee*

**Enriqueta Bond** *President Emeritus, Burroughs Wellcome Fund*

**Purnell W. Choppin** *President Emeritus, Howard Hughes Medical Institute*

**Michael T. Clegg** *Professor of Biological Sciences, University of California–Irvine*

**Jared L. Cohon** *President, Carnegie Mellon University*

**Stephen Corman** *President, Corman Enterprises*

**Gowher Rizvi** *Vice Provost of International Programs, University of Virginia*

**Linda Rosenstock** *Dean, School of Public Health, University of California–Los Angeles*

**Henry Schacht** *Managing Director, Warburg Pincus; Former Chairman and Chief Executive Officer, Lucent Technologies*

**Warren M. Washington** *Senior Scientist, National Center for Atmospheric Research; Former Chair, National Science Board*

**Archibald Cox, Founding Chair** *1980–2001*

**Donald Kennedy, Vice Chair Emeritus** *Editor-in-Chief Emeritus, Science; President Emeritus and Bing Professor of Biological Sciences, Stanford University*

## Health Research Committee

**David L. Eaton, Chair** *Associate Vice Provost for Research and Director, Center for Ecogenetics and Environmental Health, School of Public Health, University of Washington–Seattle*

**David T. Allen** *Gertz Regents Professor in Chemical Engineering; Director, Center for Energy and Environmental Resources, University of Texas–Austin*

**Joe G.N. Garcia** *Vice Chancellor for Research and Professor of Medicine, University of Illinois–Chicago*

**Uwe Heinrich** *Professor, Medical School Hannover; Executive Director, Fraunhofer Institute for Toxicology and Experimental Medicine, Hannover, Germany*

**Grace LeMasters** *Professor of Epidemiology and Environmental Health, University of Cincinnati College of Medicine*

**Sylvia Richardson** *Professor of Biostatistics, Department of Epidemiology and Public Health, Imperial College School of Medicine, London, United Kingdom*

**Richard L. Smith** *Director, Statistical and Applied Mathematical Sciences Institute, University of North Carolina–Chapel Hill*

**James A. Swenberg** *Kenan Distinguished Professor of Environmental Sciences, Department of Environmental Sciences and Engineering, University of North Carolina–Chapel Hill*

**Ira B. Tager** *Professor of Epidemiology, School of Public Health, University of California–Berkeley*

# HEI BOARD, COMMITTEES, and STAFF

## Health Review Committee

**Homer A. Boushey, Chair** *Professor of Medicine, Department of Medicine, University of California–San Francisco*

**Ben Armstrong** *Reader in Epidemiological Statistics, Public and Environmental Health Research Unit, Department of Public Health and Policy, London School of Hygiene and Tropical Medicine, United Kingdom*

**Michael Brauer** *Professor, School of Environmental Health, University of British Columbia, Canada*

**Bert Brunekreef** *Professor of Environmental Epidemiology, Institute of Risk Assessment Sciences, University of Utrecht, the Netherlands*

**Mark W. Frampton** *Professor of Medicine and Environmental Medicine, University of Rochester Medical Center*

**Stephanie London** *Senior Investigator, Epidemiology Branch, National Institute of Environmental Health Sciences*

**Armistead Russell** *Georgia Power Distinguished Professor of Environmental Engineering, School of Civil and Environmental Engineering, Georgia Institute of Technology*

**Lianne Sheppard** *Professor of Biostatistics, School of Public Health, University of Washington–Seattle*

## Officers and Staff

**Daniel S. Greenbaum** *President*

**Robert M. O’Keefe** *Vice President*

**Rashid Shaikh** *Director of Science*

**Barbara Gale** *Director of Publications*

**Jacqueline C. Rutledge** *Director of Finance and Administration*

**Helen I. Dooley** *Corporate Secretary*

**Kate Adams** *Staff Scientist*

**Aaron J. Cohen** *Principal Scientist*

**Maria G. Costantini** *Principal Scientist*

**Philip J. DeMarco** *Compliance Manager*

**Suzanne Gabriel** *Editorial Assistant*

**Hope Green** *Editorial Assistant (part time)*

**L. Virgi Hepner** *Senior Science Editor*

**Anny Luu** *Administrative Assistant*

**Francine Marmenout** *Senior Executive Assistant*

**Sumi Mehta** *Senior Scientist*

**Nicholas Moustakas** *Policy Associate*

**Hilary Selby Polk** *Senior Science Editor*

**Sarah Rakow** *Science Administrative Assistant*

**Robert A. Shavers** *Operations Manager*

**Geoffrey H. Sunshine** *Senior Scientist*

**Annemoon M.M. van Erp** *Senior Scientist*

**Katherine Walker** *Senior Scientist*

**Morgan Younkin** *Research Assistant*





HEALTH  
EFFECTS  
INSTITUTE

101 Federal Street, Suite 500  
Boston, MA 02110, USA  
+1-617-488-2300  
*[www.healtheffects.org](http://www.healtheffects.org)*

RESEARCH  
REPORT

Number 153  
December 2010